

Homodyne Detection and Quantum State Reconstruction[†]

Dirk–Gunnar Welsch

Friedrich-Schiller-Universität Jena, Theoretisch-Physikalisches Institut
Max-Wien Platz 1, D-07743 Jena, Germany

Werner Vogel

Universität Rostock, Fachbereich Physik
Universitätsplatz 3, D-18051 Rostock, Germany

Tomáš Opatrný

Palacký University, Faculty of Natural Sciences
Svobody 26, 77146 Olomouc, Czech Republic

[†]In *Progress in Optics*, Vol. XXXIX, ed. E. Wolf (Elsevier, Amsterdam, 1999), p. 63–211.

Contents

1. Introduction	4
2. Phase-sensitive measurements of light	7
2.1. Optical homodyning	7
2.1.1. Basic scheme	7
2.1.2. Quadrature-component statistics	9
2.1.3. Multimode detection	13
2.1.4. Q function	16
2.1.5. Probability operator measures	20
2.1.6. Positive P function	22
2.1.7. Displaced-photon-number statistics	23
2.1.8. Homodyne correlation measurements	25
2.2. Heterodyne detection	26
2.3. Parametric amplification	26
2.4. Measurement of cavity fields	27
3. Quantum-state reconstruction	31
3.1. Optical homodyne tomography	31
3.2. Density matrix in quadrature-component bases	35
3.3. Density matrix in the Fock basis	37
3.3.1. Sampling of quadrature-components	37
3.3.2. Sampling of the displaced Fock-states on a circle	43
3.3.3. Reconstruction from propensities	45
3.4. Multimode density matrices	46
3.5. Local reconstruction of $P(\alpha; s)$	48
3.6. Reconstruction from test atoms in cavity QED	49
3.6.1. Quantum state endoscopy and related methods	49
3.6.2. Atomic beam deflection	52
3.7. Alternative proposals	54
3.8. Reconstruction of specific quantities	56
3.8.1. Normally ordered photonic moments	57
3.8.2. Quantities admitting normal-order expansion	59
3.8.3. Canonical phase statistics	60
3.8.4. Hamiltonian and Liouvillian	63
3.9. Processing of smeared and incomplete data	64
3.9.1. Experimental inaccuracies	64
3.9.2. Least-squares method	69
3.9.3. Maximum-entropy principle	70
3.9.4. Bayesian inference	72
4. Quantum states of matter systems	74
4.1. Molecular vibrations	74
4.1.1. Harmonic regime	75
4.1.2. Anharmonic vibrations	76
4.2. Trapped-atom motion	78
4.2.1. Quadrature measurement	78

4.2.2.	Measurement of the Jaynes–Cummings dynamics	81
4.2.3.	Entangled vibronic states	84
4.3.	Bose–Einstein condensates	85
4.4.	Atomic matter waves	87
4.4.1.	Transverse motion	87
4.4.2.	Longitudinal motion	90
4.5.	Electron motion	91
4.5.1.	Electronic Rydberg wave packets	91
4.5.2.	Cyclotron state of a trapped electron	92
4.5.3.	Electron beam	93
4.6.	Spin and angular momentum systems	93
4.7.	Crystal lattices	95
A. Radiation field quantization		97
B. Quantum-state representations		98
B.1.	Fock states	98
B.2.	Quadrature-component states	99
B.3.	Coherent states	99
B.4.	\mathfrak{s} -Parametrized phase-space functions	101
B.5.	Quantum state and quadrature components	102
C. Photodetection		103
D. Elements of least-squares inversion		104
References		107

1. Introduction

Since the experimental demonstration of tomographic quantum-state measurement on optical fields by Smithey, Beck, Raymer and Faridani [1993] based on the theoretical work of Vogel, K., and Risken [1989] a boom in studying quantum-state reconstruction problems has been observed. Numerous workers have considered various schemes and methods for extracting all knowable information on the state of a quantum system from measurable data, and early work has been recovered. In the history of quantum theory the concept of quantum state including quantum-state measurement has been a matter of intense discussion.

The state of a quantum object is commonly described by a normalized Hilbert-space vector $|\Psi\rangle$ or, more generally, by a density operator $\hat{\rho} = \sum_i p_i |\Psi_i\rangle\langle\Psi_i|$ which is a Hermitian and non-negative valued Hilbert-space operator of unit-trace. The Hilbert space of the object is usually spanned up by an orthonormalized set of basic vectors $|A\rangle$ representing the eigenvectors (eigenstates) of Hermitian operators \hat{A} associated with a complete set of simultaneously measurable observables (physical quantities) of the object.¹ The eigenvalues A of these operators are the values of the observables that can be registered in a measurement. Here it must be distinguished between an individual (single) and an ensemble measurement (i.e., in principle, an infinitely large number of repeated measurements on identically prepared objects). Performing a single measurement on the object, a totally unpredictable value A is observed in general, and the state of the object has *collapsed* to the state $|A\rangle$ according to the von Neumann's projection definition of a measurement (von Neumann [1932]). If the same measurement is repeated immediately after the first measurement (on the same object), the result is now well predictable – the same value A as in the first measurement is observed. Obviously, owing to the first measurement the object has been prepared in the state $|A\rangle$. Repeating the measurement many times on identically prepared object, the relative rate at which the result A is observed approaches the diagonal density-matrix element $\langle A|\hat{\rho}|A\rangle$ as the number of measurements tend to infinity. Measuring $\langle A|\hat{\rho}|A\rangle$ for all values of A the statistics of \hat{A} (and any function of \hat{A}) are known. To completely describe the quantum state, i.e., to determine all the quantum-statistical properties of the object, knowledge of all density-matrix elements $\langle A|\hat{\rho}|A'\rangle$ is needed. In particular, the off-diagonal elements essentially determine the statistics of such sets of observables \hat{B} that are not compatible with \hat{A} ($[\hat{A}, \hat{B}] \neq 0$) and cannot be measured simultaneously with \hat{A} . Obviously, the statistics of \hat{B} can also be obtained directly – similar to the statistics of \hat{A} – from an ensemble measurement yielding the diagonal density-matrix elements $\langle B|\hat{\rho}|B\rangle$ in the basis of the eigenvectors $|B\rangle$ of \hat{B} . Now one can proceed to consider other sets of observables that are not compatible with \hat{A} and \hat{B} , and the rather old question arises of which and how many incompatible observables must be measured in order to obtain all the information contained in the density matrix of an arbitrary quantum state. Already Pauli [1933] addressed the question whether or not the wave function of a particle can be reconstructed from the position and momentum probability distributions, i.e., the diagonal density-matrix elements in the position and momentum basis.

Roughly speaking, there have been two routes to collect measurable data for

¹For notational convenience we write \hat{A} , without further specifying the quantities belonging to the set.

reconstructing the quantum state of an object under consideration. In the first, which closely follows the line given above, a succession of (ensemble) measurements is made such that a set of noncommutative object observables is measured which carries the complete information about the quantum state. A typical example is the tomographic quantum-state reconstruction mentioned at the beginning. Here, the probability distributions $p(x, \varphi) = \langle x, \varphi | \hat{\rho} | x, \varphi \rangle$ of the quadrature components $\hat{x}(\varphi)$ of a radiation-field mode for all phases φ within a π interval are measured, i.e., the expectation values of the quadrature-component projectors $|x, \varphi\rangle\langle x, \varphi|$. In the second, the object is coupled to a reference system (whose quantum state is well known) such that measurement of observables of the composite system corresponds to “simultaneous” measurement of noncommutative observables of the object. In this case the number of observables (of the composite system) that must be measured in a succession of (ensemble) measurements can be reduced drastically, but at the expense of the image sharpness of the object. As a result of the additional noise introduced by the reference system only fuzzy measurements on the object can be performed, which just makes a “simultaneous” measurement of incompatible object observables feasible. A typical example is the Q function of a radiation-field mode, which is given by the diagonal density-matrix elements in the coherent-state basis, $Q(\alpha) = \pi^{-1} \langle \alpha | \hat{\rho} | \alpha \rangle$. It can already be obtained from one ensemble measurement of the complex amplitude α , which corresponds to a fuzzy measurement of the “joint” probability distribution of two canonically conjugated observables $\hat{x}(\varphi)$ and $\hat{x}(\varphi + \pi/2)$ of the object.

Since the sets of quantities measured via the one or the other route (or an appropriate combination of them) carry the complete information on the quantum state of the object, they can be regarded, in a sense, as representations of the quantum state, which can be more or less close to (or far from) familiar quantum-state representations, such as the density matrix in the Fock basis or the Wigner function. In any case, the question arises of how to reconstruct from the measured data specific quantum-state representations (or specific quantum-statistical properties of the object for which a direct measurement scheme is not available). Again, there have been two typical concepts for solving the problem. In the first, equations that relate the measured quantities to the desired quantities are derived and tried to be solved either analytically or numerically in order to obtain the desired quantities in terms of the measured quantities. In practice, the measured data are often incomplete, i.e., not all quantities needed for a precise reconstruction are measured,² and moreover, the measured data are inaccurate. Obviously, any experiment can only run for a finite time, which prevents one, on principle, from performing an infinite number of repeated measurements in order to obtain precise expectation values. These inadequacies give rise to systematic and statistical errors of the reconstructed quantities, which can be quantified in terms of confidence intervals. In the second, statistical methods are used from the very beginning in order to obtain the best *a posteriori* estimation of the desired quantities on the basis of the available (i.e., incomplete and/or inaccurate) data measured. However the price to pay may be high. Whereas in the first concept linear equations are typically to be handled and estimates of the desired quantities (including statistical errors) can often be directly sampled from the measured data, application of purely statistical methods, such as the principle of *maximum entropy* or

²To compensate for incomplete data, some *a priori* knowledge of the quantum state is needed.

Bayesian inference, require nonlinear equations to be considered, and reconstruction in *real time* is impossible in general.

The aim of this review is to familiarize physicists with the recent progress in the field of quantum-state reconstruction and draw attention to important contributions in the large body of work. Although in much of what follows we consider the reconstruction of quantum states of travelling optical fields, the basic-theoretical concepts also apply to cavity fields and matter systems. Section 2. reviews the experimental schemes that have been considered for quantum-state measurement on optical fields, with special emphasis on optical homodyne (§ 2.1.). It begins by formulating the basic ideas of four-port homodyne detection of the quadrature components of single-mode fields (§§ 2.1.1. and 2.1.2.) and then proceeds to extend the scheme to multimode fields and multipoint homodyne detectors (§ 2.1.3.), which can also be used for “simultaneous” measurement of noncommuting signal observables (§§ 2.1.4. – 2.1.6.). Section 2.1.7. returns to the four-port scheme in § 2.1.1. and explains its use for measuring displaced Fock states. Homodyne correlation measurements are shown to yield insight in phase-sensitive field properties even in the case of low detection efficiencies (§ 2.1.8.). After addressing heterodyne detection (§ 2.2.) and parametric amplification (§ 2.3.), typical schemes for quantum-state measurement in high- Q cavity QED by test atoms are outlined (§ 2.4.).

Section 3. reviews typical methods for reconstruction of quantum-state representations and specific quantum-statistical properties of optical fields from sets of measurable quantities carrying the complete information on the quantum state. In § 3.1. – 3.5. we focus on the reconstruction of quantum-state representations from quantities measurable in homodyne detection of travelling optical fields. The next subsection (§ 3.6.) presents methods of reconstruction of quantum-state representations of high- Q cavity fields from measurable properties of test atoms probing the cavity fields, and in § 3.7. alternative proposals are outlined. Section 3.8. then addresses the problem of direct reconstruction of specific quantities from the measured data – an important problem with respect to quantities for which direct measurement schemes have not been found so far. Whereas in §§ 3.1. – 3.8. it is assumed that all the data needed for a precise reconstruction of the desired quantities can be precisely measured, at least in tendency, in § 3.9. statistical methods for processing smeared and inaccurately measured incomplete data are outlined with the aim to obtain optimum estimations of the quantum states.

Section 4. summarizes methods for measurement and reconstruction of quantum-state representations of matter system, with special emphasis on optical methods and experimental demonstrations. In § 4.1. the problem of reconstruction of the vibrational quantum state in an excited electronic state of a two-atom molecule is addressed. Typical schemes for determining the motional quantum state of trapped atoms are outlined in § 4.2., and in § 4.3. the problem of quantum-state measurement on Bose–Einstein condensates is considered. Sections 4.4. and 4.5., respectively, present schemes suitable for determining the motional quantum state of atom- and electron-wave packets. In the debate on quantum-state measurement, which is nearly as old as quantum mechanics, spin systems has been attracted much attention, because of low-dimensional Hilbert space. Section 4.6. outlines the main ideas in this field. Finally, § 4.7. explains the basic ideas of Compton and X -ray scattering for measuring the single-particle quantum state of crystal lattices.

2. Phase-sensitive measurements of light

The statistical properties of a classical radiation field are known when the amplitude statistics and the phase statistics are known. Whereas the amplitude statistics can be obtained from intensity measurements, determination of the phase statistics needs phase-sensitive measurement. Obviously the same is true in quantum optics. In order to obtain the complete information about the quantum state a radiation field is prepared in interferometric measurements that respond to amplitude and phase variables must be performed.

2.1. Optical homodyning

Homodyne detection has been a powerful method for measuring phase sensitive properties of travelling optical fields which are suitable for quantum-state reconstruction, and a number of sophisticated detection schemes have been studied. In the four-port basic scheme, a signal field is combined, through a lossless beam splitter, with a highly stable reference field which has the same mid-frequency as the signal field. The reference field, also called local oscillator, is usually prepared in a coherent state of large photon number. The superimposed fields impinge on photodetectors, the numbers of the emitted (and electronically processed) photoelectrons being the homodyne detection output (for the basic ideas, see Yuen and Shapiro, J.H. [1978a,b, 1980]; Shapiro, J.H., and Yuen [1979]; Shapiro, J.H., Yuen and Machado Mata [1979]). The observed interference fringes, which vary with the difference phase between the two fields, reflect the quantum statistics of the signal field and can be used – under certain circumstances – to obtain the quantum state of the signal field. The homodyne output can be fully given in terms of the joint-event probability distribution of the detectors in the output channels. In balanced homodyning, difference-event distributions are measured. In particular, the difference-event statistics measurable by a perfect four-port homodyne detector directly yields the quadrature-component statistics of the signal field, which has offered novel possibilities of quantum-state measurement.

2.1.1. Basic scheme

Let us start the analysis with the four-port scheme and first restrict attention to single-mode fields mode-matched to the local-oscillator (Fig. 1).³ The action of a lossless beam splitter (as an example of a linear four-port coupler) on quantum fields has widely been studied (see, e.g., Richter, G., Brunner and Paul, H., [1964]; Brunner, Paul, H., and Richter, G., [1965]; Paul, H., Brunner and Richter, G., [1966]; Yurke, McCall and Klauder [1986]; Prasad, Scully and Martienssen [1987]; Ou, Hong and Mandel [1987a]; Fearn and Loudon [1987]; Campos, Saleh and Teich [1989]; Leonhardt [1993]; Vogel, W., and Welsch [1994]; Luis and Sánchez-Soto [1995]), and it is well known that the input–output relations can be characterized by the SU(2) Lie algebra.

In the Heisenberg picture, the photon destruction operators of the outgoing modes, \hat{a}'_k ($k = 1, 2$), can be obtained from those of the incoming modes, \hat{a}_k , by a unitary

³Here and in the following spatial-temporal modes are considered. They are nonmonochromatic in general and defined with a particular spatial, temporal and spectral form (Appendix A.).

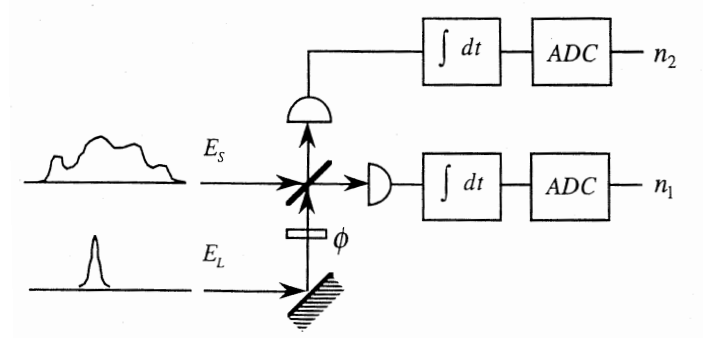


Figure 1: A signal pulse field E_S interferes with a shorter local-oscillator pulse E_L at a 50/50 beam splitter. The local-oscillator phase ϕ determines which quadrature amplitude of the signal is detected. The superposed fields are detected with high-efficiency photodiodes having response times much longer than the pulse durations. The photocurrents are integrated and sampled by analog-to-digital converters, to yield pulse photoelectron numbers n_1 and n_2 . (After Raymer, Cooper, Carmichael, Beck and Smithey [1995].)

transformation

$$\hat{a}'_k = \sum_{k'=1}^2 U_{kk'} \hat{a}_{k'}, \quad (1)$$

where U_{11} and U_{21} are the transmittance and reflectance of the beam splitter from one side, and U_{22} and U_{12} are those from the other side. The unitarity of the scattering matrix $U_{kk'} = |U_{kk'}| e^{i\varphi_{kk'}}$ implies that the following restrictions are placed on it:

$$|U_{11}|^2 + |U_{21}|^2 = 1, \quad |U_{22}| = |U_{11}|, \quad |U_{12}| = |U_{21}|, \quad (2)$$

$$\varphi_{11} - \varphi_{21} + \varphi_{22} - \varphi_{12} = \pm\pi. \quad (3)$$

The relations (2) and (3) ensure that the bosonic commutation relations for the photon creation and destruction operators are preserved. Using the angular momentum representation, the unitary transformation (1) can be given by

$$\hat{a}'_k = \hat{V} \hat{a}_k \hat{V}^\dagger, \quad (4)$$

where the operator \hat{V} reads as⁴

$$\hat{V} = e^{-i\alpha\hat{L}_3} e^{-i\beta\hat{L}_2} e^{-i\gamma\hat{L}_3} e^{-i\delta\hat{N}}. \quad (5)$$

Here, $\hat{N} = \hat{n}_1 + \hat{n}_2$ is the operator of the total photon number ($\hat{n}_k = \hat{a}_k^\dagger \hat{a}_k$), and the operators

$$\hat{L}_1 = \frac{1}{2} (\hat{a}_1^\dagger \hat{a}_2 + \hat{a}_2^\dagger \hat{a}_1), \quad \hat{L}_2 = \frac{1}{2i} (\hat{a}_1^\dagger \hat{a}_2 - \hat{a}_2^\dagger \hat{a}_1), \quad \hat{L}_3 = \frac{1}{2} (\hat{a}_1^\dagger \hat{a}_1 - \hat{a}_2^\dagger \hat{a}_2) \quad (6)$$

obey the familiar commutation relations of angular-momentum operators.

⁴The parameters in eq. (5) are related to the parameters in eqs. (2) and (3) as $\alpha = \frac{1}{2}(\varphi_{11} - \varphi_{22} + \varphi_{21} - \varphi_{12} \pm \pi)$, $\gamma = \frac{1}{2}(\varphi_{11} - \varphi_{22} - \varphi_{21} + \varphi_{12} \mp \pi)$, $\cos^2(\beta/2) = |U_{11}|^2$, $\sin^2(\beta/2) = |U_{21}|^2$, $\delta = \frac{1}{2}(\varphi_{11} + \varphi_{22})$.

In the Schrödinger picture the photonic operators are left unchanged, but the state is transformed. Let $\hat{\rho}$ and $\hat{\rho}'$ be the input- and output-state density operator of the two modes, respectively. It is easily seen that if they are related to each other as

$$\hat{\rho}' = \hat{V}^\dagger \hat{\rho} \hat{V}, \quad (7)$$

then the two pictures lead to identical expectation values of arbitrary field quantities.

Let us now assume that the operation of the photodetectors in the two output channels of the beam splitter can be described by means of the standard photodetection theory as outlined in Appendix C.; i.e., the numbers of photoelectric events counted in a given time interval (integrated photocurrents) are proportional to the numbers of photons falling on the detectors. From eq. (C.8) the joint-event distribution of measuring m_1 and m_2 events in the two output channels 1 and 2, respectively, is then given (in the Heisenberg picture) by

$$P_{m_1, m_2} = \left\langle : \prod_{k=1}^2 \frac{1}{m_k!} (\eta_k \hat{n}'_k)^{m_k} e^{-\eta_k \hat{n}'_k} : \right\rangle, \quad (8)$$

where

$$\hat{n}'_k = \hat{a}'_k{}^\dagger \hat{a}'_k, \quad (9)$$

with \hat{a}'_k being given by eq. (1) [or eq. (4)]. Note that for $\eta=1$ (i.e., perfect detection) P_{m_1, m_2} is nothing more than the joint-photon-number distribution of the two outgoing modes. In particular when the reference mode is prepared in a coherent state $|\alpha_L\rangle$, then in the expectation values of normally ordered operator functions, \hat{a}'_k can be replaced with ($\hat{a} \equiv \hat{a}_1$)

$$\hat{a}'_k = U_{k1} \hat{a} + U_{k2} \alpha_L. \quad (10)$$

2.1.2. Quadrature-component statistics

Let us now turn to the question of what information on the quantum statistics of the signal mode can be obtained from the homodyne output. From eq. (9) together with eqs. (10) and (3) we easily find that the output photon number \hat{n}'_k can be rewritten as

$$\hat{n}'_k = |U_{k2}|^2 |\alpha_L|^2 + |U_{k1}|^2 \hat{a}^\dagger \hat{a} + (-1)^{k+1} |U_{k2}| |U_{k1}| \hat{F}(\varphi), \quad (11)$$

where

$$\hat{F}(\varphi) = 2^{1/2} |\alpha_L| \hat{x}(\varphi), \quad (12)$$

with

$$\hat{x}(\varphi) = 2^{-1/2} (\hat{a} e^{-i\varphi} + \hat{a}^\dagger e^{i\varphi}) \quad (13)$$

being the quadrature-component operator, and

$$\varphi = \varphi_L + \varphi_{12} - \varphi_{11}. \quad (14)$$

We see that \hat{n}'_k consists of three terms. The first and the second terms represent the photon numbers of the local oscillator and the signal, respectively. More interestingly, the third term that arises from the interference of the two modes is proportional to a quadrature component of the signal mode, $\hat{x}(\varphi)$, the rapidly varying optical phase ωt that usually occurs in a field strength (quadrature component) is replaced with

the phase parameter φ . In particular, when the signal and the local oscillator come from the same source, then the phase parameter φ can be controlled easily, so that the dependence on φ of $\hat{x}(\varphi)$ can be monitored; e.g., by shifting the phase difference between the signal and the local oscillator in the input ports of the beam splitter in Fig. 1.

If a balanced (i.e., 50%:50%) beam splitter is used, the relation $|U_{k2}| = |U_{k1}| = 1/\sqrt{2}$ is valid, and hence the difference photon number is a signal-mode field strength $\hat{F}(\varphi)$,

$$\hat{n}'_1 - \hat{n}'_2 = \hat{F}(\varphi); \quad (15)$$

i.e., it is proportional to a signal-mode quadrature component. This result suggests that it is advantageous to use a balanced scheme and to measure the difference events or the corresponding difference of the photocurrents of the detectors in the two output channels in order to eliminate the intensities of the two input fields from the measured output. The method is also called *balanced* homodyning and can be used advantageously in order to suppress perturbing effects due to classical excess noise of the local oscillator (Mandel [1982]; Yuen and Chan [1983]; Abbas, Chan and Yee [1983]; Schumaker [1984]; Shapiro, J.H., [1985]; Yurke [1985]; Loudon [1986]; Collett, Loudon and Gardiner [1987]; Yurke and Stoler [1987]; Yurke, Grangier, Slusher and Potasek [1987]; Drummond [1989]; Blow, Loudon, Phoenix and Shepherd [1990]; Huttner, Baumberg, Ryan and Barnett [1992]). In particular, when the local oscillator is much stronger than the signal field, then even small intensity fluctuations of the local oscillator may significantly disturb the signal-mode quadrature components that are desired to be observed. For example, if the quadrature-component variance is intended to be derived from the variance of events measured by a single detector, the classical noise of the local oscillator and the quantum noise of the signal would contribute to the measured data in the same manner, so that the two effects are hardly distinguishable. Since in the two output channels identical classical-noise effects are observed, in the balanced scheme they eventually cancel in the measured signal due to the subtraction procedure.

Strictly speaking, from the arguments given above it is only established that for chosen phase parameters the mean value of the measured difference events or photocurrents is proportional to the expectation value of a quadrature component of the signal mode. From a more careful (quantum-mechanical) analysis it can be shown that in perfect balanced homodyning the quadrature-component statistics of the signal mode are indeed measured, provided that the local oscillator is sufficiently strong; i.e., $|\alpha_L|^2$ is large compared with the mean number of signal photons (Carmichael [1987]; Braunstein [1990]; Vogel, W., and Grabow [1993]; Vogel, W., and Welsch [1994]; Raymer, Cooper, Carmichael, Beck and Smithey [1995]; Munroe, Boggavarapu, Anderson, Leonhardt and Raymer [1996]). The probability distribution of the difference events,

$$\Delta m = m_1 - m_2, \quad (16)$$

can be derived from the joint-event distribution (8) as

$$P_{\Delta m} = \sum_{m_2} P_{\Delta m + m_2, m_2}. \quad (17)$$

Examples of the dependence of the difference-event distribution $P_{\Delta m}$ on the local-oscillator strength and the detection efficiency are shown in Fig. 2. In the limit of

the local oscillator being sufficiently strong, so that $|\alpha_L|^2$ is large compared with the average number of photons in the signal mode, the difference-event distribution $P_{\Delta m}$ can be given by (assuming that the two detectors have the same quantum efficiency η)

$$P_{\Delta m} = \frac{1}{\eta\sqrt{2}|\alpha_L|} p\left(x = \frac{\Delta m}{\eta\sqrt{2}|\alpha_L|}, \varphi; \eta\right), \quad (18)$$

with the phase φ being determined by the phase parameters of the apparatus and of the local oscillator according to eq. (14). In eq. (18), $p(x, \varphi; \eta)$ is a convolution of the quadrature-component distribution of the signal mode, $p(x, \varphi) = \langle x, \varphi | \hat{\rho} | x, \varphi \rangle$ [cf. Appendix B.], with a Gaussian:⁵

$$p(x, \varphi; \eta) = \int dx' p(x', \varphi) p(x - x'; \eta), \quad (19)$$

$$p(x; \eta) = \sqrt{\frac{\eta}{\pi(1-\eta)}} \exp\left(-\frac{\eta x^2}{1-\eta}\right). \quad (20)$$

In particular, for perfect detection, $\eta = 1$, the measured difference-event distribution

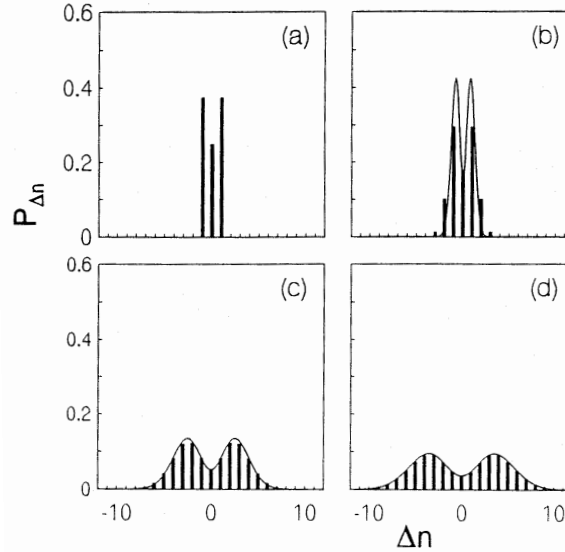


Figure 2: Difference statistics $P_{\Delta n}$ for a single-photon state, quantum efficiency $\eta = 0.75$, and various photon numbers of the local oscillator: $|\alpha_L|^2 = 0$ (a), 0.5 (b), 5 (c), 10 (d). The solid curves represent the smeared quadrature-component distribution $p(x, \varphi; \eta)$, eq. (19), which is a convolution of $p(x, \varphi)$ with $p(x; \eta)$. (After Vogel, W., and Grabow [1993].)

$P_{\Delta m}$ is identical with the difference-photon-number distribution. In this case $p(x; \eta)$ reduces to a δ function; i.e., $p(x, \varphi; \eta = 1) = p(x, \varphi)$, and hence $P_{\Delta m}$ is (apart from a scaling factor) exactly a quadrature-component distribution $p(x, \varphi)$ of the signal mode. Note that when the local oscillator is sufficiently strong, then $\Delta m / (\sqrt{2}|\alpha_L|)$ in eq. (18) is effectively continuous. In other words, single-photon resolution is not

⁵This result is obtained directly (in the limit of a strong local oscillator) from the basic equations (8), (17) of photocounting theory (Vogel, W., and Grabow [1993]), which include the effects of imperfect detection.

needed in order to measure the (continuous) quadrature-component statistics with high accuracy. In this case, highly efficient linear response photodiodes can be used, which do not discriminate between single photons, but nearly reach 100% quantum efficiency (Polzik, Carri and Kimble [1992]).

The Gaussian $p(x; \eta)$ [with dispersion $\sigma^2 = (1 - \eta)/(2\eta)$] obviously reflects the noise associated with nonperfect detection ($\eta < 1$). In particular, for 50% quantum efficiency (i.e., $\eta = 1/2$) the function $p(x; \eta)$ is the (phase-independent) quadrature-component distribution of the vacuum ($\sigma^2 = 1/2$). Obviously, the measured quadrature-component distribution $p(x, \varphi; \eta)$ does not correspond to the quadrature component $\hat{x}(\varphi)$ of the signal mode, but it corresponds to the quadrature component $\hat{x}(\varphi; \eta)$ of a superposition of the quadrature component of the signal, $\hat{x}(\varphi)$, and that of an additional (Gaussian) noise source, $\hat{x}_N(\varphi)$,

$$\hat{x}(\varphi; \eta) = \sqrt{\eta} \hat{x}(\varphi) + \sqrt{1 - \eta} \hat{x}_N(\varphi), \quad (21)$$

so that $\hat{x}(\varphi; \eta)$ is effectively a combined two-mode quadrature component. In particular, eq. (21) reveals that the effect of nonperfect detection can be modelled, assuming a (virtual) beam splitter is placed in front of a perfect detector, since eq. (21) exactly corresponds to a beam-splitter transformation (§ 2.1.1.) (Yurke and Stoler [1987]; Leonhardt and Paul, H., [1993b, 1994a,b]). In this case the fields are only partly detected, together with some fraction of vacuum noise introduced through the “unused” input ports of the beam splitters.⁶

If the signal field is not perfectly mode-matched to the local-oscillator mode, the non-mode-matched part can give rise to additional noise in the measured quadrature-component distributions of the mode-matched signal (Raymer, Cooper, Carmichael, Beck and Smithey [1995]). It can be shown that when the local oscillator is strong enough to dominate the mode-matched signal field but not necessarily the non-matched signal, then the detection efficiency reduces to

$$\tilde{\eta} = \eta \left(1 + \frac{\bar{N}_B}{|\alpha_L|^2} \right)^{-1}, \quad (22)$$

where \bar{N}_B is the mean number of photons in the nonmatched signal; i.e., η is replaced with $\tilde{\eta}$ in eq. (18). As expected, $\tilde{\eta}$ approaches η only in the limit $|\alpha_L|^2 \gg \bar{N}_B$.

In terms of the characteristic functions of the distributions involved, the content of eqs. (18) – (20) can be given by

$$\Omega_\Delta(y) = \Psi(\sqrt{2}y, \varphi; \eta) = \exp \left[-\frac{(s-1)\eta + 1}{2\eta} y^2 \right] \Phi(iye^{i\varphi}; s). \quad (23)$$

Here,

$$\Omega_\Delta(y) = \sum_{\Delta m} P_{\Delta m} \exp \left(i \frac{\Delta m}{\eta |\alpha_L|} y \right) \quad (24)$$

is the characteristic function of the measured probability distribution of the scaled difference events $\Delta m/(\eta |\alpha_L|)$, and $\Psi(z, \varphi; \eta)$ and $\Phi(\beta; s)$, respectively, are the characteristic functions, i.e., the Fourier transforms, of the (owing to nonperfect detection)

⁶For a discussion of eqs. (19) and (20) in terms of moments of the quadrature components $\hat{x}(\varphi; \eta)$ and $\hat{x}(\varphi)$, see Banaszek and Wódkiewicz [1997a].

smearred quadrature-component distribution $p(x, \varphi; \eta)$ and the s -parametrized phase-space function $P(\alpha; s)$ [see eqs. (B.26)⁷ and (B.23)]. Equation (23) reveals that in the case of perfect detection the characteristic function of the (scaled) difference-event distribution is equal, along a line in the complex plane, to the characteristic function of the Wigner function, which can be regarded as a suitable representation of the quantum state of the signal mode. Hence, when the difference-event statistics are measured on a sufficiently dense grid of phases φ within a π interval, then all knowable information on the signal-mode quantum state can be obtained. The result is obviously a consequence of the fact that knowledge of the quadrature-component distribution for all phases within a π interval is equivalent to knowledge of the quantum state; see Appendix B.5. (Vogel, K., and Risken [1989]).

2.1.3. Multimode detection

Relations of the type given in eq. (23) are also valid for (higher than four-port) multiport homodyning (Walker [1987]; Kühn, Vogel, W., and Welsch [1995]; Ou and Kimble [1995]). Let us consider a linear, lossless $2(N+1)$ -port coupler (Fig. 3) and assume, e.g., that N spatially separated signal modes (channels $1, \dots, N$) and a strong local-oscillator mode (channel $N+1$) of the same frequency are mixed to obtain $(N+1)$ output modes impinging on photodetectors.⁸ The input and output photon operators \hat{a}_k and \hat{a}'_k , respectively, are then related to each other by a $SU(N+1)$ transformation, extending eq. (1) to

$$\hat{a}'_k = \sum_{k'=1}^{N+1} U_{kk'} \hat{a}_{k'} \quad (25)$$

($k = 1, \dots, N+1$). Note that any discrete finite-dimensional unitary matrix can be constructed in the laboratory using devices, such as beam splitters, phase shifters and mirrors (Reck, Zeilinger, Bernstein and Bertani [1994]; for further readings, see Jex, Stenholm and Zeilinger [1995]; Mattle, Michler, Weinfurter, Zeilinger and Zukowski [1995]; Stenholm [1995]; Törmä, Stenholm and Jex [1995]; Törmä, Jex and Stenholm [1996]). Simultaneous detection of the output modes yields an $(N+1)$ -fold joint event distribution $P_{m_1, \dots, m_{N+1}}$. With regard to difference-event measurements, let us consider the scaled difference events

$$\Delta \tilde{m}_l = \frac{m_l}{\eta_l |\alpha_L|} - \frac{|U_{lN+1}|^2}{|U_{\bar{k}N+1}|^2} \frac{m_{\bar{k}}}{\eta_{\bar{k}} |\alpha_L|}. \quad (26)$$

Here, $l = 1, \dots, \bar{k}-1, \bar{k}+1, \dots, N+1$, the reference channel being denoted by \bar{k} . It can be shown that when the photon number $|\alpha_L|^2$ of the coherent-state local oscillator is much greater than unity and dominates all the signal modes at the detectors,⁹ then

⁷The characteristic function $\Psi(z, \varphi; \eta)$ of $p(x, \varphi; \eta)$ is defined according to eq. (B.26) with $p(x, \varphi; \eta)$ in place of $p(x, \varphi)$. It is seen to be related to the characteristic function $\Psi(z, \varphi)$ of $p(x, \varphi)$ as $\Psi(z, \varphi; \eta) = \exp[-\frac{1}{4}(\eta^{-1} - 1)z^2] \Psi(z, \varphi)$.

⁸All the modes are assumed to be matched to each other.

⁹Apart from this condition, the analysis also allows the local oscillator to be in other than coherent states (Walker [1987]; Leonhardt [1995]; Kim, M.S., and Sanders [1996]; for measuring the degree of *squeezing* in a signal field by using squeezed local oscillators, see Kim, C., and Kumar [1994]). This can be done by writing the local-oscillator state $\hat{\rho}_L$ in the form $\hat{\rho}_L = \hat{D}(\alpha_L) \hat{\rho}'_L \hat{D}^\dagger(\alpha_L)$, where $\hat{D}(\alpha_L)$ is the coherent displacement operator and $\hat{\rho}'_L$ is a state that remains finite as the complex amplitude $|\alpha_L|$ becomes large.

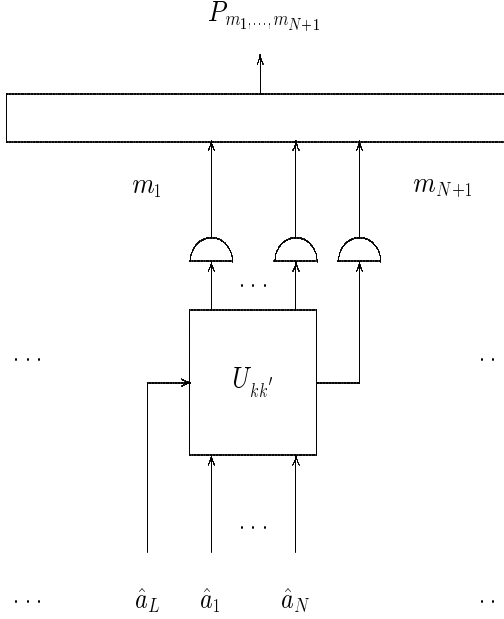


Figure 3: Scheme of homodyne $2(N + 1)$ -port detection. N signal modes \hat{a}_k ($k = 1, \dots, N$) of frequency ω and a strong local oscillator \hat{a}_L of the same frequency are combined by a lossless $2(N + 1)$ -port device to give $N + 1$ output modes ($U_{kk'}$: unitary transformation matrix of the device). Simultaneous detection of the $N + 1$ output modes yields the $(N + 1)$ -fold joint count distribution P_{m_1, \dots, m_N} . (After Vogel and Welsch [1995].)

the characteristic function of the joint probability distribution of the scaled difference events, $\Omega_\Delta(\{y_l\})$, can be related to the characteristic function of the s -parametrized multimode phase-space function of the signal field, $\Phi(\{\beta_n\}; s)$, $n = 1, \dots, N$, as¹⁰

$$\Omega_\Delta(\{y_l\}) = \exp\left[-\frac{(s-1)\eta+1}{2\eta} \sum_{n=1}^N |\beta_n|^2\right] \Phi(\{\beta_n\}; s), \quad (27)$$

where equal detection efficiencies have been assumed ($\eta_k = \eta_{k'} \equiv \eta$), and

$$\beta_n = ie^{i\varphi_L} \sum_{k=1}^{N+1} U_{kN+1} U_{kn}^* y_k, \quad \text{with} \quad \sum_{k=1}^{N+1} |U_{kN+1}|^2 y_k = 0 \quad (28)$$

(Kühn, Vogel, W., and Welsch [1995]). Note that when $N = 1$ (four-port apparatus) and $|U_{k2}| = |U_{k1}| = 1/\sqrt{2}$, then eq. (27) [together with eq. (28)] reduces to eq. (23). It should be pointed out that joint measurements on combinations of multiports of the above described type can also be used in order to detect (groups of) correlated modes of different frequencies. In particular, the combination of two balanced four-port schemes can be used to measure the joint quadrature-component distribution $p(x_1, x_2, \varphi_1, \varphi_2)$ of a (correlated) two-mode signal field for all values of the two phases φ_1 and φ_2 within π intervals in order to determine the two-mode quantum state (Raymer, Smithey, Beck, Anderson and McAlister [1993]).

¹⁰Note that $\Phi(\{\beta_j\}; s) = \exp[\sum_n \frac{1}{2} s |\beta_n|^2] \langle \hat{D}(\{\beta_n\}) \rangle$, where $\hat{D}(\{\beta_n\})$ is the N -mode coherent displacement operator, and the Fourier transform of $\Phi(\{\beta_n\}; s)$ is the s -parametrized N -mode phase-space function.

From eqs. (27) and (28) it can be seen that for perfect detection the characteristic function of the N -fold joint scaled difference-event distribution is nothing other than the characteristic function of the Wigner function of the N -mode input radiation field at certain values of the N complex arguments β_n , and it corresponds to the characteristic function of a joint quadrature-component distribution. To obtain all knowable information on the N -mode quantum state, i.e., the joint quadrature-component distributions for all relevant phases or the complete Wigner function, the arguments β_n must be allowed to attain arbitrary complex values. This may be achieved by means of an appropriate succession of (ensemble) measurements or one (ensemble) measurement, including in the apparatus appropriately chosen reference modes whose quantum states are known (or a combination of the two methods) (Vogel, W., and Welsch [1995]). In the first case, phase shifters in the apparatus may be used to appropriately vary (similar to the four-port scheme) the scattering matrix $U_{kk'}$ from measurement to measurement. In the second case, the scattering matrix is left unchanged, but additional reference inputs are used, so that a joint quadrature-component distribution of signal and reference modes is effectively measured (see § 2.1.4.).

Instead of measuring the N -fold joint difference-event statistics in a $2(N+1)$ -port scheme, the information on the N -mode signal field can also be obtained from the difference-event statistics measured in a standard four-port scheme with controlled signal-mode superposition (Opatrný, Welsch and Vogel, W., [1996, 1997a,b]; Raymer, McAlister and Leonhardt [1996]; McAlister and Raymer [1997a,b]). In the scheme, which applies to both spatially separable and nonseparable modes, the signal input is formed as a superposition of all the signal modes. Controlling the expansion coefficients in the superposition, from the measured difference-event distributions the same information on the quantum statistics of the N -mode signal-field can be obtained as from the N -fold joint difference-event distribution measured in a $2(N+1)$ -port scheme.

If the signal modes are separated spatially, they can be superimposed using an optical multiport interferometer such that each of the signal modes is fed into a separate input channel of the interferometer and the superimposed mode in one of the output channels is used as the (signal) input of a four-port homodyne detector. If the signal field is a pulse-like mode, the signal pulse can be combined, through the beam splitter in the four-port scheme, with a sequence of short local-oscillator pulses in order to analyse the signal pulse in terms of the modes associated with the local-oscillator pulses. In this case the superposition of the component modes to be measured is achieved by a proper formation of the local oscillator pulses.

To illustrate the method, let us consider the simplest case when a (correlated) two-mode field is perfectly detected (Fig. 4). Then the measured quantity is a weighted sum of the quadrature components $\hat{x}_1(\varphi_1)$ and $\hat{x}_2(\varphi_2)$ of the two modes,

$$\hat{x} = \hat{x}_1(\varphi_1) \cos \alpha + \hat{x}_2(\varphi_2) \sin \alpha, \quad (29)$$

where the phases φ_1 and φ_2 and the relative weight [superposition parameter α , $\alpha \in (0, \pi/2)$] are assumed to be controlled in the measurement. For spatially separated modes [Fig. 4(a)] the phases can be controlled by phase shifters placed in front of a beam splitter used for mixing the modes, and the parameter α can be

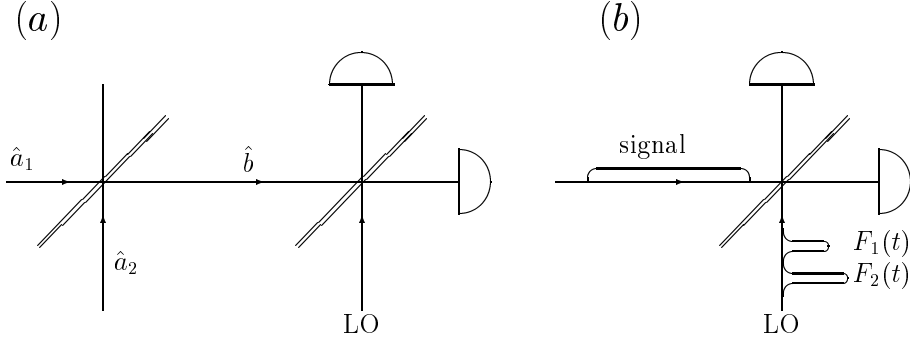


Figure 4: Two possible schemes for reconstructing two-mode density matrices via measurement of combined quadrature components. (a) Two modes (\hat{a}_1 and \hat{a}_2) are mixed by a beam splitter and one of the interfering output modes (\hat{b}) is used as signal mode in balanced homodyning in order to measure the sum quadratures of the two modes (LO is the strong local oscillator). (b) A signal pulse and a sequence of two short (strong) local-oscillator pulses with envelopes $F_1(t)$ and $F_2(t)$ are superimposed in balanced homodyne detection. (After Opatrný, Welsch and Vogel, W., [1997b].)

controlled by the transmittance (reflectance) of the beam splitter. If the quadrature statistics of a signal pulse are measured in a set of short local-oscillator pulses [Fig. 4(b)], then the parameter α can be controlled by changing the mutual intensities of the two pulses. Again, the phases can be controlled interferometrically.¹¹ Let $p_J(x_1, x_2, \varphi_1, \varphi_2)$ and $p_S(x, \alpha, \varphi_1, \varphi_2)$ be respectively, the joint quadrature-component distribution and the (measured) sum quadrature-component distribution of the two modes, and $\Psi_J(z_1, z_2, \varphi_1, \varphi_2)$ and $\Psi_S(z, \alpha, \varphi_1, \varphi_2)$ the corresponding characteristic functions. It can be shown that

$$\Psi_J(z \cos \alpha, z \sin \alpha, \varphi_1, \varphi_2) = \Psi_S(z, \alpha, \varphi_1, \varphi_2). \quad (30)$$

In other words, the joint-quadrature component distribution for all phase values (within π intervals) can be obtained from the sum quadrature component distribution for all phase values and all values of the weighting factor, which shows the possibility to obtain the two-mode quantum state from the measured statistics of the summed quadratures. The effect of nonperfect detection can be taken into account according to eq. (23).

2.1.4. Q function

As mentioned in § 2.1.3., the $2N$ -fold manifold of data necessary for a reconstruction of the quantum state of an N -mode signal field can be obtained by including additional reference modes in the detection scheme in Fig. 3 whose quantum states are known, such as the vacuum inputs in “unused” input channels. Let us suppose that the $2(N+1)$ -port apparatus is extended to a $2(2N+1)$ -port device, N input channels

¹¹If signal and local oscillator come from different sources, only the phase difference $\delta\varphi = \varphi_1 - \varphi_2$ can be controlled.

being “unused”. Since the vacuum inputs are not correlated to each other and to the signal input, the characteristic function of the quantum state of the $(2N)$ -mode input field can be factorized,

$$\Phi(\{\beta_n\}; s) = \Phi(\{\beta_i\}; s) \Phi(\{\beta_j\}; s), \quad \text{with} \quad \Phi(\{\beta_j\}; s) = \prod_{j=N+1}^{2N} e^{(s-1)|\beta_j|^2/2} \quad (31)$$

($i = 1, \dots, N$, signal channels; $j = N + 1, \dots, 2N$, vacuum channels). Equation (28) (with $2N$ in place of N) can then be inverted easily in order to obtain $2N$ real arguments y_l of the characteristic function $\Omega_\Delta(\{y_l\})$ of the measured distribution for any (freely chosen) N complex arguments β_i of the characteristic function $\Phi(\{\beta_i\}; s)$ of the N -mode signal-quantum state. In other words, in the extended detection scheme there is a one-to-one correspondence between the measured $(2N)$ -fold joint difference-event distribution and the quantum state of the N -mode signal field (Vogel, W., and Welsch [1995]).

Obviously, one local oscillator per group of (equal-frequency) signal modes and one additional reference input per signal mode are sufficient for measuring a joint difference-event distribution that can be regarded as a measure of the signal-mode quantum state. Needless to say, both the number of local oscillators and/or the number of additional reference inputs may be increased, and the quantum state of the signal may of course be expressed in terms of an appropriately chosen joint difference-event distribution recorded in such an extended measurement scheme. In the case of a single-mode signal field a six-port scheme is the minimum in order to determine the quantum state of the signal (Zucchetti, Vogel, W., and Welsch [1996]; Paris, Chizhov and Steuernagel [1997]). The situation is quite similar to classical optics, in which the six-port scheme is the minimum in order to determine the complex amplitude (Walker [1987]). Let us consider a 3×3 coupler and assume that the reference mode is in the vacuum state (Fig. 5). In this case, it can be shown that application of eqs. (27), (28) and (31) yields

$$\Phi(\beta; s) = \exp\left(\frac{1}{2}s|\beta|^2\right) \Phi(\beta) = \exp\left\{\frac{1}{2}|\beta|^2 \left[s + (2-\eta)\eta^{-1}\right]\right\} \Omega_\Delta(y_1, y_2), \quad (32)$$

where β is related to y_1 and y_2 as

$$\beta = \frac{1}{3}i[(\phi^* - 1)y_1 + (\phi - 1)y_2] e^{i\varphi_L}, \quad (33)$$

with $\phi = \exp(-i2\pi/3)$ [$\Phi(\beta) \equiv \Phi(\beta; 0)$]. Equation (33) reveals that $\Phi(\beta; s = 1 - 2\eta^{-1}) = \Omega_\Delta(y_1, y_2)$; i.e., measurement of the joint difference-event distribution $P_{\Delta m_1, \Delta m_2}$ in balanced six-port homodyning is equivalent to measurement of a phase-space function $P(\alpha; s)$ of the signal mode (in non-orthogonal coordinates in the phase space):

$$P_{\Delta m_1, \Delta m_2} = \frac{\sqrt{3}}{2\eta^2|\alpha_L|^2} P(\alpha; s), \quad (34)$$

with

$$\alpha = -\frac{\Delta m_1}{\eta\alpha_L^*} \sqrt{\phi} - \frac{\Delta m_2}{\eta\alpha_L^*} \sqrt{\phi^*} \quad (35)$$

and $s = 1 - 2\eta^{-1}$ [$\sqrt{\phi} = \exp(-i\pi/3)$]. The function $P(\alpha; s = 1 - 2\eta^{-1})$ can be regarded as a smoothed Q function of the signal mode, which approaches the Q function as the

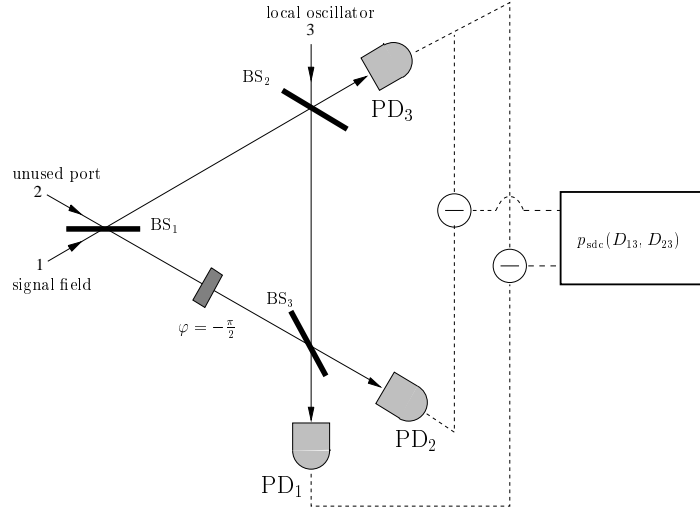


Figure 5: Scheme of balanced six-port homodyning for the detection of the Q function. Three input fields (signal, local oscillator, vacuum) are combined by three symmetric beam splitters BS_i ($i = 1, 2, 3$) and a $(-\pi/2)$ phase shifter, where two $(1/2 : 1/2)$ beam splitters (BS_1 and BS_3) and one $(2/3 : 1/3)$ beam splitter (BS_2) are used. The joint difference statistics is recorded by the detectors PD_i in the output channels [$p_{\text{sdc}}(D_{13}, D_{23})$ corresponds to $P_{\Delta m_1, \Delta m_2}$ in eq. (34)]. (After Zucchetti, Vogel, W., and Welsch [1996].)

quantum efficiency η goes to unity. In particular for perfect detection ($\eta = 1$) the Q function of the signal mode is measured (in non-orthogonal phase-space coordinates).

Identifying in eq. (B.25) s' with $1 - 2\eta^{-1}$, this equation can be regarded as a prescription for obtaining other phase-space functions $P(\alpha; s)$ from the measured one. When $s < 1 - 2\eta^{-1}$ is valid, then the β integration in eq. (B.25) can be performed separately to obtain $P(\alpha; s)$ as a convolution of $P(\alpha; s = 1 - 2\eta^{-1})$ with a Gaussian, which reveals that all the phase-space functions which are typically broader than the measured one can be obtained simply by convolving the measured distribution with a Gaussian. In the opposite case, when $s > 1 - 2\eta^{-1}$, then the integration over γ must be done first in eq. (B.25). However, experimental inaccuracies may be exploding via the inverse Gaussian and prevent a stable reconstruction of $P(\alpha; s)$ with reasonable precision. Since the maximum value of s for an always stable reconstruction, i.e., $s = 1 - 2\eta^{-1}$, tends to minus unity as η goes to unity, the upper boundary of s corresponds to the Q function.

As mentioned above, higher than six-port homodyne detectors can also be used in order to measure the signal-mode quantum state in the phase space. Among them, eight-port homodyne detection has widely been studied (Walker and Carroll [1984]; Walker [1987]; Lai and Haus [1989]; Noh, Fougères and Mandel [1991, 1992a,b]; Hradil [1992]; Freyberger and Schleich [1993]; Freyberger, Vogel, K., and Schleich [1993a,b]; Leonhardt and Paul, H., [1993a]; Luis and Peřina [1996a]). Let us consider two modes that are superimposed, in accordance with eq. (1), by a 50%:50% beam splitter, and assume that one of the incoming modes, say, the second is in the vacuum. It can then be shown that the joint probability distribution of the two outgoing quadrature

components $\hat{x}'_1(\varphi)$ and $\hat{x}'_2(\varphi + \pi/2)$ is the (scaled) Q function of the first incoming mode,¹²

$$p(x'_1, x'_2, \varphi, \varphi + \pi/2) \sim Q[\alpha_1 = 2^{-1/2}(x'_1 + ix'_2)] \quad (36)$$

(Lai and Haus [1989]; Leonhardt and Paul, H., [1993a]; for details, also see Leonhardt and Paul, H., [1995]; Leonhardt [1997c]). Hence, using the two outgoing modes of the beam splitter as incoming signal modes in two separate balanced four-port homodyne detectors and measuring (for a $\pi/2$ phase difference) the joint difference-event statistics of the two homodyne detectors, the Q function of the original signal mode is obtained, provided that perfect detection is accomplished.¹³ Altogether the setup forms an balanced eight-port homodyne detector, with a signal input, a vacuum input and two local-oscillator inputs. Alternatively, the beam splitter and the two four-port homodyne detectors can be combined into an eight-port apparatus with two vacuum inputs and one local-oscillator input (Fig. 6). A straightforward calculation

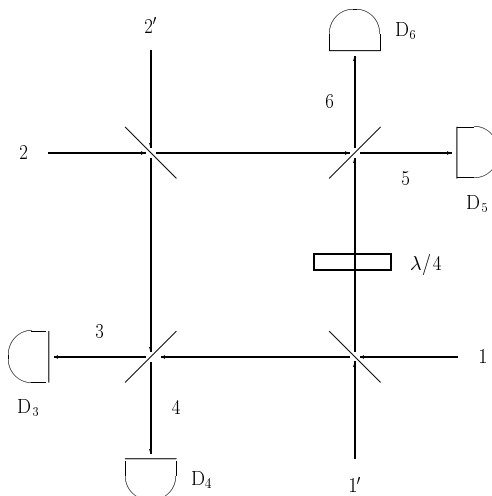


Figure 6: Balanced homodyne eight-port detection scheme for measuring the Q function, using 50%:50% beam splitters and a $\lambda/4$ phase shifter. The signal is fed into port 1 and the strong local oscillator is fed into port 2, and vacuum is fed into the ports 1' and 2'. The joint difference-event probability distribution $P_{\Delta m_1, \Delta m_2}$, eq. (37), is measured in the channels 3 and 4 (Δm_1) and 5 and 6 (Δm_2). (After Vogel, W., and Welsch [1994].)

¹²Equation (36) can be proved correct, applying the beam splitter transformation (1) and expressing the characteristic function of the two-mode (outgoing) quadrature-component distribution $p(x'_1, x'_2, \varphi, \varphi + \pi/2)$ in terms of the characteristic function of the single-mode (incoming) Q function $Q(\alpha_1)$.

¹³Note that $\hat{x}(\varphi)$ and $\hat{x}(\varphi + \pi/2)$ play the same role as position and momentum of a harmonic oscillator in quantum mechanics, because of $[\hat{x}(\varphi), \hat{x}(\varphi + \pi/2)] = i$. Therefore also the notations $\hat{q} \equiv \hat{x}(\varphi)$ and $\hat{p} \equiv \hat{x}(\varphi + \pi/2)$ are frequently used. Equation (36) is an example of “simultaneous” measurement of a pair of conjugate quantities. Actually, the quantities $\hat{q}'_1 \equiv \hat{x}'_1(\varphi)$ and $\hat{p}'_2 \equiv \hat{x}'_2(\varphi + \pi/2)$ are measured, which can be regarded as the conjugate quantities $\hat{q}_1 \equiv \hat{x}_1(\varphi)$ and $\hat{p}_1 \equiv \hat{x}_1(\varphi + \pi/2)$, respectively, “smoothed” by the introduction of additional (vacuum) noise necessary for a simultaneous (but approximate) measurement of \hat{q}_1 and \hat{p}_1 . Accordingly, an additional uncertainty is introduced in the measurement, and it can be shown that the uncertainty product for \hat{q}'_1 and \hat{p}'_2 is twice that of the measurements of \hat{q}_1 and \hat{p}_1 made individually, $\Delta q'_1 \Delta p'_2 \geq 1$ (Arthurs and Kelly [1965]; for a review, see Stenholm [1992]).

shows (similar to the six-port homodyne detector) that measurement of the joint difference-event distribution $P_{\Delta m_1, \Delta m_2}$ again yields the phase-space function $P(\alpha; s = 1 - 2\eta^{-1})$,

$$P_{\Delta m_1, \Delta m_2} = \frac{1}{\eta^2 |\alpha_L|^2} P\left(\alpha = -\frac{\Delta m_1 - i\Delta m_2}{\eta \alpha_L^*}; s = 1 - 2\eta^{-1}\right) \quad (37)$$

(Freyberger and Schleich [1993]; Freyberger, Vogel, K., and Schleich [1993a,b]; Leonhardt and Paul, H., [1993b]; Vogel, W., and Welsch [1994]; D’Ariano, Macchiavello and Paris [1995]; Kočański and Wódkiewicz [1997]). Compared with the six-port scheme, $P_{\Delta m_1, \Delta m_2}$ is the (scaled) function $P(\alpha; s = 1 - 2\eta^{-1})$ in an orthogonal basis [cf. eqs. (34) and (37)]. The balanced eight-port homodyne detector was first used by Walker and Carroll in order to demonstrate the feasibility of measuring the components of the complex amplitude of optical signals, extending earlier microwave techniques (Walker and Carroll [1984]).

Finally, it was proposed to measure the Q function by *projection synthesis*, mixing the signal mode with a reference mode that is prepared in a quantum state such that, for appropriately chosen parameters, the joint-photon-number probabilities in the two output channels of the beam splitter realize the coherent-state projector $\hat{\Pi}(\alpha) = \pi^{-1} |\alpha\rangle\langle\alpha|$ for truncated signal states (Baseia, Moussa and Bagnato [1997]). The method was first introduced to synthesize (for truncated states) the phase-state projector $\hat{\Pi}(\phi) = |\phi\rangle\langle\phi|$ (Barnett and Pegg [1996]; cf. § 3.8.3.).

2.1.5. Probability operator measures

As mentioned, the reference mode with which a signal mode is mixed has not necessarily to be in the vacuum state in order to obtain, in principle, all knowable information on the quantum state of the signal mode. If the reference mode is allowed to be prepared in a quantum state $\hat{\rho}_R$, then a joint measurement of the ($\pi/2$ -shifted) quadrature-components of the interfering fields can be regarded as a realization of a complex amplitude measurement (Walker [1987]). Each $\hat{\rho}_R$ implies a *probability operator measure* (POM) over the complex amplitude which can be characterized by a positive valued Hermitian operator

$$\hat{\Pi}(\alpha) = \pi^{-1} \hat{D}(\alpha) \hat{\rho}_R \hat{D}^\dagger(\alpha), \quad (38)$$

with

$$\int d^2\alpha \hat{\Pi}(\alpha) = \hat{I}. \quad (39)$$

The joint probability density $\text{prob}(\alpha)$ of obtaining a result $\alpha = \text{Re } \alpha + i\text{Im } \alpha$ from a measurement described by this POM is¹⁴

$$\text{prob}(\alpha) = \langle \hat{\Pi}(\alpha) \rangle. \quad (40)$$

¹⁴The concept of POM was introduced in quantum theory in order to generalize the familiar quantum probability theory based on orthogonal projectors (Davies, E.B., and Lewis [1970]; Holevo [1973]; Davies, E.B., [1976]; Helstrom [1976]). In particular, it can be used for describing “simultaneous” measurement of noncommuting observables of an object, the corresponding POM being related to a quantum measurement of commuting observables in some extended Hilbert space. Note that for nonperfect detection ($\eta < 1$) the photocounting formula (C.8) is also a POM.

Note that from the properties of $\hat{\Pi}(\alpha)$ it follows that $\text{prob}(\alpha) \geq 0$ and $\int d^2\alpha \text{prob}(\alpha) = 1$. The operational probability density distribution $\text{prob}(\alpha)$ in eq. (40), which is also called *propensity* (Popper [1982]), can be given by a convolution of the Wigner function $W(\alpha)$ of the signal prepared in a state $\hat{\rho}$ with the Wigner function $W_R(\alpha)$ of the reference mode prepared in a state $\hat{\rho}_R$,

$$\text{prob}(\alpha) = \int d^2\beta W_R(\beta - \alpha) W(\beta) \quad (41)$$

(Husimi [1940]; Arthurs and Kelly, Jr., [1965]; Kano [1965]; Wootters and Zurek [1979]; O'Connell and Rajagopal [1982]; Rajagopal, A.K., [1983]; Wódkiewicz [1984, 1986, 1988]; Takahashi and Saitô [1985]; Walker [1987]; Lai and Haus [1989]; Hradil [1992]; Lalović, Davidović and Bijedić [1992]; Stenholm [1992]; Davidović, Lalović and Bijedić [1993]; Leonhardt [1993]; Leonhardt and Paul, H., [1993b, 1995]; Chaturvedi, Agarwal and Srinivasan [1994]; Raymer [1994]; Bužek, Keitel and Knight [1995a,b]; Paris, Chizhov and Steuernagel [1997]; Wünsche and Bužek [1997]). Obviously, the reference mode acts as a filter and smoothes the Wigner function of the signal. A filter system of this type is also called *quantum ruler* (Aharonov, Albert and Au [1981]). It is needed in order to resolve the noncommutative quadrature components of the signal.

The particular realization of the filter strongly influences the outcome of the measurement. The class of phase-space functions that can be obtained includes the s -parametrized functions with $s \leq -1$. In particular, detection of the Q -function implies that $\hat{\rho}_R = |0\rangle\langle 0|$, so that $\hat{\Pi}(\alpha) = \pi^{-1}|\alpha\rangle\langle\alpha|$, and hence $\text{prob}(\alpha) = \pi^{-1}\langle\alpha|\hat{\rho}|\alpha\rangle = Q(\alpha)$. This is the case when vacuum is fed into the reference channels in the homodyne detection schemes in Figs. 5 and 6, and the signal is mixed with it. If the signal is mixed with a squeezed vacuum, then the POMs of the form given in eq. (38) with $\hat{\rho}_R = \hat{S}(\xi)|0\rangle\langle 0|\hat{S}^\dagger(\xi)$ can be realized (Walker [1987]; Lai and Haus [1989]; Leonhardt [1993]; Kim, M.S., and Sanders [1996]; Kočański and Wódkiewicz [1997]).¹⁵

Probability operator measures over the complex amplitude and the photon number can also be defined such that the joint probability density for an outcome $\alpha = \text{Re } \alpha + i\text{Im } \alpha$ and n is given by

$$\text{prob}(\alpha, n) = \langle \hat{\Pi}(\alpha, n) \rangle, \quad (42)$$

where $\hat{\Pi}(\alpha, n)$ must be a positive valued Hermitian operator that can be used to resolve the identity,

$$\sum_n \int d^2\alpha \hat{\Pi}(\alpha, n) = \hat{I}. \quad (43)$$

A probability operator measure of this form can be realized by ten-port homodyne detection (Luis and Peřina [1996b]).¹⁶ In the scheme, a signal mode is fed into one of the input channels of an unbalanced beam splitter whose second input channel is “unused”. The mode in one of the output channels of the beam splitter (say, the transmitted signal) is used as the input mode in an eight-port homodyne detector,

¹⁵It should be noted that these POMs can also be realized in heterodyne detection (§ 2.2.) (Yuen and Shapiro, J.H., [1980]; Yuen [1982]). Further, they can be realized in an unbalanced homodyne scheme with vacuum input but not equal-part signal-beam splitting (Leonhardt [1993, 1997c]).

¹⁶The ten-port scheme can be regarded as a reduced twelve-port scheme, the latter being suited for measuring simultaneously the Stokes parameters of a two-mode field.

and a photodetector is placed in the other output channel in order to measure the photon-number statistics of the mode in this channel,¹⁷ together with the eight-port complex-amplitude measurement. The realized POM is related closely to photon-added coherent states,

$$\hat{\Pi}(\alpha, n) = g_n(\alpha) \hat{a}^{\dagger n} |\alpha\rangle \langle \alpha| \hat{a}^n, \quad (44)$$

where $g_n(\alpha) = \pi^{-1} t^{-2} \exp[|\alpha|^2(1-t^{-2})] (1-t^2)^n/n!$, with t being the (absolute value of the) transmittance of the beam splitter ($0 < t < 1$). Note that when $t \rightarrow 1$ then $\hat{\Pi}(\alpha, n) \rightarrow \pi^{-1} |\alpha\rangle \langle \alpha| \delta_{n0}$; i.e., the familiar coherent-state POM is realized.

2.1.6. Positive P function

It is well known that for $s > -1$ the s -parametrized phase-space functions $P(\alpha; s)$ (see Appendix B.4.) do not necessarily exist as positive functions, and for $s > 0$ they are not necessarily well-behaved. The latter also applies to the P function, which is widely used to calculate averages of normally ordered (i.e., measurable) quantities. In order to avoid using singular functions, generalized P representations may be used (Drummond and Gardiner [1980]; see also Gardiner [1983, 1991]), such as the positive P function,¹⁸

$$P(\alpha, \alpha') = \frac{1}{4\pi^2} \exp\left(-\frac{1}{4}|\alpha - \alpha'^*|^2\right) \left\langle \frac{1}{2}(\alpha + \alpha'^*) \middle| \hat{\rho} \middle| \frac{1}{2}(\alpha + \alpha'^*) \right\rangle. \quad (45)$$

The possibility of measuring the single-mode Q function in perfect (six-port or eight-port) homodyne detection offers also the possibility of measuring the quantum state of the mode in terms of the positive P distribution using more involved multipoint homodyne detection schemes (Agarwal and Chaturvedi [1994]). Let us again consider a signal mode and a reference mode that are superimposed by a 50%:50% beam splitter and assume that the reference mode is in the vacuum. It can then be shown that the joint Q function of the two outgoing modes, $Q(\alpha_1, \alpha_2)$, is related to the Q function of the signal mode, $Q(\alpha)$, as¹⁹

$$Q(\alpha_1, \alpha_2) = \frac{1}{\pi^2} \exp\left(-\frac{1}{2}|\alpha_1 - \alpha_2|^2\right) Q\left(\alpha = \frac{\alpha_1 + \alpha_2}{\sqrt{2}}\right), \quad (46)$$

which reveals that $Q(\alpha_1, \alpha_2)$ is nothing but the (scaled) positive P function of the signal mode,

$$Q(\alpha_1, \alpha_2) = 4P\left(\alpha = \sqrt{2}\alpha_1, \beta = \sqrt{2}\alpha_2^*\right). \quad (47)$$

Hence, if each of the two output modes of the beam splitter is used as an input mode of a multipoint apparatus (such as the six- or eight-port homodyne detector outlined in § 2.1.4.) that measures the Q function, then measurement of the joint Q function of the two modes yields the positive P function of the signal-mode under study. Needless to say that for imperfect detection a smeared positive P function is measured.

¹⁷For a direct measurement of the photon-number statistics, see § 2.1.7..

¹⁸Note that $\hat{\rho} = \int d^2\alpha \int d^2\alpha' |\alpha\rangle \langle \alpha'^*| ((\alpha'^*|\alpha))^{-1} P(\alpha, \alpha')$ in this representation.

¹⁹Equation (46) can be proved correct, applying the beam splitter transformation (1) and expressing the characteristic function of the two-mode (outgoing) Q function $Q(\alpha_1, \alpha_2)$ in terms of the characteristic function of the signal-mode (incoming) Q function $Q(\alpha)$. Note that $Q(\alpha_1, \alpha_2)$ is the two-mode s -parametrized phase-space function $P(\alpha_1, \alpha_2; s = -1)$.

The positive P function is an example of a measurable phase-space function²⁰ that is defined as a function of two complex amplitudes α and β (per mode). The concept can also be extended – similar to § 2.1.5. – to other than vacuum reference inputs (in the beam splitter and/or the multiport homodyne detectors) in order to obtain generalized phase-space functions defined in a four-dimensional phase space. A simple example is the smeared positive P function mentioned.

2.1.7. Displaced-photon-number statistics

Let us return to the four-port homodyne detection scheme (Fig. 1) and answer the question of which quantity is measured when a signal mode is mixed with a local-oscillator mode by an unbalanced beam splitter and only a single-channel homodyne output is measured. We rewrite eq. (10) as

$$\hat{a}'_k = U_{k1}(\hat{a} - \alpha) = U_{k1}\hat{D}(\alpha)\hat{a}\hat{D}^\dagger(\alpha), \quad (48)$$

where

$$\alpha = -\frac{U_{k2}}{U_{k1}}\alpha_L, \quad (49)$$

and apply the photocounting formula (C.5). The probability of detecting m events in the k th output channel can then be given by

$$P_m = \left\langle : \frac{1}{m!} [\eta\hat{n}(\alpha)]^m e^{-\eta\hat{n}(\alpha)} : \right\rangle, \quad (50)$$

where $\hat{n}(\alpha) = \hat{D}(\alpha)\hat{n}\hat{D}^\dagger(\alpha)$ is the displaced photon-number operator of the signal mode, and $\eta = |U_{k1}|^2\eta_D$ (with η_D being the quantum efficiency of the detector used). Equation (50) reveals that the observed probability distribution P_m is nothing but the displaced photon-number distribution of the signal field measured with quantum efficiency η . In particular, when a signal and a strong local oscillator, $|\alpha_L| \rightarrow \infty$, are mixed by a beam splitter with high transmittance, $|U_{11}| = |U_{22}| \rightarrow 1$, and low reflectance, $|U_{21}| = |U_{12}| \rightarrow 0$, such that the product $|U_{12}||\alpha_L|$ is finite, then for high quantum efficiency ($\eta \rightarrow 1$) the displaced photon-number probability distribution of the signal is measured (Wallentowitz and Vogel, W., [1996a]; Banaszek and Wódkiewicz [1996]; Paris [1996a]),

$$P_m \rightarrow p_m(\alpha) = \langle m, \alpha | \hat{\rho} | m, \alpha \rangle, \quad (51)$$

where $|m, \alpha\rangle = \hat{D}(\alpha)|m\rangle$ are the displaced photon-number states. It should be noted that for chosen m the quantity $p_m(\alpha)$ as a function of α can be regarded (apart from the factor π^{-1}) as a propensity for the signal-mode complex amplitude, which can also be measured in multiport homodyning (see § 2.1.5.). For chosen α it is an ordinary probability for the displaced signal-mode photon number, which can already be obtained from the four-port detector outlined here. In order to obtain in this scheme $p_m(\alpha)$ as a function of α , a succession of (ensemble) measurements must be performed. Hence, measurement of the displaced-signal-mode photon-number statistics

²⁰For a method suggested to measure the positive P function of a quantum-mechanical particle, see Braunstein, Caves and Milburn [1991].

as a function of the complex parameter α is equivalent to measurement of the signal-mode quantum state, and it is expected that it yields more data than the minimum necessary for reconstructing it (§ 3.).

In contrast to balanced homodyning, measurement of the displaced photon-number statistics in unbalanced homodyning requires highly efficient photodetectors that can discriminate between n and $n + 1$ photons in order to resolve the discrete nature of the photon number. Presently, such detectors are not available. Photomultipliers and streak cameras can discriminate between single photons, provided that the field does not contain more than about 10 photons, but the quantum efficiency of about 10% – 20% is extremely low. Currently available avalanche photodiodes operating in the Geiger regime may reach about 80% quantum efficiency (Kwiat, Steinberg, Chiao, Eberhard and Petroff [1993]), but they do not discriminate between single photons. They can only indicate the presence of photons, because of saturation.

The problem may be overcome using multichannel coincidence-event measurement techniques also called *photon chopping*. In particular it was proposed to use highly efficient avalanche photodiodes and a beam splitter array to divide the number of readout photons among the photodiodes, so that none is likely to receive more than one photon (Ho, Lane, La Porta, Slusher and Yurke [1990]; Song, Caves and Yurke [1990]; Paul, H., Törmä, Kiss and Jex [1996a]).²¹ Alternatively, it was proposed to directly defocus the field to be measured onto an array of photodiodes (Wallentowitz and Vogel, W., [1996a]).

Let us assume that the mode to be detected enters one of the input ports of a balanced linear $2N$ -port apparatus (the other input ports being “unused”), and multiple coincidences are measured at the output, placing avalanche photodiodes in the N output channels. If the signal mode contains less than $N + 1$ photons, then there is a one-to-one correspondence between the measured coincidence-event distribution $\tilde{p}_n(N)$ and the photon-number distribution p_n of the signal. To be more specific, it can be shown that²²

$$\tilde{p}_m(N) = \sum_{n=m}^N \tilde{P}_{m|n}(N) p_n, \quad (52)$$

where

$$\tilde{P}_{m|n}(N) = \frac{1}{N^n} \binom{N}{m} \sum_{i=0}^m (-1)^i \binom{m}{i} (m - i)^n \quad \text{if } m \leq n \leq N, \quad (53)$$

and $\tilde{P}_{m|n}(N) = 0$ if $n < m$ (Paul, H., Törmä, Kiss and Jex [1996a]). Here, $\tilde{P}_{m|n}(N)$ is the probability of registration of m clicks under the condition that n photons are present. The probabilities $\tilde{P}_{m|n}(N)$ form an $N \times N$ upper triangular matrix $A_{mn} = \tilde{P}_{m|n}(N)$ which can be inverted in order to calculate p_n from $\tilde{p}_n(N)$,

$$p_n = \sum_{m=n}^N (A^{-1})_{nm} \tilde{p}_m. \quad (54)$$

²¹For detection of squeezing via coincidence-event measurement, see Janszky, Adam, P., and Yushin [1992]; for Fock state detection and preparation, see Paul, H., Törmä, Kiss and Jex [1996b].

²²Here it is assumed that the balanced $2N$ -port realizes a unitary transformation $\mathbf{U}_N = \mathbf{U}_2 \otimes \mathbf{U}_{N/2}$.

2.1.8. Homodyne correlation measurements

As already mentioned, the accuracy with which a (quantum) field can be measured by a homodyne detector is limited by the overall quantum efficiency of the device [see, e.g., Eqs (19) and (20)]. To overcome this limitation, one may perform homodyne correlation measurements (Ou, Hong and Mandel [1987b]). In contrast to ordinary balanced homodyning, the (time-delayed) intensity correlation between the two outgoing fields is measured. In particular, the information on squeezing is obtained from the time dependence of the measured correlation function. Since the measured coincidence events are proportional to the product of the detection efficiencies of the two detectors, small quantum efficiencies may reduce the measured signal (which could be compensated by longer measurement times) but do not smooth out the desired information. However, a drawback of the method is that the classical noise of the local oscillator is not balanced out, i.e., even small relative fluctuations of the (strong) local oscillator may prevent the quantum noise effects of a weak signal from being measured.

It was therefore proposed to use a weak local oscillator whose intensity is comparable to that of the signal (Vogel, W., [1991, 1995]). In this case, the classical noise of the (highly stabilized) local oscillator may be reduced below the level of the quantum fluctuations of the signal. Moreover, simultaneous measurement of different kinds of correlation functions of the signal field is possible. To illustrate this, let us consider the difference between the measured second-order intensity correlation function $G^{(2)}(t, t + \tau)$ for short and long delay times τ ,

$$\Delta G^{(2)}(t) = G^{(2)}(t, t) - \lim_{\tau \rightarrow \infty} G^{(2)}(t, t + \tau), \quad (55)$$

and restrict attention to stationary fields, so that the time argument t can be omitted. Decomposing $\Delta G^{(2)}$ with respect to powers of the local-oscillator amplitude E_L , one may observe the following effects. The zeroth-order term yields the normally ordered intensity (I) fluctuation of the signal,

$$\Delta G_0^{(2)} \sim \langle : (\Delta \hat{I})^2 : \rangle. \quad (56)$$

The second-order term is related to the normally ordered electric-field variance of the signal,

$$\Delta G_2^{(2)} \sim E_L^2 \langle : [\Delta \hat{E}(\varphi)]^2 : \rangle, \quad (57)$$

where $\hat{E}(\varphi)$ corresponds to the quadrature-component operator $\hat{x}(\varphi)$, φ being the phase difference between signal and local oscillator. Eventually, the first-order term represents the correlation between the two signal-field observables,

$$\Delta G_1^{(2)} \sim E_L \langle : \Delta \hat{E}(\varphi) \Delta \hat{I} : \rangle. \quad (58)$$

Note that all these quantum-statistical moments can be separated from each other by using their dependences on the phase shift φ (for the measurement of the corresponding spectral properties, see Vogel, W., [1995]).

2.2. Heterodyne detection

It is worth noting that multiport homodyning for measurement of the complex amplitude is equivalent to (four-port) *heterodyne* detection (Yuen and Shapiro, J.H., [1980]; Yuen [1982]; Yuen and Chan [1983]; Shapiro, J.H., [1985]; Shapiro, J.H., and Wagner [1984]; Caves and Drummond [1994]). In the scheme, an optical field is combined, through a beam splitter, on the surface of a photodetector with a strong local oscillator whose frequency ω_0 is offset by an amount $\Delta\omega$ from that of the signal mode in the optical field ($\Delta\omega \ll \omega_0$). The measured photocurrent is electrically filtered in order to select the complex valued component at frequency $\Delta\omega$. The classical statistics of this component correspond, under certain circumstances, to the quantum statistics of the two-mode operator

$$\hat{\alpha} = \hat{a}_S + \hat{a}_I^\dagger, \quad (59)$$

where the subscripts S and I , respectively, are used to denote the signal mode at frequency $\omega_0 + \Delta\omega$ and the imaging mode at frequency $\omega_0 - \Delta\omega$. Obviously, the imaging mode can be used to probe the signal mode. To show this, we first note that the measured quantity $\hat{\alpha}$ can always be brought into the form

$$\hat{\alpha} = \hat{\alpha}_1 + i\hat{\alpha}_2, \quad (60)$$

where $\hat{\alpha}_1$ and $\hat{\alpha}_2$ are commuting Hermitian operators having a quantum-mechanical joint probability density $p(\alpha) \equiv p(\alpha_1, \alpha_2)$, which can be found easily through its characteristic function

$$\phi(\beta) = \langle e^{\beta\hat{\alpha}^\dagger - \beta^*\hat{\alpha}} \rangle = \int d^2\alpha e^{\beta\alpha^* - \beta^*\alpha} p(\alpha). \quad (61)$$

In particular, if the imaging mode is in the vacuum, then measurement of $p(\alpha)$ can be seen to yield the Q function of the signal mode, because of

$$\phi(\beta) = \langle e^{-\beta^*\hat{a}_S} e^{\beta\hat{a}_S^\dagger} \rangle = \Phi(\beta; s = -1) \quad (62)$$

(cf. Appendix B.4.).

2.3. Parametric amplification

Finally it should be mentioned that linear amplification of a signal mode and measurement of the complex amplitude of the amplified signal may be regarded as an equivalent of the homodyne measurement of the complex amplitude of the original signal (Bandilla and Paul, H., [1969, 1970]; Paul, H., [1974]). If the signal mode is strongly enhanced such that it behaves classically, the conjugated quadrature components can be measured simultaneously. The scheme can be realized by (nondegenerate) parametric amplification, in which the photon destruction operators \hat{a}'_S and \hat{a}'_I , respectively, of the amplified signal and idler modes are obtained from the $SU(1,1)$ input-output relations

$$\hat{a}'_S = \sqrt{g}\hat{a}_S + \sqrt{g-1}\hat{a}_I^\dagger \quad (63)$$

$$\hat{a}'_I = \sqrt{g-1}\hat{a}_S + \sqrt{g}\hat{a}_I^\dagger, \quad (64)$$

where g is the (linear) signal-gain factor (for details, see, e.g., Mollow and Glauber [1967a,b]; Caves and Schumaker [1985]; Yurke, McCall and Klauder [1986]).

It can be shown that when the signal mode is mixed with an idler mode that is initially in the vacuum state and the strong-amplification limit is realized, i.e., $g \rightarrow \infty$, then the Q function of the original signal mode can be inferred from the measured distribution function for the complex amplitude of the amplified signal mode by appropriately rescaling this distribution (Leonhardt [1994]; see also Leonhardt and Paul, H., [1995]). It is worth noting that a degenerate parametric amplifier that operates as a squeezer [$\hat{a}_I^\dagger \rightarrow e^{i\phi} \hat{a}_S^\dagger$ in eq. (63)] may be used to (partially) compensate for the detection losses in balanced four-port homodyne detection for measuring quadrature components (Leonhardt and Paul, H., [1994a]; § 3.9.1.), since it makes it possible to amplify a quadrature component with no increase of noise (Caves [1982]).

Further, parametric amplification can be used to determine the quantum state of the signal mode by direct photodetection of the amplified signal if the idler mode is initially prepared in, e.g., a coherent state, without restriction to the Q function and without restriction to the strong-amplification limit (Kim, M.S., [1997a]; § 3.5.). In particular, when the idler mode is prepared in a strong coherent state such that it can be treated classically, $\hat{a}_I \rightarrow \alpha_I$, then – with regard to the photocounting formula (C.5) for detecting the amplified signal – eq. (63) takes the form of eq. (48), with $\alpha = -[(g-1)/g]^{1/2} \alpha_I^*$ in place of eq. (49). In this case, eq. (50) also applies to the detection of the amplified signal, where now $\hat{n} = \hat{n}_S$ and $\eta = g \eta_D$.²³

2.4. Measurement of cavity fields

Let us now consider the possibilities of phase-sensitive measurements of high- Q cavity fields. The realization of such fields, for example in a micromaser (Meschede, Walther and Müller [1985]; Rempe, Walther and Klein [1987]; Brune, Raimond, Goy, Davidovich and Haroche [1987]), necessitates a strong suppression of cavity losses. That is, only a very small fraction of the field escapes from the cavity and could be used, e.g., in homodyne detection. Since the quantum efficiency of such a scheme is very low, it is impossible, in general, to extract the (complete) quantum statistics of the field inside the cavity from the homodyne data measured outside the cavity. To overcome the problem, methods have been developed which use atoms that travel through the cavity and probe the field inside. The system that is directly observed in the experiment is not the cavity field itself but the atoms after their interaction with the field. Under certain circumstances, the measured atomic occupation probabilities can then be related uniquely (in a more or less direct way) to the quantum state of the cavity field (§ 3.6.). Let us consider a measurement scheme typically used in Rydberg-atom superconducting cavity QED (see, e.g., Brune and Haroche [1994] and references therein).²⁴ The atoms that cross the cavity are prepared, after

²³Note that eq. (63) implies that the signal and idler operators in the photocounting formula (C.5) are subject to different orderings, so that eq. (48) does not apply in general.

²⁴Here circular Rydberg atoms are used in which one electron is placed on a highly excited energy level with large value of principal quantum number n , and the angular momentum takes its maximum value ($l = m = n - 1$). For $n \approx 50$ the atomic-dipole decay time is of the order of magnitude of 10^{-2} s. The cavity damping time is of the order of magnitude of $10^{-3} \dots 10^{-1}$ s for superconducting cavities at subKelvin temperatures. The Q factor defined as the ratio of the cavity frequency to the cavity damping rate (inverse damping time) then reaches values of about $10^8 \dots 10^{10}$. The Rabi frequency,

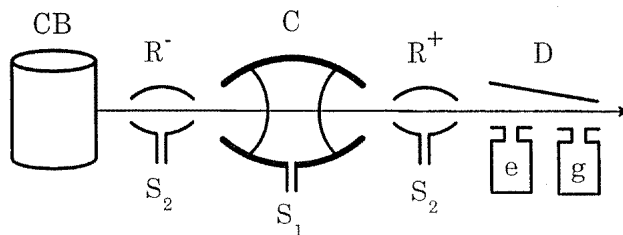


Figure 7: Set-up for the detection of a high- Q cavity mode. The Rydberg atoms are prepared in the state $|e\rangle$ in the box CB and cross a microwave zone R^- (source S_2) between CB and C which mixes the (excited) state $|e\rangle$ and the (ground) state $|g\rangle$ before the atoms enter the cavity C. A second microwave pulse (source S_2) applied between C and D in the zone R^+ again mixes the states $|e\rangle$ and $|g\rangle$ before the atoms reach the detector D, which renders it possible to detect linear superpositions of these two states. The microwave source S_1 can be used to feed into the cavity a (classical) field. (After Brune and Haroche [1994].)

leaving an oven and before entering the cavity, into a superposition of Rydberg states $|e\rangle$ and $|g\rangle$ of different energies (Fig. 7). After preparation of the state $|e\rangle$, which involves laser and radiofrequency excitation, a microwave (Ramsey) zone can be used to apply a resonant pulse to the atoms, mixing the state $|e\rangle$ with another state $|g\rangle$ of different energy. In this way an initial atomic state of the form $c_e|e\rangle + c_g|g\rangle$ can be injected into the cavity. The atoms then interact with the cavity mode while crossing it. After leaving the cavity, the atoms can again cross a microwave zone in order to realize state mixing before they enter a detector for measuring their energies by field ionization. This detection can be made energy-sensitive and one can thus count the atoms in $|e\rangle$ and $|g\rangle$. The dependence of the measured data on the various parameters characterizing the experimental conditions (such as state mixing and interaction time) can then be used to gain insight into the quantum state of the cavity mode (Vogel, W., Welsch and Leine [1987]; Bardroff, Mayr and Schleich [1995]; Bardroff, Mayr, Schleich, Domokos, Brune, Raimond and Haroche [1996]).

The cavity and the atomic transition can be tuned to coincide (resonant regime) or slightly detuned (dispersive regime), with a frequency difference $\delta\omega$ such that any exchange of energy between atom and field is made impossible. In the resonance regime, the system can be described (in its simplest version) by the Jaynes–Cummings model (Jaynes and Cummings [1963]; Paul, H., [1963]; for a review, see, e.g., Shore and Knight [1993]). The Hamiltonian consists of three terms describing the free two-level (circular Rydberg) atom, the free cavity mode and the atom–field coupling, the latter being given by

$$\hat{H}' = \hbar\kappa (\hat{\sigma}_+ \hat{a} + \hat{a}^\dagger \hat{\sigma}_-). \quad (65)$$

Here, $\hat{\sigma}_+ = |e\rangle\langle g|$ and $\hat{\sigma}_- = |g\rangle\langle e|$, respectively, are the atomic raising and lowering operators, and κ is the coupling constant between the atom and the cavity mode

which is typically of the order of magnitude of 10 . . . 100 kHz, is large compared with the atomic and the cavity decay rates, so that relaxation can be disregarded in first approximation (strong coupling regime).

($\Omega = 2\kappa$ is the vacuum Rabi frequency, which is the rate at which the atom and the empty cavity exchange a photon at exact resonance.)

In the dispersive regime, the atom–field interaction produces a dephasing of the field and also dephases the atom’s wave function by an angle depending upon the number of photons in the cavity and on the quantum state of the atom. The nonresonant interaction can be described by an effective Hamiltonian,

$$\hat{H}'' = \hbar \frac{\kappa^2}{\delta\omega} (\hat{\sigma}_- \hat{\sigma}_+ \hat{a}^\dagger \hat{a} - \hat{a} \hat{a}^\dagger \hat{\sigma}_+ \hat{\sigma}_-). \quad (66)$$

The phase difference induced by the interaction of the two parts of the system can be measured when the two microwave zones in Fig. 7 are active. It can be shown that the probability that a probe atom which is initially prepared in the state $|e\rangle$ is finally detected in the state $|g\rangle$ (i.e., after the combined action of the two microwave zones on it) oscillates as a function of the microwave frequency, the position of the interference (Ramsey) fringes being dependent on the additional dephasing produced by the cavity mode. It is worth noting that the Ramsey interferometer outlined here can serve as an apparatus for a *quantum non-demolition measurement* (QND) (Braginsky, Vorontsov and Khalili [1977]; also see Braginsky and Khalili [1992]) of the photon number in the cavity (Brune, Haroche, Lefevre, Raimond and Zagury [1990]; Brune, Haroche, Raimond, Davidovich and Zagury [1992]).

When in the dispersive regime an additional microwave generator is used in order to resonantly couple a classical (strong) oscillator to the cavity mode, then the Wigner function of the cavity mode can, in principle, be measured directly (Lutterbach and Davidovich [1997]). Owing to the coupling of the classical oscillator to cavity mode, a displacement in phase space of the (initial) quantum state of the cavity mode is performed such that the density operator $\hat{\rho}$ is replaced with $\hat{D}^\dagger(\alpha)\hat{\rho}\hat{D}(\alpha)$.²⁵ The atoms initially prepared in state $|e\rangle$ cross the first Ramsey zone where they see a $\pi/2$ pulse, so that $|e\rangle \rightarrow 2^{-1/2}(|e\rangle + e^{i\psi}|g\rangle)$. The atoms then interact dispersively with the cavity field, and after that they undergo a $\pi/2$ pulse in the second Ramsey zone before detection. Let P_e and P_g be the probabilities of detecting a probe atom in the states $|e\rangle$ and $|g\rangle$, respectively. It can be shown that the difference between these probabilities is

$$\Delta P = P_e - P_g = -\text{Re} \left\{ e^{i(\psi+\phi)} \left\langle \hat{D}(\alpha) e^{2i\phi\hat{a}^\dagger\hat{a}} \hat{D}^\dagger(\alpha) \right\rangle \right\}, \quad (67)$$

where $\phi = (\Omega^2/\delta)\tau$ is the additional dephasing of the atoms in the cavity, with τ being the interaction time. In particular, if $\phi = \psi = \pi/2$, then

$$\Delta P = \frac{1}{2}\pi W(\alpha), \quad (68)$$

which reveals that indeed the Wigner function is detected, provided that during the (ensemble) measurement the phases are controlled and each probe atom meets the cavity field in exactly the same state.

The method of displaced states²⁶ can also be used for quantum-state measurement in the resonance regime, without phase-sensitive state mixing (Wilkins and Meystre

²⁵Note that this coupling acts in a similar way as the mode mixing at an unbalanced beam splitter outlined in § 2.1.7..

²⁶An analogous method can be used in order to determine the quantum state of the center-of-mass motion of trapped ions (cf. § 4.2.2.).

[1991]; Bodendorf, Antesberger, Kim, M.S., and Walther [1998]). Here, the probe atoms are prepared in one of the two considered states $|e\rangle$ and $|g\rangle$ or in a statistical mixture of them. The measured two-level occupation statistics of the atoms as a function of the interaction time and/or the displacement parameter contain all knowable information on the quantum state of the cavity mode.

The method of probing a cavity field using two-level atoms that travel through the cavity can also be extended to other than purely two-level probe atoms. So it was proposed to completely transfer, by adiabatic passage, the quantum state of the field onto an internal Zeeman submanifold of an atom (Walser, Cirac and Zoller [1996]). Utilizing a tomography of atomic angular momentum states by Stern–Gerlach measurements (Newton and Young [1968]), this angular momentum state can then be determined uniquely, by a finite number of magnetic dipole measurements.

The spatial variation of the cavity mode implies a dependence on the atomic position of the Rabi frequency, which offers the possibility of probing the quantum state of the mode via atomic deflection (Akulin, Fam and Schleich [1991]; Herkommer, Akulin and Schleich [1992]; Freyberger and Herkommer [1994]). In the scheme in Fig. 8 a narrow beam of resonant atoms is proposed to pass through a node region of the mode, where the interaction Hamiltonian can be assumed to be a linear function of the atomic position. The cavity photons repulse the atoms so that the transverse momentum distribution of the atoms is changed during their passage through the cavity. When the cavity mode is (initially) in a pure state, then the measurable change provides (for appropriately prepared atoms) all the information needed for reconstructing it.

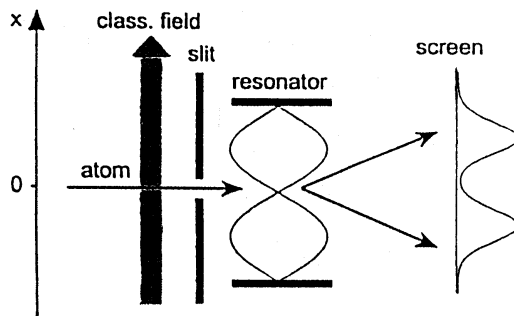


Figure 8: Atomic-deflection measurement scheme. A classical field prepares the two-level atoms in a superposition $|g\rangle + e^{i\varphi}|e\rangle$ of the ground state $|g\rangle$ and the excited state $|e\rangle$. The so-prepared atoms pass a narrow slit which confines them to a region $\Delta x \ll \lambda$ centred around the node of the standing light field at $x=0$. After the resonant interaction with the field the deflected atoms travel to a screen put up far away from the resonator. The spatial distribution on this screen reflects the momentum distribution of the atoms right after the interaction. (After Freyberger and Herkommer [1994].)

To extend the method to the reconstruction of mixed states, the effects of the classical field and the cavity field on the atoms can be combined such that the classical field travels orthogonally with respect to the cavity mode and both fields overlap in the region where the atoms cross them (Schneider, Herkommer, Leonhardt and Schleich

[1997]). In particular, when the classical field is sufficiently strong, then it can play a similar role as the local oscillator in balanced four-port optical homodyning. It is worth noting that under certain circumstances the transverse momentum distribution of the atoms which is observed in the dispersive regime is nothing but a smeared quadrature-component distribution of the cavity mode (§ 3.6.2.).

3. Quantum-state reconstruction

When in an experiment a sequence of quantities \hat{A}_i ($\hat{A}_i = \hat{A}_i^\dagger$) can be measured, such that the density operator of the system under study can be given by

$$\hat{\rho} = \sum_i \hat{B}_i \langle \hat{A}_i \rangle, \quad (69)$$

then all knowable information on the quantum state of the system can be obtained in principle (Fano [1957]).²⁷ In practice it must be ensured that enough data can be measured and that they can be decoded with reasonable accuracy and acceptable effort – a task which is not trivial in general. In particular if the measured data are directly related to a smeared quantum-state representation in the phase space, it may be an effort to derive from it the quantum state in another basis for studying specific quantum-statistical properties. Typical examples of complete and overcomplete basis sets of observables for which measurement schemes have been designed are the generalized projectors $\hat{A}_i \rightarrow \hat{\Pi}(x, \varphi) = \pi^{-1} |x, \varphi\rangle \langle x, \varphi|$ [see eq. (B.31)] and $\hat{A}_i \rightarrow \hat{\Pi}(\alpha) = \pi^{-1} |\alpha\rangle \langle \alpha|$ [see eq. (B.20) with $s = -1$], respectively, for the quadrature-component states and the coherent states. If a scheme is not designed for measuring at least a [in the sense of eq. (69)] complete set of observables, then some *a priori* knowledge of the quantum state is required in order to compensate for the lack of data.

3.1. Optical homodyne tomography

From § 2.1.2. we know that in a succession of (phase-shifted) balanced four-port homodyne measurements the quadrature-component distribution $p(x, \varphi)$ of a signal mode can be obtained for various values of the phase φ , provided that 100% quantum efficiency is realized. The quantum state is then known when $p(x, \varphi)$ is known for all values of φ within a π interval (Vogel, K., and Risken [1989]). That is to say, all quantum-statistical properties can be obtained from the quadrature-component distributions measured in a π interval.

In particular, $p(x, \varphi)$ can be used to reconstruct the Wigner function. From eq. (B.28) ($s = 0$) it can be derived that

$$p(x, \varphi) = \int dy W(x \cos \varphi - y \sin \varphi, x \sin \varphi + y \cos \varphi), \quad (70)$$

²⁷In connection with the study of the Pauli problem (Pauli [1933]) the sufficient set of observables that has to be measured in order to obtain the complete information on the quantum state was also called *quorum* of a quantum-state measurement (Park and Band [1971]). It was shown that for the one-dimensional motion of a particle a quorum can be given by all symmetrized products of powers of position and momentum (cf. § 3.8.1.) or alternatively, all time derivatives of all powers of the position (Band and Park [1979]; Park, Band and Yourgrau [1980]).

where the definition $W(q, p) \equiv 2^{-1} W[\alpha = 2^{-1/2}(q + ip)]$ is used. Equation (70) reveals that the quadrature-component distributions can be regarded as marginals of the Wigner function. An integral relation of the form given in eq. (70) is also called *Radon transformation* (Radon [1917]). Inversion of the Radon transformation (70) yields the Wigner function in terms of the quadrature-component distribution.²⁸ From eq. (B.29) ($s = 0$) the Wigner function is derived to be²⁹

$$W(q, p) = \frac{1}{4\pi^2} \int_0^\pi d\varphi \int dz \int dx |z| \exp[iz(q \cos \varphi + p \sin \varphi - x)] p(x, \varphi). \quad (71)$$

Performing the z integral first would lead to an integral kernel that is not well-behaved. To overcome this difficulty in the numerical calculation, regularization techniques can be used. In the *filtered back projection algorithm*, the z integral is truncated such that

$$W(q, p) \simeq W_c(q, p) = \frac{1}{2\pi^2} \int_0^\pi d\varphi \int dx K_c(q \cos \varphi + p \sin \varphi - x) p(x, \varphi), \quad (72)$$

with

$$K_c(y) = \frac{1}{2} \int_{-z_c}^{+z_c} dz |z| e^{iyz} \quad (73)$$

($z_c > 0$). Here, rapid variations of the quadrature-component distributions which correspond to frequencies higher than the cut-off frequency z_c are suppressed, i.e., the exact distributions are effectively replaced with somewhat smeared ones.

In the pioneering experimental demonstration of the method also called *optical homodyne tomography* (Smithey, Beck, Raymer and Faridani [1993]; Smithey, Beck, Cooper, Raymer and Faridani [1993]), a pulsed signal field is superimposed with a pulsed coherent-state field much stronger than the signal. The quadrature-component distributions are measured for a squeezed signal field and a vacuum signal field. The squeezed field is generated by using a walk-off compensated, travelling-wave optical parametric amplifier. The generated down-conversion signal centred at 1064 nm consists of two orthogonally polarized fields, the signal and idler, and has a bandwidth estimated to be 10^4 times that of the laser pump (532 nm, 300 ps, 420 pulses per second). The laser pump and the local-oscillator field (1064 nm, 400 ps) are obtained from a common laser source, and each local-oscillator pulse contains a mean number of photons of about 4×10^6 . The interfering fields are detected with high-quantum-efficiency ($\sim 85\%$) photodiodes, and the resulting current pulses are temporally integrated and subtracted. The measurements and reconstructions are performed for a squeezed signal field and for a vacuum signal field, Figs. 9 and 10, the field mode detected being selected by the spatial-temporal mode of the local-oscillator field. The method of optical homodyne tomography was also extended subsequently to the continuous wave-regime, including squeezed vacuum with a high degree of quantum noise reduction (Breitenbach, Müller, Pereira, Poizat, Schiller and Mlynek [1995]; Schiller, Breitenbach, Pereira, Müller and Mlynek [1996]) and bright squeezed light (Breitenbach and Schiller [1997]; Breitenbach, Schiller and Mlynek [1997]).

²⁸Inverse Radon transformation techniques are well known from *tomographic imaging* (for mathematical details, see, e.g., Natterer [1986]). In quantum mechanics, the problem of tomographic reconstruction of the Wigner function of a particle moving in one dimension was first addressed by Bertrand and Bertrand [1987].

²⁹For phase-randomized states, see Leonhardt and Jex [1994].

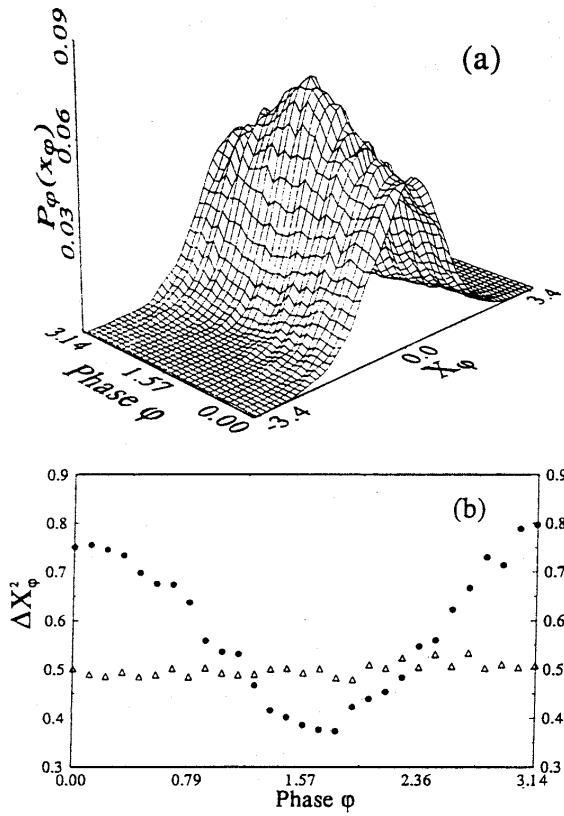


Figure 9: (a) In balanced four-port homodyne detection measured quadrature-component distributions at various values of the local-oscillator phase [$P_\varphi(x_\varphi)$ corresponds to $p(x, \varphi)$]. (b) Variances of quadrature components vs local-oscillator phase: circles, squeezed state; triangle, vacuum state. In the experiment 4000 repeated measurements of the photoelectron difference number at 27 values of the relative phase φ are made. (After Smithey, Beck, Raymer and Faridani [1993].)

As mentioned in § 2.1.2., the measured quadrature-component distributions do not correspond, in general, to the true signal mode, but they must be regarded as the distributions of a superposition of the signal and an additional noise source [eq. (21)], because of non-perfect detection. Substituting in eq. (70) for $p(x, \varphi)$ the measured distributions $p(x, \varphi; \eta)$ with $\eta < 1$ [eq. (19)] and performing the inverse Radon transform on them, the Wigner function of a noise-assisted signal field is effectively reconstructed. Equivalently, the reconstructed Wigner function can be regarded as an s -parametrized phase-space function of the true signal field, however with $s < 0$. The characteristic function $\Psi(z, \varphi; \eta)$ of $p(x, \varphi; \eta)$ typically measured when $\eta < 1$ and the characteristic function $\Phi(\beta; s)$ of the phase-space function $P(\alpha; s)$ are related to each other according to eq. (B.27), with $\Psi(z, \varphi; \eta)$ in place of $\Psi(z, \varphi)$ and $s - 1 + \eta^{-1}$ in place of s in the exponential [cf. eq. (23) and footnote 7]. Hence, making in the exponentials in eqs. (B.28) and (B.29) for s the substitution $s - 1 + \eta^{-1}$ yields the relations between $P(\alpha; s)$ and $p(x, \varphi; \eta)$. In particular, eq. (B.29) can be used to obtain any phase-space function $P(q, p; s) \equiv 2^{-1} P[\alpha = 2^{-1/2}(q + ip; s)]$ from the measured

quadrature-component distributions in principle:³⁰

$$P(q, p; s) = \frac{1}{4\pi^2} \int_0^\pi d\varphi \int dz \int dx \left\{ \exp\left[\frac{1}{4}(s-1+\eta^{-1})z^2\right] \right. \\ \left. \times |z| \exp[iz(q \cos \varphi + p \sin \varphi - x)] p(x, \varphi; \eta) \right\}. \quad (74)$$

Obviously, when $s = 1 - \eta^{-1}$, then eq. (74) takes the form of eq. (71); i.e., replacing in eq. (70) $p(x, \varphi)$ with $p(x, \varphi; \eta)$, inverse Radon transformation yields the signal-mode phase-space function $P(q, p; s = 1 - \eta^{-1})$ in place of the Wigner function,

$$p(x, \varphi; \eta) = \int dy P(x \cos \varphi - y \sin \varphi, x \sin \varphi + y \cos \varphi; s = 1 - \eta^{-1}). \quad (75)$$

The proposal was made to combine squeezing and balanced homodyning such that generalized quadrature-components

$$\hat{x}(\mu, \nu) = \mu \hat{q} + \nu \hat{p} \quad (76)$$

for all real parameters μ and ν can be measured, and to reconstruct the quantum state from the corresponding distributions $p(X, \mu, \nu)$ (Mancini, Man'ko, V.I., and Tombesi [1995]; D'Ariano, Mancini, Man'ko, V.I., and Tombesi [1996]; Man'ko, O.V., [1996]; Mancini, Man'ko, V.I., and Tombesi [1997]).³¹ In fact, $\hat{x}(\mu, \nu)$ can be related to $\hat{x}(\varphi)$ since it represents a scaled quadrature-component,

$$\hat{x}(\mu, \nu) = |F| \left(\hat{a} e^{-i\varphi} + \hat{a}^\dagger e^{i\varphi} \right) = 2^{1/2} |F| \hat{x}(\varphi), \quad (77)$$

with

$$2^{1/2} |F| = \sqrt{\mu^2 + \nu^2}, \quad \tan \varphi = \frac{\nu}{\mu} \quad (78)$$

(cf. § 2.1.2. and Appendix B.), which implies that

$$p(x, \mu, \nu) = \frac{1}{\sqrt{\mu^2 + \nu^2}} p\left(\frac{x}{\sqrt{\mu^2 + \nu^2}}, \varphi = \arctan \frac{\nu}{\mu}\right). \quad (79)$$

Hence, measurement of a particularly scaled quadrature-component distribution by means of an ordinary homodyne detector already yields all scaled quadrature components. Performing the analysis with a variable scaling parameter, it can be shown that eqs. (70) and (71), respectively, can be given in terms of $p(x, \mu, \nu)$ by³²

$$p(x, \mu, \nu) = \frac{1}{2\pi} \int dk \int dq \int dp e^{-ik(x - q\mu - p\nu)} W(q, p) \quad (80)$$

³⁰When $s > 1 - \eta^{-1}$, then in eq. (74) an inverse Gaussian occurs which may lead to an artificial enhancement of the inaccuracies of the measured data, so that a stable deconvolution might be impossible and the noise dominates the reconstruction of $P(q, p; s)$. This effect is not observed when $s \leq 1 - \eta^{-1}$, and hence a stable reconstruction with reasonable precision of $P(\alpha; s)$ for $s \leq 1 - \eta^{-1}$ may therefore be expected to be feasible for any quantum state (see also § 3.9.). In particular, reconstruction of the Q function is always possible if $\eta > 1/2$. When $s < 1 - \eta^{-1}$, then in eq. (74) the z integral can be performed first to obtain $P(q, p; s)$ in a form suited for application of sampling techniques (§ 3.3.1.): $P(q, p; s) = \int_0^\pi d\varphi \int dx K(q, p, x, \varphi; s; \eta) p(x, \varphi; \eta)$, with $K(q, p, x, \varphi; s; \eta)$ being a well-behaved integral kernel.

³¹For an application of the method (also called *symplectic tomography*) to trapped-ion quantum state reconstruction, see Mancini, Man'ko, V.I. and Tombesi [1996]; Man'ko, O.V. [1997].

³²For a detailed discussion of the transformation properties, see also Wünsche [1997].

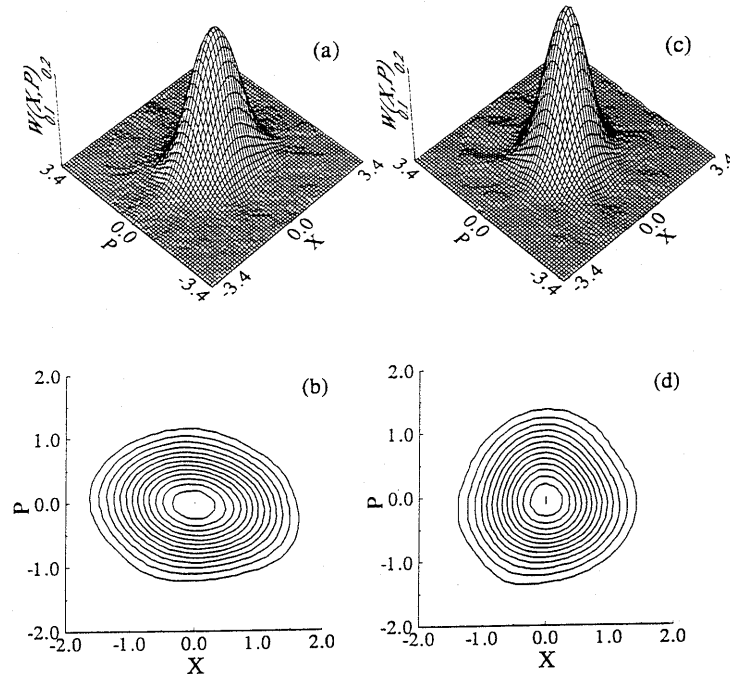


Figure 10: From the measured quadrature-component distributions reconstructed Wigner distributions for (a),(b) a squeezed state and (c),(d) a vacuum state, viewed in 3D and as contour plots, with equal numbers of constant-height contours [$W(X, P)$ corresponds to $W(q, p)$]. The reconstruction is performed by using inverse Radon transformation according to eq. (72). (After Smithey, Beck, Raymer and Faridani [1993].)

and

$$W(q, p) = \frac{z^2}{(2\pi)^2} \int dx \int d\mu \int d\nu e^{iz(x-q\mu-p\nu)} p(x, \mu, \nu). \quad (81)$$

Comparing eq. (81) with eq. (71), we see that in any case a three-fold Fourier transformation is required in order to obtain the Wigner function from the homodyne data. Note that z in eq. (81) can be chosen arbitrarily, which reflects the above mentioned fact of overcomplete data.

3.2. Density matrix in quadrature-component bases

The reconstructed Wigner function can be used in order to calculate the density matrix in a quadrature-component basis (Smithey, Beck, Raymer and Faridani [1993]; Smithey, Beck, Cooper, Raymer and Faridani [1993]). The definition of the Wigner function given in Appendix B.4. can be rewritten, on expanding the density operator in a quadrature-component basis, as

$$W(q, p) = \frac{1}{\pi} \int dx' e^{2iyx'} \langle x-x', \varphi | \hat{\rho} | x+x', \varphi \rangle, \quad (82)$$

with

$$x = q \cos \varphi + p \sin \varphi, \quad y = -q \sin \varphi + p \cos \varphi, \quad (83)$$

which for $\varphi = 0$ is nothing but the well-known Wigner formula (Wigner [1932]). Hence the density matrix in a quadrature-component basis can be obtained by Fourier transforming the Wigner function:

$$\langle x-x', \varphi | \hat{\rho} | x+x', \varphi \rangle = \int dy e^{-2ix'y} W(x \cos \varphi - y \sin \varphi, x \sin \varphi + y \cos \varphi). \quad (84)$$

Note that eq. (84) reduces to eq. (70) for $x' = 0$.

It is worth noting that the reconstruction of the density matrix from the homodyne data can be accomplished with two Fourier integrals, avoiding the detour via the Wigner function (Kühn, Welsch and Vogel, W., [1994]; Vogel, W., and Welsch [1994]). Writing the density-matrix elements as

$$\langle x-x', \varphi | \hat{\rho} | x+x', \varphi \rangle = \frac{1}{2\pi} \int dz e^{-ixz} \Psi(z, x', \varphi), \quad (85)$$

the characteristic function $\Psi(z, x', \varphi)$ can be shown to be the characteristic function of a quadrature-component distribution,

$$\Psi(z, x', \varphi) = \Psi(\tilde{z}, \tilde{\varphi}), \quad (86)$$

with

$$\tilde{z} = \tilde{z}(z, x') = [z^2 + (2x')^2]^{1/2} \quad \text{and} \quad \tilde{\varphi} = \varphi - \frac{1}{2}\pi + \arg(2x' + iz). \quad (87)$$

Hence, the density-matrix elements can be obtained from the quadrature-component distributions by means of a simple two-fold Fourier transformation:³³

$$\langle x-x', \varphi | \hat{\rho} | x+x', \varphi \rangle = \frac{1}{2\pi} \int dz e^{-ixz} \int d\tilde{x} e^{i\tilde{z}\tilde{x}} p(\tilde{x}, \tilde{\varphi}). \quad (88)$$

It is worth noting that eq. (88) can be used to obtain the density matrix in different representations, by varying the phase of the quadrature component defining the basis. Further, eq. (88) can also be extended, in principle, to imperfect detection, expressing $\Psi(z, \varphi)$ in eq. (85) in terms of $\Psi(z, \varphi; \eta)$ (cf. footnote 7; for details, see Kühn, Welsch and Vogel, W., [1994]; Vogel, W., and Welsch [1994]).

For the numerical implementation of the reconstruction based on eq. (88) spline-expansion techniques can be used (Zucchetti, Vogel, W., Tasche and Welsch [1996]),³⁴

$$\langle x-x', \varphi | \hat{\rho} | x+x', \varphi \rangle \simeq \sum_{m,n} K_{mn}(x, x', \varphi) p(\tilde{x}_{m+1}, \tilde{\varphi}_{n+1}), \quad (89)$$

where

$$K_{mn}(x, x', \varphi) = (2\pi)^{-1} \sum_k \underline{B}_{\Delta\tilde{x}_m, m}[\tilde{z}(\xi_{k+1}, x')] B_{\Delta z_n, n}(\xi_{k+1}) \underline{B}_{\Delta\xi_k, k}(-x), \quad (90)$$

with $z_n = -2x' \cot(\tilde{\varphi}_n - \varphi) [\underline{B}_{(\dots)}(k)$, Fourier transform of $B_{(\dots)}(x)]$. As an illustration of this method, in Figs. 11(a) and 11(b) the reconstructed density matrices in the

³³For the two-fold Fourier transformation that relates the density-matrix elements to $p(x, \mu, \nu)$, eq. (80), see D'Ariano, Mancini, Man'ko and Tombesi [1996].

³⁴Choosing a finite set of nodes $\{x_n\}$, an approximate spline function $f_s(x)$ of $f(x)$ is given by $f_s(x) = \sum_n f(x_{n+1}) B_{\Delta x_n, n}(x)$, where $B_{\Delta x_n, n}(x) = (x - x_n) / \Delta x_n$ if $x_n \leq x \leq x_{n+1}$, $B_{\Delta x_n, n}(x) = (x_{n+2} - x) / \Delta x_{n+1}$ if $x_{n+1} \leq x \leq x_{n+2}$, and $B_{\Delta x_n, n}(x) = 0$ elsewhere, and $\Delta x_n = x_{n+1} - x_n$; for mathematical details of spline expansion, see de Boor [1987].

“position” basis, $\varphi = 0$, and the “momentum” basis, $\varphi = \pi/2$, of a squeezed vacuum state are shown. The homodyne data were recorded by T. Coudreau, A.Z. Khoury and E. Giacobino. In the underlying experimental scheme the squeezing effect is obtained in a probe beam that interacts with cold atoms in a nearly single-ended cavity (Lambrech, Coudreau, Steinberg and Giacobino [1996]). The phases $\varphi = 0$ and $\varphi = \pi/2$ that define the quadrature-component bases in Fig. 11 coincide with the phases of minimal and maximal field noise, respectively.

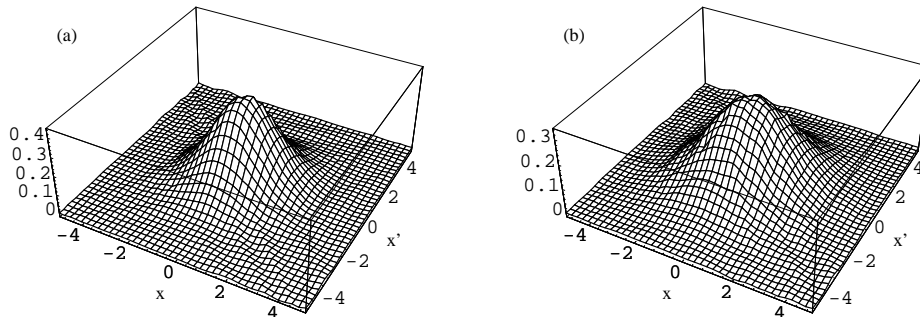


Figure 11: From measured quadrature-component distributions reconstructed (real) density matrix $\langle x, \varphi | \hat{\rho} | x', \varphi \rangle$ of a squeezed state in (a) the “position” basis ($\varphi = 0$) and (b) the “momentum” basis ($\varphi = \pi/2$). The homodyne data were obtained by T. Coudreau, A.Z. Khoury and E. Giacobino, using the experimental setup reported by Lambrecht, Coudreau, Steinberg and Giacobino [1996]. In the experiment, the quadrature-components were measured at 48 phases, and at each phase 7812 measurements were performed.

3.3. Density matrix in the Fock basis

Stimulated by the tomographic reconstruction of the Wigner function (§ 3.1.) much effort has been made to obtain the density matrix in the Fock basis from measurable data as direct as possible. Let us again start with analysing balanced four-port homodyning.

3.3.1. Sampling of quadrature-components

The problem of reconstruction of the density matrix in the Fock basis from the quadrature-component distributions can be solved, in principle, by relating the density-matrix elements to derivatives of the Q function (cf. § 3.3.3.) and expressing the Q function in terms of the quadrature-component distributions, using eq. (B.29), with $s = -1$ (D’Ariano, Macchiavello and Paris [1994a,b]). An equivalent formalism, which is suited for practice and which can also be applied to the reconstruction of the density matrix in other than the photon-number basis, is based on the expansion of the density operator as given in eq. (B.31). In the photon-number basis this equation

reads as³⁵

$$\varrho_{mn} = \langle m|\hat{\varrho}|n\rangle = \int_0^\pi d\varphi \int dx K_{mn}(x, \varphi) p(x, \varphi). \quad (91)$$

The integral kernel (also called *pattern function*)

$$K_{mn}(x, \varphi) = \langle m|\hat{K}(x, \varphi)|n\rangle = f_{mn}(x) e^{i(m-n)\varphi}, \quad (92)$$

with

$$\hat{K}(x, \varphi) = \frac{1}{2\pi} \int dz |z| \exp\{iz [\hat{x}(\varphi) - x]\}, \quad (93)$$

is studied in detail in a number of papers (D'Ariano [1995]; D'Ariano, Leonhardt and Paul, H., [1995]; Leonhardt, Paul, H., and D'Ariano [1995]; Leonhardt, Munroe, Kiss, Richter, Th., and Raymer [1996]; Richter, Th., [1996a]; Wünsche [1997]). The function $f_{mn}(x)$ (Fig. 12) is well behaved, and it is worth noting that it can be given by (Richter, Th., [1996a]; Leonhardt, Munroe, Kiss, Richter, Th., and Raymer [1996])

$$f_{mn}(x) = \frac{d}{dx} [\psi_m(x)\varphi_n(x)], \quad (94)$$

where $\psi_m(x)$ and $\varphi_m(x)$ are the regular and irregular (real) solutions of the harmonic-oscillator Schrödinger equation for a chosen energy value E_m .³⁶

Equation (91) reveals that the density matrix in the Fock basis can be sampled directly from the measured quadrature-component statistics, since ϱ_{mn} can be regarded as a statistical average of the (bounded) sampling function $K_{mn}(x, \varphi)$ (D'Ariano, Leonhardt and Paul, H., [1995]; Leonhardt, Paul, H., and D'Ariano [1995]; Leonhardt, Munroe, Kiss, Richter, Th., and Raymer [1996]; Leonhardt [1997c]; D'Ariano [1997a]). In an experiment each outcome x of $\hat{x}(\varphi)$, with $\varphi \in [0, \pi)$, contributes individually to ϱ_{mn} , so that ϱ_{mn} is gradually building up during the data collection. That is to say, ϱ_{mn} can be sampled from a sufficiently large set of homodyne data in *real time*, and the mean value obtained from different experiments can be expected to be normal-Gaussian distributed around the true value, because of the central-limit theorem. Moreover, the sampling method can also be used to estimate the statistical error (see also § 3.9.1.).

Experimentally, the method was successfully applied to the determination of the density matrix of squeezed light generated by a continuous-wave optical parametric amplifier (Schiller, Breitenbach, Pereira, Müller and Mlynek [1996]; Breitenbach and Schiller [1997]; Breitenbach, Schiller and Mlynek [1997]). In the experiment the spectral component of the photocurrent in a small band around a radiofrequency Ω is measured (overall quantum efficiency $\sim 82\%$). In this case the measurement is on a two-mode quadrature-component $\hat{x}(\varphi) = e^{i\phi_R} [\hat{a}(\omega + \Omega)e^{-i\varphi} + \hat{a}(\omega - \Omega)e^{i\varphi}]$, ϕ_R being the phase of the radio-frequency local oscillator, so that the scheme is basically a heterodyne detector. Examples of reconstructed diagonal density-matrix elements are shown in Fig. 13 (for reconstructed off-diagonal density-matrix elements, see, e.g., Schiller, Breitenbach, Pereira, Müller and Mlynek [1996]; Breitenbach and Schiller [1997]).

³⁵For the relation between the density-matrix elements and $p(x, \mu, \nu)$, eq. (80), see D'Ariano, Mancini, Man'ko and Tombesi [1996]).

³⁶Strictly speaking, the irregular (i.e., not normalizable) function $\varphi_n(x)$ has to be chosen such that $\psi_n\varphi'_n - \psi'_n\varphi_n = 2/\pi$ (for details, see Leonhardt [1997c]). Note that $f_{mn}(x)$ is not determined uniquely.

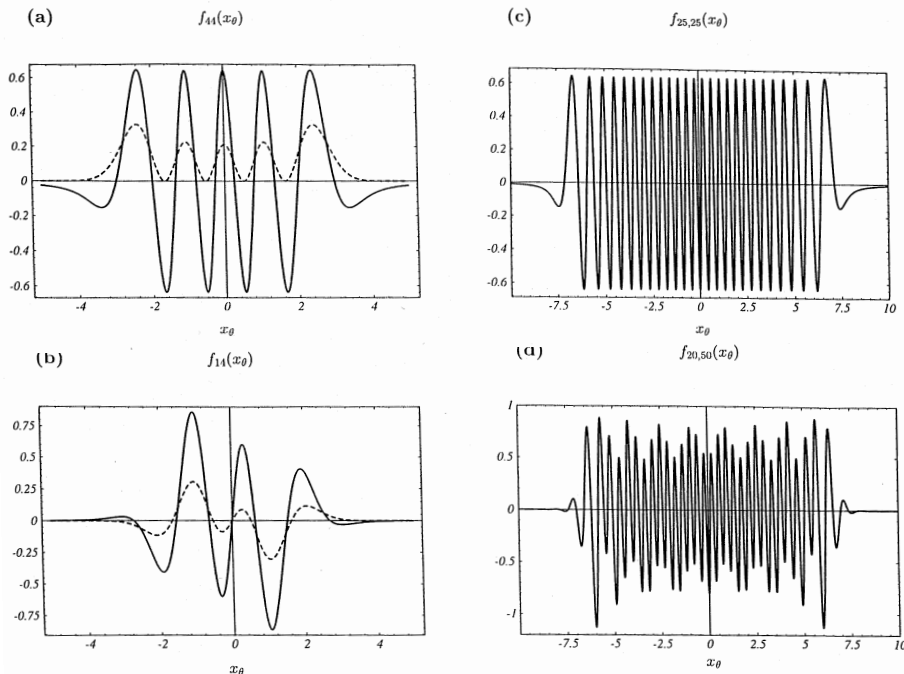


Figure 12: Plots of some typical pattern functions $f_{mn}(x)$ (lines) along with the products of regular wave functions $\psi_n(x)\psi_m(x)$ (dashed lines). In (a) the diagonal pattern function with $n = m = 4$ is depicted. Oscillations between $-2/\pi$ and $+2/\pi$ are clearly visible in the classically allowed region. Then the function swings over and decays like x^{-2} . In (b) the off-diagonal pattern function with $n = 1$, $m = 4$ is depicted. It is less oscillating than the diagonal pattern function and it decays faster in the forbidden zone. In (c) and (d) highly oscillating pattern functions are shown for (c) $n = m = 25$ and (d) $n = 20$, $m = 50$. (After Leonhardt, Munroe, Kiss, Raymer and Richter, Th., [1996].)

Further, the method was used successfully to measure the time-resolved photon-number statistics of a 5 ns pulsed field with a sampling time of 330 fs, set by the duration of the local-oscillator pulse (Munroe, Boggavarapu, Anderson and Raymer [1995]). From eqs. (91) and (92) it is easily seen that the photon-number probability distribution $p_n = \varrho_{nn}$ can be given by

$$p_n = \pi \int dx f_{nn}(x) \bar{p}(x), \quad (95)$$

where $\bar{p}(x) = (2\pi)^{-1} \int d\varphi p(x, \varphi)$ is the phase-averaged quadrature-component distribution. Equation (95) reveals that for sampling the photon-number statistics the phase need not be controlled – a situation that is typically realized when the signal and the local oscillator come from different sources. In the experiment, an argon-laser-pumped Ti:sapphire laser is used in combination with a chirped-pulse regenerative amplifier to generate ultrashort, transform limited local-oscillator pulses (330 fs) at a wavelength of 830 nm and a repetition rate of 4 kHz with approximately 10^6 photons per pulse. The signal is from a laser diode of wavelength 830 nm and pulse width 5 ns. Figure 14 shows examples of the (with $\sim 65\%$ overall quantum efficiency) measured quadrature-component probability distributions and the resulting

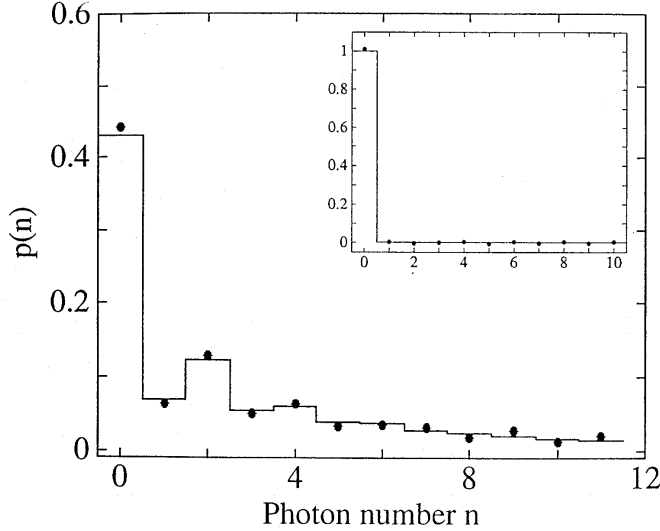


Figure 13: Photon-number distribution of a squeezed vacuum and the vacuum state (inset) reconstructed from the quadrature-component distributions according to eq. (91). Solid points refer to experimental data, histograms to theory. The experimentally determined statistical error is 0.03. (After Schiller, Breitenbach, Pereira, Müller and Mlynek [1996].)

photon-number probability distributions at two times in the signal pulse. In particular, the photon-number statistics are seen to change from nearly Poissonian statistics (laser above threshold) to thermal-like statistics (laser below threshold) (for ultrafast homodyne detection of two-time photon-number correlations, see § 3.8.1.).

So far in the formulas, perfect detection has been assumed. The problem of extending eq. (91) to imperfect detection such that $p(x, \varphi)$ and $K_{mn}(x, \varphi)$, respectively, are replaced with $p(x, \varphi; \eta)$ and a sampling function $K_{mn}(x, \varphi; \eta)$ that compensates for the losses has also been considered,³⁷

$$K_{mn}(x, \varphi; \eta) = \langle m | \hat{K}(x, \varphi; \eta) | n \rangle, \quad (96)$$

where

$$\hat{K}(x, \varphi; \eta) = \frac{1}{2\pi} \int dz |z| \exp\left\{ iz [\hat{x}(\varphi) - x] + \frac{1}{4}(\eta^{-1} - 1)z^2 \right\} \quad (97)$$

(D'Ariano [1995]; D'Ariano, Leonhardt and Paul, H., [1995]; Leonhardt, Paul, H., and D'Ariano [1995]; D'Ariano [1997a]; D'Ariano and Paris [1997a]). It has been shown that $K_{mn}(x, \varphi; \eta)$ is a well-behaved bounded function provided that $\eta > 1/2$.

It is worth noting that the reconstruction formula (91) also applies to other than harmonic-oscillator systems (Leonhardt and Raymer [1996]; Richter, Th., and Wünsche [1996a,b]; Krähmer and Leonhardt [1997b, 1997c]; Leonhardt [1997a]; Leonhardt and Schneider [1997]). To be more specific, $p(x, \varphi)$ in terms of ϱ_{mn} reads as³⁸

$$p(x, \varphi) = \sum_{m,n} g_{mn}(x) e^{-i(m-n)\varphi} \varrho_{mn}, \quad (98)$$

³⁷Equation (96) follows from eqs. (B.31) and (B.32), expressing $\Psi(z, \varphi)$ in terms of $\Psi(z, \varphi; \eta)$; see footnote 7.

³⁸Note that substituting in eq. (91) for $p(x, \varphi)$ the expression on the right-hand side of eq. (98), carrying out the φ integral and using the orthonormalization relation (100) just yields an identity.

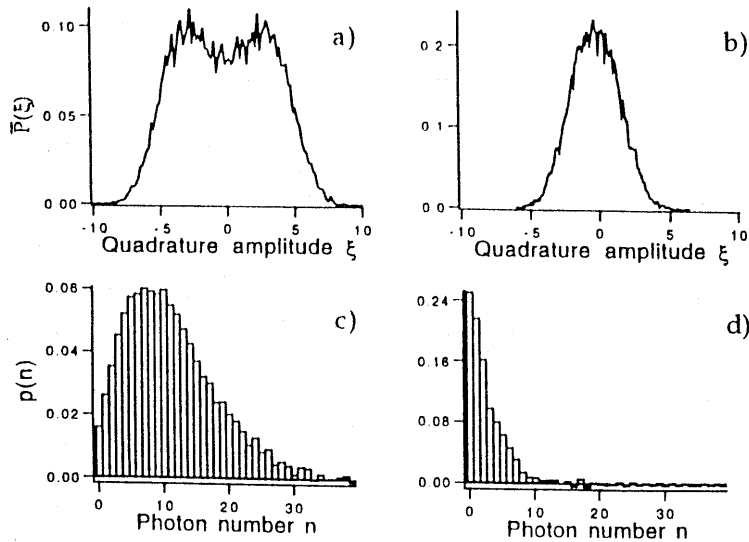


Figure 14: Measured phase-averaged quadrature-component distributions for (a) $t=4.0$ ns and (b) $t=6.0$ ns, and the the resulting time-resolved photon-number distributions for (c) $t=4.0$ ns and (d) $t=6.0$ ns, obtained from (a) and (b) by using eq. (95). $\bar{P}(\xi)$ and $p(n)$, respectively, correspond to $\bar{p}(x)$ and p_n . (After Munroe, Boggavarapu, Anderson and Raymer [1995].)

where

$$g_{mn}(x) = \psi_m(x) \psi_n(x), \quad (99)$$

and from eqs. (91) and (98) together with eqs. (92), (94) and (99) it follows that the functions $\pi f_{mn}(x)$, eq. (94), are orthonormal to products of energy eigenfunctions $g_{mn}(x)$, eq. (99),

$$\pi \int dx f_{mn}(x) g_{m'n'}(x) = \delta_{mm'} \delta_{nn'} \quad \text{for} \quad E_m - E_n = E_{m'} - E_{n'}. \quad (100)$$

It can be shown that $\psi_m(x)$ and $\varphi_m(x)$ can be the regular and irregular solutions, respectively, which solve a Schrödinger equation

$$\left[-\frac{1}{2} \frac{d^2}{dx^2} + U(x) \right] \phi_m(x) = E_m \phi_m(x) \quad (101)$$

for chosen energy E_m , with $U(x)$ being an arbitrary potential.³⁹ This offers the possibility of reconstruction of the density matrix (in the energy representation) of a particle in an arbitrary one-dimensional potential $U(x)$ from the time-dependent position distribution of the particle. The quadrature-component distribution in eq. (91) has to be regarded as a time-dependent position distribution $p(x, t) = \langle x | \hat{\rho}(t) | x \rangle$ and the phase integral converts into a time integral,

$$\varrho_{mn} = \lim_{T \rightarrow \infty} \frac{\pi}{T} \int_{-T/2}^{+T/2} dt \int dx e^{i\nu_{mn}t} f_{mn}(x) p(x, t), \quad (102)$$

$[\varrho_{mn} = \varrho_{mn}(t)|_{t=0}$; ν_{mn} , transition frequencies]. Obviously, the position distribution $p(x, t)$ can also be used for reconstruction of other quantum-state representations,

³⁹For a proof, see, e.g., Leonhardt and Schneider [1997]; Leonhardt [1997c].

such as tomographic reconstruction of the Wigner function. Note that the time interval T , in which the position distribution can be measured is limited in general (for a data analysis scheme for determining the quantum state of a freely evolving one-dimensional wave packet, see Raymer [1997]; see also § 4.4.1.).

In the numerical implementation of eq. (91) [or eq. (102)] the sampling function can be calculated on the basis of the analytical result given in eqs. (92) and (94), using appropriate numerical routines (Leonhardt, Munroe, Kiss, Richter, Th., and Raymer [1996]). An alternative way is the direct inversion of the underlying basic equation (98) that expresses the quadrature-component distributions $p(x, \varphi)$ in terms of the density-matrix elements ϱ_{mn} (Tan [1997]).⁴⁰ For any physical quantum state the density-matrix elements ϱ_{mn} must eventually decrease to zero with increasing $m(n)$. Therefore it follows that the expression on the right-hand side of eq. (98) can always be approximated to any desired degree of accuracy by setting $\varrho_{mn} \approx 0$ for $m(n) > n_{\max}$. To obtain the (finite) number of density-matrix elements from the measured quadrature-component distributions, the resulting equation can always be inverted numerically, using standard methods, such as least-squares inversion (Appendix D.; see also § 3.9.2.). It should be pointed out that the method also applies when the detection efficiency is less than unity. Recalling eqs. (19) and (20), it is easily seen that $p(x, \varphi; \eta)$ is related to ϱ_{mn} according to eq. (98), with $g_{mn}(x)$ being replaced with

$$g_{mn}(x; \eta) = \int dx' \psi_m(x') \psi_n(x') p(x - x'; \eta). \quad (103)$$

When the characteristic function $\Psi(z, \varphi)$ of the quadrature-component distribution $p(x, \varphi)$ can be measured directly (§ 4.2.1.), then the density matrix in the Fock basis can be obtained from $\Psi(z, \varphi)$ by replacing in eqs. (91) and (92) the x integral with the z integral over $\underline{f}_{mn}(z)\Psi(z, \varphi)$, where

$$\underline{f}_{mn}(z) = \int dx e^{izx} f_{mn}(x). \quad (104)$$

More explicitly, the result can be given by (Wallentowitz and Vogel, W., [1996b])

$$\varrho_{n+n+k} = \int_0^\pi d\varphi e^{-ik\varphi} \int_0^\infty dz S_n^{(k)}(z) \begin{cases} \operatorname{Re} \Psi(z, \varphi) & \text{if } k \text{ even,} \\ \operatorname{Im} \Psi(z, \varphi) & \text{if } k \text{ odd} \end{cases} \quad (105)$$

($k \geq 0$), with

$$S_n^{(k)}(z) = \frac{\sqrt{2}}{\pi} \sqrt{\frac{2n!}{(n+k)!}} \left(\frac{z}{2}\right)^{k+1} L_n^{(k)}(z^2/2) e^{-z^2/4} \begin{cases} (-2)^{k/2} & \text{if } k \text{ even,} \\ (-2)^{(k-1)/2} & \text{if } k \text{ odd} \end{cases} \quad (106)$$

[$L_n^{(k)}(x)$, Laguerre polynomial].

So far, reconstruction of arbitrary quantum states has been considered, which can require measurement of the quadrature components at a large number of phases (see also §3.9.1.), which reveals that the Pauli problem [i.e., reconstructing a quantum

⁴⁰The underlying basic equation for eq. (102) is given by eq. (98) with $p(x, t)$ and $e^{-i\nu_{mn}t}$ in place of $p(x, \varphi)$ and $e^{-i(m-n)\varphi}$, respectively. Inverting it numerically, the time need not be infinitely large as it might be suggested from the analytical result given in eq. (102) (Opatrný, Welsch and Vogel, W., [1997c]).

state from $p(x, \varphi)$ and $p(x, \varphi + \pi/2)$] cannot be uniquely solved in general. However, if there is some *a priori* information on the quantum state to be reconstructed, then $p(x, \varphi)$ need not be known for all phases within a π interval. In particular when the state is known to be a pure state that is a finite superposition of Fock states,

$$|\Psi\rangle = \sum_{n=0}^{n_{\max}} c_n |n\rangle, \quad (107)$$

then it can be reconstructed from two quadrature-component distributions $p(x, \varphi)$ and $p(x, \varphi + \pi/2)$.⁴¹ In this case the problem reduces to solving blocks of linear equations for the unknown coefficients in the Fock-state expansion of the state (Orłowski and Paul, H. [1994]).⁴²

3.3.2. Sampling of the displaced Fock-states on a circle

From § 2.1.7. we know that in unbalanced homodyning the photon-number distribution of the transmitted signal mode is, under certain conditions, the displaced photon-number distribution of the signal mode, $p_m(\alpha)$, the displacement parameter $\alpha = |\alpha|e^{i\varphi}$ being controlled by the local-oscillator complex amplitude [see eq. (51)]. Expanding the density operator in the Fock basis, $p_m(\alpha)$ can be related to the density matrix of the signal mode as

$$p_m(\alpha) = \langle m, \alpha | \hat{\rho} | m, \alpha \rangle = \sum_{k,n} \langle n | m, \alpha \rangle \langle k | m, \alpha \rangle^* \varrho_{kn}, \quad (108)$$

where the expansion coefficients $\langle n | m, \alpha \rangle$ can be taken from eq. (B.15) or eq. (B.16). Equation (108) can always be inverted in order to obtain ϱ_{mn} in terms of $p_k(\alpha)$ (Mancini, Tombesi and Man'ko, V.I. [1997]; Mancini, Man'ko, V.I., and Tombesi [1997]).⁴³

$$\varrho_{mn} = \sum_{k=0}^{\infty} \int d^2\alpha K_{mn}^k(\alpha) p_k(\alpha), \quad (109)$$

where

$$K_{mn}^k(\alpha) = \langle m | \hat{K}^k(\alpha) | n \rangle = \frac{2}{(1-s)} \left(\frac{s+1}{s-1} \right)^k \langle m | \hat{\delta}(\alpha - \hat{a}; -s) | n \rangle \quad (110)$$

⁴¹The Pauli problem of determining the quantum state of a particle from the position distribution and the momentum distribution has been studied widely, and it has turned out that it cannot be solved uniquely even if the particle moves in a one-dimensional potential and is prepared in a pure but arbitrary state (for the problem including finite dimensional spin systems, see Pauli [1933]; Feenberg [1933]; Kemble [1937]; Reichenbach [1946]; Gale, Guth and Trammell [1968]; Lamb [1969]; Trammell [1969]; Band and Park [1970, 1971]; Park and Band [1971]; d'Espagnat [1976]; Kreinovich [1977]; Corbett and Hurst [1978]; Prugovečki [1977]; Corbett and Hurst [1978]; Vogt [1978]; Band and Park [1979]; Park, Band and Yourgrau [1980]; Ivanović [1981, 1983] Moroz [1983, 1984]; Royer [1985, 1989]; Friedman [1987]; Pavičić [1987]; Wiesbrock [1987]; Busch and Lahti [1989]; Wootters and Fields [1989]; Stulpe and Singer [1990]; Bohn [1991]; Weigert [1991]).

⁴²These coefficients can also be obtained from $p(x, \varphi)$ and $\partial/\partial\varphi p(x, \varphi)|_{\varphi=0}$ (Richter, Th., [1996c]). More generally, it can be shown that a pure state can always be determined from $p(x, \varphi)$ and $\partial/\partial\varphi p(x, \varphi)$, i.e., from the position distribution and its time derivative in the case of a particle that moves in a one-dimensional potential and is prepared in an arbitrary pure state (Feenberg [1933], for the problem, also see Gale, Guth and Trammell [1968]; Royer [1989]).

⁴³Equation (109) directly follows from eqs. (B.20) and (129).

is bounded for $s \in (-1, 0]$, the $\hat{\delta}$ operator being given by eq. (B.19). This offers the possibility of direct sampling of ϱ_{mn} from the displaced Fock-state probability distribution $p_m(\alpha)$.

Since $p_m(\alpha)$ as a function of α for chosen m already determines the quantum state (§§ 2.1.5. and 3.3.3.), it is clear that when m is allowed to be varying, then – in contrast to eq. (109) – $p_m(\alpha)$ need not be known for all complex values of α in order to reconstruct the density-matrix elements ϱ_{kn} from $p_m(\alpha)$. In particular, it is sufficient to know $p_m(\alpha)$ for all values of m and all phases φ , $|\alpha|$ being fixed (Leibfried, Meekhof, King, Monroe, Itano and Wineland [1996]⁴⁴; Opatrný and Welsch [1997]; Opatrný, Welsch, Wallentowitz and Vogel, W., [1997]). For chosen $|\alpha|$ we regard $p_m(\alpha)$ as a function of φ and introduce the Fourier coefficients

$$p_m^s(|\alpha|) = \frac{1}{2\pi} \int_0^{2\pi} d\varphi e^{is\varphi} p_m(\alpha) \quad (111)$$

($s = 0, 1, 2, \dots$), which are related to the density-matrix elements whose row and column indices differ by s as

$$p_m^s(|\alpha|) = \sum_{n=0}^{\infty} G_{mn}^s(|\alpha|) \varrho_{n+s, n}, \quad (112)$$

where

$$G_{mn}^s(|\alpha|) = e^{-|\alpha|^2} m! \sqrt{n!(n+s)!} \times \sum_{j=0}^J \sum_{l=0}^L \frac{(-1)^{j+l} |\alpha|^{2(m+n-j-l)+s}}{j!(m-j)!(n+s-j)!l!(m-l)!(n-l)!}, \quad (113)$$

with $J = \min(m, n+s)$ and $L = \min(m, n)$. Inverting eq. (112) for each value of s yields the sought density matrix. Since there has not been an analytical solution, eq. (112) has been inverted numerically,⁴⁵ setting $\varrho_{mn} \approx 0$ for $m(n) > n_{\max}$ (cf. the last paragraph but two of § 3.3.1.) and using least-squares inversion (Appendix D.; § 3.9.2.). In this way $\varrho_{m+s, m}$ can be given by

$$\varrho_{m+s, m} = \sum_{n=0}^N F_{mn}^s(|\alpha|) p_n^s(|\alpha|), \quad (114)$$

where it is assumed that p_n is measured for $n = 0, 1, 2, \dots, N$, with $N \leq n_{\max}$, and the matrix $F_{mn}^s(|\alpha|)$ is calculated numerically. Combining eqs. (114) and (111), $\varrho_{m+s, m}$ can be given in a form suitable for statistical sampling.

An extension of eq. (112) to nonperfect detection is straightforward. In this case eq. (50) applies, and the measured probability distribution $P_m(\alpha; \eta)$ can be related to $p_m(\alpha)$ as shown in Appendix C.. From eqs. (111) and (C.3) it can be seen that when in eq. (112) the Fourier component $p_m^s(|\alpha|)$ is replaced with the actually measured one, then the matrix $G_{mn}^s(|\alpha|)$ has to be replaced with the matrix

$$G_{mn}^s(|\alpha|, \eta) = \sum_l P_{m|l}(\eta) G_{ln}^s(|\alpha|). \quad (115)$$

⁴⁴Here the method was first used for reconstructing experimentally the density matrix of the center-of-mass motion of a trapped ion (also see § 4.2.2.).

⁴⁵For examples, see, e.g., Opatrný, Welsch, Wallentowitz and Vogel, W., [1997].

Similarly, multichannel detection of the photon-number distribution can be taken into account. In particular when a photon-chopping scheme as outlined in § 2.1.7. is used, then the Fourier components of the measured N -coincidence-event probability distribution can again be related to the density-matrix elements according to eq. (112), but now with

$$G_{mn}^s(|\alpha|, \eta, N) = \sum_{k,l} \tilde{P}_{m|k}(N) P_{k|l}(\eta) G_{ln}^s(|\alpha|) \quad (116)$$

in place of $G_{mn}^s(|\alpha|, \eta)$, where $\tilde{P}_{m|k}(N)$ can be taken from eq. (53).

3.3.3. Reconstruction from propensities

As already mentioned, the displaced-Fock-state probability $p_m(\alpha)$, eq. (108), as a function of α defines for each m a propensity $\text{prob}(\alpha) = \pi^{-1} p_m(\alpha)$ of the type given in eq. (40). The simplest example is the Q function ($m=0$), which can be measured in perfect eight-port balanced homodyne detection, with the vacuum as quantum filter (§ 2.1.4.). Propensities contain all knowable information on the quantum state, and therefore all relevant properties of it can be obtained from them in principle. However, in order to obtain the “unfiltered” quantum state, the additional noise introduced by the filter must be “removed”, which may be an effort in practise.

When the Q function is known, then the density matrix in the photon-number basis can be calculated straightforwardly, using the well-known relation⁴⁶

$$\varrho_{mn} = \langle m | \hat{\varrho} | n \rangle = \frac{\pi}{\sqrt{m!n!}} \left. \frac{\partial^{m+n}}{\partial \alpha^{*m} \partial \alpha^n} e^{|\alpha|^2} Q(\alpha) \right|_{\alpha=\alpha^*=0}, \quad (117)$$

which corresponds to

$$\hat{\varrho} = \pi \exp\left(\hat{a}^\dagger \frac{\partial}{\partial \alpha^*}\right) \exp\left(\hat{a} \frac{\partial}{\partial \alpha}\right) Q(\alpha) \Big|_{\alpha=\alpha^*=0} \quad (118)$$

(Wünsche [1991, 1996a]). Equation (118) can also be extended to other than vacuum filters, in order to obtain the density operator in terms of derivatives of more general propensities of the type given in eq. (40) (Wünsche and Bužek [1997]). In order to obtain the density matrix from the homodyne data measured, derivatives on them must be carried out, which probably could be done with sufficient accuracy only for states that contain very few photons.

In practice it may be more convenient to handle integrals rather than derivatives. It can be shown that⁴⁷

$$\varrho_{mn} = \left(\frac{s-1}{2}\right)^n \sqrt{\frac{n!}{m!}} \sum_{p=0}^{\infty} \int d^2\alpha P(\alpha; s) \alpha^{m-n} \binom{p+n}{p} \left(\frac{1-s}{2}\right)^p L_{p+n}^{m-n} \left(\frac{2|\alpha|^2}{1-s}\right), \quad (119)$$

where $m \geq n$ and $s \leq -1$, $L_n^m(z)$ being the Laguerre polynomial (Paris [1996b]). In particular when $s = 1 - 2\eta^{-1}$, then $P(\alpha; s)$ is just the smoothed Q function measured

⁴⁶Writing $\pi e^{|\alpha|^2} Q(\alpha) = e^{|\alpha|^2} \langle \alpha | \hat{\varrho} | \alpha \rangle = \sum_{m,n} e^{|\alpha|^2} \langle \alpha | m \rangle \langle m | \hat{\varrho} | n \rangle \langle n | \alpha \rangle$ and recalling that $\langle n | \alpha \rangle = (n!)^{-1/2} \alpha^n e^{-|\alpha|^2/2}$, eq. (117) can be derived easily.

⁴⁷Equation (119) can be derived, applying eq. (B.22) to $\hat{F} = |n\rangle\langle m|$ and calculating the c -number function $F(\alpha; s)$ associated with \hat{F} in chosen order. Note that for $s = -1$ the integral form (119) corresponds to the differential form (117).

in nonperfect detection (cf. § 2.1.4.). Unfortunately, eq. (119) is not suitable for statistical sampling, since the integral must be performed first and after that the summation can be carried out. Moreover, the inaccuracies of the measured $P(\alpha; s)$ together with the Laguerre polynomials can give rise to an error explosion in the reconstructed density matrix, so that an exact reconstruction of the density matrix from measured data may be expected to be possible only for states that contain finite (and not too large) numbers of photons. In this case the p sum in eq. (119) can be truncated at $p = N - m$, where the value N has to be chosen large enough to ensure that $\langle \hat{a}^\dagger{}^i \hat{a}^j \rangle = 0$ for $i, j \geq N$. Now the p sum can be performed first, and a (state-dependent) integral kernel for statistical sampling can be calculated (Paris [1996b, 1996c]).

3.4. Multimode density matrices

The extension of the methods outlined in §§ 3.2. and 3.3. to the reconstruction of multimode density matrices from the corresponding multimode joint quadrature-component distributions or multimode joint propensities is straightforward. The situation is somewhat different when combined distributions, i.e., distributions that are related to linear combinations of the modes, are measured. Let us consider the two-mode detection schemes shown in Fig. 4 in § 2.1.3.. When the sum quadrature-component distribution of two modes, $p_S(x, \alpha, \varphi_1, \varphi_2)$, is known for all phases φ_1 and φ_2 within π intervalls and all superposition parameters $\alpha \in (0, \pi/2)$, then it can be shown, on recalling eq. (30), that the reconstruction of the two-mode density matrix in a quadrature-component basis can be accomplished with a three-fold Fourier integral (Opatrný, Welsch and Vogel, W., [1996, 1997b]):

$$\begin{aligned} & \langle x_1 - x'_1, x_2 - x'_2, \varphi | \hat{\rho} | x_1 + x'_1, x_2 + x'_2, \varphi \rangle \\ &= \left(\frac{1}{2\pi} \right)^2 \int dz_1 \int dz_2 e^{-i(x_1 z_1 + x_2 z_2)} \int dx e^{iyx} p_S(x, \alpha, \tilde{\varphi}_1, \tilde{\varphi}_2), \end{aligned} \quad (120)$$

where

$$y = \sqrt{z_1^2 + z_2^2 + (2x'_1)^2 + (2x'_2)^2}, \quad \tan \alpha = \sqrt{\frac{z_2^2 + (2x'_2)^2}{z_1^2 + (2x'_1)^2}}, \quad (121)$$

and

$$\tilde{\varphi}_k = \varphi - \frac{1}{2}\pi + \arg(2x'_k + iz_k) \quad (122)$$

($k = 1, 2$).⁴⁸

The generalization to the N -mode case is straightforward. Suppose that we can measure the probability distribution of a weighted sum of quadratures $\hat{x} = \sum_{k=1}^N f_k(\{\alpha_l\}) \hat{x}_k$, where α_l are $N - 1$ parameters that can be controlled in the experiments, $l = 1, 2, \dots, N - 1$, and f_k are real functions which satisfy $\sum_{k=1}^N f_k^2(\{\alpha_l\}) = 1$ identically for each set of parameters $\{\alpha_l\}$. Let g_l be the inversions of f_k , $g_l[\{f_k(\{\alpha_m\})\}] = \alpha_l$ (i.e., the set $\{\alpha_l\}$ parameterizes the surface of an N -dimensional sphere). From the measured sum quadrature-component probability distribution $p_S(x, \{\alpha_l\}, \{\varphi_k\})$ its characteristic function $\Psi_s(z, \{\alpha_l\}, \{\varphi_k\})$ can be calculated as a Fourier transform.

⁴⁸For an extension to imperfect detection, see Opatrný, Welsch and Vogel, W., [1997b].

The characteristic function of the joint quadrature-component probability distribution can then be calculated as

$$\Psi_j(\{z_k\}, \{\varphi_k\}) = \Psi_s(z, \{g_l(\{z_k/z\}, \{\varphi_k\})\}), \quad (123)$$

[$z \equiv (\sum_{k=1}^N z_k^2)^{1/2}$], from which the N -mode density matrix can be obtained by an N -fold Fourier transform; the whole N -mode density matrix reconstruction is thus accomplished by an $N+1$ -fold integration of the measured data.

In the Fock basis the reconstruction of a two-mode density matrix from the combined quadrature-component distribution $p_s(x, \alpha, \varphi_1, \varphi_2)$ can be accomplished with a four-fold integration (Raymer, McAlister and Leonhardt [1996]; McAlister and Raymer [1997b]; Richter, Th., [1997a]):

$$\langle m_1, m_2 | \hat{\rho} | n_1, n_2 \rangle = \int dx \int_0^\pi d\alpha \int_0^\pi d\varphi_1 \int_0^\pi d\varphi_2 R_{m_1 n_1}^{m_2 n_2}(x, \alpha, \varphi_1 \varphi_2) p_s(x, \alpha, \varphi_1, \varphi_2), \quad (124)$$

where the integral kernel $R_{m_1 n_1}^{m_2 n_2}(x, \alpha, \varphi_1 \varphi_2)$ is suitable for application of statistical sampling. It can be given by

$$R_{m_1 n_1}^{m_2 n_2}(x, \alpha, \varphi_1 \varphi_2) = r_{m_1 n_1}^{m_2 n_2}(x, \alpha) e^{i(m_1 - n_1)\varphi_1} e^{i(m_2 - n_2)\varphi_2}, \quad (125)$$

where

$$r_{m_1 n_1}^{m_2 n_2}(x, \alpha) = \frac{1}{2\pi} \int dy f_{m_2 n_2}(y) \frac{\partial^2}{\partial x^2} \psi_{m_1}\left(\frac{x - y \cos \alpha}{\sin \alpha}\right) \psi_{n_1}\left(\frac{x - y \cos \alpha}{\sin \alpha}\right). \quad (126)$$

Here, $\psi_{m_1}(y)$ and $\psi_{n_1}(y)$ are harmonic-oscillator energy eigenfunctions, and $f_{m_2 n_2}(y)$ is given by eq. (94). An alternative integral expression for $r_{m_1 n_1}^{m_2 n_2}(x, \alpha)$ reads

$$r_{m_1 n_1}^{m_2 n_2}(x, \alpha) = \frac{1}{(2\pi)^2} \int dz |z| e^{-izx} \underline{f}_{m_1 n_1}(z \cos \alpha) \underline{f}_{m_2 n_2}(z \sin \alpha), \quad (127)$$

with $\underline{f}_{mn}(z)$ being given by eq. (104). Since $\underline{f}_{mn}(z)$ is the kernel function for reconstruction of the single-mode density matrix in the Fock basis from the quadrature-component characteristic function $\Psi(z, \phi)$, from eqs. (105) and (106) it is seen that it can be expressed in terms of the associated Laguerre polynomial. Using this in eq. (127), then the integral can be performed to obtain a representation of $r_{m_1 n_1}^{m_2 n_2}(x, \alpha)$ as a finite sum over confluent hypergeometric functions (Richter, Th., [1997a]).

Finally, the problem of reconstruction of the quantum state of unpolarized light was studied, by considering the (two-mode) density operator

$$\hat{\rho} = \sum_{n=0}^{\infty} p_n \left(\frac{1}{n+1} \sum_{k=0}^{\infty} |k, n-k\rangle \langle k, n-k| \right) \quad (128)$$

(Lehner, Leonhardt and Paul, H., [1996]). Obviously, the probability distribution p_n of finding n completely unpolarized photons in the signal field characterizes uniquely the quantum state (128). Two schemes for determining p_n were studied. First, expressions for the sampling function were derived for the case when the two orthogonal polarization modes are delivered to two balanced homodyne detectors and the joint quadrature-component distributions are measured (Krähmer and Leonhardt [1997a]). Second, it was shown that measurement of the quadrature-component distributions of any linearly polarized component of the signal field is sufficient to determine p_n , the corresponding sampling function being closely related to the single-mode function (Richter, Th., [1997b]).

3.5. Local reconstruction of $P(\alpha; s)$

The displaced photon-number statistics that is measurable in unbalanced homodyning (§ 2.1.7.) can be used for a pointwise reconstruction of s -parametrized phase-space functions (Wallentowitz and Vogel, W., [1996a]; Banaszek and Wódkiewicz [1996]).⁴⁹ From eq. (B.21) together with eqs. (B.19) and (B.13) it is easily seen (cf. also Moyacessa and Knight [1993])

$$P(\alpha; s) = \frac{2}{\pi(1-s)} \sum_{m=0}^{\infty} \left(\frac{s+1}{s-1}\right)^m p_m(\alpha). \quad (129)$$

Hence, all the phase-space functions $P(\alpha; s)$, with $s < 1$, can be obtained from $p_m(\alpha)$ for each phase-space point α in a very direct way, without integral transformations. In particular when $s = -1$, then eq. (129) reduces to the well-known result that $Q(\alpha) = \pi^{-1}p_0(\alpha)$, with $p_0(\alpha) = \langle \alpha | \hat{\rho} | \alpha \rangle$. Further, choosing $s = 0$ in eq. (129), we arrive at the Wigner function,

$$W(\alpha) = \frac{2}{\pi} \sum_{m=0}^{\infty} (-1)^m p_m(\alpha). \quad (130)$$

Equation (130) reflects nothing but the well-known fact that the Wigner function is proportional to the expectation value of the displaced parity operator (Royer [1977]).⁵⁰ Experimentally, the method was first applied to the reconstruction of the Wigner function of the center-of-mass motion of a trapped ion (Leibfried, Meekhof, King, Monroe, Itano and Wineland [1996]; § 4.2.2.).

From § 2.1.7. we know that in unbalanced homodyning the quantum efficiency $\eta = |U_{k1}|^2 \eta_D$ is always less than unity even if $\eta_D = 1$, because of $|U_{k1}| < 1$. Equation (129) can be extended to imperfect detection in order to obtain (Wallentowitz and Vogel, W., [1996a]; Banaszek and Wódkiewicz [1997b])⁵¹

$$P(\alpha; s) = \frac{2}{\pi(1-s)} \sum_{m=0}^{\infty} \left[\frac{\eta(s-1)+2}{\eta(s-1)} \right]^m P_m \quad (131)$$

[$\alpha = -(U_{k2}/U_{k1})\alpha_L$, eq. (49)], where the measured photon-number distribution P_m can be regarded as a smoothed displaced photon-number distribution $p_m(\alpha; \eta)$ of the signal mode. The method works very well and is well suited for statistical sampling if $s < 1 - \eta^{-1}$; i.e., when the weighting factors improve the convergence of the series.⁵² Hence reconstruction of the Q function with reasonable precision is always possible if $\eta > 1/2$ (for computer simulations of measurements, see Wallentowitz and Vogel, W., [1996a]; Banaszek and Wódkiewicz [1997b]).

As already mentioned in § 2.3., measurement of the photon-number distribution of a linearly amplified signal can also be used – similarly to measurement of the

⁴⁹For a squeezed coherent local oscillator, see Banaszek and Wódkiewicz [1998].

⁵⁰For proposals of measuring the Wigner function of a particle using this fact, see (Royer [1985, 1989]).

⁵¹This can be easily proved correct, applying eq. (C.4) and expressing $p_m(\alpha)$ in eq. (129) in terms of P_m , eq. (50).

⁵²The feasibility of reconstruction of the Wigner function of truncated states was also demonstrated for $\eta < 1$ (Wallentowitz and Vogel, W., [1996a]).

displaced photon-number statistics in unbalanced homodyning – for reconstructing the quantum state of the signal mode. It can be shown that when the idler mode is prepared in a coherent state, then the phase-space function $P(\alpha; s)$ of the signal mode can be related to the measured photon-number distribution as⁵³

$$P(\alpha; s) = \frac{2g}{\pi(2-g-s)} \sum_{m=0}^{\infty} \left[\frac{\eta_D(s+g-2)+2}{\eta_D(s+g-2)} \right]^m P_m \quad (132)$$

(Kim, M.S., [1997a,b]), where $\alpha = -[(g-1)/g]^{1/2} \alpha_I^*$. Note that the gain factor g and the quantum efficiency η_D of the detector enter separately into eq. (132) [in contrast to $\eta = |U_{k1}|^2 \eta_D$ in eq. (131)].

3.6. Reconstruction from test atoms in cavity QED

Let us now turn to the problem of reconstruction of the quantum state of a high- Q cavity field from measurable properties of test atoms in detection schemes outlined in § 2.4.. Though at a first glance the schemes look quite different from the homodyne detection schemes, there are a number of remarkable similarities between them.

3.6.1. Quantum state endoscopy and related methods

Let us first consider a two-level (test) atom that resonantly interacts with a single-mode cavity field according to a k -photon Jaynes–Cummings model, the atom–field interaction Hamiltonian being given by

$$\hat{H}^{(k)} = \hbar \kappa^{(k)} (\sigma_+ \hat{a}^k + \hat{a}^{\dagger k} \hat{\sigma}_-), \quad (133)$$

which for $k=1$ reduces to eq. (65). When the atoms are initially prepared in superposition states $|\pm\rangle = 2^{-1/2} (|g\rangle \pm e^{-i\psi} |e\rangle)$ and the excited-state occupation probabilities $P_e^\pm(t)$ are measured as functions of time, then the cavity-mode density-matrix elements ϱ_{nn+k} can be determined (Vogel, W., Welsch and Leine [1987]). To be more specific, it can be shown that the difference $P_e^-(t) - P_e^+(t)$ reads as

$$P_e^-(t) - P_e^+(t) = 2 \sum_{n=0}^{\infty} a_n^{(k)} \sin(\Omega_{nn+k} t), \quad (134)$$

where $\Omega_{nn+k} = 2\kappa^{(k)} \{(n+1) \cdots (n+k)\}^{1/2}$, and

$$a_n^{(k)} = \frac{e^{i\psi}}{2i} \varrho_{nn+k} + \text{c.c.}; \quad (135)$$

i.e., the off-diagonal density-matrix elements ϱ_{nn+k} can be obtained directly from the coefficients $a_n^{(k)}$ for two phases ψ , such as $\psi = 0$ and $\psi = \pi/2$. Provided that the interaction time t can be varied in a sufficiently large interval $(0, T)$, the Fourier

⁵³From eq. (C.5) it can be found that for $\alpha=0$, eq. (129) relates the measured distribution P_m to the phase-space function of the detected mode at the origin of the phase space, $P_{\text{det}}(0, s)$. Equation (132) can then be proved correct, using the unitary transformation (63) and expressing $P_{\text{det}}(\alpha, s)$ in terms of phase-space functions of the signal and idler modes by convolution (see also Leonhardt [1994]; Kim, M.S., and Imoto [1995]).

transform of $P_e^-(t) - P_e^+(t)$ consists of sharp peaks, whose values yield the sought coefficients $a_n^{(k)}$ as⁵⁴

$$a_n^{(k)} = \frac{2}{T} \int_0^T dt \sin(\Omega_{nn+k}t) [P_e^-(t) - P_e^+(t)] \quad (136)$$

($T \rightarrow \infty$). To measure the diagonal density-matrix elements ϱ_{nn} , it is sufficient to prepare the atom in the excited state, $P_e(t)|_{t=0} = 1$, and observe (for arbitrary k) the atomic-state inversion $\Delta P = P_e - P_g = 2P_e - 1$,

$$\Delta P(t) = \sum_{n=0}^{\infty} \varrho_{nn} \cos(\Omega_{nn+k}t), \quad (137)$$

from which ϱ_{nn} can be obtained by Fourier transformation.⁵⁵

In cavity QED the 1-photon Jaynes–Cummings model is typically realized, so that the method – also called *quantum state endoscopy* – does not yield the off-diagonal density-matrix elements ϱ_{nn+k} with $k > 1$. When the quantum state is *a priori* known to be a pure state such that ϱ_{mn} is given by $\varrho_{mn} = c_m c_n^*$ with $c_m c_{m+1}^* \neq 0 \forall m$,⁵⁶ then eq. (134) [together with eq. (135)] can be taken at a sufficiently large number of time points (and at least at two phases) in order to obtain [after truncating the state at a sufficiently large photon number n_{\max} according to eq. (107)] a system of conditional equations for the expansion coefficients c_m , which can be solved numerically (Bardroff, Mayr and Schleich [1995]; Bardroff, Mayr, Schleich, Domokos, Brune, Raimond and Haroche [1996]).

The reconstruction problem for arbitrary quantum states can be solved by performing a displacement of the initial state of the cavity field such that $\hat{\varrho}$ is replaced with $\hat{D}^\dagger(\alpha)\hat{\varrho}\hat{D}(\alpha)$, and hence ($k = 1$)

$$\Delta P(t) = \sum_{n=0}^{\infty} \varrho_{nn}(\alpha) \cos(\Omega\sqrt{n+1}t) \quad (138)$$

($\Omega = 2\kappa$, $\kappa \equiv \kappa^{(1)}$), where $\varrho_{nn}(\alpha) = \langle n | \hat{D}^\dagger(\alpha)\hat{\varrho}\hat{D}(\alpha) | n \rangle = \langle n, \alpha | \hat{\varrho} | n, \alpha \rangle$. Now $\varrho_{nn}(\alpha)$ can again be obtained from $\Delta P(t)$ by Fourier transformation, and from $\varrho_{nn}(\alpha)$ the quantum state of the cavity mode can be obtained, applying, e.g., the methods outlined in §§ 3.3.2. and 3.5.. Alternatively, the quantum state can also be reconstructed when the interaction time is left fixed and only $\alpha = |\alpha|e^{i\varphi}$ is varied (Bodendorf, Antesberger, Kim, M.S., and Walther [1998]). Regarding the measured atomic occupation probabilities as functions of $\alpha = |\alpha|e^{i\varphi}$, $\Delta P(t) = \Delta P(t, \alpha)$, and introducing for chosen t and $|\alpha|$ the Fourier coefficients

$$\Delta P^s(t, |\alpha|) = \frac{1}{2\pi} \int_0^{2\pi} d\varphi e^{is\varphi} \Delta P(t, \alpha) \quad (139)$$

⁵⁴If T is not large enough, then the peaks in the Fourier integral contain non-negligible contributions of the tails of the corresponding sinc functions. In this case, the coefficients $a_n^{(k)}$ can be calculated from a set of linear equations obtained from eq. (134) for different times.

⁵⁵For $k=1$ very precise measurements of the Rabi oscillations have been performed recently (Brune, Schmidt–Kaler, Maali, Dreyer, Hagley, Raimond and Haroche [1996]), the peaked structure of the Fourier-transformed data being interpreted as a direct experimental verification of field quantization in a cavity.

⁵⁶This condition is not satisfied, e.g., for even and odd coherent states as typical examples of *Schrödinger-cat*-like states. For even and odd coherent states, see Dodonov, Malkin and Man’ko, V.I., [1974]. For a review of Schrödinger cats, see Bužek and Knight [1995].

($s=0, 1, 2, \dots$), it can be shown that they are related to the density-matrix elements by equations of the form of

$$\Delta P^s(t, |\alpha|) = \sum_n^{\infty} Y_n^s(t, |\alpha|) \varrho_{n+sn} \quad (140)$$

(for explicit expressions for $Y_n^s(t, |\alpha|)$, see Bodendorf, Antesberger, Kim, M.S., and Walther [1998]). Inverting eq. (140), which resembles, in a sense, eq. (112) in § 3.3.2., for each value of s then yields the density matrix of the cavity mode. Similarly to eq. (112), the inversion can be carried out numerically; e.g., by means of least-squares inversion (Appendix D.), choosing an appropriate set of values of $|\alpha|$.

In the two-mode *nonlinear atomic homodyne detection* scheme (Wilkins and Meystre [1991]) it is assumed that the signal cavity mode is mixed with a local-oscillator cavity mode according to the interaction Hamiltonian

$$\hat{H}' = \hbar\kappa \left[\hat{\sigma}_+(\hat{a} + \hat{a}_L) + (\hat{a}^\dagger + \hat{a}_L^\dagger)\hat{\sigma}_- \right]. \quad (141)$$

Equation (138) can then be found treating the effect of the local oscillator semiclassically (i.e., replacing the operator \hat{a}_L with a c number α_L , $\hat{a}_L \rightarrow \alpha_L$). In this case the scheme is obviously equivalent to an initial displacement $\alpha = -\alpha_L$ of the density operator of the cavity mode, so that the atomic-state inversion $\Delta P(t)$ is exactly given by eq. (138). In particular, when $|\alpha_L|$ is sufficiently large, then $\Delta P(t)$ can be rewritten as

$$\Delta P(t) = \frac{1}{2} \left[e^{i2\kappa t|\alpha_L|} \Phi\left(ie^{i\varphi_L}\kappa t\right) + \text{c.c.} \right]. \quad (142)$$

In other words, for $|\alpha_L| \rightarrow \infty$ the atomic occupation probabilities $P_{e(g)}(t)$ can be related directly to the characteristic function $\Phi(\beta)$ of the Wigner function $W(\beta)$ of the cavity mode. Varying the interaction time and the phase φ_L of α_L , the whole function $\Phi(\beta)$ can be scanned in principle. Knowing $\Phi(\beta)$, the Wigner function can then be obtained by Fourier transformation.⁵⁷ Since for appropriately chosen arguments $\Phi(\beta)$ is nothing but the characteristic function of the quadrature-component distribution $p(x, \vartheta)$ for all values of ϑ within a π interval (see Appendix B.5.), the density matrix in both a quadrature-component basis and the photon number basis can be reconstructed straightforwardly from eq. (142) (§§ 3.2. and 3.3.1.). Later it was found that the semiclassical treatment of the local oscillator restricts the time scale to times less than a vacuum Rabi period, because of the quantum fluctuations in the local-oscillator cavity mode (Zaugg, Wilkins and Meystre [1993]; Dutra, Knight and Moya-Cessa [1993]), and it was shown that this difficulty can be overcome when the atoms are weakly coupled to the local oscillator but strongly coupled to the signal (Dutra and Knight [1994]).

A priori knowledge on the quantum state to be measured is required in *magnetic tomography* (Walser, Cirac and Zoller [1996]). Here, the idea of quantum state mapping between multilevel atoms and cavity modes prepared in truncated states (Parkins, Marte, Zoller, Carnal and Kimble [1995]) is combined with a tomography of atomic angular momentum states by Stern-Gerlach measurements (Newton and Young [1968]). It is assumed that an angular-momentum degenerate two-level atom

⁵⁷Recall that in the dispersive regime the Wigner function can be measured directly (Lutterbach and Davidovich [1997]; see § 2.4.), without any reconstruction algorithm.

passes adiabatically through the spatial profile of a classical laser beam [Rabi frequency: $\Omega(t)$] and, with a spatiotemporal displacement $\tau > 0$, through the profile of a quantized cavity mode [atom–cavity coupling: $g(t - \tau)$] such that the coupled atom–cavity system evolves according to the time-dependent Hamiltonian

$$\begin{aligned} \hat{H}(t) = & \hbar\omega\hat{a}^\dagger\hat{a} + \hbar\omega_{eg} \sum_{m_e=-J_e}^{J_e} |J_e, m_e\rangle\langle J_e, m_e| \\ & - i\hbar\Omega(t) \left(e^{i\omega_L t} \hat{A}_1 - \hat{A}_1^\dagger e^{-i\omega_L t} \right) + i\hbar g(t-\tau) \left(\hat{a}^\dagger \hat{A}_0 - \hat{A}_0^\dagger \hat{a} \right), \end{aligned} \quad (143)$$

where the atomic deexcitation operators $\hat{A}_0, \hat{A}_{\pm 1}$ are defined by

$$\hat{A}_\sigma = \sum_{|m_g| \leq J_g, |m_e| \leq J_e} |J_g, m_g\rangle\langle J_e, m_e| C_{\sigma, m_g, m_e}^{1, J_g, J_e}, \quad (144)$$

$C_{\sigma, m_g, m_e}^{1, J_g, J_e}$ being Clebsch–Gordan coefficients.

It can be shown that if the time-dependent change of the Hamiltonian during the total interaction time is much less than the characteristic transition energies and if the delay and shape of the pulse sequences are chosen such that

$$0 \xleftarrow{-\infty \leftarrow t} g(t-\tau)/\Omega(t) \xrightarrow{t \rightarrow +\infty} \infty, \quad (145)$$

then a coupled atom–cavity-field density operator $\hat{\varrho}_{AF}$ that can be factorized initially into a pure atomic state and a field state containing less than $2J_g$ photons will be mapped to a product of atomic ground state superpositions and the cavity vacuum

$$|J_g, J_g-1\rangle\langle J_g, J_g-1| \otimes \hat{\varrho}_F \xleftarrow{-\infty \leftarrow t} \hat{\varrho}_{AF}(t) \xrightarrow{t \rightarrow +\infty} \hat{\varrho}_A \otimes |0\rangle\langle 0|, \quad (146)$$

with

$$\hat{\varrho}_F = \sum_{m, n=0}^{2J_g-1} (\varrho_F)_{mn} |m\rangle\langle n| \quad (147)$$

and⁵⁸

$$\hat{\varrho}_A = \sum_{m, n=0}^{2J_g-1} s_m s_n (\varrho_F)_{mn} |J_g, J_g-m-1\rangle\langle J_g, J_g-n-1|, \quad (148)$$

s_m, s_n being possible sign changes. Hence, the original cavity-field density matrix $\langle m|\hat{\varrho}_F|n\rangle$ is known if the final atomic density matrix $\langle J_g, J_g-m-1|\hat{\varrho}_A|J_g, J_g-n-1\rangle$ is known. Atomic states of this type can be determined from magnetic dipole measurements using conventional Stern–Gerlach techniques (see § 4.5).

3.6.2. Atomic beam deflection

When a cavity mode is known to be in a pure state, then the expansion coefficients of the state in the photon-number basis can be inferred from the measured deflection of two-level probe atoms during their passage through the cavity (Freyberger and Herkommer [1994]; for an application of related schemes to the reconstruction of the transverse motional quantum state of two-level atoms, see § 4.4.1.). A narrow slit

⁵⁸Note that with reverse adiabatic passage, an internal atomic state is prepared uniquely by reading out the cavity state.

put in front of one node of the standing wave (see Fig. 8) transmits the atoms only in a small region $\Delta x \ll \lambda$ centered around $x=0$ (x , atomic center-of-mass position; λ , wavelength of the mode). The dependence on \hat{x} of the coupling strength $\kappa = \kappa(\hat{x}) = \kappa' \sin(k\hat{x})$ in eq. (65) can then be approximated by $\kappa = \kappa' k \hat{x}$, $k = 2\pi/\lambda$, so that the interaction Hamiltonian of the combined system reads as

$$\hat{H}' = \hbar \kappa' k \hat{x} (\hat{\sigma}_+ \hat{a} + \hat{a}^\dagger \hat{\sigma}_-). \quad (149)$$

It is further assumed that the system is initially prepared in a state $|\Psi\rangle = |\Psi_F\rangle |\Psi_A\rangle$, where

$$|\Psi_F\rangle = \sum_{n=0}^{\infty} c_n |n\rangle, \quad |\Psi_A\rangle = 2^{-1/2} \int dx \psi(x) |x\rangle (|g\rangle + ce^{i\varphi}|e\rangle). \quad (150)$$

The subscripts F and A label the states of the cavity field and the atom, respectively, $\psi(x)$ being the initial wave function of the atomic center-of-mass motion. Assuming $c=1$ and calculating the temporal evolution of the state vector in the Raman–Nath regime,⁵⁹ it can be shown that the atomic momentum probability density for the interaction time t is given by

$$P(p, t) = \frac{1}{4} \hbar k \sum_{n=1}^{\infty} |\underline{\psi}(p + \sqrt{n} \hbar k \kappa' t)|^2 |c_n + e^{i\varphi} c_{n-1}|^2 + \frac{1}{4} \hbar k \sum_{n=1}^{\infty} |\underline{\psi}(p - \sqrt{n} \hbar k \kappa' t)|^2 |c_n - e^{i\varphi} c_{n-1}|^2 + \frac{1}{2} \hbar k |\underline{\psi}(p)|^2 |c_0|^2, \quad (151)$$

where $\underline{\psi}(p)$ is the initial wave function of the atomic center-of-mass motion in the momentum basis. For an initial position distribution $|\psi(x)|^2$, such as a Gaussian, with $\Delta x \ll \lambda$, and sufficiently strong interaction, i.e., $\kappa' t \rightarrow \infty$, the corresponding shifted momentum distribution $|\underline{\psi}(p \pm \sqrt{n} \hbar k \kappa' t)|^2$ becomes sharply peaked at $p = \mp \sqrt{n} \hbar k \kappa' t$, $n = 1, 2, \dots$. In this case, $|\underline{\psi}(p)|^2$ and $|\underline{\psi}(p \pm \sqrt{n} \hbar k \kappa' t)|^2$ obviously select in the measured momentum distribution $P(p, t)$ a sequence of peaks whose heights are proportional to $|c_0|^2$ and $|c_n \pm e^{i\varphi} c_{n-1}|^2$, respectively, for $n=0$ and $n>0$. In this way $|c_0|^2$ and – if the measurement is performed at two phases φ – the sequence of products $c_0^* c_1$, $c_1^* c_2$, \dots can be obtained, from which (after truncating the state at a sufficiently large photon number n_{\max}) the expansion coefficients c_n can be calculated easily (up to an unimportant overall phase factor).⁶⁰

To allow the cavity mode to be prepared in a mixed state, a running reference field aligned along the y -axis (i.e., perpendicular with respect to the standing-wave cavity field aligned along the x -axis and the z -direction of the moving atoms) can be included in the scheme such that the atoms initially prepared in the electronic ground state simultaneously interact with the two fields (Schneider, Herkommer, Leonhardt and Schleich [1997]). In the dispersive regime the effective interaction Hamiltonian

⁵⁹In this approximation it is assumed that the transverse displacement of the atoms during the interaction time t is small compared to the wavelength of the field, so that the kinetic energy of the atomic center-of-mass motion can be disregarded in the Hamiltonian of the combined system. For times longer than the interaction time the now deflected atoms move freely, and the spatial distribution of the atoms on a screen put up far away from the resonator is a picture of their momentum distribution at the moment when they leave the interaction zone.

⁶⁰For an analysis of a diffuse peak structure, see Freyberger and Herkommer [1994].

for the system can then [on extending eq. (66) to two modes] be given by

$$\begin{aligned} \hat{H}'' = \hbar \frac{\kappa^2(\hat{x})}{\delta\omega} (\hat{\sigma}_- \hat{\sigma}_+ \hat{a}^\dagger \hat{a} - \hat{a} \hat{a}^\dagger \hat{\sigma}_+ \hat{\sigma}_-) + \hbar \frac{\kappa_L^2}{\delta\omega} (\hat{\sigma}_- \hat{\sigma}_+ \hat{a}_L^\dagger \hat{a}_L - \hat{a}_L \hat{a}_L^\dagger \hat{\sigma}_+ \hat{\sigma}_-) \\ + \hbar \frac{\kappa(\hat{x})\kappa_L}{\delta\omega} [(\hat{\sigma}_- \hat{\sigma}_+ - \hat{\sigma}_+ \hat{\sigma}_-) (\hat{a}^\dagger \hat{a}_L e^{i\hat{y}} + e^{-i\hat{y}} \hat{a}_L^\dagger \hat{a})]. \end{aligned} \quad (152)$$

Here the index L refers to the running reference field, which has the same frequency as the cavity field and can play a similar role as the local oscillator in a homodyne detector. In the calculations it is assumed that the atoms are initially prepared in a state $|\Psi_A\rangle$ of the form given in eq. (150) with $c=0$, and the reference field is prepared in a strong coherent state and can be treated classically ($\hat{a}_L \rightarrow \alpha_L = |\alpha_L| e^{i\varphi_L}$, $|\alpha_L| \rightarrow \infty$).⁶¹ The cavity field can be prepared in an arbitrary mixed state described by a density operator $\hat{\rho}$. Again making the approximation $\kappa(\hat{x}) \approx \kappa' k \hat{x}$ and assuming that the initial atomic wave function $\psi(x, y)$ factorizes into a very narrow y -wave function $\cong \delta(y - y_0)$ and a Gaussian in the x -direction, it can be shown that the transverse momentum distribution $P(p, t)$ of the atoms for an interaction time t is a (scaled) smeared quadrature-component distribution $p(x, \varphi; \eta)$ of the cavity mode,

$$P(p, t) = \frac{\eta}{\sqrt{2}|\tilde{\kappa}|} p\left(x = \frac{p}{\sqrt{2}|\tilde{\kappa}|}, \varphi; \eta\right), \quad (153)$$

$\tilde{\kappa} = \Omega_L \kappa' \hbar k |\alpha_L| t / \delta$. Here, the quantum efficiency η with which the quadrature-component distribution is measured is given by

$$\eta = \left(1 + \frac{(\hbar k)^2}{2(\Delta x)^2 \tilde{\kappa}^2}\right)^{-1}, \quad (154)$$

and the phase φ is determined by the reference-field phase and the position y_0 , $\varphi = -\varphi_L - k y_0$. The result proves that the atomic probe carries the (smeared) quadrature-component information on the cavity field that corresponds to the reference angle φ . Hence, after having measured the transverse momentum probability distribution $P(p, t)$ of the deflected atoms for a sequence of phases φ_L of the (local-oscillator) reference field, the phase-space function $P(q, p; s = 1 - \eta^{-1})$ of the cavity mode can be reconstructed from eq. (75) by means of tomographic imaging (§ 3.1.). Note that the larger the effective coupling constant $\tilde{\kappa}$ is, the closer is $P(p, q; s)$ to the Wigner function. However the initial position uncertainty must not exceed a fraction of the wavelength of the cavity mode, because of the approximations made. Needless to say, the interaction time t must be small compared to the decay time of the cavity mode.

3.7. Alternative proposals

Since the quantum state of a radiation field mode is known when its density-matrix elements ϱ_{mn} in the photon-number basis are known, it was proposed to measure them directly (Steuernagel and Vaccaro [1995]). The diagonal elements can be measured by direct photodetection in principle. In order to measure the off-diagonal elements,

⁶¹Note that an atom that is initially in the electronic ground state ($c=0$) stays in the electronic ground state, because of the effective Hamiltonian (152).

it was proposed to prepare a probe field in a superposition of two photon-number states,

$$|a_{mn}\rangle = N_a(|m\rangle + a|n\rangle), \quad (155)$$

$N_a = (1 + |a|^2)^{-1/2}$, and combine it with the signal mode at a beam splitter. The observed joint photon-number probability in the two output channels of the beam splitter then reads as ($m > n$)

$$p_{q,k+m-q} \sim \langle b_{kl} | \hat{\rho} | b_{kl} \rangle, \quad (156)$$

$l - k = m - n$, where $|b_{kl}\rangle$ is again a state of the type given in eq. (155), so that

$$\langle b_{kl} | \hat{\rho} | b_{kl} \rangle = N_b^2 \left(\varrho_{kk} + |b|^2 \varrho_{ll} + b \varrho_{kl} + b^* \varrho_{kl}^* \right). \quad (157)$$

When for chosen difference $k - l = n - m$ the diagonal elements ϱ_{ll} and ϱ_{kk} are known from a direct photon-number measurement, then the off-diagonal elements $\varrho_{k,k+m-n}$, $k = 0, 1, 2, \dots$, can be obtained from two (ensemble) measurements for different superposition parameters. The whole density matrix can then be obtained by means of a succession of (ensemble) measurements, varying the difference $m - n$ of photon numbers in the reference state (155) from measurement to measurement. The presently unresolved problem, however, consists in building an apparatus that prepares travelling waves in superpositions of two photon-number states $|m\rangle$ and $|n\rangle$ for arbitrary difference $m - n$ in a controllable way.

For a radiation-field mode that is known to be prepared in a pure state $|\Psi\rangle$ and that contains only a finite number of photons, eq. (107), it was proposed to extend the method of photon chopping outlined in § 2.1.7. to a complete determination of the expansion coefficients c_n (Paul, H., Törmä, Kiss and Jex [1996a, 1997a]).⁶² First the photon-number distribution $p_n = |c_n|^2$ is determined according to eqs. (52) – (54). Then the balanced $2N$ -port apparatus ($N \geq n_{\max}$) is used for mixing the signal mode with $N - 2$ reference modes in the vacuum state and one reference mode prepared in a coherent state $|\alpha\rangle$ (in place of the N vacuum reference inputs in § 2.1.7.). Using the selected statistics when only photons in the first $N/2$ output channels are observed, it can be shown that the probability $p_n(N)$ of detecting n photons with at most one photon in each channel is given by (Paul, H., Törmä, Kiss and Jex [1996a])

$$p_n(N) = \binom{N/2}{n} \frac{e^{-|\alpha|^2}}{N^n} \left| \sum_{m=0}^n \binom{n}{m} \sqrt{(n-m)!} \alpha^m c_{n-m} \right|^2. \quad (158)$$

Determining the coincidence probability distribution $p_n(N)$ for two coherent states with different phases, the phases φ_n of the expansion coefficients $c_n = |c_n| e^{i\varphi_n}$ can be calculated step by step (for known amplitudes $|c_n|$ and up to an overall unimportant phase) from the two measured coincidence-event distributions. More involved formulas are obtained in the case when the complete coincidence statistics is included in the analysis; i.e., photons are allowed to be observed in any output channel and realistic photodetection is considered (Paul, H., Törmä, Kiss and Jex [1997a]). It turns out that the reconstruction scheme with two coherent states requires photodetectors that

⁶²For a proposal to extend the method to a two-mode signal field, see Paul, H., Törmä, Kiss and Jex [1997b].

can discriminate between 0, 1, 2, . . . photons, i.e., detectors that have rather low quantum efficiency. Using avalanche photodiodes, which can have high quantum efficiency, the reconstruction might become rather involved, because additional reference beams with different phase properties must be used. Similarly, when a mixed quantum state is tried to be reconstructed, then extra reference beams (reference phases) must be used, the maximum number of reference beams being limited by the cutoff in the photon number.

It can also be shown (Białynicka-Birula and Białynicki-Birula [1994]; Vaccaro and Barnett [1995]) that when a radiation-field mode is prepared in a pure state $|\Psi\rangle$ that is a finite superposition of photon-number states, eq. (107), then it can be reconstructed from the photon-number distribution $p_n = |c_n|^2$ and the (Pegg–Barnett)⁶³ truncated canonical phase distribution $P_{PB}(\phi) = |\psi(\phi)|^2$, with⁶⁴

$$\psi(\phi) = |\psi(\phi)|e^{i\lambda(\phi)} = \frac{1}{\sqrt{n_{\max}+1}} \sum_{n=0}^{n_{\max}} |c_n| e^{i\varphi_n} e^{in\phi}. \quad (159)$$

Taking eq. (159) at $2(n_{\max}+1)$ values of ϕ , such as $\phi_l = l\pi/(n_{\max}+1)$, the resulting equations can be regarded as conditional equations for the unknown phases φ_n , provided that all absolute values $|\psi(\phi_l)|$ and $|c_n|$ are known. Apart from the fact that the quantum state must be known to be a pure state, the question remains of how to obtain the phase statistics (see also § 3.8.3.).

3.8. Reconstruction of specific quantities

Since the density matrix in any basis contains the full information about the quantum state of the system under consideration, all quantum-statistical properties can be inferred from it. Let \hat{F} be an operator whose expectation value,

$$\langle \hat{F} \rangle = \sum_{mn} F_{nm} \varrho_{mn}, \quad (160)$$

is desired to be determined. One may be tempted to calculate it from the reconstructed density matrix (or another measurable quantum-state representation). However, an experimentally determined density matrix always suffers from various inaccuracies which can propagate (and increase) in the calculation process (cf. § 3.9.1.). Therefore it may be advantageous to determine directly the quantities of interest from the measured data, without reconstructing the whole quantum state. In particular, substituting in eq. (160) for ϱ_{mn} the integral representation (91) one can try to obtain an integral representation

$$\langle \hat{F} \rangle = \int_0^\pi d\varphi \int dx K_F(x, \varphi) p(x, \varphi), \quad (161)$$

with

$$K_F(x, \varphi) = \sum_{mn} F_{nm} f_{mn}(x) e^{i(m-n)\varphi}, \quad (162)$$

suitable for direct sampling of $\langle \hat{F} \rangle$ from the quadrature component distributions $p(x, \varphi)$ [provided that both the sampling function $K_F(x, \varphi)$ and the integral in eq. (161) exist].

⁶³See Pegg and Barnett [1988].

⁶⁴Note that $\psi(\phi) = \langle \Phi_{PB}(\phi) | \Psi \rangle$, where $|\Psi\rangle$ is given by eq. (107), and the truncated phase state $|\Phi_{PB}(\phi)\rangle$ reads as $|\Phi_{PB}(\phi)\rangle = (n_{\max}+1)^{-1/2} \sum_{n=0}^{n_{\max}} e^{-in\phi} |n\rangle$ (cf. § 3.8.3.).

3.8.1. Normally ordered photonic moments

It is often sufficient to know some moments of the photon creation and destruction operators of a radiation-field mode rather than its overall quantum state. Let us again consider the measurement of the quadrature-component probability distributions $p(x, \varphi)$ in balanced homodyning (§ 2.1.2.). Then the normally ordered moments of the creation and destruction operators, $\langle \hat{a}^{\dagger n} \hat{a}^m \rangle$ can be related to $p(x, \varphi)$ as⁶⁵

$$\langle \hat{a}^{\dagger n} \hat{a}^m \rangle = \frac{n!m!}{\pi 2^{(n+m)/2} (n+m)!} \int_0^\pi d\varphi \int dx p(x, \varphi) H_{n+m}(x) e^{i(m-n)\varphi}, \quad (163)$$

where $H_n(x)$ is the Hermite polynomial (Richter, Th., [1996b]).⁶⁶ Equation (163) is just of the type given in eq. (161) and offers the possibility of direct sampling of normally ordered moments $\langle \hat{a}^{\dagger n} \hat{a}^m \rangle$ from the homodyne data. It is worth noting that knowledge of $p(x, \varphi)$ at all phases within a π interval is not necessary to reconstruct $\langle \hat{a}^{\dagger n} \hat{a}^m \rangle$ exactly, and therefore the φ integral in eq. (163) can be replaced with a sum. It was shown that any normally ordered moment $\langle \hat{a}^{\dagger n} \hat{a}^m \rangle$ can already be obtained from $p(x, \varphi)$ at $N = n + m + 1$ discrete different phases φ_k (Wünsche [1996b, 1997]).

The method is especially useful, e.g., for a determination of the moments of photon number. Note that for finding the mean number of photons $\langle \hat{n} \rangle$ from the Fock-basis density matrix a relatively large number of measured diagonal elements ϱ_{nn} must be included into the calculation, in general, each of which being determined with some error. After calculation of the sum $\langle \hat{n} \rangle = \sum_n n \varrho_{nn}$ the error of the result can be too large to be acceptable, and for higher-order moments severe error amplification may be expected. Equation (163) can easily be extended to nonperfect detection ($\eta < 1$), since replacing $p(x, \varphi)$ with $p(x, \varphi; \eta)$ simply yields $\eta^{(n+m)/2} \langle \hat{a}^{\dagger n} \hat{a}^m \rangle$.⁶⁷

Provided that the whole manifold of moments $\langle \hat{a}^{\dagger n} \hat{a}^m \rangle$ has been determined, then the quantum state is known in principle (Wünsche [1990, 1996b]; Lee [1992]; Herzog [1996b]).⁶⁸ To be more specific, the density operator can be expanded as [cf. eq. (69)]

$$\hat{\varrho} = \sum_{k,l=0}^{\infty} \hat{a}_{k,l} \langle \hat{a}^{\dagger k} \hat{a}^l \rangle, \quad (164)$$

where

$$\hat{a}_{k,l} = \sum_{j=0}^{\{k,l\}} \frac{(-1)^j |l-j\rangle \langle k-j|}{j! \sqrt{(k-j)! (l-j)!}} \quad (165)$$

$\{k, l\} = \min(k, l)$, provided that $\langle \hat{a}^{\dagger k} \hat{a}^l \rangle$ exists for all values of k and l and the series (164) (in chosen basis) exists as well. Since all the moments do not necessarily exist for

⁶⁵Equation (163) can be proven correct if both sides are expressed in terms of the density matrix in the photon-number basis and standard summation rules for the Hermite polynomials are used.

⁶⁶A more involved transformation was suggested by Białynicka-Birula and Białynicki-Birula [1995]; see footnote 77.

⁶⁷Recall that an imperfect detector can be regarded as a perfect detector with a beam splitter in front of it, so that the destruction operator \hat{a} of the mode that is originally desired to be detected is transformed according to a beam-splitter transformation (§ 2.1.1.), $\hat{a}(\eta) = \sqrt{\eta} \hat{a} + \sqrt{1-\eta} \hat{b}$, where \hat{b} is the photon destruction operator of a reference mode prepared in the vacuum state.

⁶⁸This is also true for other than normally ordered moments, such as symmetrically ordered moments (Band and Park [1979]; Park, Band and Yourgrau [1980]).

any quantum state, and the series need not necessarily converge for existing moments, the quantum-state description in terms of density matrices is more universal than that in terms of normally ordered moments.⁶⁹

The extension of the method to the reconstruction of normally-ordered moments of multimode fields from joint quadrature-component distributions is straightforward. Moreover, normally-ordered moments of multimode fields can also be reconstructed from combined distributions considered in § 2.1.3. (Opatrný, Welsch and Vogel, W., [1996, 1997a]; McAlister and Raymer [1997a,b]; Richter, Th., [1997a]). For simplicity, let us restrict attention here to two-mode moments $\langle \hat{a}_1^{\dagger n_1} \hat{a}_2^{\dagger n_2} \hat{a}_1^{m_1} \hat{a}_2^{m_2} \rangle$ (the subscripts 1 and 2 refer to the two modes) and assume that the weighted sum $\hat{x} = \hat{x}_1(\varphi_1) \cos \alpha + \hat{x}_2(\varphi_2) \sin \alpha$, eq. (29), is measured in a homodyne detection scheme outlined in § 2.1.3. (see Fig. 4). Measuring the moment $\langle \hat{x}^n \rangle$ for $n + 1$ values of α , a set of $n + 1$ linear algebraic equations can be obtained whose solution yields the two-mode quadrature-component moments $\langle \hat{x}_1^{n-k}(\varphi_1) \hat{x}_2^k(\varphi_2) \rangle$ ($k = 0, 1, 2, \dots, n$). Varying φ_1 and φ_2 , the procedure can be repeated to obtain the dependence on φ_1 and φ_2 of the two-mode quadrature-component moments. These can then be used to determine the normally ordered moments of the photon creation and destruction operators of the two modes step by step. In a closed form, $\langle \hat{a}_1^{\dagger n_1} \hat{a}_2^{\dagger n_2} \hat{a}_1^{m_1} \hat{a}_2^{m_2} \rangle$ can be obtained from the combined quadrature-component distribution $p_S(x, \alpha, \varphi_1, \varphi_2)$ as

$$\begin{aligned} \langle \hat{a}_1^{\dagger n_1} \hat{a}_2^{\dagger n_2} \hat{a}_1^{m_1} \hat{a}_2^{m_2} \rangle &= C_{n_1 m_1} C_{n_2 m_2} \int dx \int_{\Omega} d\alpha \int_0^{\pi} d\varphi_1 \int_0^{\pi} d\varphi_2 \left[p_S(x, \alpha, \varphi_1, \varphi_2) \right. \\ &\quad \left. \times H_{n_1+n_2+m_1+m_2}(x) F_{n_2+m_2}^{(n_1+n_2+m_1+m_2)}(\alpha) e^{i(n_1-m_1)} e^{i(n_2-m_2)} \right] \quad (166) \end{aligned}$$

[$C_{nm} = n!m! / (\pi 2^{(n+m)/2} (n+m)!)$]. The functions $F_k^{(l)}(\alpha)$ form a biorthonormal system to the functions $G_k^{(l)}(\alpha) = \binom{l}{k} \cos^{l-k} \alpha \sin^k \alpha$ in some Ω interval, so that $\int_{\Omega} d\alpha F_k^{(l)}(\alpha) G_{k'}^{(l)}(\alpha) = \delta_{kk'}$. Note that since for given l there is a finite number of functions $G_k^{(l)}(\alpha)$, the system of functions $F_k^{(l)}(\alpha)$ is not uniquely determined and can be chosen in different ways. In particular when only the phase difference $\Delta\varphi = \varphi_2 - \varphi_1$ is controlled and the overall phase φ_1 is averaged out (this is the case when the signal and the local oscillator stem from different sources), then the moments $\langle \hat{a}_1^{\dagger n_1} \hat{a}_2^{\dagger n_2} \hat{a}_1^{m_1} \hat{a}_2^{m_2} \rangle$ can be reconstructed for $n_1 - m_1 = m_2 - n_2$. If both phases φ_1 and φ_2 are averaged out, then those moments $\langle \hat{a}_1^{\dagger n_1} \hat{a}_2^{\dagger n_2} \hat{a}_1^{n_1} \hat{a}_2^{n_2} \rangle$ can still be obtained, which carry the information about the photon-number correlation in the two modes.

The method was used to experimentally demonstrate the determination of the ultrafast two-time photon number correlation of a 4 ns optical pulse (McAlister and Raymer [1997a]). In the experiment, the local-oscillator pulses are derived from a Ti:sapphire-based laser system which generates ultrashort, near transform-limited pulses (150 fs) at a wavelength of 830 nm and a repetition rate of 1 kHz. The signal is from a single-spatial-mode superluminescent diode. The broadband emission at 830 nm is spectrally filtered to produce a 4 ns pulse having a 0.22 nm spectral width.

⁶⁹An example of nonexisting normally ordered moments is realized by a quantum state whose photon-number distribution behaves like $p_n \sim n^{-3}$ for $n \rightarrow \infty$. Even though it is a normalizable state with finite energy, its moments $\langle \hat{n}^k \rangle$ do not exist for $k \geq 2$. For a thermal state the relation $\langle \hat{a}^{\dagger n} \hat{a}^m \rangle = \delta_{nm} n! \bar{n}^n$ is valid (\bar{n} , mean photon number), which implies that the series (164) for ρ_{mn} does not exist. Note that the problem of nonconvergence of the series (164) may be overcome by analytic continuation.

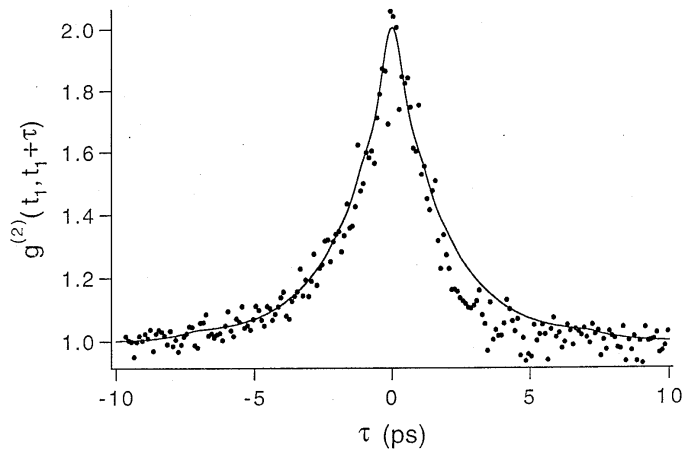


Figure 15: The second-order coherence, eq. (167), experimentally determined via balanced four-port homodyne detection (dots) and from the measured optical spectrum (solid line). The value of t_1 is set to occur near the maximum of the signal pulse. (After McAlister and Raymer [1997a].)

For each value of the relative delay $\Delta t = t_1 - t_2$ between two local-oscillator pulses the phase-averaged combined quadrature-component distribution $\bar{p}_S(x, \alpha) = (2\pi)^{-2} \int d\varphi_1 \int d\varphi_2 p_S(x, \alpha, \varphi_1, \varphi_2)$ is measured for three different values of α : 0, $\pi/2$ and $\pi/4$. From these the normalized second-order coherence function

$$g^{(2)}(t_1, t_2) = \frac{\langle \hat{a}_1^\dagger \hat{a}_2^\dagger \hat{a}_1 \hat{a}_2 \rangle}{\langle \hat{a}_1^\dagger \hat{a}_1 \rangle \langle \hat{a}_2^\dagger \hat{a}_2 \rangle}, \quad (167)$$

is computed (\hat{a}_1 and \hat{a}_2 being the photon destruction operators of the spatial-temporal modes defined by the local-oscillator pulses centered at times t_1 and t_2). This experiment represents an extension of measurements of the Hanbury-Brown–Twiss correlations⁷⁰ to a sub-picosecond region. Results are shown in Fig. 15.

3.8.2. Quantities admitting normal-order expansion

The basic relation (163) can also be used [similar to eqs. (160) – (162)] to find sampling formulas for the mean values of quantities that can be given in terms of normally ordered moments of photon creation and destruction operators (D’Ariano [1997b]). Let us consider an operator \hat{F} and assume that it can be given by a normal-order expansion as

$$\hat{F} = \sum_{n,m=0}^{\infty} f_{nm} \hat{a}^{\dagger n} \hat{a}^m. \quad (168)$$

⁷⁰See Hanbury Brown and Twiss [1956a,b,1957a,b]; for a more discussion of the Hanbury Brown and Twiss experiments, see Peřina [1985], Mandel and Wolf [1995].

The mean value $\langle \hat{F} \rangle$ can then be obtained from $p(x, \varphi; \eta)$ according to⁷¹

$$\langle \hat{F} \rangle = \int_0^\pi d\varphi \int dx K_F(x, \varphi; \eta) p(x, \varphi; \eta), \quad (169)$$

where the integral kernel

$$K_F(x, \varphi; \eta) = \text{Tr} \left[\hat{F} \hat{K}(x, \varphi; \eta) \right] \quad (170)$$

[$\hat{K}(x, \varphi; \eta)$ being defined in eq. (97)] can be given by

$$K_F(x, \varphi; \eta) = \frac{1}{\pi \sqrt{2\pi\eta^{-1}}} \int dy e^{-\eta y^2/2} G_F\left(y + i\sqrt{2\eta^{-1}}x, \varphi\right), \quad (171)$$

with

$$G_F(z, \varphi) = \sum_{n,m=0}^{\infty} f_{nm} \binom{n+m}{m}^{-1} (-iz)^{n+m} e^{i(m-n)\varphi}. \quad (172)$$

Here it is assumed that the integral kernel $K_F(x, \varphi; \eta)$ exists and the x integral in eq. (169) exists as well.⁷² The integral kernel (171) exists if for $z \rightarrow \infty$ the function $G_F(z, \varphi)$ grows slower than $e^{\eta z^2/2}$, so that the integral in eq. (171) converges (for examples, see D'Ariano [1997b]; D'Ariano and Paris [1997b]).⁷³ The integral kernel (171) is therefore applicable to such quantum states whose (smeared) quadrature-component distributions $p(x, \varphi; \eta)$ tend to zero sufficiently fast as $|x|$ goes to infinity such that eq. (169) converges even if $K_F(x, \varphi; \eta)$ increases with $|x|$. At this point it should be noted that $K_F(x, \varphi; \eta)$ is determined only up to a function $\Theta(x, \varphi)$; i.e., $K_F(x, \varphi; \eta)$ in eq. (169) can be replaced with $K'_F(x, \varphi; \eta) = K_F(x, \varphi; \eta) + \Theta(x, \varphi)$ such that

$$\int_0^\pi d\varphi \int dx \Theta(x, \varphi) p(x, \varphi; \eta) = 0 \quad (173)$$

for any normalizable quantum state. Hence, if the integral kernel $K_F(x, \varphi; \eta)$ that is obtained from eq. (171) is unbounded for $|x| \rightarrow \infty$ such that the x integral in eq. (169) does not exist for any normalizable quantum state, it cannot be concluded that \hat{F} cannot be sampled from the quadrature-component distributions of any normalizable quantum state, since a different, bounded kernel may exist.

3.8.3. Canonical phase statistics

The quantum-mechanical description of the phase and its measurement has turned out to be troublesome and is still a matter of discussion. Many papers have dealt with the problem and an extensive literature is available (for reviews, see Lukš and

⁷¹Recall that when the c -number function $F(\alpha; s)$ that is associated with an operator \hat{F} in s order exists for $s \leq -1$, then $\langle \hat{F} \rangle$ can be obtained from the phase-space function $P(\alpha; s)$ (measurable, e.g., in balanced eight-port homodyning; see § 2.1.4.) according to eq. (B.22), provided that the integral exists.

⁷²Equations (169) – (172) can be obtained by taking the average of eq. (168), substituting for $\langle \hat{a}^{\dagger n} \hat{a}^m \rangle$ the right-hand side (multiplied by $\eta^{-(n+m)/2}$) of eq. (163), and using the generating function of the Hermite polynomials with the argument $(i/\sqrt{2\eta})(d/dz)$.

⁷³Since the integral kernel $K_F(x, \varphi; \eta)$ does not depend on φ if \hat{F} is a function of the photon-number operator, this case can be regarded as the first realization of Helstrom's *quantum roulette wheel* (D'Ariano and Paris [1997b]).

Peřinová [1994], Lynch [1995], Royer [1996], Pegg and Barnett [1997]). Here we confine ourselves to the canonical phase that is obtained in the attempt – in close analogy to the classical description – to decompose the photon destruction operator into amplitude and phase such that $\hat{a} = \hat{E}\sqrt{\hat{n}}$. The (nonorthogonal and unnormalizable) phase states,

$$|\phi\rangle = \sum_{n=0}^{\infty} e^{in\phi}|n\rangle \quad (174)$$

(London [1926, 1927]), which are the right-hand eigenstates of the one-sided unitary operator \hat{E} , $\hat{E}|\phi\rangle = e^{i\phi}|\phi\rangle$, can then be used to define – in the sense of a POM – the canonical phase distribution $P(\phi) = \langle \hat{\Pi}(\phi) \rangle$, with $\hat{\Pi}(\phi) = |\phi\rangle\langle\phi|$.⁷⁴ Note that the Hermitian operators $\hat{C} = (\hat{E} + \hat{E}^\dagger)/2$ and $\hat{S} = (\hat{E} - \hat{E}^\dagger)/(2i)$ are the Susskind–Glogower sine and cosine operators (Susskind and Glogower [1964]).⁷⁵

Various proposals have been made to measure $P(\phi)$ using homodyne detection or related schemes.⁷⁶ So the Wigner function or the density matrix reconstructed from the homodyne data could be used to infer the phase statistics in principle (Beck, Smithey and Raymer [1993]; Smithey, Beck, Cooper and Raymer [1993]; Breitenbach and Schiller [1997]). Further it was proposed to obtain $P(\phi) = \langle \hat{\Pi}(\phi) \rangle$ from a homodyne measurement of (all) normally ordered moments $\langle \hat{a}^{\dagger m+n} \hat{a}^n \rangle$, because $\hat{\Pi}(\phi)$ has a series expansion of the type given in eq. (168),

$$\hat{\Pi}(\phi) = (2\pi)^{-1} \left[1 + \sum_{m=1}^{\infty} \sum_{n=0}^{\infty} \left(e^{im\phi} \hat{a}^{\dagger m+n} \hat{a}^n + e^{-im\phi} \hat{a}^{\dagger n} \hat{a}^{m+n} \right) \right], \quad (175)$$

(Białyńska-Birula and Białyński-Birula [1995]).⁷⁷ Unfortunately $\langle \hat{\Pi}(\phi) \rangle$ cannot be given (even for $\eta = 1$) by an integral relation of the form (169) suited to statistical sampling, because the integral kernel does not exist (see footnote 79). It was therefore proposed to introduce parametrized phase distributions $P(\phi, \epsilon)$ such that for any $\epsilon > 0$ $P(\phi, \epsilon)$ can be obtained by direct sampling from $p(x, \varphi)$, and $P(\phi, \epsilon) \rightarrow P(\phi)$ for $\epsilon \rightarrow 0$ (Dakna, Knöll and Welsch [1997a,b]). The sampling functions can then be obtained as convergent sums of the sampling functions for the density-matrix elements in the Fock-basis (see § 3.3.). Since the value of the parameter ϵ for which $P(\phi, \epsilon) \approx P(\phi)$ is determined by the number of photons at which the quantum state under study can effectively be truncated, the method is state-dependent. Further, it was proposed to measure the canonical phase by projection synthesis, mixing the signal mode with a reference mode that is prepared in a quantum state such that, for appropriately chosen parameters, the joint-photon-number probabilities in the two output channels of the beam splitter directly correspond to the canonical phase statistics of the signal mode (Barnett and Pegg [1996]; Pegg, Barnett and Phillips [1997]). Apart from the

⁷⁴For a two-mode orthogonal projector realization in the relative-photon-number basis, see Ban [1991a–d, 1992, 1993]; Hradil [1993].

⁷⁵For constructing the operators corresponding to classical phase-dependent quantities, see Bergou and Englert [1991].

⁷⁶The proposal was made to regard the quadrature-component distribution at $x=0$ as (unnormalized) phase distribution, $P(\phi) \sim p(x=0, \phi)$ (Vogel, W., and Schleich [1991]), which yields a phase statistics that is quite different from the canonical phase statistics in general (for an improvement, see Bužek and Hillery [1996]).

⁷⁷Here it was proposed to obtain $\langle \hat{a}^{\dagger m+n} \hat{a}^n \rangle$ from the homodyne data via the $(2n+m)$ th derivative of $\int_0^{2\pi} d\varphi e^{-im\varphi} e^{-\lambda^2/2} \langle \exp[i\lambda\hat{x}(\varphi - \pi/2)] \rangle$.

direct photon-number measurement needed and the fact that the quantum state under study must again be truncated, so that the method is state-dependent, the difficult problem remains to design an apparatus that produces the reciprocal binomial states needed.

The problem of homodyne measurement of the canonical phase can be solved when the exponential phase moments Ψ_k [i.e., the Fourier components of $P(\phi)$] are considered and not the phase distribution itself,

$$P(\phi) = (2\pi)^{-1} \sum_{k=-\infty}^{+\infty} e^{-ik\phi} \Psi_k, \quad (176)$$

where $\Psi_k = \langle \hat{E}^k \rangle$ if $k > 0$, and $\Psi_k = \Psi_{-k}^*$ if $k < 0$ ($\Psi_0 = 1$). Then it can be shown that ($k > 0$)

$$\Psi_k = \int_0^{2\pi} d\varphi \int dx e^{ik\varphi} K_k(x) p(x, \varphi) \quad (177)$$

(Opatrný, Dakna and Welsch [1997, 1998]; Dakna, Opatrný and Welsch [1998]). The integral kernel $K_k(x)$ (Fig. 16) can be used for sampling the exponential phase moments from the homodyne data for any normalizable state.⁷⁸ In particular, $K_k(x)$

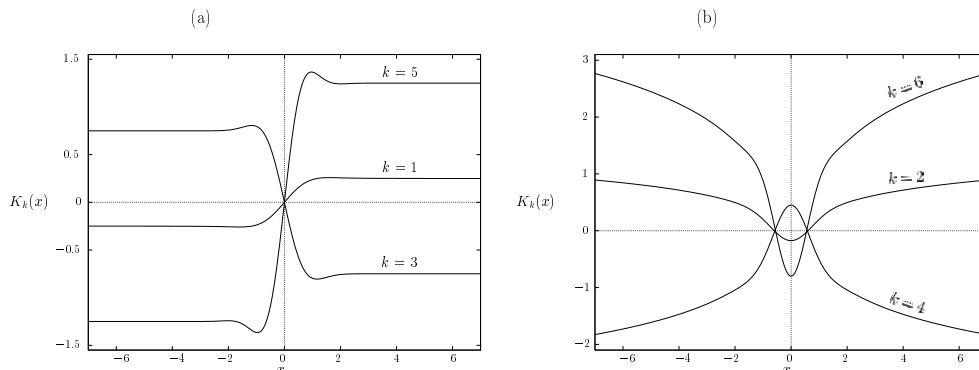


Figure 16: The x -dependent part $K_k(x)$ of the sampling function $K_k(x, \varphi) = e^{ik\varphi} K_k(x)$ for the determination of the exponential moments $\Psi_k = \langle \hat{E}^k \rangle$ of the canonical phase from the quadrature-component distributions $p(x, \varphi)$ according to eq. (177) for various (a) odd and (b) even k . (After Dakna, Opatrný and Welsch [1998].)

rapidly approaches the classical limit⁷⁹

$$K_k^{(cl)}(x) = \begin{cases} \frac{1}{4}(-1)^{(k-1)/2} k \operatorname{sign} x & \text{if } k \text{ odd,} \\ (2\pi)^{-1}(-1)^{(k+2)/2} k \ln x & \text{if } k \text{ even} \end{cases} \quad (178)$$

as $|x|$ increases, and it differs from the classical limit only in a small interval around the origin. It is worth noting that the method applies to quantum and classical

⁷⁸Note that when $K_k(x)$ is calculated according to eq. (171), then it does not apply to all normalizable states (for analytical expressions and properties of $K_k(x)$, including nonperfect detection, see Dakna, Opatrný and Welsch [1998]).

⁷⁹Already from the classical kernel (178) it is seen that $\sum_{k=-\infty}^{+\infty} e^{ik(\varphi-\phi)} K_k(x)$ does not exist, and hence $P(\phi)$ cannot be obtained from $p(x, \varphi)$ by means of an integral transformation of the form given in eq. (177).

systems in a unified way and bridges the gap between quantum and classical phase. In particular, the integral kernel $K_k^{(cl)}(x)$ as given in eq. (178) is nothing but the integral kernel for determining the radially integrated Wigner function, which reveals that in the classical limit the canonical phase distribution is simply the radially integrated probability density for the complex amplitude α . Note that any radially integrated propensity $\text{prob}(\alpha)$, such as the radially integrated Q function measurable, e.g., in balanced eight-port homodyne detection, can be used to define an operational phase probability density (Noh, Fougères and Mandel [1991, 1992a,b, 1993a,b,c]), which in the quantum regime differs from the canonical phase distribution in general (for further readings, see Turski [1972]; Paul, H., [1974]; Shapiro, J.H., and Wagner [1984]; Hradil [1992, 1993]; Vogel, W., and Welsch [1994]; Leonhardt, Vaccaro, Böhmer and Paul, H., [1995]; Leonhardt [1997c]).

3.8.4. Hamiltonian and Liouvillian

So far, measurement and reconstruction of quantum-state representations and averages of particular quantities at certain time have been considered. The quantum state of an object at chosen time t is of course a result of state evolution from an initial time t_0 , the state evolution being governed by the Hamiltonian \hat{H} of the system or a Liouvillian \hat{L} in the more general case of the system being open. Since the Liouvillian of an object expresses in most concentrated form the dynamics of the object, knowledge of the Liouvillian is essential for understanding the behaviour of the object, and the question may arise of how to experimentally determine its form. To answer the question, it was proposed to appropriately apply quantum-state reconstruction routines, such as direct sampling of the density matrix in balanced homodyning (D'Ariano and Maccone [1997]).

Let us consider a system that is initially prepared in some known state $\hat{\rho}_{\text{in}} \equiv \hat{\rho}(t_0)$ and assume that in the further course of time it evolves to a state $\hat{\rho}_{\text{out}} \equiv \hat{\rho}(t)$ at time t ,

$$\hat{\rho}_{\text{out}} = \hat{G} \hat{\rho}_{\text{in}}, \quad (179)$$

where for a system that is homogeneous in time the superoperator $\hat{G} \equiv \hat{G}(t, t_0)$ can be given by the exponential of the (time-independent) Liouvillian \hat{L} of the system,

$$\hat{G} = e^{\hat{L}(t-t_0)}. \quad (180)$$

The superoperators \hat{G} and \hat{L} can then be obtained by measuring (reconstructing) $\hat{\rho}_{\text{out}}$ for various probe inputs $\hat{\rho}_{\text{in}}$. A typical example may be a radiation-field mode which (at time t_0) is fed into a nonlinear resonator-like equipment giving rise to amplification and damping. The quantum state of the outgoing mode (at time t) can then be related to that of the incoming mode according to eq. (179). In the Fock basis, eq. (179) reads as

$$\langle m | \hat{\rho}_{\text{out}} | n \rangle = \sum_{l,k=0}^{\infty} G_{mn}^{lk} \langle l | \hat{\rho}_{\text{in}} | k \rangle. \quad (181)$$

Now let us assume that in a succession of measurements the quantum states of the outgoing mode are reconstructed for an appropriately chosen (overcomplete) set of

input quantum states $\hat{\rho}_{\text{in}}^{\mu}$, $\mu = 1, 2, \dots$, such that for chosen m and n the block of equations

$$\langle m | \hat{\rho}_{\text{out}}^{\mu} | n \rangle = \sum_{l,k=0}^{\infty} G_{mn}^{lk} \langle l | \hat{\rho}_{\text{in}}^{\mu} | k \rangle \quad (182)$$

can be used as conditional equations for the matrix elements G_{mn}^{lk} . Repeating the procedure for all values of m and n , the G matrix and [by using eq. (180)] the L matrix can be calculated in principle. Apart from a truncation of the Hilbert space in numerical implementations, the main problem that remains in practice is of course the (controlled) initial-state preparation such that all (relevant) matrix elements of the Liouvillian can be probed.

In particular, when the Liouvillian is phase-insensitive, then mixtures of Fock states evolves into mixtures of Fock states. For this case a setup was proposed which uses correlated twin beams produced by a nondegenerate parametric amplifier in combination with conditional photon-number measurement on one beam in order to prepare the other beam in (random) photon-number states. These states can then be used as initial states for probing the Liouvillian. To realize the scheme with available techniques, it should be noted that the reconstruction algorithm can be extended such that the quantum efficiency of the photon-number measurement need not be unity (D'Ariano [1997c]).

3.9. Processing of smeared and incomplete data

In practice, there are always experimental inaccuracies that limit the precision with which the quantum state in a chosen representation can be determined. Typical examples of inaccuracies⁸⁰ are data smearing owing to nonperfect detection, finite number of measurement events, and discretization of continuous parameters, such as the quadrature-component phase in balanced homodyning. In particular, the latter is an example of leaving out observables \hat{A}_i in the expansion (69) of the density operator $\hat{\rho}$. Whereas in balanced homodyning the distance between neighboring phases can be diminished such that the systematic error is reduced, in principle, below any desired level, there are also cases in which a principally incomplete set of observables is available. Then either additional knowledge of the quantum state is necessary to compensate for the lack of observables or other principles must be used to reconstruct the density operator according to the actual observation level.

3.9.1. Experimental inaccuracies

Since in a realistic experiment the quantum efficiency η is always less than unity, the probability distributions of the measured quantities are always more or less smeared, because of losses. The problem of compensating for losses in direct sampling of the quantum state from the quadrature-component distributions measurable in balanced homodyning (§ 2.1.2.) has been studied widely. As mentioned in § 2.3., active loss compensation may be realized, in principle, by means of a squeezer, such as a degenerate parametric amplifier (Leonhardt and Paul, H., [1994a]; see also Leonhardt

⁸⁰For limits upon the measurement of state vectors expressed in terms of channel capacities for the transmission of information by finite numbers of identical copies of state vectors, see Jones, K.R.W., [1994].

and Paul, H., [1995]). When the signal mode is preamplified before detection by means of a squeezer [eq. (63) with $e^{i\phi}\hat{a}_S^\dagger$ in place of \hat{a}_I^\dagger], then it can be shown that for appropriately phase matching the (scaled) quadrature-component distribution of the preamplified signal measured with quantum efficiency η reads as⁸¹

$$p'(\sqrt{g}x, \varphi; \eta) = \int dx' p(x', \varphi) p[\sqrt{g}(x-x'); \eta] \quad (183)$$

(g , amplification factor), with $p(x; \eta)$ being given by eq. (20). From eq. (183) together with eq. (20) it is seen that η is effectively replaced with $g\eta/(1-\eta+g\eta)$, and hence $\sqrt{g} p'(\sqrt{g}x, \varphi; \eta)$ tends to $p(x, \varphi)$ as the amplification becomes sufficiently strong.⁸² Note that the degree of improving the quantum efficiency is limited by the realizable mode-matching in degenerate parametric amplification, which deteriorates with increasing pump strength.

Without active manipulation of the signal, it has been well established that above a lower bound for η , it is always possible to compensate for detection losses, introducing a modified sampling function that depends on η such that performing the sampling algorithm on the really measurable (i.e., the smeared) quadrature-component distributions $p(x, \varphi; \eta)$ yields the correct quantum state (D'Ariano, Leonhardt and Paul, H., [1995]). This bound depends on the chosen state representation in general. In particular, reconstruction of the density matrix in the photon-number basis is always possible if $\eta > 1/2$. In this case,

$$\varrho_{mn} = \int_0^\pi d\varphi \int dx K_{mn}(x, \varphi; \eta) p(x, \varphi; \eta), \quad (184)$$

where the now η -dependent sampling function $K_{mn}(x, \varphi; \eta)$ is defined by eq. (96) [together with eq. (97)].

Another approach to the problem of loss compensation is that the sampling function is left unchanged [i.e., $K_{mn}(x, \varphi; \eta) \rightarrow K_{mn}(x, \varphi) = K_{mn}(x, \varphi; \eta = 1)$ in eq. (184)] and, at the first stage, the density matrix $\varrho_{mn}(\eta)$ of the quantum state that corresponds to the smeared quadrature-component distributions $p(x, \varphi; \eta)$ is reconstructed. After that, at the second stage, the true density matrix $\varrho_{mn} = \varrho(\eta = 1)$ is calculated from $\varrho_{mn}(\eta)$ (Kiss, Herzog and Leonhardt [1995]; Herzog [1996a]). Extending the Bernoulli transformation (C.3) and the inverse Bernoulli transformation (C.4) to off-

⁸¹Note that squeezing the local oscillator has the same effect as antisqueezing the signal field under the assumption that the coherent component is large (Kim, M.S., and Sanders [1996]; see also Kim, M.S., [1997b]).

⁸²For details, see also Vogel, W., and Welsch [1994], and for a discussion of eqs. (183) and (20) in terms of moments of the measured quadrature components and those of $\hat{x}(\varphi)$, see Marchiolli, Mizrahi and Dodonov [1997]).

diagonal density-matrix elements, ϱ_{mn} can be calculated from $\varrho_{mn}(\eta)$ as⁸³

$$\varrho_{mn} = \eta^{-(m+n)/2} \sum_{k=0}^{\infty} \binom{n+k}{n}^{1/2} \binom{m+k}{m}^{1/2} \left(1 - \frac{1}{\eta}\right)^k \varrho_{m+k, n+k}(\eta). \quad (185)$$

It is worth noting that eq. (185) is exact. In other words, when (for precisely given overall detection efficiency) $\varrho_{mn}(\eta)$ is exactly known, then ϱ_{mn} can always be calculated precisely, irrespective of the value of η .

In practice however, η is not known precisely in general, and the experimentally determined values of $\varrho_{mn}(\eta)$ always differ from the exact ones. In particular, when $\eta \leq 1/2$ and the error of $\varrho_{mn}(\eta)$ does not vanish with increasing m and n , and when there is no *a priori* information about the quantum state, such as the photon number at which it can be truncated, then ϱ_{mn} cannot be obtained – for chosen number of measurements – from the measured $\varrho_{kl}(\eta)$, because of error explosion. A typical example of such an error is the statistical error with which $\varrho_{mn}(\eta)$ is sampled from the quadrature-component distributions measured in balanced homodyning. In this case loss compensation (for arbitrary quantum states) is only possible if $\eta > 1/2$ (D’Ariano and Macchiavello [1998]).⁸⁴ Clearly when the quantum state to be reconstructed can be truncated at some maximum photon number n_{\max} , then the sum in eq. (185) is finite and the density-matrix elements ϱ_{mn} can also be obtained for $\eta < 1/2$, the accuracy being determined by that of $\varrho_{mn}(\eta)$.

Limitations on variables in real experiments always give rise to systematic errors. This is the case, e.g., when the quadrature components $\hat{x}(\varphi)$ are measured at discrete phases φ_k or when only some part of the π interval can be scanned experimentally (for an example, see § 4.4.1.). In particular, in balanced homodyning the quadrature-component distribution $p(x, \varphi)$ is measured at a finite number of phases φ_k within a π interval and finite x -resolution. When $p(x, \varphi)$ is measured precisely at N equidistant phases $\varphi_k = (\pi/N)k$, then the reconstructed density-matrix elements are given by

$$\varrho_{mn}(N) = \frac{\pi}{N} \sum_{k=0}^{N-1} \int dx K_{mn}(x, \varphi_k) p(x, \varphi_k), \quad (186)$$

in place of eq. (91). A measure of the systematic error is the difference $\Delta\varrho_{mn} =$

⁸³Replacing in eq. (185) η^{-1} with η yields $\varrho_{mn}(\eta)$ in terms of ϱ_{mn} , which corresponds to a generalization of the Bernoulli transformation (C.3) to off-diagonal density-matrix elements. Since an imperfect detector can be regarded as a perfect detector with a beam splitter in front of it, $\hat{\varrho}(\eta)$ and $\hat{\varrho}$ can be related to each other applying the beam-splitter transformation (7), $\hat{\varrho}(\eta) = {}_2\langle 0|e^{i\beta\hat{L}_2}\hat{\varrho}e^{-i\beta\hat{L}_2}|0\rangle_2$, with \hat{L}_2 according to eq. (6) and $\cos^2(\beta/2) = \eta$ (the mode indices 1 and 2, respectively, refer to the signal and vacuum inputs). It can then be proved easily that $\hat{\varrho}(\eta) = \eta^{\hat{L}}\hat{\varrho}$, where $\hat{L} = \frac{1}{2}(\hat{a}^\dagger\hat{a}\hat{\varrho} + \hat{\varrho}\hat{a}^\dagger\hat{a} - 2\hat{a}\hat{\varrho}\hat{a}^\dagger)$, which corresponds to the time evolution of a damped harmonic oscillator at zero temperature ($\eta \rightarrow e^{-t}$).

⁸⁴When the density matrix at initial time $t=0$ of a signal mode that undergoes phase-insensitive damping or amplification is tried to be reconstructed from the quadrature-component distributions $p(x, \varphi, t; \eta)$ measured at time $t > 0$, then the additional (phase-insensitive) noise gives rise to a modified overall quantum efficiency η_* , so that $\eta_* > 1/2$ must be valid in order to compensate for the losses (D’Ariano [1997b]; D’Ariano and Sterpi [1997]).

$\varrho_{mn}(N) - \varrho_{mn}$, which reads as⁸⁵

$$\Delta\varrho_{mn} = \sum_{j=1}^{\infty} \sum_{k,l} G_{kl}^{mn} \varrho_{kl}, \quad \text{with } k-l = m-n \pm 2jN \quad (187)$$

[$G_{kl}^{mn} = \pi \int dx f_{mn}(x) g_{kl}(x)$] (Leonhardt and Munroe [1996]; Leonhardt [1997b]). Equation (187) reveals that when the quantum state can be truncated such that

$$\varrho_{mn} = 0 \quad \text{for } |m-n| \geq N, \quad (188)$$

then the density matrix-elements ϱ_{mn} for $|m-n| < N$ can be reconstructed precisely from $p(x, \varphi)$ at N phases φ_k according to eq. (186). In particular, one phase is required to reconstruct a completely dephased quantum state that contains only diagonal density-matrix elements. Since any quantum state can be approximated to any desired degree of accuracy by setting $\varrho_{mn} \approx 0$ for $m(n) > n_{\max}$, there is always an $N \approx n_{\max}$ for which the condition (188) can be assumed to be satisfied, so that all (essentially nonvanishing) density-matrix elements can be reconstructed precisely. If N is not known *a priori*, the quantum state can be reconstructed in an iterative way, increasing N in a sequence of (ensemble) measurements until $|\Delta\varrho_{mn}|$ is sufficiently small. Note that any normally ordered moment $\langle \hat{a}^{\dagger n} \hat{a}^m \rangle$ can exactly be reconstructed from $p(x, \varphi)$ at $N = n + m + 1$ phases (Wünsche [1996b]; see § 3.8.1.).

The methods for quantum-state reconstruction are based on ensemble measurements; i.e., on a sequence of individual measurements carried out on identically prepared systems.⁸⁶ Since the number of individual measurements is principally finite, the measured quantities are always estimates of the true ones. Hence all the quantities that can be inferred from the measured quantities are also estimates, and the statistical error with which the original quantities are measured propagates to the quantities inferred from them. In particular, when the quantities which are desired to be determined can be sampled directly from the measured data, then the statistical error can be estimated straightforwardly by also using the sampling method. The problem of statistical error in quantum-state reconstruction has been studied in a number of papers, with special emphasis on balanced four-port homodyne detection (Leonhardt, Munroe, Kiss, Raymer and Richter, Th., [1996]; D'Ariano [1997b]; D'Ariano and Paris [1997a]; D'Ariano, Macchiavello and Sterpi [1997]; Leonhardt [1997c]). Let us consider a quantity \hat{F} and assume that it can be sampled directly from the quadrature-component statistics according to eq. (161). When in an experiment $n(\varphi_k)$ individual measurements are performed at phase φ_k , $k = 0, 1, \dots, N-1$, then $\langle \hat{F} \rangle$ can be estimated as

$$\langle \hat{F}^{(\text{est})}(N) \rangle = \frac{\pi}{N} \sum_{k=0}^{N-1} \frac{1}{n(\varphi_k)} \sum_{n=1}^{n(\varphi_k)} K_F[x_n(\varphi_k), \varphi_k], \quad (189)$$

where $x_n(\varphi_k)$ is the result of the n th individual measurement at phase φ_k . Taking the average over all estimates $\langle \hat{F}^{(\text{est})}(N) \rangle$ yields $\langle \hat{F}(N) \rangle$; i.e., the desired quantity within

⁸⁵Equation (187) can be derived by substituting in eq. (186) for $p(x, \varphi)$ the result of eq. (98) and recalling eqs. (92) and (100). Note that $G_{kl}^{mn} = \delta_{mk}\delta_{nl}$ only holds for $k-l = m-n$.

⁸⁶For the problem of measuring the state of single quantum systems, see Ueda and Kitagawa [1992]; Aharonov and Vaidman [1993]; Aharonov, Anandan and Vaidman [1993]; Imamoğlu [1993]; Royer [1994, 1995]; Alter and Yamamoto [1995]; D'Ariano and Yuen [1996].

the systematic error owing to phase discretization,

$$\overline{\langle \hat{F}^{(\text{est})}(N) \rangle} = \langle \hat{F}(N) \rangle = \frac{\pi}{N} \sum_{k=0}^{N-1} \overline{K_F[x(\varphi_k), \varphi_k]} \quad (190)$$

where

$$\overline{K_F[x(\varphi_k), \varphi_k]} = \int dx p(x, \varphi_k) K_F(x, \varphi_k). \quad (191)$$

Accordingly, the statistical fluctuation of $\langle \hat{F}^{(\text{est})}(N) \rangle$ in terms of the averaged estimates of the variance of $\langle \hat{F}^{(\text{est})}(N) \rangle$ can be given by, on taking into account that the individual measurement are statistically independent of each other,⁸⁷

$$\sigma_{\langle \hat{F} \rangle}^2 = \frac{\pi}{N} \sum_{k=1}^{N-1} N^{-1}(\varphi_k) \overline{\{\Delta K_F[x(\varphi_k), \varphi_k]\}^2}, \quad (192)$$

where

$$\overline{\{\Delta K_F[x(\varphi_k), \varphi_k]\}^2} = \int dx p(x, \varphi_k) K_F^2(x, \varphi_k) - \left[\int dx p(x, \varphi_k) K_F(x, \varphi_k) \right]^2 \quad (193)$$

is the variance of the sampling function, and $N(\varphi_k)$ is the number of measurements per phase interval, $N(\varphi_k) = n(\varphi_k)N/\pi$.

Let us mention that when the kernel $K_F(x, \varphi)$ is a strongly varying function of x in regions where $p(x, \varphi)$ is non-negligible, then the first term in eq. (193) is much larger than the second one. In this case the second term can be neglected and the statistical error can be approximated by averaging the square of the kernel. Note that the same result is obtained if one assumes that the numbers of events yielding the values of $x(\varphi_k)$ in given intervals of x (bins) are independent Poissonian variables (Leonhardt, Munroe, Kiss, Raymer and Richter, Th., [1996]; Leonhardt [1997c]; McAlister and Raymer [1997b]). However, these variables are neither strictly independent [their sum is always $N(\varphi_k)$] nor Poissonian [probability that there is more than $N(\varphi_k)$ events in a bin is zero]. Therefore, care must be taken before one decides to use the simplified error estimation. Whereas for the Fock-basis density matrix elements the simplified estimation is very good (the kernels are strongly oscillating), for the exponential moments of canonical phase one has to take into account both terms in eq. (193), otherwise the error would be overestimated (the kernels are slowly varying functions).

From eq. (192) it can be expected that the statistical error depends sensitively on the analytical form of the sampling function. To give an example, let us consider the integral kernels $K_{mn}(x, \varphi)$, eq. (92), needed for sampling the density-matrix elements in the photon-number basis, ϱ_{mn} . For chosen φ , $K_{mn}(x, \varphi)$ is an oscillating function of x , and with increasing distance $d = |m - n|$ from the diagonal the oscillations become faster and the oscillation range slowly increases. It turns out that with increasing m the diagonal-element variance $\sigma_{\varrho_{mm}}^2$ becomes independent of m ; i.e., saturation of the statistical error for sufficiently large m is observed, $\sigma_{\varrho_{mm}}^2 \leq 2/\bar{N}$ (\bar{N} , mean number of measurements per phase interval). On the contrary, the off-diagonal statistical error increases with d , without saturation. The influence of the quantum efficiency η on the statistical error of the density-matrix elements is very strong in general. For

⁸⁷For simplicity, in eq. (192) it is assumed that F is a real quantity.

chosen m and n the oscillation range of $K_{mn}(x, \varphi; \eta)$, eq. (96), increases very rapidly as η approaches the lower bound $\eta=1/2$, and the statistical error increases rapidly as well (for numerical examples, see D’Ariano, Macchiavello and Sterpi [1997]).⁸⁸ Using the experimentally sampled density-matrix elements for calculating the expectation values of other quantities, such as $\langle \hat{F} \rangle$ according to eq. (160), the resulting statistical error is determined by the law of error propagation. It is worth noting that error propagation can lead to additional noise which is not observed if the quantities are also directly sampled from the measured data (provided that the sampling method applies).

3.9.2. Least-squares method

In the quantum-state reconstruction problems outlined in the foregoing sections a set of measurable quantities (in the following also referred to as data vector) is related linearly to a set of quantities (state vector) that can be used to characterize the quantum state of the system under study. Both sets of quantities can be discrete or continuous or of mixed type. Typical examples are the relations (70) and (98), respectively, between the Wigner function and the density-matrix elements in the Fock basis, and the relations (112) and (140) between the Fourier components of the displaced Fock-state distributions and the atomic-state inversion, respectively, and the density-matrix elements in the Fock basis. A powerful method for inversion of such relations has been least-squares inversion.⁸⁹ The method has been used for quantum-state reconstruction in balanced optical homodyning (Tan [1997]), unbalanced homodyning (Opatrný and Welsch [1997]; Opatrný, Welsch, Wallentowitz and Vogel, W., [1997]), cavity QED (Bardroff, Mayr, Schleich, Domokos, Brune, Raimond and Haroche [1996]; Bodendorf, Antesberger, Kim, M.S. and Walther [1998]) and for orbital electronic motion (Cline, van der Burgt, Westerveld and Risley [1994]). It has been used further to reconstruct the quantum state of the center-of-mass motion of trapped ions (Leibfried, Meekhof, King, Monroe, Itano and Wineland [1996]), the quantum state of a particle in an anharmonic potential and the quantum state of a particle that undergoes a damped motion in a harmonic potential (Opatrný, Welsch and Vogel, W., [1997c]).

An advantage of least-squares inversion is that it is a linear method – the density matrix elements can be reconstructed in *real time* together with an estimation of the statistical error. Moreover, it allows for an easy incorporation in the reconstruction of various experimental peculiarities, such as non-unity quantum efficiency, finite resolution or discretization of the data, finite observation time, dissipative decay of the system, etc.. These aspects can hardly be treated on the basis of analytically determined (and existing) sampling functions. On the other hand, the method does not guarantee (similarly as any other linear method) that a reconstructed density matrix is exactly positive-definite (cf. § 3.9.3.).

⁸⁸For the error of the exponential phase moments sampled from the quadrature-component distributions in balanced homodyning, see Dakna, Opatrný and Welsch [1998], and for the error in quantum-state measurement via unbalanced homodyning and direct photocounting, see Wallentowitz and Vogel, W., [1996a]; Banaszek and Wódkiewicz [1997b]; Opatrný, Welsch, Wallentowitz and Vogel, W., [1997].

⁸⁹The method of least squares was discovered by Legendre [1805] and Gauss [1809,1821] for solving the problem of reconstruction of orbits of planetoids from measured data.

To illustrate the method, let us assume that a distribution $p(x, \varphi)$ of the type of a quadrature-component distribution is measured, and that $p(x, \varphi)$ can be given by a linear combination of all density-matrix elements $\varrho_{nn'}$ of the quantum state to be reconstructed, with linearly independent coefficient functions $S_{nn'}(x, \varphi)$,

$$p(x, \varphi) = \sum_{n, n'} S_{nn'}(x, \varphi) \varrho_{nn'}, \quad (194)$$

where $S_{nn'}(x, \varphi)$ need not be of the form used in eq. (98).⁹⁰ Since the density matrix of any physical state can be truncated at some value n_{\max} , the sum in eq. (194) is effectively finite. Direct application of least-squares inversion (Appendix D.) yields the reconstructed density-matrix elements $\varrho_{nn'}^{(M)}$ as

$$\varrho_{nn'}^{(M)} = \int_X dx \int_{\Phi} d\varphi K_{nn'}(x, \varphi) p^{(M)}(x, \varphi), \quad (195)$$

where $p^{(M)}(x, \varphi)$ is the experimentally measured distribution, X and Φ being the intervals accessible to measurement. The integral kernel $K_{nn'}(x, \varphi)$ is given by

$$K_{nn'}(x, \varphi) = \sum_{m, m' \leq n_{\max}} F_{nn'; mm'} S_{mm'}^*(x, \varphi), \quad (196)$$

and $\mathbf{F} = \mathbf{G}^{-1}$, with the matrix \mathbf{G} being defined by

$$G_{mm'; nn'} = \int_X dx \int_{\Phi} d\varphi S_{mm'}^*(x, \varphi) S_{nn'}(x, \varphi). \quad (197)$$

It can be proved by direct substitution that if the data correspond to the exact quantities $p(x, \varphi)$, i.e., $p^{(M)}(x, \varphi) = p(x, \varphi)$, then the reconstructed density matrix equals the correct one, i.e., $\varrho_{nn'}^{(M)} = \varrho_{nn'}$. On the other hand, if the experimental data suffer from some inaccuracies, then the reconstructed density matrix has the property that it reproduces the data as truly as possible (in the sense of least squares). In the above given formulas we have assumed that x and φ are continuous variables, and n is discrete. The formulas for other combinations of discrete and/or continuous arguments can be obtained in a quite similar way.

An essential point of the method is the inversion of the matrix \mathbf{G} , which requires the matrix to be sufficiently far from singularity; i.e., the data must carry enough information about all the density-matrix elements that are desired to be reconstructed. Otherwise regularized inversion must be applied (Appendix D.). Regularized inversion usually decreases the statistical error of the reconstructed density-matrix elements, but on the other hand they are biased. Therefore, in practice such a degree of regularization should be used for which the introduced bias is just below the statistical noise.

3.9.3. Maximum-entropy principle

As already mentioned, it is principally impossible to measure the exact expectation values of an infinite number of operators \hat{A}_i in an expansion of the density operator

⁹⁰In particular, when x is the position of a moving particle and φ corresponds to the time t , and the particle undergoes damping, then the quantum state evolves according to a master equation whose solution then determines $S_{nn'}(x, t)$.

of the type given in eq. (69), because any realistic experiment can only run for a finite time. So far, the exact formulas have been applied to the analysis of the incomplete measurements including an estimation of the error made. However the question may arise of how to obtain an optimum result of reconstruction of a quantum state when only a finite number of $\langle \hat{A}_i \rangle$ has been measured in the experiment. An answer can be given using the Jaynes principle of *maximum entropy*⁹¹ (Bužek, Adam, G., and Drobný [1996a,b]; Bužek, Drobný, Adam, G., Derka and Knight [1997]).

Let us assume that the expectation values $\langle \hat{A}_i \rangle$ of n quantities \hat{A}_i , $i = 1, \dots, n$ are experimentally determined.⁹² The set of measured quantities can be regarded as a measure of the realized observation level. Certainly, there are a number of potential density operators $\hat{\rho}$, $\text{Tr} \hat{\rho} = 1$, which are compatible with the experimental results, i.e.,

$$\text{Tr}(\hat{\rho} \hat{A}_i) = \langle \hat{A}_i \rangle, \quad i = 1, \dots, n. \quad (198)$$

Among them that density operator is chosen that maximizes the von Neumann entropy⁹³

$$S[\hat{\rho}] = -\text{Tr}(\hat{\rho} \ln \hat{\rho}). \quad (199)$$

Introducing Lagrange multipliers, the resulting density operator $\hat{\rho} = \hat{\rho}_S$ takes the familiar (grand-canonical ensemble) form

$$\hat{\rho}_S = Z^{-1} \exp\left(-\sum_{i=1}^n \lambda_i \hat{A}_i\right), \quad (200)$$

where

$$Z = \text{Tr}\left[\exp\left(-\sum_{i=1}^n \lambda_i \hat{A}_i\right)\right], \quad (201)$$

and represents a partially reconstructed (estimated) density operator on the chosen observation level. Substituting in eq. (198) for $\hat{\rho}$ the density operator $\hat{\rho}_S$ from eq. (200), a set of n nonlinear equations is obtained for the calculation of the n Lagrange multipliers λ_i from the measured expectation values $\langle \hat{A}_i \rangle$. Any incomplete observational level can be extended to a more complete observational level, in principle, by including additional observables in the scheme, which is usually associated with a decrease of the entropy. However, since rather involved calculations are required to be performed, the method has been studied for reconstructing the quantum state of a radiation-field mode on particular (not very high) observational levels (Bužek, Adam, G., and Drobný [1996a,b]; Bužek, Drobný, Adam, G., Derka and Knight [1997]) and/or low-dimensional systems, such as spin states (Bužek, Drobný, Adam, G., Derka and Knight [1997]).

⁹¹See Jaynes [1957a,b]. Probability distributions (or density operators) describe our stage of knowledge about physical systems. If we do not know anything, we usually assign uniform distributions to the quantities (or a multiple of the unity operator to the density operators). If we have partial knowledge, we choose such distributions which are as broad as possible and still reflect our stage of knowledge. A suitable measure of the breadth is the entropy, one therefore seeks for such distributions (density operators) which maximize the entropy under the condition that known quantities are reproduced.

⁹²Note that the determination of $\langle \hat{A}_i \rangle$ already requires an infinite number of individual measurements which cannot be realized during a finite measurement time.

⁹³See von Neumann [1932].

Since the expectation values $\langle \hat{A}_i \rangle$ cannot be measured with infinite precision, only estimates can be inserted into eq. (198), and therefore it can happen that the solution does not exist; i.e., the non-precisely measured averages are not compatible with any density operator. To overcome this problem, the method can be combined with least-squares minimization (Wiedemann [1996]⁹⁴); i.e., the sum of squares of differences

$$C(\{\lambda_i\}) = \sum_{j=1}^n \left\{ \langle \hat{A}_j \rangle^{(M)} - \text{Tr}[\hat{\rho}_S(\{\lambda_i\})\hat{A}_j] \right\}^2 \quad (202)$$

as a function of the parameters λ_i is tried to be minimized, $\langle \hat{A}_j \rangle^{(M)}$ being the non-precisely measured averages.

3.9.4. Bayesian inference

The statistical fluctuations of the data are taken into account in the *Bayesian inference* scheme (Helstrom [1976], Holevo [1982], Jones, K.R.W., [1991, 1994]; Derka, Bužek, Adam, G., [1996]; Derka, Bužek, Adam, G., and Knight [1996]). Let us assume that the system under consideration is prepared in a pure state that belongs to a continuous manifold of states in a *state space* Ω and consider a repeated N -trial measurement of observables \hat{A}_i , $i = 1, \dots, n$, with eigenvalues A_{j_i} . The determination of the quantum state of the measured system is then performed in a repeated three-step procedure:

- (i) As a result of a (single) measurement of \hat{A}_i a conditional probability $p(A_{j_i}|\hat{\rho})$ is defined which specifies the result A_{j_i} if the measured system is in state $\hat{\rho} = |\Psi\rangle\langle\Psi|$,

$$p(A_{j_i}|\hat{\rho}) = \text{Tr}(\hat{P}_{A_{j_i}}\hat{\rho}), \quad (203)$$

where $\hat{P}_{A_{j_i}} = |A_{j_i}\rangle\langle A_{j_i}|$.

- (ii) A probability distribution $p_0(\hat{\rho})$ defined on the space Ω is specified such that it describes the *a priori* knowledge of the state to be reconstructed. The joint probability distribution $p(A_{j_i}, \hat{\rho})$ is then given by

$$p(A_{j_i}, \hat{\rho}) = p(A_{j_i}|\hat{\rho})p_0(\hat{\rho}). \quad (204)$$

When no initial information about the measured system is available, then the prior probability distribution $p_0(\hat{\rho})$ is chosen to be constant.

- (iii) Finally, the Bayes rule⁹⁵ is used to obtain the probability $p(\hat{\rho}|A_{j_i})$ of the system being in state $\hat{\rho}$ under the condition that A_{j_i} is measured,

$$p(\hat{\rho}|A_{j_i}) = \frac{p(A_{j_i}, \hat{\rho})}{\int_{\Omega} d\Omega p(A_{j_i}, \hat{\rho})}. \quad (205)$$

⁹⁴In this paper, which is unfortunately unpublished, the operators \hat{A}_i are identified with the photon number \hat{n} and quadrature-component projectors $|x_l, \varphi_k\rangle\langle x_l, \varphi_k|$, where the subscript l labels a finite subset of the continuous quadrature-components at chosen phase φ_k . Due to computational limits 4 phases and 13 values of x at each phase are considered. The partial reconstruction of the quantum state (in phase space) from computer-simulated homodyne data is performed for various states and yields results that reflect typical properties of the states sufficiently well.

⁹⁵The Bayes rule expresses the relation between the conditional probabilities $p(x|y)$ and $p(y|x)$ as $p(x|y)p(y) = p(x, y) = p(y|x)p(x)$, and hence $p(y|x) = p(x, y)/p(x) = p(x, y) / \int dy p(x, y)$.

Now the procedure can be repeated, making a second measurement of some observable \hat{A}_k ($\hat{A}_k = \hat{A}_i$ or $\hat{A}_k \neq \hat{A}_i$) and using $p(\hat{\rho}|A_{j_i})$ obtained from the first measurement as the prior probability distribution for the second measurement. Proceeding in the way outlined, the N -trial conditional probability distribution $p(\hat{\rho}|\{A_{j_i}\})$ is given by

$$p(\hat{\rho}|\{A_{j_i}\}) = \frac{\mathcal{L}(\hat{\rho}) p_0(\hat{\rho})}{\int_{\Omega} d\Omega \mathcal{L}(\hat{\rho}) p_0(\hat{\rho})}, \quad (206)$$

where

$$\mathcal{L}(\hat{\rho}) = \prod_{i=1}^N p(A_{j_i}|\hat{\rho}) \quad (207)$$

is the *likelihood function* (regarded as a function of $\hat{\rho}$; the measured values $\{A_{j_i}\}$ playing the role of parameters). Note that $\mathcal{L}(\hat{\rho})$ is the probability distribution of finding the result $\{A_{j_i}\}$ in the sequence of N measurements under the condition that the state of the system is $\hat{\rho}$. The partially reconstructed density operator $\hat{\rho}_B$ is then taken as the average over all the possible states $\hat{\rho}$,⁹⁶

$$\hat{\rho}_B = \int_{\Omega} d\Omega p(\hat{\rho}|\{A_{j_i}\}) \hat{\rho}. \quad (208)$$

To apply the method, the state space Ω of the measured system and the corresponding integration measure $d\Omega$ must be defined and the prior probability $p_0(\hat{\rho})$ must be specified. In particular, the integration measure has to be invariant under unitary transformations in the space Ω . This requirement uniquely determines the form of the measure. It should be pointed out that this is no longer valid when Ω is tried to be extended to mixed states. Since a system which is in a mixed state can always be considered as a subsystem of a composite system that is in a pure state, the Bayesian reconstruction can be applied to the composite system and tracing the resulting density operator over the degrees of freedom of the other subsystem (Derka, Bužek and Adam, G., [1996], Derka, Bužek, Adam, G., and Knight [1996]). As already mentioned, the prior probability $p_0(\hat{\rho})$ can be chosen constant if there is no *a priori* information about the state to be reconstructed.⁹⁷ It turns out that with increasing number of measurements the method becomes rather insensitive to the prior probability. In particular, when the number of measurements approaches infinity, $N \rightarrow \infty$, eq. (208) corresponds, on chosen observation level, to the principle of maximum entropy on a microcanonical ensemble.⁹⁸ Contrary to least-squares inversion, Bayesian inference always yields a (partially) reconstructed density operator which is (formally) positive definite and normalized to unity. However the price to pay is a rather involved procedure that has to be carried out in practice. For this reason, the method has been mostly considered – similar to the method of maximum entropy – for spin systems; i.e., for systems with small dimension of the state space

⁹⁶Note that $\hat{\rho}_B$ can correspond to a mixed state even though it is assumed that the system is prepared in a pure state.

⁹⁷Note that when the integration measure $d\Omega$ is not uniquely defined, then a prior probability that is constant with respect to a chosen integration measure need not be constant with respect to another one.

⁹⁸Note that on a chosen (incomplete) observational level the two methods yield different fluctuations of the observables in general.

(Jones, K.R.W., [1991], Derka, Bužek and Adam, G., [1996], Derka, Bužek, Adam, G., and Knight [1996]).

Another statistical method closely related to the Bayesian reconstruction method is the quantum state estimation based on the maximization of the likelihood function $\mathcal{L}(\hat{\rho})$, eq. (207). Here, that state $\hat{\rho}$ in the state space is selected for which $\mathcal{L}(\hat{\rho})$ attains its maximum. Because of the difficulty of finding the maximum of $\mathcal{L}(\hat{\rho})$ in higher-dimensional state spaces, a procedure was proposed which is based on a sequence of general inequalities satisfied by the likelihood function (Hradil [1997]). In this way, the problem can be transformed to that of the diagonalization of an operator given by a linear combination of the projectors $\hat{P}_{A_{j_i}}$, where the expansion coefficients must solve a set of nonlinear algebraic equations. The method simplifies the Bayesian treatment but still guarantees the positive definiteness. Significantly, all the solutions based on the deterministic relation (69) between counted data (frequencies) and the desired density matrix are involved. Whenever such solution exists as a positively defined density matrix, then it should maximize the likelihood function as well. The method was applied successfully to the reconstruction of (low-dimensional) density matrices in the photon-number basis of a radiation-field mode from computer-simulated homodyne data, and a comparison with direct inversion of the linear basic relation between the measurable quantities and the density-matrix elements was given (Mogilevtsev, Hradil and Peřina [1997]).

4. Quantum states of matter systems

In the preceding sections we have considered phase sensitive measurements of radiation fields and methods for reconstructing the quantum state of the fields from the measured data. The problem of quantum-state measurement and reconstruction has also been studied for various matter systems. Different matter systems require, in general, different detection schemes for measuring specific quantities that carry the full information on the quantum state of the system. Although these methods may be, at first glance, quite different from the methods outlined in § 2. for phase-sensitive measurements of light, there have been a number of analogies between the reconstruction concepts for radiation and matter.

4.1. Molecular vibrations

It was shown and demonstrated experimentally that the quantum state of molecular vibrations can be determined using a tomographic method (Dunn, Walmsley and Mukamel [1995]) which resembles the one for a light mode outlined in § 3.1.. The method, called *molecular emission tomography*, is based on the fact that the time resolved emission spectrum of a molecule allows one to visualise the time dependence of a vibrational wave packet within the excited electronic state from which the emission originates (Kowalczyk, Radzewicz, Mostowski and Walmsley [1990]). Alternatively, the desired information on the wave-packet dynamics can be obtained by photoelectron spectroscopy (Assion, Geisler, Helbing, Seyfried and Baumert [1996]).

Let us assume that the molecule is prepared in a given vibrational quantum state in the excited electronic state. As can be seen from Fig. 17, for appropriately displaced

potential energy surfaces of the molecule the position of the vibrational wave packet can be effectively mapped onto the frequency of the emitted light. This fact is used for the tomographic reconstruction of the vibrational wave packet by measuring the time-resolved emission spectrum with a time resolution that is fast compared with the characteristic time period of the molecular state to be studied. The experimental

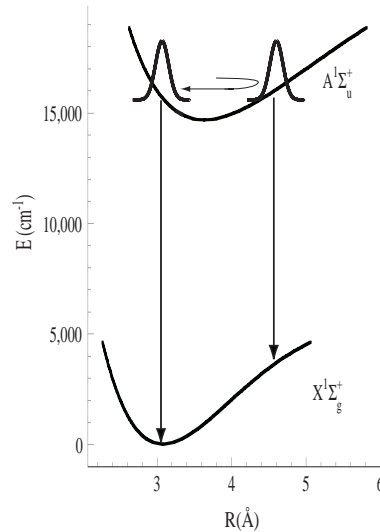


Figure 17: The vibronic energies for the $A^1\Sigma_u^+ \rightarrow X^1\Sigma_g^+$ transition of Na_2 clearly show the possibility to display the vibrational motion (in the excited state) in the time-resolved emission spectrum. (After Kowalczyk, Radzewicz, Mostowski and Walmsley [1990].)

realization has been performed as follows (Dunn, Walmsley and Mukamel [1995]). A sample of Na_2 molecules is illuminated by a 4 kHz train of laser pulses of 60 fs duration and mean wavelength of 630 nm. The laser pulses generate vibrational wave packets in the $A^1\Sigma_u^+$ state of the sodium dimer, which evolve with a time period of 310 fs. A fraction of the pulses is split off and plays the role of a time-gate shutter. The light emitted from the molecular sample is collected and focused synchronously with the split-off part of the exciting pulse onto a nonlinear crystal. A prism monochromator is used to filter the resulting sum-frequency and the field is recorded by a photon-counting photomultiplier. The resulting temporal resolution of the device is about 65 fs.

4.1.1. Harmonic regime

The first reconstruction of the quantum state of molecular vibrations from a time-resolved emission spectrum was based on the assumption that only low vibrational quantum states are excited such that the relevant potentials can be approximated by harmonic ones. Furthermore, it was assumed that the vibrational frequencies in the two electronic quantum states, which contribute to the emission spectrum, are nearly equal. In this case, the vibronic coupling is caused solely by the displacement of the equilibrium positions of the potentials in the two electronic states. When these approximations are justified, then the time-gated spectrum $S(\Omega, T)$ can be related to

the s -parametrized phase-space distribution $P(q, p; s) \equiv 2^{-1}P[\alpha = 2^{-1/2}(q + ip); s]$ as (Dunn, Walmsley and Mukamel [1995])

$$S(\Omega, T) = \int dy P[x(\Omega) \cos(\nu T) + y \sin(\nu T), y \cos(\nu T) - x(\Omega) \sin(\nu T); s]. \quad (209)$$

Here, Ω and T are the setting frequency of the spectral filter and the setting time of the time gate, respectively (ν , vibrational frequency). The function $x(\Omega) = (\Omega - \kappa^2\nu)/\sqrt{2}\kappa\nu$ describes the mapping of the position of the wave packet onto the emitted frequency, κ being the ratio of the displacement of the potentials to the width of the vibrational ground state. The ordering parameter s in eq. (209) is related to the temporal width Γ^{-1} of the time gate as $s = -(\Gamma/\kappa\nu)^2$.

Obviously, the relation (209) between the phase-space distribution $P(q, p; s)$ of the molecular vibration and the measured spectrum $S(\Omega, T)$ is very close to the basic relation (70) of optical homodyne tomography. Thus $P(q, p; s)$ can be obtained from $S(\Omega, T)$ by means of inverse Radon transform (see § 3.1.). A typical experimental result is shown in Fig. 18.

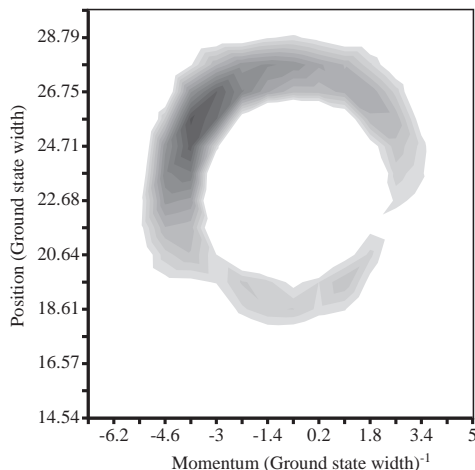


Figure 18: Tomographic reconstruction of an s -parametrized phase-space function for a vibrational wave packet in sodium from a measured set of emission spectra. The time gate duration was 65 fs, which implies $s = -0.8$. (After Dunn, Walmsley and Mukamel [1995].)

4.1.2. Anharmonic vibrations

In general, molecular vibrations are known to be significantly anharmonic when their excitations are not restricted to very small numbers of vibrational quanta. In such cases one cannot apply the approximate reconstruction procedure based on eq. (209). Due to the anharmonicity effects it is no longer possible to reconstruct the quantum state only from one half of a vibrational period.

It was proposed (Shapiro, M., [1995]) to reconstruct the vibrational quantum state from the time-resolved (spectrally integrated) intensity $I(T) = \int d\Omega S(\Omega, T)$ of the light emitted by the molecular sample, which can be related to the density-matrix

elements ϱ_{mn} of the vibrational mode in the excited electronic state as

$$I(T) \sim \sum_{m,n} \varrho_{mn} \sum_k \lambda_{km} \lambda_{kn}^* \exp(-i\nu_{mn}T). \quad (210)$$

Here, ν_{mn} are the vibrational transition frequencies in the excited electronic state, and $\lambda_{km} \sim (\omega_{21}^{mk})^2 {}_1\langle k|m\rangle_2$ is determined by the Franck-Condon overlap ${}_1\langle k|m\rangle_2$ of the vibrational wave functions in the two electronic states and the vibronic transition frequency ω_{21}^{mk} . Equation (210) reveals that, as long as the transition frequencies ν_{mn} are nondegenerate, the corresponding density-matrix elements ϱ_{mn} can be obtained, in principle, from an analysis of $I(T)$ as a function of T . However, the separation of the density-matrix elements from each other may require a rather long time series. Further, the dimension of the set of equations to be inverted can be large, because of the large number of density-matrix elements that may contribute to the intensity of the emitted light. In the degenerate case, which is observed for the diagonal elements of the density matrix and for some off-diagonal elements due to the anharmonicities, additional information is needed. It was proposed to use the stationary spectrum of the light, whose determination requires an additional measurement. Alternatively, the two measurements can be combined such that the density-matrix elements are reconstructed from the time-resolved spectrum (Trippenbach and Band [1996]).⁹⁹

It is worth noting that the dimension of the sets of equations that must be inverted numerically can be reduced substantially by employing the full information inherent in the time-resolved spectrum:

$$S(\Omega, T) \sim \sum_{m,n} \varrho_{mn} \sum_k \lambda_{km} \lambda_{kn}^* \exp(-i\nu_{mn}T) g(\Omega - \omega_{21}^{mk}) g(\Omega - \omega_{21}^{nk}) \quad (211)$$

(Waxer, Walmsley and Vogel, W., [1997]). In eq. (211), the blurring function $g(\omega) = \exp(-\omega^2/4\Gamma^2)$ is determined by the resolution time Γ^{-1} of the time gate (see § 4.1.1.). In practice, the time-dependent spectrum is available only in a finite time interval of size τ , which can be taken into account by multiplying $S(\Omega, T)$ by the corresponding sampling-window function $G(T, \tau)$ in order to obtain $S'(\Omega, T) = S(\Omega, T)G(T, \tau)$. The Fourier transform of $S'(\Omega, T)$ with respect to T reads

$$\underline{S}'(\Omega, \nu) \sim \sum_{m,n} \varrho_{mn} \sum_k \lambda_{km} \lambda_{kn}^* \underline{G}(\nu - \nu_{mn}, \tau) g(\Omega - \omega_{21}^{mk}) g(\Omega - \omega_{21}^{nk}), \quad (212)$$

with $\underline{G}(\nu - \nu_{mn}, \tau)$ being the Fourier transform of the sampling window. Fixing the frequency ν of the time-series spectrum, the structure of the window function ensures that only some of the density matrix elements contribute at this frequency, depending on the chosen size τ of the sampling window. Let us assume that the density matrix elements $\varrho_{m_i n_i}$ ($i=1, 2, 3, \dots, N$) contribute to the spectrum at chosen frequency ν . By choosing N frequencies $\Omega = \Omega_i$ of the emission spectrum, one gets from eq. (212) a linear set of N equations of rather low dimension that can be inverted numerically.¹⁰⁰ In this way, the method allows one to reconstruct rather complicated

⁹⁹Trippenbach and Band [1996] also discussed the inclusion of molecular rotations in the reconstruction.

¹⁰⁰Note that the emission frequencies Ω_i are determined by the two vibrational potentials involved in the vibronic emission, whereas the degenerate values of the vibrational frequencies ν_{mn} are determined solely by the vibrational potential in the excited electronic state. The (within the resolution of the sampling window) degenerate density-matrix elements usually contribute to the emission spectrum at distinct frequencies Ω_i .

quantum states on a time scale that can be shorter than the fractional revival time, as was demonstrated in a computer simulation of measurements (Waxer, Walmsley and Vogel, W., [1997]). Note that a reduction of the dimension of the set of equations to be inverted improves the robustness of the method with respect to the noise in the experimental data.

It was also proposed to reconstruct the density matrix from the time-dependent position distribution according to eq. (102) (Leonhardt and Raymer [1996]; Richter, Th., and Wünsche [1996a,b]; Leonhardt [1997a]; Leonhardt and Schneider [1997]). This requires a scheme suitable for measuring either the position distribution of molecular vibrations or another set of quantities that can be mapped onto the position at different times. Note that this is hardly possible in molecular emission tomography in general. Finally it was proposed to use a wave-packet interference technique (Chen and Yeazell [1997]; § 4.5.1.) for reconstructing pure vibrational states in the excited electronic state (Leichtle, Schleich, Averbukh and Shapiro, M., [1998]).

4.2. Trapped-atom motion

Since the first observation of a single ion in a *Paul trap*¹⁰¹ (Neuhauser, Hohenstatt, Toschek and Dehmelt [1980]) much progress has been achieved with respect to laser manipulation of the quantized motion of single atoms in trap potentials. Such systems are of particular interest since the quantized low-frequency (\sim MHz) motion is very stable, and laser manipulations allow one to prepare very interesting nonclassical states. Until now, motional Fock states and squeezed states (Meekhof, Monroe, King, Itano and Wineland [1996]) as well as Schrödinger-cat type superposition states (Monroe, Meekhof, King and Wineland [1996]) have been realized experimentally.

One might expect that the reconstruction of the quantum state of the center-of-mass motion of a trapped atom may be very similar to the reconstruction of molecular vibrations. However, the vibronic couplings in the two systems are basically different. In the case of a molecule, the vibrating atoms are close together within atomic dimensions and the change of the electronic state substantially alters the potential of the nuclear motion. In the case of an atom in a Paul trap the potential of the center-of-mass motion is externally given by the trap. In this case, electronic transitions can hardly affect the potential. The vibronic interaction in this system is induced by the interaction with radiation. Therefore one may expect that appropriate interactions of a trapped atom with laser fields may open various possibilities for measuring the motional quantum state.

4.2.1. Quadrature measurement

The first proposals to reconstruct the motional quantum state of a trapped atom were based on measuring the quadrature components of the atomic center-of-mass motion in the (harmonic) trap potential. In the scheme in Fig. 19 a weak electronic transition $|g\rangle \equiv |1\rangle \leftrightarrow |e\rangle \equiv |2\rangle$ of the atom is proposed to be simultaneously driven by two (classical) laser beams whose frequencies ω_r and ω_b , respectively, are tuned to the first motional sidebands, $\omega_r = \omega_{21} - \nu$ and $\omega_b = \omega_{21} + \nu$ of the electronic transition of frequency ω_{21} (Wallentowitz and Vogel, W., [1995,1996b]). Since the

¹⁰¹For the trap, see Paul, W., Osberghaus and Fischer [1958].

linewidth of the transition is very small, the motional sidebands can be well resolved. For a long-living transition and in the *Lamb–Dicke regime*¹⁰² these interactions are well described by Hamiltonians of the Jaynes–Cummings (and anti Jaynes–Cummings) type.¹⁰³ Assuming that the Rabi frequencies of the two (classically treated) laser fields are equal, the two Jaynes–Cummings interactions can be combined to an electron–vibration coupling that in the interaction picture reads as

$$\hat{H}' = \frac{1}{2}\hbar\Omega_L\sqrt{2}(\hat{\sigma}_- + \hat{\sigma}_+)\hat{x}(\varphi), \quad (213)$$

where Ω_L is the vibronic Rabi frequency of the driven transitions, and φ is the phase difference of the two lasers which can be controlled precisely. Assuming that the

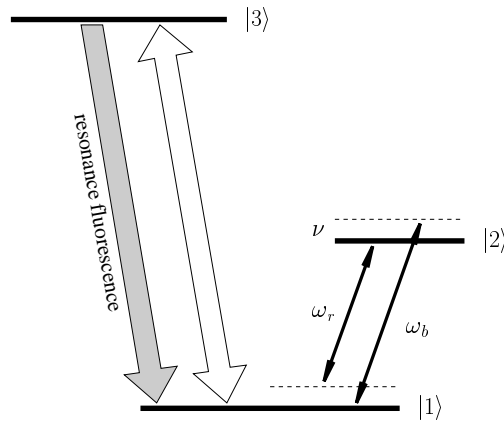


Figure 19: Scheme of a trapped ion with a weak transition $|1\rangle \leftrightarrow |2\rangle$ and a strong transition $|1\rangle \leftrightarrow |3\rangle$. Two incident lasers of frequencies $\omega_r = \omega_{21} - \nu$ and $\omega_b = \omega_{21} + \nu$ are detuned from the electronic transition by the vibrational frequency ν to the red and blue respectively. The laser driving the strong transition is used for testing the ground state occupation probability by means of resonance fluorescence. (After Wallentowitz and Vogel, W., [1995].)

atom is initially prepared in the electronic ground state, $P_g(t)|_{t=0} = 1$ (incoherent preparation), it can be shown that the atomic-state inversion at time t is nothing but the real part of the (scaled) characteristic function $\Psi(x, \varphi)$ of the quadrature-component distribution $p(x, \varphi)$ at phase φ of the center-of-mass motion,

$$\Delta P^{(\text{inc})}(t) = -\text{Re} \Psi\left(\sqrt{2}\Omega_L t, \varphi\right) \quad (214)$$

¹⁰²In this regime, the (one-dimensional) spread of the motional wave packet, Δx , is small compared with the laser wavelength λ_L over 2π , $\Delta x \ll \lambda_L/2\pi$. The Lamb-Dicke parameter, $\eta_{LD} = 2\pi(\Delta x)_0/\lambda_L$, is a measure of the spread of the motional wave packet in the ground state of the trap potential relative to the wavelength.

¹⁰³For the description of the dynamics in the Lamb–Dicke regime by a Jaynes–Cummings type Hamiltonian, see Blockley, Walls and Risken [1992]; Wineland, Bollinger, Itano, Moore, and Heinzen [1992], Cirac, Blatt, Parkins and Zoller [1994]. Note that the fact that the method is based on the Lamb–Dicke regime is not a serious limitation. In recent experiments (Meekhof, Monroe, King, Itano and Wineland [1996]) the frequency of the weak transition is in the GHz range and it is driven by two lasers in a Raman configuration. In this case the Lamb–Dicke parameter can be changed easily by the laser beam geometry.

$[\Delta P = P_e - P_g]$. Similarly, the imaginary part of the characteristic function can be obtained by preparing the atom initially in an appropriate coherent superposition of the two electronic quantum states such that

$$\Psi(\sqrt{2}\Omega_L t, \varphi) = -\Delta P^{(\text{inc})}(t) - \Delta P^{(\text{coh})}(t). \quad (215)$$

Hence, varying the phase difference between the two driving laser beams, the complete information about the motional quantum state can be determined from the time evolution of the atomic-state inversion of the weak transition. This occupation probability can be probed by testing an auxiliary, strong transition $|1\rangle \leftrightarrow |3\rangle$ for the appearance of fluorescence (cf. Fig. 19). The existence and the absence of fluorescence detects the weak transition in state $|1\rangle$ and $|2\rangle$, respectively. This method has an almost ideal quantum efficiency which is a great advantage for the present purpose.¹⁰⁴ Applying eqs. (85) – (87), the reconstruction of density matrix of the center-of-mass motion in a quadrature-component basis from the measured signal can be accomplished with a single Fourier integral, and application of eqs. (105) and (106) offers the possibility of direct sampling of the density matrix in the Fock basis from the fluorescence signal. Further, using eqs. (B.24) and (B.27), s -parametrized phase-space functions can be inferred from the signal by performing a two-fold integral.

The latter was demonstrated in another proposal suitable for measuring $\Psi(z, \varphi)$ (D’Helon and Milburn [1996]). Here, the $|1\rangle \leftrightarrow |2\rangle$ transition (Fig. 19) is driven by a standing-wave laser pulse tuned to ω_{21} whose duration τ_P is much shorter than the vibrational period, $\nu\tau_P \ll 1$, and it is assumed that the center of the trap potential coincides with a node of the standing wave. In the interaction picture, the interaction Hamiltonian in the Lamb-Dicke regime then reads as¹⁰⁵

$$\hat{H}' = \frac{1}{2}\hbar\Omega_L(t)\sqrt{2}(\hat{\sigma}_- + \hat{\sigma}_+)\hat{x}(t). \quad (216)$$

Here, $\hat{x}(t)$ corresponds to the freely evolving position operator of the center-of-mass motion, which for the harmonic motion considered is simply given by the quadrature-component operator at phase $\varphi = \nu t$, and the time-dependent (slowly varying) Rabi frequency $\Omega_L(t)$ includes the shape of the pulse. Owing to the shortness of the driving pulse it can be assumed that its action at time t gives rise to a unitary kick described by the operator

$$\hat{K} = T \exp\left[-i\hbar^{-1} \int dt' H'(t')\right] \approx \exp\left[-i\frac{1}{2}\theta(\hat{\sigma}_- + \hat{\sigma}_+)\hat{x}(t)\right], \quad (217)$$

where $\theta = \int dt' \Omega(t')$ is the pulse area. Obviously, its action on the state is formally the same as the action of the unitary operator that corresponds to the interaction Hamiltonian (213). Hence, $\Delta^{(\text{inc})}P(t)$ and $\Delta^{(\text{coh})}P(t)$ measured immediately after application of the pulse at time t are again related to $\Psi(z, \varphi)$ according to eq. (215), but now with θ and νt in place of $\Omega_L t$ and φ , respectively.¹⁰⁶

¹⁰⁴For the experimental detection of a weak transition via fluorescence from another, strong transition, see Nagourney, Sandberg and Dehmelt [1986]; Sauter, Neuhauser, Blatt and Toschek [1986]; Bergquist, Hulet, Itano and Wineland [1986].

¹⁰⁵Note that the Hamiltonian (216) is not based on a vibrational rotating wave approximation as it is the case for the Hamiltonian (213). In eq. (216) the position operator results from the Lamb-Dicke approximation of the (operator-valued) mode function of the standing wave, $\sin(k_L \hat{x}) \approx k_L \hat{x}$.

¹⁰⁶Whereas in the scheme of Wallentowitz and Vogel, W., [1995] the phase difference between the two laser beams must be controlled, the scheme of D’Helon and Milburn [1996] requires control of short-pulse areas.

It is well known that a squeezed coherent state approaches a quadrature-component eigenstate as the strength of squeezing goes to infinity; i.e.,

$$|x, \varphi\rangle \propto \lim_{|\xi| \rightarrow \infty} \hat{D}(xe^{i\varphi}/\sqrt{2}) \hat{S}(|\xi|e^{i2\varphi})|0\rangle, \quad (218)$$

with $\hat{D}(\alpha)$ the coherent displacement operator, and $\hat{S}(\xi) = \exp[(\xi^* \hat{a}^2 - \xi \hat{a}^{\dagger 2})/2]$ the squeeze operator.¹⁰⁷ Hence, the quadrature-component distribution $p(x, \varphi)$ can be asymptotically given by

$$p(x, \varphi) \propto \lim_{|\xi| \rightarrow \infty} \langle 0 | \hat{\rho}' | 0 \rangle, \quad (219)$$

where $\hat{\rho}'$ is a coherently displaced and squeezed version of the density operator $\hat{\rho}$ to be determined,

$$\hat{\rho}' = \hat{S}^\dagger(|\xi|e^{i2\varphi}) \hat{D}^\dagger(xe^{i\varphi}/\sqrt{2}) \hat{\rho} \hat{D}(xe^{i\varphi}/\sqrt{2}) \hat{S}(|\xi|e^{i2\varphi}). \quad (220)$$

Equations (219) and (220) reveal that when the quantum state to be measured can be squeezed strongly and displaced coherently, then the quadrature-component distributions can be obtained, in principle, from the occupation probability of the motional ground state that is measured after these manipulations, the phase being controlled by the free evolution of the vibrating system (Poyatos, Walser, Cirac, Zoller and Blatt [1996]). To realize the scheme, the following procedure was proposed:

- (i) Wait for a time t such that $\varphi = \nu t$.
- (ii) Perform a sudden displacement of the center of the trap to the right for a distance d such that $x = \sqrt{m\nu/(2\hbar)} d$, m being the mass of the atom.
- (iii) Change the trap frequency instantaneously from ν to (lower) ν' .¹⁰⁸
- (iv) Determine the population of the motional ground state.¹⁰⁹

Knowing $p(x, \varphi)$ for all phases φ in a π interval, the complete information on the motional quantum state is available and the (tomographic) methods of quantum-state reconstruction outlined in § 3. applies.¹¹⁰

4.2.2. Measurement of the Jaynes–Cummings dynamics

Let us consider the dynamics of a trapped ion that is driven by a single (classical) laser beam in a resolved sideband regime¹¹¹ and assume that the laser frequency is tuned to the (red) k th-order motional sideband of the weak electronic transition $|1\rangle \leftrightarrow |2\rangle$,

¹⁰⁷For a proof, see, e.g., Vogel, W., and Welsch [1994].

¹⁰⁸The sudden change of the trap frequency leads to squeezing with the squeeze parameter being $|\xi| = \ln(\nu/\nu')/2$ (Janszky and Yushin [1986]). Note that a significant change of the trap frequency is needed since the measurement scheme requires strong squeezing.

¹⁰⁹It was demonstrated experimentally that the motional number statistics can be determined from the measured Jaynes–Cummings revivals (Meekhof, Monroe, King, Itano and Wineland [1996]; § 4.2.2.).

¹¹⁰The steps (i), (ii) and (iv) were proposed in order to measure the Q function.

¹¹¹In the practical realization the single laser may also be replaced with two lasers driving a dipole-forbidden transition in a Raman configuration, which essentially yields the same basic Hamiltonian.

$\omega_{21} = \omega_l - k\nu$. In this case the resulting coupling (in the interaction picture) between the electronic transition and the center-of-mass motion has the form of a nonlinear multiquantum Jaynes-Cummings interaction (Vogel, W., and de Matos Filho [1995]),

$$\hat{H}' = \frac{1}{2}\hbar\Omega_L\hat{\sigma}_+\hat{f}^{(k)}(\hat{a}^\dagger\hat{a})\hat{a}^k + \text{H.c.}, \quad (221)$$

where the operator function \hat{f}_k reads in normally ordered form as

$$\hat{f}^{(k)}(\hat{a}^\dagger\hat{a}) = e^{-\eta_{LD}^2/2} \sum_{l=0}^{\infty} \frac{(i\eta_{LD})^{2l+k}}{l!(l+k)!} \hat{a}^{\dagger l} \hat{a}^l \quad (222)$$

(η_{LD} , Lamb-Dicke parameter). It describes the influence of the interference between the driving laser wave and the (extended) atomic wave function on the dynamics of the system. The nonlinear Jaynes-Cummings model can be solved exactly. In particular, when the atom is initially prepared in the excited electronic state, then the atomic-state inversion is given by an equation of the type of eq. (137),¹¹²

$$\Delta P(t) = \sum_{n=0}^{\infty} \varrho_{nn} \cos(\Omega_{n,n+k}t), \quad (223)$$

where now $\Omega_{n,n+k} = \Omega_L \langle n | \hat{f}^{(k)} \hat{a}^k | n+k \rangle$, and ϱ_{nn} are the motional density-matrix elements at the initial time $t=0$.

The motional quantum state can be reconstructed from the measured (nonlinear) Jaynes-Cummings dynamics by applying typical methods outlined in § 3.. When the motional quantum state which is desired to be reconstructed is coherently shifted [$\hat{\rho} \rightarrow \hat{D}^\dagger(\alpha)\hat{\rho}\hat{D}(\alpha)$] before $\Delta P(t)$ is measured, then the Fock-state probability distribution $p_n = \varrho_{nn}$ in eq. (223) must be replaced with the displaced Fock-state probability distribution $p_n(\alpha) = \varrho_{nn}(\alpha) = \langle n, \alpha | \hat{\rho} | n, \alpha \rangle$ [cf. eq. (138)], and inversion of eq. (223) yields $p_n(\alpha)$. Changing α in a succession of (ensemble) measurements, the complete information about the original (unshifted) motional quantum state can be inferred from the measured data. In particular, applying the method outlined in § 3.5., pointwise reconstruction of phase-space functions is feasible. This was demonstrated successfully by reconstructing the Wigner function [eq. (130)] of a single ${}^9\text{Be}^+$ ion that is stored in a rf Paul trap (Leibfried, Meekhof, King, Monroe, Itano and Wineland [1996]). In the experiment, the relevant oscillation frequency in the trap potential is $\nu/2\pi \approx 11.2$ MHz, and the transition between the states $|g\rangle$ and $|e\rangle$ is a stimulated Raman transition between the hyperfine ground states ${}^2S_{1/2}$ ($F=2$, $m_F=-2$) and ${}^2S_{1/2}$ ($F=1$, $m_F=-1$), respectively, which are separated by about 1.25 GHz. The coherent displacement of the initially prepared motional quantum state is realized by applying a classical, spatially uniform rf field. In Fig. 20 an example of a reconstructed Wigner function of a motional number state is shown.

The density matrix in the Fock basis, ϱ_{mn} , can be obtained from the displaced Fock-state probability on a circle, applying the method outlined in § 3.3.2.. This was also demonstrated in the above mentioned experiment (Leibfried, Meekhof, King, Monroe, Itano and Wineland [1996]). In Fig. 21 an example of a reconstructed density matrix of a superposition of two Fock states is shown.

¹¹²The dynamics were realized experimentally and used to determine the (initial) excitation statistics ϱ_{nn} of the motional state by inverting eq. (223) (Meekhof, Monroe, King, Itano and Wineland [1996]). The same dynamics can be realized by tuning the laser onto the corresponding blue sideband, $\omega_{21} = \omega_l + k\nu$, and preparing the electronic subsystem initially in the ground state.

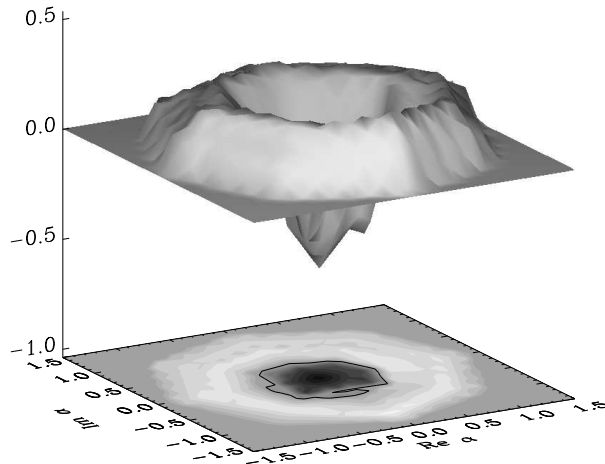


Figure 20: Surface and contour plots of the reconstructed Wigner function $W(\alpha)$ of the $|n=1\rangle$ motional number state. The plotted points are the result of fitting a linear interpolation between the actual data points to a 0.1 by 0.1 grid. The octagonal shape is an artifact of the eight measured phases per radius. (After Leibfried, Meekhof, King, Monroe, Itano and Wineland [1996].)

The method of coherently displacing the motional quantum state to be detected can be extended in order to measure the Wigner function rather than reconstructing it from the measured data (Lutterbach and Davidovich [1997]).¹¹³ For this purpose the laser driving the Jaynes–Cummings dynamics is tuned on resonance to the electronic transition, so that the Hamiltonian (221) for $k=0$ applies. For sufficiently small Lamb–Dicke parameter, $\eta_{LD} \ll 1$, the nonlinear function $\hat{f}^{(0)}$ in eq. (222) can be approximated by $\hat{f}^{(0)} \approx 1 - \eta_{LD}^2 (\hat{a}^\dagger \hat{a} + 1/2)$. Consequently, the vibronic Rabi frequencies read as $\Omega_{nn} \approx \Omega_L [1 - \eta_{LD}^2 (n + 1/2)]$. Inserting this result into eq. (223), with $\varrho_{nn}(\alpha)$ in place of ϱ_{nn} , and choosing the interaction time as $t = t_W = \pi / (\Omega \eta_{LD}^2)$ yields

$$\Delta P(t_W) \approx \sin(\pi/\eta_{LD}^2) \sum_{n=0}^{\infty} \varrho_{nn} (-1)^n = \frac{1}{2} \pi \sin(\pi/\eta_{LD}^2) W(\alpha), \quad (224)$$

which reveals that under the conditions given the measured electronic-state occupation probability directly gives the Wigner function at the phase-space point α .

Further it was proposed to reconstruct the density matrix in the Fock basis following a line similar to that given by eqs. (134) – (136) for cavity QED (Bardroff, Leichtle, Schrade and Schleich [1996]). In cavity QED the k -photon transitions needed to calculate the off-diagonal density matrix elements $\varrho_{n, n+k}$ from the measured atomic-state inversion (provided that initially a coherent superposition of the two states is prepared) can hardly be realized for larger values of k . In the case of a trapped ion the situation is improved significantly. The k -quantum interaction of Jaynes–Cummings type as given by eq. (221) can be realized as outlined above, by tuning the laser on

¹¹³For comparison, see the approach to direct measurement of the Wigner function in cavity QED as outlined in § 2.4..

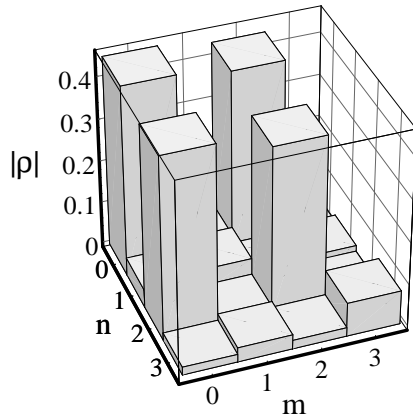


Figure 21: Reconstructed density-matrix amplitudes $|\rho| \equiv |\rho|_{mn}$ of an approximate $1/\sqrt{2}(|n=0\rangle - i|n=2\rangle)$ motional state. The state was displaced by $|\alpha| = 0.79$ for eight phases on the circle. (After Leibfried, Meekhof, King, Monroe, Itano and Wineland [1996].)

resonance to the k th motional sideband. This enables one to reconstruct the density matrix elements $\rho_{n,n+k}$ for all k in principle, by successively tuning the laser on all sidebands. Needless to say, this requires sufficiently large values of the Lamb–Dicke parameter, since otherwise the coupling of the laser to high-order sidebands is very small. Formally, the difference to cavity QED only consists in the frequencies $\Omega_{n,n+k}$, which are different for the two systems.¹¹⁴

It was also proposed to reconstruct the density matrix in the coherent-state basis by combining coherent displacements with motional ground state measurements (Freyberger [1997]). The scheme allows a pure motional quantum state to be reconstructed by coherent displacements on a circle. Reconstruction of the density matrix of a mixed state requires additional variation of the displacement amplitude. A first displacement is introduced before a filtering measurement is performed in order to decide whether or not the atom is in the motional ground state. A second displacement is performed which is followed by detecting the probability that the atom is in the motional ground state, which may be obtained from the Jaynes–Cummings dynamics as outlined above.

4.2.3. Entangled vibronic states

Let us consider the situation where the motional state is entangled with the electronic state of the system and ask for measuring the complete vibronic state. Such a measurement may be realized by the interaction Hamiltonian (221) for $k=0$ (Wallentowitz, de Matos Filho and Vogel, W., [1997]). In the scheme the initially prepared vibronic state $\hat{\rho}$ is first displaced coherently in the phase space of the motional sub-

¹¹⁴At this point it should be noted that in a Paul trap the applied rf field may modulate the motion of a trapped atom, which gives rise to the so-called *micromotion*. The rf frequency is usually large compared to the (effective) motional frequency, and its effect may consist in a modification of the excitation-dependent function $\hat{f}^{(k)}$ in the interaction Hamiltonian (221) (Bardroff, Leichtle, Schrade and Schleich [1996]). Apart from such modifications, the structure of the Hamiltonian is preserved. For details of the treatment of the micromotion, see the original article.

system, $\hat{\rho} \rightarrow \hat{\rho}(\alpha) = \hat{D}^\dagger(\alpha) \hat{\rho} \hat{D}(\alpha)$. Next the driving laser causing the electron-motional coupling is switched on for an interaction time τ . This procedure is followed by probing the atom for fluorescence on the strong, auxiliary transition. Provided the atom is detected in the excited electronic state $|e\rangle$ (no fluorescence), the density operator $\hat{\rho}(\tau)$ of the system reduces to

$$\hat{\rho}'(\tau) \sim |e\rangle\langle e| \otimes \hat{\rho}_M(\tau), \quad (225)$$

where $\hat{\rho}_M(\tau) \sim \langle e|\hat{\rho}(\tau)|e\rangle$ is the corresponding density operator of the motional subsystem. Its diagonal elements in the Fock basis read

$$\begin{aligned} [\varrho_M(\tau)]_{nn} &\sim \text{Im} \left[\varrho_{ge}^{nn}(\alpha) \right] \sin(\Omega_{nn}\tau) \\ &+ \varrho_{ee}^{nn}(\alpha) \cos^2\left(\frac{1}{2}\Omega_{nn}\tau\right) + \varrho_{gg}^{nn}(\alpha) \sin^2\left(\frac{1}{2}\Omega_{nn}\tau\right). \end{aligned} \quad (226)$$

Equation (226) reveals that appropriately chosen interaction times τ allow the displaced vibronic density-matrix elements $\varrho_{ab}^{nn}(\alpha)$ to be mapped onto the reduced motional number statistics $[\varrho_M(\tau)]_{nn}$. It is worth noting that the underlying vibronic coupling is not only suited for this mapping but also for a QND measurement of the reduced motional number statistics, since the Hamiltonian commutes with the motional number operator.¹¹⁵ Note that the reduced motional number statistics can also be determined using other methods, such as the methods outlined in § 4.2.2..

Knowing the displaced vibronic density-matrix elements $\varrho_{ab}^{nn}(\alpha)$ as functions of α , the density matrix ϱ_{ab}^{mn} of the original vibronic quantum state can be reconstructed, following the lines given in § 3.. In particular, the elements $\varrho_{ab}^{nn}(\alpha)$ can be summed up to obtain the vibronic quantum state in terms of the Wigner-function matrix $W_{ab}(\alpha)$,

$$W_{ab}(\alpha) = \frac{2}{\pi} \sum_{n=0}^{\infty} (-1)^n \varrho_{ab}^{nn}(\alpha) \quad (227)$$

(Wallentowitz, de Matos Filho and Vogel, W., [1997]). The Wigner-function matrix $W_{ab}(\alpha)$ has the following properties. Its trace with respect to the electronic subsystem is the (reduced) motional Wigner function. Integrating $W_{ab}(\alpha)$ with respect to the motional phase-space amplitude α yields the (reduced) electronic density matrix. A typical quantum state for which such a measurement scheme would be of interest is an entangled state of the type $|\psi\rangle \sim (|2\rangle|\alpha\rangle \pm |1\rangle|-\alpha\rangle)$.¹¹⁶ Clearly, the nonclassical features of such a state are completely lost when one measures only the reduced motional quantum state.

4.3. Bose–Einstein condensates

The recent progress in evaporative cooling of an atomic gas has rendered it possible to realize Bose–Einstein condensation experimentally (Anderson, Ensher, Matthews,

¹¹⁵For the application of this type of vibronic coupling to QND measurement of the motional excitation of a trapped atom, see de Matos Filho and Vogel, W., [1996]; Davidovich, Orszag and Zagury [1996].

¹¹⁶States of this type have been realized experimentally (Monroe, Meekhof, King and Wineland [1996]). For a reconstruction of $W_{ab}(\alpha)$ from a computer simulation of measurements, see Wallentowitz, de Matos Filho and Vogel, W., [1997]).

Wieman and Cornell [1995]; Bradley, Sackett, Tollett and Hulet [1995]; Davies, Mewes, Andrews, van Druten, Durfee, Kurn and Ketterle [1995]). The Bose–Einstein condensate (BEC) represents a macroscopic occupation of the ground state of the gas, which is an important signature of quantum-statistical mechanics. Moreover, coherence effects, such as interference fringes between two condensates, could be demonstrated (Mewes, Andrews, Kurn, Durfee, Townsend and Ketterle [1997], Andrews, Townsend, Miesner, Durfee, Kurn and Ketterle [1997]; for a theoretical interpretation, see Wallis, Röhrl, Naraschewski and Schenzle [1997]). In view of these feasibilities it is interesting to get more insight in the exact nature of the quantum state of BEC.

Let us consider a two-mode BEC consisting of N atoms,¹¹⁷ where the two modes may correspond to different hyperfine states. To reconstruct the quantum state, it was proposed to introduce a controllable phase shift ϕ between the modes and to mix them by applying a (lossless) beam-splitter transformation. The numbers of atoms in the two modes are counted, and the two-mode quantum state is inferred from joint counting statistics (Bolda, Tan and Walls [1997], Mancini and Tombesi [1997b], Walser [1997]).¹¹⁸ Neglecting collisions between the atoms, the two-mode density operator $\hat{\rho}$ is transformed as

$$\hat{\rho}' = \hat{U}^\dagger(\beta, \phi) \hat{\rho} \hat{U}(\beta, \phi), \quad (228)$$

with

$$\hat{U}(\beta, \phi) = \exp\left[\frac{1}{2}i\beta \left(\hat{a}_1^\dagger \hat{a}_2 e^{i\phi} + \hat{a}_2^\dagger \hat{a}_1 e^{-i\phi}\right)\right]. \quad (229)$$

[cf. eq. (7)], where the mode subscripts 1 and 2 label the corresponding hyperfine states. Raman transitions between these states can be made by optical pulses that are off-resonance from an excited state 3. An rf field may be used to couple state 1 to another state 4, and atoms in state 4 are repelled from the trap. The beam splitter transformation can be realized by applying two copropagating light pulses that are detuned from the 1 – 3 and 2 – 3 transitions. The phase ϕ is controlled by the phase difference of the lasers. The pulses are followed by an rf π -pulse that transfers the state 1 to 4. Consequently, the atoms in state 4 fall freely and those in state 2 remain trapped. Eventually, the separate groups of trapped and untrapped atoms are counted (for the experimental setup, see also Mewes, Andrews, Kurn, Durfee, Townsend and Ketterle [1997], Andrews, Townsend, Miesner, Durfee, Kurn and Ketterle [1997]). The probability $P_m(\phi) \equiv P_{n, N-n}(\phi)$ of counting n and $N - n$ atoms, respectively, in the modes 1 and 2 for a phase shift setting of ϕ can be given by¹¹⁹

$$P_m(\phi) = \langle m | \hat{U}^\dagger(\beta, \phi) \hat{\rho} \hat{U}(\beta, \phi) | m \rangle = \sum_{l, l'} T_m^{ll'}(\phi) \rho_{ll'}, \quad (230)$$

where $T_m^{ll'}(\phi)$ is defined by the corresponding matrix elements of the beam splitter transformation in the basis of the states $|m\rangle$.

¹¹⁷The two-mode BEC is considered in view of the lack of a coherent reference state within a condensate of a fixed number of atoms.

¹¹⁸The three proposals are basically similar. Concerning the practical realization of such a measurement, we briefly outline the rather detailed scheme proposed by Bolda, Tan, and Walls [1997]. For the interaction with radiation of an atomic Bose gas in an isotropic harmonic oscillator potential, see also Javanainen [1994].

¹¹⁹For simplicity, the abbreviating notation $|m\rangle$ for the two-mode states $|n\rangle_1 \otimes |N - n\rangle_2$ is used.

The density matrix of the two-mode state can be obtained by numerically inverting eq. (230) (Bolda, Tan and Walls [1997], Mancini and Tombesi [1997b]) by means of the least-squares method (Appendix D.; see also § 3.9.2.). A further simplification can be achieved by taking the Fourier transform of $P_m(\phi)$ with respect to ϕ (Bolda, Tan and Walls [1997]). Since the s th Fourier component $P_m^s = (2\pi)^{-1} \int_0^{2\pi} d\phi e^{is\phi} P_m(\phi)$ is related only to the matrix elements whose row and column indices differ by s , the corresponding blocks of equations can be inverted separately (cf. § 3.3.2.). Alternatively, the inversion can also be performed analytically by applying orthogonality relations for Clebsch-Gordan coefficients (Walser [1997]).

The complex amplitude of a BEC field, $\psi(\mathbf{r}, t) = \langle \hat{\psi}(\mathbf{r}, t) \rangle$, is frequently assumed to satisfy a nonlinear Schrödinger equation

$$i\hbar \frac{\partial \psi}{\partial t} = \left(-\frac{\hbar^2}{2m} \Delta + U + g|\psi|^2 \right) \psi \quad (231)$$

(m , particle mass; U , potential; g , atom–atom interaction constant). The density of particles $|\psi|^2$ can be measured by phase-contrast imaging (Andrews, Mewes, van Druten, Durfee, Kurn and Ketterle [1996]). In order to determine $\psi(\mathbf{r}, t)$ for given $|\psi(\mathbf{r}, t)|^2$, it was proposed to use a nonlinear propagation for a trial function φ , so that the correct function ψ can be found by adaptive modification of the trial function (Leonhardt and Bardroff [1997]).

4.4. Atomic matter waves

Stimulated by the successful experimental demonstration of atom interferometry (Carnal and Mlynek [1991], Keith, Ekstrom, Turchette and Pritchard [1991]) the study of coherence properties of atomic matter waves has been of increasing interest. In particular, several methods have been considered for determining the (single-particle) quantum state of both the transverse and the longitudinal center-of-mass motion of the atoms, and first experiments have been performed.

4.4.1. Transverse motion

The density matrix of the (with respect to the direction of propagation) transverse motion of a single particle can be determined by methods of refractive (atom) optics (Raymer, Beck and McAlister [1994], Janicke and Wilkens [1995]). Combining the effect of lenses and propagation, it is possible to reconstruct the quantum state from measured position distributions by tomographic methods (§ 3.1.). The desired rotation of the quadrature components can be realized by appropriately changing the parameters of the experimental set-up, such as the focal lengths of the lenses, their positions and the positions of the detectors (Raymer, Beck and McAlister [1994]).¹²⁰

In the first experimental reconstruction of the transverse quantum state of an atomic matter wave (Kurtsiefer, Pfau and Mlynek [1997], Pfau and Kurtsiefer [1997]) the scheme is simplified by avoiding the use of lenses. Metastable helium atoms are used whose quantum state of the transverse motion is prepared by a combination of

¹²⁰For possible realizations of optical elements in atom optics, see, e.g., Adams, Sigel and Mlynek [1994].

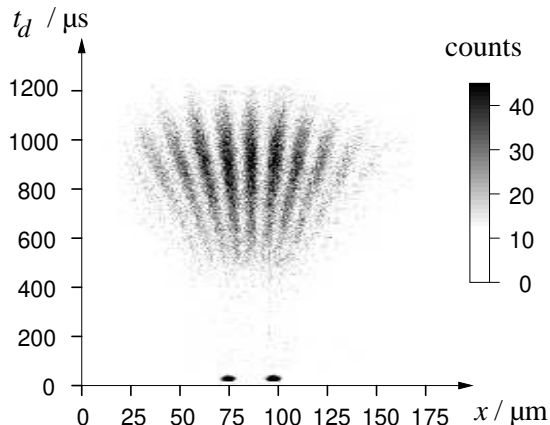


Figure 22: Measured time-resolved spatial atomic distribution in the Fraunhofer diffraction limit. The two wave packets emerging from the individual slits overlap almost completely, and a maximal visibility of the interference fringes is observed. (After Pfau and Kurtsiefer [1997].)

an entrance slit and a double slit, which realizes a nonclassical two-peaked atom-wave state. The atoms then propagate for some distance to a time- and space-resolving detector, which allows one to measure the transverse atomic distribution of the atoms with a spatial resolution down to 500 nm, and the arrival time of the atoms with an accuracy of 100 ns. This renders it possible to record spatial atomic distributions for different free-evolution times of the atom-wave packet after the double slit (Fig. 22), which are suited for reconstructing the quantum state. The measured distributions are position distributions of the sheared Wigner function

$$W(x, p, t) = W\left(x - \frac{p}{m}t, p, 0\right) \quad (232)$$

(m , mass of the atom) of the freely evolving atom-wave packet after the double slit. Knowing the position distributions for a sufficiently large set of evolution times, the original quantum state can be obtained (§ 3.3.1.; for reconstruction of an original Wigner function from marginals of the sheared Wigner function, see also Lohmann [1993]). In particular, the measured position distributions correspond to the quadrature-component distributions whose phase parameter is given by

$$\varphi = \arctan\left(\frac{t\hbar}{mx_0^2}\right), \quad (233)$$

(x_0 , scaling length). Obviously, the phase φ can only be scanned between 0 and $\pi/2$, and in a real experiment this interval is further reduced in general. Since a precise reconstruction of the quantum state requires a phase interval of size π , some *a priori* information about the state should be available (cf. § 3.9.1.). In the present case it may be possible to assume symmetry in position space for the Wigner function, because of the preparation of the quantum state by a double slit. The Wigner function

reconstructed (with a limited range of phases φ) from the measured diffraction pattern in Fig. 22 by applying inverse Radon transform (§ 3.1.) is shown in Fig. 23.

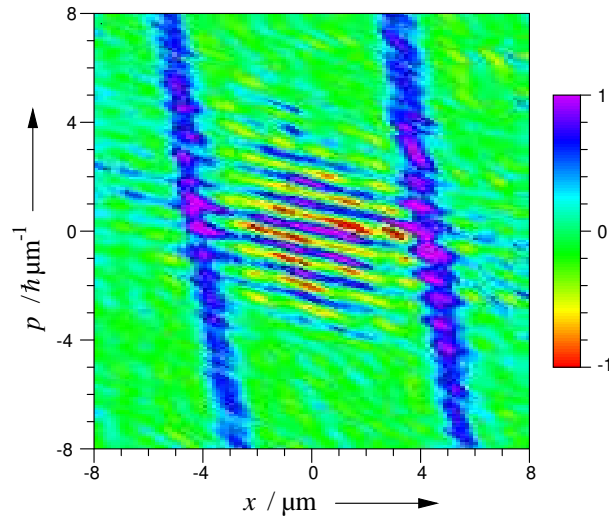


Figure 23: Wigner function of the atomic motional state immediately behind the double slit, reconstructed from the measured time-resolved spatial atomic distribution in Fig. 22. (After Pfau and Kurtsiefer [1997].)

Although the shape of the Wigner function and especially the oscillating interference part are well reproduced, there is a systematic error owing to the limited range of phases accessible in the experiment. For example, the reconstructed Wigner function appears sheared. This shear could be avoided by forced symmetrization of the Wigner function in position. Using the *Wittaker-Shannon sampling theorem* (see, e.g., Marks [1991]), it can be proved which features of the reconstructed Wigner function of an atom-wave packet are obtained correctly when the set of data is not tomographically complete (Raymer [1997]). The analysis shows that the density matrix in the momentum basis is correct everywhere except in an excluded region of width $(\delta p)_{\min}$ around the diagonal, with $(\delta p)_{\min}$ being inversely proportional to the time interval over which the diffraction pattern is recorded. Transferring this result to the reconstructed Wigner function, it turns out that there is a low-frequency error in $W(x, p)$ as a function of x , whereas the high-frequency behaviour is essentially correct.

In another tomographic scheme for reconstructing the Wigner function of an initially prepared transverse motional state, a set-up is considered, in which a classical standing light field that is strongly detuned from the atomic transition serves as a thick gradient-index lens for two-level atoms which are prepared in the ground state and cross the light field close to a node (Kienle, Fischer, Schleich, Yakovlev and Freyberger [1997]; for a set-up of this type, see also Fig. 8). It was found that here the phase φ of the quadrature-component distribution associated with the measured time-resolved position distribution can be tuned over a complete π interval.

In a modified (interferometric) scheme it is assumed that the phase φ_L of the mode function of the standing-wave laser field can be controlled via a movable mirror, which is used to create the standing wave (Freyberger, Kienle and Yakovlev [1997]; Kienle, Fischer, Schleich, Yakovlev and Freyberger [1997]). It is shown that when a pure

motional state is realized, then the phase of the free-evolving wave function can be inferred from the atomic position distributions for phases of the laser field $\varphi_L = -\pi/4, 0, \pi/4$ and $\pi/2$ at chosen time. Knowing from a pre-measurement the absolute value of the wave function for this time, the initial wave function can then be reconstructed by inverting the free time evolution.

4.4.2. Longitudinal motion

In order to determine the quantum state of the longitudinal center-of-mass motion of atoms in an atomic beam, it was proposed to reconstruct the Wigner function tomographically via state-selective time-dependent measurement of longitudinal position distributions (Kokorowski and Pritchard [1997]). In the scheme, two-level atoms that are initially prepared in the ground state are considered. Located at an adjustable position in the apparatus is an electromagnetic excitation region that is assumed to be effectively a π pulse; i.e., any particle exposed to the radiation in the region is completely excited. Downstream, a state-selective detector counts the number of particles which have made a transition into the excited state owing to the π pulse. Time dependence may be introduced either by operating the excitation region in short pulses at definite times, or by using an excited state whose lifetime is much shorter than the desired time resolution. In the latter case, detection consists of observing spontaneously emitted radiation, and the time is simply the time of detection. Measurement of the longitudinal position distribution as a function of time then yields, similar to eq. (233), the quadrature-component distributions for phase parameters in a $\pi/2$ interval. Again, symmetry assumptions may be made in order to compensate for the lack of accessible phases.

It was also proposed to reconstruct the quantum state in terms of the density matrix in the energy basis by using an interferometric method that is based on a generalization of Ramsey's classic separated oscillatory fields technique¹²¹ and the observation that the longitudinal momentum of an atom can be shifted coherently via interaction with off-resonant radiation (Dhirani, Kokorowski, Rubenstein, Hammond, Rohwedder, Smith, Roberts and Pritchard [1997]). In the interferometer an atom-wave in the internal (electronic) ground state is split into ground-state and excited-state components by an electromagnetic field (detuning δ_1) at position z_1 . The excited-state component receives a momentum shift $\hbar\Delta k_1$ ($\approx \delta_1/v$ if the kinetic energy $mv^2/2$ is much larger than $\hbar\delta_1$). The remaining ground-state component is split again by a second field (detuning δ_2) at x_2 , where the excited-state component is momentum-shifted by $\hbar\Delta k_2$. Both field regions are assumed to have different detunings ($\delta_1 \neq \delta_2$). The excited state detected at the interferometer output contains a coherent superposition of two distinct energy components, each with a different corresponding longitudinal momentum. It can be shown that the probability of detecting an atom in the excited state at location z (output port) and time t is given by¹²²

$$P_e(z, t) = \int d\Omega' \int d\Omega'' \varrho(\Omega', \Omega'') \exp[-i(\Omega' - \Omega'')(t - z/v')] \\ \times \cos^2\left\{\frac{1}{2}[(\delta_1 - \delta_2)t - \Delta k'_1(z - z_1) + \Delta k'_2(z - z_2)]\right\}, \quad (234)$$

¹²¹For details, see Ramsey [1956].

¹²²Here it is assumed that $\Omega' - \Omega'' \ll \Omega', \Omega''$; for the relation without this restriction, see Dhirani, Kokorowski, Rubenstein, Hammond, Rohwedder, Smith, Roberts and Pritchard [1997].

where $\rho(\Omega', \Omega'')$ is the motional density matrix in the energy basis (strictly speaking, $\Omega = E/\hbar$). Equation (234) reveals that the measured excited-state probability $P_e(z, t)$ is determined by a convolution of the density-matrix elements $\rho(\Omega', \Omega'')$ with two factors. The exponential represents the free evolution of the density matrix, and the cosine squared contains the phase difference accumulated by the two paths of the interferometer. Eventually, eq. (234) can be inverted in order to obtain $\rho(\Omega', \Omega'')$ in terms of $P_e(z, t)$ by Fourier transforming twice after appropriate change of the variables (for details, see Dhirani, Kokorowski, Rubenstein, Hammond, Rohwedder, Smith, Roberts, and Pritchard [1997]).

4.5. Electron motion

So far knowledge of electronic quantum states has been typically required in order to reconstruct motional and vibrational quantum states of atoms and molecules. This may have brought the reconstruction of the motional quantum state of electrons into question (for the spin, see § 4.6.).

4.5.1. Electronic Rydberg wave packets

Highly excited Rydberg states have offered novel possibilities of preparing electron-wave packets. Since the early experiments at the end of the 1980s (Yeazell and Stroud, Jr., [1988]; ten Wolde, Noordam, Lagendijk and van Linden van den Heuvell [1988]) various schemes have been used in order to produce Rydberg wave packets (for a brief review of generation and detection of Rydberg wave packets, see Noordam and Jones, R.R., [1997]). A Rydberg wave packet is produced whenever several Rydberg states are excited coherently. In particular, it has also been possible to prepare an atomic electron in a coherent superposition of two wave packets which are localized spatially at the opposite extremes of a Kepler orbit (Noel and Stroud, Jr. [1996]). On a sufficiently short time scale these nonclassical states are close to the even/odd coherent states of the harmonic oscillator. To demonstrate important features of these states, two kinds of measurements have been used. State selective ionization allows one to verify that only every other atomic level is populated, and a Ramsey fringe measurement verifies the coherence of the superposition.

A wave-packet interference technique was proposed to measure engineered atomic Rydberg wave functions (Chen and Yeazell [1997]).¹²³ It is assumed that the Rydberg wave packet is produced by (a sequence of) short optical (Gaussian) pulses whose interaction with the atomic system can be treated in lowest-order perturbation theory. Describing the atomic system by the radial wave function,

$$\Psi(r, t) = a_g(t)e^{-i\omega_g t}u_g(r) + \sum_n a_n(t)e^{-i\omega_n t}u_n(r), \quad (235)$$

where a_n and ω_n are the Schrödinger amplitudes and eigenenergies for the Rydberg states and a_g and ω_g are these for the ground state, the excited-state amplitudes after the last excitation pulse, a_n , are given by

$$a_n = -\frac{1}{2}i\Omega_n e^{-\Delta_n^2 \sigma^2 / 2} z_n, \quad (236)$$

¹²³The method was also proposed for reconstructing pure vibrational states in a molecule (Leichtle, Schleich, Averbukh and Shapiro, M., [1998]).

where $z_n = 1 + \sum_i \exp[i(\omega + \Delta_n)\tau_i]$ (Ω_n , Rabi frequency of the excitation between the ground state and a given Rydberg state n ; $\Delta_n = \omega_n - \omega$, detuning; σ , pulse width; τ_i , time delay for the i th individual pulse). When a probe pulse (identical to the previous pulses) interacts with the atom, then the new excited-state amplitudes

$$a'_n = -\frac{1}{2}i\Omega_n e^{-\Delta_n^2 \sigma^2 / 2} \{z_n + \exp[i(\omega + \Delta_n)\tau]\} \quad (237)$$

are produced (τ , delay time for the probe pulse). By measuring the population in each eigenstate, $|a'_n|^2$, for different phases between excitation and probe pulses (on applying high-resolution technique, such as state-selective field ionization), the complex quantities z_n can be obtained; i.e., the (radial) wave function created by the excitation pulse may be inferred. Note that the pump and probe pulses need not be identical, but they must be phase coherent with each other.

Using optical pulses, Rydberg wave packets can usually be detected when they are near to an ionic core. This limitation can be overcome by using subpicosecond, unipolar electromagnetic field (half-cycle) pulses,¹²⁴ which have been a powerful tool for studying dynamics in weakly bound systems (Jones, R.R., You and Bucksbaum [1993]). Such pulses can track the wave packet throughout its orbit and detect wave-packet motion anywhere in the atom, as was demonstrated experimentally (Raman, Conover, Sukenik and Bucksbaum [1996]). In particular, it has been possible to monitor the momentum-space probability of the wave packet as a function of time (Jones, R.R., [1996]; for details, see also Noordam and Jones, R.R., [1997]). In the experimental demonstration of the method also called *impulsive momentum retrieval* Na atoms are first excited by a tunable nanosecond laser to the $25d$ Rydberg state. Subsequently, two half-cycle pulses are applied. Kicking the electron with the first pulse, the Rydberg population is redistributed and a complicated, dynamically evolving wave packet is created. The second pulse is used to measure the ionization as a function of its peak field and delay relative to the first pulse. If the duration of the probe pulse is negligible compared with the time scale for variations in the position and momentum of the electron, then the energy gained (or lost) by the electron depends only on its initial momentum (i.e., the momentum immediately before the application of the pulse) and the time-integrated field. By measuring the ionization probability (at threshold) as a function of field, the momentum distribution of the initial state along the field axis can be obtained.

4.5.2. Cyclotron state of a trapped electron

Let us consider an electron in a *Penning trap*¹²⁵ and assume a uniform magnetic field along the positive z axis. The cyclotron and the axial motions are well separated in their frequency ranges (for a review, see Brown, L.S., and Gabrielse [1986]). It was proposed to reconstruct the cyclotron state by mapping it onto the axial degree of freedom (Mancini and Tombesi [1997a]). By applying appropriate fields on the trapped electron, a coupling between the two degrees of freedom may be realized such that the Hamiltonian in the (cyclotron) interaction picture is of the form

$$\hat{H} = \hbar\nu_z \left(\hat{a}_z^\dagger \hat{a}_z + \frac{1}{2} \right) + \hbar g \hat{x}_c(\varphi) \hat{z}. \quad (238)$$

¹²⁴For these pulses, commonly referred to as HCP's, see also Greene, Federici, Dykaar, Jones, R.R., and Bucksbaum [1991]; You, Jones, R.R., Bucksbaum and Dykaar [1993].

¹²⁵For the trap, see Penning [1936].

Here, \hat{a}_z^\dagger (\hat{a}_z) is the creation (annihilation) operator for the axial motion of frequency ν_z , and \hat{z} and $\hat{x}_c(\varphi)$, respectively, are the axial position operator and the quadrature operator of the cyclotron motion, g being the (field induced) coupling constant. For an interaction time that is short compared with the axial period, $\tau \ll 2\pi/\nu_z$, the Hamiltonian (238) gives rise to a unitary kick and the time evolution of the mean axial momentum yields the mean of the quadrature operator,

$$\langle \hat{p}_z(t+\tau) \rangle = \langle \hat{p}_z(t) \rangle + \hbar g \tau \langle \hat{x}_c(\varphi) \rangle \cos(\nu_z t). \quad (239)$$

By measuring the current due to the induced charge variation on the cap electrodes of the trap, one may obtain the axial momentum and then the cyclotron quadrature component. Knowing the cyclotron quadrature-component statistics, the quantum state can be derived; e.g., by applying the methods of §§ 3.1., 3.2. and 3.3.1..

To determine the cyclotron state from the displaced number statistics (§§ 3.3.2. and 3.5.), it was proposed to perform a QND measurement of the cyclotron excitation number (Mancini and Tombesi [1997a]). Using a magnetic bottle configuration (Brown, L.S., and Gabrielse [1986]), an interaction Hamiltonian of the type

$$\hat{H}' = \hbar \kappa \hat{a}_c^\dagger \hat{a}_c \hat{z}^2 \quad (240)$$

may be realized. It gives rise to a dependence of the axial angular frequency on the number of cyclotron excitations, which may be obtained by probing the resonance frequency of the output electric signal. The displacement of the cyclotron state may be realized by a driving field acting immediately before the measurement process induced by the Hamiltonian (240).

4.5.3. Electron beam

A method was also proposed for determining the quantum state of the (one-dimensional) transverse motion of a beam of identically prepared electrons (Tegmark [1996]). Originating from the electron source, the beam crosses a magnetic field and in conjunction with collimators a highly monochromatic beam is prepared. This beam enters a shielded box, wherein a harmonic potential acts in the x -direction. The needed potential is obtained by subdividing the walls of the box into a large number of metal plates which are insulated from one another, and by fixing the potentials of the plates appropriately. A slidable detector (along the z -direction of longitudinal motion of the beam) allows one to measure the particle density $p(x)$ along the x -direction. Performing these measurements for a series of locations of the slidable detector, the density matrix characterizing the transverse motion of the electrons of the beam may be reconstructed.

4.6. Spin and angular momentum systems

In the history of quantum-state measurement spin (angular momentum) systems have played a particular role, because of the finite-dimensional Hilbert space (see, e.g., Fano [1957] and the references in footnote 41 for the Pauli problem). Spin-quantum-state reconstruction is usually based on data obtained from Stern–Gerlach experiments, in which particles with magnetic momentum are deflected in a magnetic-field gradient

and the spin (or angular momentum) projection onto the direction of the field gradient is measured (Stern [1921], Gerlach and Stern [1921, 1922]; Feynman, Leighton and Sands [1965]; for the optical Stern–Gerlach effect, i.e., state-dependent deflection of particles in optical fields, see Kazantsev [1975, 1978], Cook [1978], Tanguy, Reynaud and Cohen-Tannoudji [1984], and for its experimental realization, see Sleator, Pfau, Balykin, Carnal and Mlynek [1992]). Interacting the particles with fields of magnetic multipoles, multipole moments of the particles can be measured (Bohn [1991]).

In a Stern–Gerlach analyzer as described by Feynman, Leighton and Sands [1965] a beam of particles is split in an inhomogeneous magnetic field into different paths provided with gates that may be opened or closed. The diagonal density-matrix elements ϱ_{mm} are then given by the probability that the particle is deflected into the corresponding m th path. Measurement of the off diagonal element ϱ_{kn} requires two analyzers. In the first analyzer, the n th and k th paths are opened while the remaining paths are closed. In the second analyzer the field gradient is in the plane that is perpendicular to the quantization axis defined by the first analyzer. Let the orientation of the field gradient of the second analyzer be φ . The probability $p_m(\varphi)$ of the particle being deflected into the m th path in the second analyzer is then given by (Gale, Guth and Trammel [1968])

$$p_m(\varphi) = N \left\{ \left[d_{mk}^{(J)}(\pi/2) \right]^2 \varrho_{kk} + \left[d_{mn}^{(J)}(\pi/2) \right]^2 \varrho_{nn} + 2|\varrho_{kn}| d_{mk}^{(J)}(\pi/2) d_{mn}^{(J)}(\pi/2) \cos[(k-n)\varphi + \varphi_{kn}] \right\}, \quad (241)$$

where $\varrho_{kn} = |\varrho_{kn}| \exp(i\varphi_{kn})$. The matrix $d_{mk}^{(J)}(\vartheta)$ is the ϑ -dependent part of the Wigner rotation matrix (see Wigner [1959]), and $N = (\varrho_{kk} + \varrho_{nn})^{-1}$. Measuring (for known ϱ_{kk} and ϱ_{nn}) the probabilities for two different orientations φ , the off diagonal-density matrix element ϱ_{kn} can be determined.

The quantum state can also be determined by using a single Stern–Gerlach apparatus with variable orientation (Newton and Young [1968]). The probability $p_m(\vartheta, \varphi)$ that the projection of the spin on the quantization axis (ϑ, φ) is m can be expressed in terms of the density matrix elements ϱ_{kn} as

$$p_m(\vartheta, \varphi) = \sum_{n,k=-J}^J e^{-i(n-k)\varphi} d_{nm}^{(J)}(\vartheta) d_{km}^{(J)}(\vartheta) \varrho_{kn}, \quad (242)$$

which can be inverted to obtain

$$\varrho_{kk+w} = \sum_{m=-J}^J \sum_{j=0}^{2J} C_{m,-m,0}^{J,J,j} C_{k+w,-k,w}^{J,J,j} \frac{(-1)^{k-m}}{d_{w,0}^{(j)}(\vartheta)} X(\vartheta)_{wm}, \quad (243)$$

where

$$X(\vartheta)_{wm} = \frac{1}{4J+1} \sum_{s=-2J}^{2J} e^{iws\varphi_s} p_m(\vartheta, \varphi_s), \quad (244)$$

$\varphi_s = 2\pi s/(4J+1)$, and $C_{k,m,w}^{J,J,j}$ are Clebsch–Gordan coefficients. It is seen that in order to reconstruct the density matrix, it is sufficient to keep ϑ fixed and take φ at $4J+1$ values such that $d_{w,0}^{(j)}(\vartheta)$ does not vanish for any combination j and w . It should be noted that the Stern–Gerlach apparatus can also be allowed to take all possible

orientations (Dodonov and Man'ko, V.I., [1997]). In this case one need not search for an optimum choice of orientations, since all possible orientations are considered on an equal footing.

As already outlined, the problem of reconstruction of spin density matrices has also been treated by means of the principle of maximum entropy (Bužek, Drobný, Adam, G., Derka and Knight [1997]; see § 3.9.3.) and Bayesian inference (Jones, K.R.W., [1991]; Derka, Bužek and Adam, G., [1996]; Derka, Bužek, Adam, G., and Knight [1996]; see § 3.9.4.). It was also proposed to tomographically reconstruct the discrete Wigner function of a spin system in analogy to the inverse Radon transform for the continuous Wigner function (Leonhardt [1995, 1996]). However, the scheme does not only require measurement of probability distributions of spin (angular momentum) components but also those of discrete phase states.

With regard to pure states, it can be shown that the spin wave function can be reconstructed from the populations of the spin projections on two directions deviated from each other by an infinitesimal angle (Weigert [1992]). Particular attention was paid to the determination of the class of pure states which are eigenstates of rotated spin projection operators $J_n = n_x J_x + n_y J_y + n_z J_z$, where $\mathbf{n} = (n_x, n_y, n_z)$ is a direction vector of unit length. As shown, measurement of spin projections on three directions is sufficient to determine the unknown direction \mathbf{n} and the corresponding spin component eigenvalue (Ivanović [1993]).

Finally, experiments for reconstructing the angular momentum density matrix of electrons in hydrogen atoms from measurements of the Stark structure of the emitted light have been reported (Havener, Rouze, Westerveld and Risley [1986]; Ashburn, Cline, Stone, van der Burgt, Westerveld and Risley [1989]; Ashburn, Cline, van der Burgt, Westerveld and Risley [1990]; Cline, van der Burgt, Westerveld and Risley [1990]; Renwick, Martell, Weaver and Risley [1993]; Seifert, Gibson and Risley [1995]). In the experiments, the density matrix is considered for the manifold of states of principal quantum number $n = 3$ and $n = 2$, the matrix elements being parametrized by the orbital and magnetic quantum numbers l and m respectively. The excited hydrogen atoms are produced by collisions of protons with noble gas atoms. Measuring the coherence parameters of the emitted light [transitions ($n = 3$) \rightarrow ($n = 2$) and ($n = 2$) \rightarrow ($n = 1$)] in dependence on the external electric field, one can infer the density-matrix elements (for theoretical results, see Jain, Lin and Fritsch [1987a,b, 1988]).

4.7. Crystal lattices

More than ten years before the first demonstration of reconstruction of the quantum state of light experiments were already performed for reconstructing off-diagonal elements of the single-particle density matrix of crystal lattices (Golovchenko, Kaplan, Kincaid, Levesque, Meixner, Robbins and Felsteiner [1981]; Schülke, Bonse and Mourikis [1981]). The methods are based on Compton scattering or X-ray scattering. Before giving the basic idea of these methods, let us outline briefly the information available in standard X-ray and Compton scattering experiments.

In conventional X-ray diffraction the Bragg diffracted intensity corresponding to a reciprocal lattice vector \mathbf{g} is proportional to the squared modulus of the form factor $F(\mathbf{g})$. Provided that the phase of the form factor can be determined, some limited

insight into the one-particle density matrix in momentum space, $\varrho(\mathbf{p}, \mathbf{p} + \mathbf{g})$, can be gained. To be more specific, the form factor yields the momentum average of the density matrix according to

$$F(\mathbf{g}) = \int d\mathbf{p} \varrho(\mathbf{p}, \mathbf{p} + \mathbf{g}). \quad (245)$$

In conventional Compton scattering one may obtain the position average of the density matrix in position space, $\varrho(\mathbf{r}, \mathbf{r}')$. The one-dimensional Fourier transform of the Compton profile, the so-called reciprocal form factor $B(\mathbf{r})$, can be given by

$$B(\mathbf{r}) = \int d\mathbf{r}' \varrho(\mathbf{r}', \mathbf{r}' + \mathbf{r}). \quad (246)$$

Obviously, conventional methods do not provide the full density matrix, neither in position nor in momentum space.

The basic idea to overcome this problem consists in the use of coherent scattering methods (Golovchenko, Kaplan, Kincaid, Levesque, Meixner, Robbins and Felsteiner [1981]; Schülke, Bonse and Mourikis [1981], Schülke and Mourikis [1986]; Schülke [1988]). Let us consider the situation in Compton scattering. In conventional experiments a propagating plane wave is used, so that each point in position space is excited equally. This explains the fact that one can only measure position-space averages of the density matrix as given in eq. (246). To avoid this limitation, one may introduce a weighting of certain positions within the elementary cell. This can be done by using a standing-wave field with a spatial periodicity of the nodes that is commensurable with the lattice periodicity. The spatial distribution of the corresponding intensity is given by

$$I(\mathbf{r}) = I_1 + I_2 + 2\sqrt{I_1 I_2} \cos(\mathbf{g} \cdot \mathbf{r} + \varphi), \quad (247)$$

where the phase φ defines the position of the nodes with respect to the atomic planes of the lattice. One may perform two measurements of the Compton profiles by choosing the values of the phase to be $\varphi = 0, \pi$. The difference of the corresponding form factors, $\Delta B(\mathbf{r}; \mathbf{g})$, is then given by

$$\Delta B(\mathbf{r}; \mathbf{g}) \sim \int d\mathbf{r}' \varrho(\mathbf{r}', \mathbf{r}' + \mathbf{r}) \cos(\mathbf{g} \cdot \mathbf{r}'). \quad (248)$$

That is, coherent Compton scattering allows to determine spatial Fourier transforms of the one-particle density matrix.

Acknowledgments

We thank all the colleagues who supported us during the preparation of this article. We are indebted to them for reading foregoing drafts and giving valuable comments that improved the final version, for bringing particular details of the subject to our attention, for providing us with experimental data and for the help in preparing figures. In particular, we are grateful to E.L. Bolda, T. Coudreau, G.M. D'Ariano, E. Giacobino, Z. Hradil, W.M. Itano, L. Knöll, D. Leibfried, U. Leonhardt, M.G.A. Paris, J. Peřina, Th. Richter, S. Wallentowitz, D.F. Walls, I.A. Walmsley, L. Waxer, D.J. Wineland and A. Zucchetti. Finally, we like to emphasize that our research in the field of phase-sensitive measurements and quantum-state reconstruction has been supported by the Deutsche Forschungsgemeinschaft.

A. Radiation field quantization

From Maxwell's theory it is well known that the vector potential of the radiation field in free space can be given by an expansion in transverse travelling waves. For dealing with radiation inside resonators, such as cavities bounded by perfectly reflecting mirrors, a standing-wave expansion is appropriate, where the spatial structure of the waves sensitively depends on the resonator geometry through the boundary conditions. An expansion of the vector potential

$$\mathbf{A}(\mathbf{r}, t) = \mathbf{A}^{(+)}(\mathbf{r}, t) + \mathbf{A}^{(-)}(\mathbf{r}, t), \quad \mathbf{A}^{(-)}(\mathbf{r}, t) = [\mathbf{A}^{(+)}(\mathbf{r}, t)]^* \quad (\text{A.1})$$

in orthogonal transverse waves,

$$\mathbf{A}^{(+)}(\mathbf{r}, t) = \sum_{\lambda} \mathbf{A}_{\lambda}(\mathbf{r}) e^{-i\omega_{\lambda} t} a_{\lambda}, \quad (\text{A.2})$$

is usually called mode expansion. The mode functions $\mathbf{A}_{\lambda}(\mathbf{r})$ satisfy the Helmholtz equation

$$\nabla \times \nabla \times \mathbf{A}_{\lambda} - \frac{\omega_{\lambda}^2}{c^2} \mathbf{A}_{\lambda} = 0, \quad (\text{A.3})$$

where the condition of transversality, $\nabla \cdot \mathbf{A}_{\lambda} = 0$, implies that $\nabla \times \nabla \times \mathbf{A}_{\lambda} = -\Delta \mathbf{A}_{\lambda}$. The mode amplitudes $a_{\lambda}(t)$ evolve according to harmonic-oscillator equations of motion,

$$\dot{a}_{\lambda} = -i\omega_{\lambda} a_{\lambda}. \quad (\text{A.4})$$

Since harmonic oscillators can be associated with the modes, quantization of radiation reduces to quantization of harmonic oscillators. In eq. (A.1), the complex amplitudes a_{λ} and a_{λ}^* are regarded as non-Hermitian destruction and creation operators \hat{a}_{λ} and $\hat{a}_{\lambda}^{\dagger}$, respectively, which satisfy the well-known (equal-time) bosonic commutation relations:

$$[\hat{a}_{\lambda}, \hat{a}_{\lambda'}^{\dagger}] = \delta_{\lambda\lambda'}, \quad [\hat{a}_{\lambda}, \hat{a}_{\lambda'}] = 0. \quad (\text{A.5})$$

The bosonic excitations introduced in this way are called photons. It should be pointed out that the expansion in monochromatic modes of the (Heisenberg) operator of the vector potential,

$$\hat{\mathbf{A}}(\mathbf{r}, t) = \hat{\mathbf{A}}^{(+)}(\mathbf{r}, t) + \hat{\mathbf{A}}^{(-)}(\mathbf{r}, t), \quad (\text{A.6})$$

$$\hat{\mathbf{A}}^{(+)}(\mathbf{r}, t) = \sum_{\lambda} \mathbf{A}_{\lambda}(\mathbf{r}) e^{-i\omega_{\lambda} t} \hat{a}_{\lambda}, \quad (\text{A.7})$$

can be used to introduce photons that are associated with other than monochromatic waves; viz.,

$$\hat{a}'_{\mu} = \sum_{\lambda} C_{\mu\lambda}^* \hat{a}_{\lambda}, \quad (\text{A.8})$$

$$\hat{\mathbf{A}}(\mathbf{r}, t) = \sum_{\mu} [\mathbf{A}'_{\mu}(\mathbf{r}, t) \hat{a}'_{\mu} + \mathbf{A}'_{\mu}^*(\mathbf{r}, t) \hat{a}'_{\mu}{}^{\dagger}], \quad (\text{A.9})$$

where $C_{\mu\lambda}$ are elements of a unitary matrix, so that the \hat{a}'_{μ} and $\hat{a}'_{\mu}{}^{\dagger}$ are again photon destruction and creation operators, respectively, and

$$\mathbf{A}'_{\mu}(\mathbf{r}, t) = \sum_{\lambda} C_{\mu\lambda} \mathbf{A}_{\lambda}(\mathbf{r}) e^{-i\omega_{\lambda} t} \quad (\text{A.10})$$

(for details, see Titulaer and Glauber [1966]). The spatial-temporal (nonmonochromatic) modes can be used advantageously for describing and analysing pulse-like radiation.

The mirrors used in resonator experiments are of course not perfectly reflecting. Moreover, fractionally transparent mirrors are deliberately used to open input and output ports in resonator equipments. Another typical example is the use of beam splitters in various interference and correlation experiments. In many cases these and related (passive) optical instruments can be regarded as macroscopic dielectric bodies that respond linearly to radiation and whose action can be included phenomenologically in the Maxwell theory through a space-dependent permittivity ε (Knöll, Vogel, W., and Welsch [1987], Glauber and Lewenstein [1991]). When the radiation under consideration is in a frequency intervall where the effect of dispersion is sufficiently small, then the dependence of the permittivity on frequency can be disregarded. Performing a mode expansion (A.2), the mode functions are now solutions of a modified Helmholtz equation (A.3), with $v = v(\mathbf{r}) = c/n(\mathbf{r})$ in place of c , where $n(\mathbf{r}) = \sqrt{\varepsilon(\mathbf{r})}$ is the (real) refractive index. The mode functions satisfy a generalized condition of transversality, $\nabla \cdot (\varepsilon \mathbf{A}_\lambda) = 0$, and the relation of orthogonality requires inclusion of ε in the space integral (for details, see Vogel, W., and Welsch [1994]), because of the dependence on \mathbf{r} of the permittivity.¹²⁶

B. Quantum-state representations

Among the wide variety of possible radiation-field states, there are some fundamental states which, with regard to representation and measurement, play a special role in quantum optics. Let us consider a (free) radiation field whose vector potential is given by a mode decomposition [eq. (A.7) or eq. (A.9)] and restrict our attention to single-mode states. The single-mode states can then be used to build up multimode states as (direct-)product states.

B.1. Fock states

A mode (with photon destruction and creation operators \hat{a} and \hat{a}^\dagger , respectively) is said to be in a Fock state (photon-number state) $|n\rangle$, when the state is an eigenstate of the photon-number operator $\hat{n} = \hat{a}^\dagger \hat{a}$,

$$\hat{n}|n\rangle = n|n\rangle, \quad n = 0, 1, 2, \dots \quad (\text{B.1})$$

Each number state $|n\rangle$ can be obtained from the vacuum state $|0\rangle$ according to

$$|n\rangle = \frac{1}{\sqrt{n!}} \hat{a}^{\dagger n} |0\rangle. \quad (\text{B.2})$$

¹²⁶For extensions to dispersive and absorbing media, see Gruner and Welsch [1996] and references therein. In this case, the permittivity is a complex function of frequency, the real and imaginary parts being related to each other according the Kramers–Kronig relations, and a mode decomposition outlined here fails.

Since the photon-number states form an orthogonal and complete set of states, the density operator of any (single-mode) quantum state can be expanded in the photon-number basis,

$$\hat{\rho} = \sum_{n,n'} |n\rangle \langle n| \hat{\rho} |n'\rangle \langle n'|, \quad (\text{B.3})$$

the diagonal elements $p_n = \langle n| \hat{\rho} |n\rangle$ being the probabilities for observing n photons.

B.2. Quadrature-component states

Next let us consider a (single-mode) field-strength operator of the type of $\hat{F}(\varphi) = |F|(\hat{a}e^{-i\varphi} + \hat{a}^\dagger e^{i\varphi})$. Depending on the choice of the (scaling) factor $|F|$, the operator \hat{F} may represent the vector potential or the electric or magnetic fields associated with the mode. In what follows we set $\hat{F} = 2^{1/2}|F|\hat{x}(\varphi)$, where

$$\hat{x}(\varphi) = 2^{-1/2}(\hat{a}e^{-i\varphi} + \hat{a}^\dagger e^{i\varphi}) \quad (\text{B.4})$$

is called quadrature-component operator. The quadrature components $\hat{x}(\varphi)$ and $\hat{x}(\varphi')$ are observables that cannot be measured simultaneously for $\varphi \neq \varphi' + k\pi$, $k=0, \pm 1, \dots$, because of $[\hat{x}(\varphi), \hat{x}(\varphi')] \neq 0$. For chosen φ quadrature-component states $|x, \varphi\rangle$ can be introduced (Schubert and Vogel, W., [1978a,b], see also Vogel, W., and Welsch [1994]), solving the eigenvalue problem

$$\hat{x}(\varphi) |x, \varphi\rangle = x |x, \varphi\rangle, \quad (\text{B.5})$$

$-\infty \leq x \leq \infty$. Obviously, $|x, \varphi\rangle$ is related to $|x\rangle = |x, \varphi=0\rangle$ as $|x, \varphi\rangle = e^{i\hat{n}\varphi} |x\rangle$, and can be given by

$$\begin{aligned} |x, \varphi\rangle &= \pi^{-1/4} e^{-x^2/2} \sum_n \frac{e^{in\varphi}}{\sqrt{2^n n!}} H_n(x) |n\rangle \\ &= \pi^{-1/4} e^{-x^2/2} \exp\left[-\frac{1}{2} \left(e^{i\varphi} \hat{a}^\dagger\right)^2 + 2^{1/2} x e^{i\varphi} \hat{a}^\dagger\right] |0\rangle \end{aligned} \quad (\text{B.6})$$

[$H_n(x)$, Hermite polynomial]. The states $|x, \varphi\rangle$ define an orthogonal Hilbert space basis for each value of φ , so that the density operator can be expanded as

$$\hat{\rho} = \int dx \int dx' |x, \varphi\rangle \langle x, \varphi| \hat{\rho} |x', \varphi\rangle \langle x', \varphi|. \quad (\text{B.7})$$

In particular, $p(x, \varphi) = \langle x, \varphi| \hat{\rho} |x, \varphi\rangle$ is the probability density for observing the value x of the quadrature component $\hat{x}(\varphi)$. Note that the symmetry relation $p(x, \varphi + \pi) = p(-x, \varphi)$ holds.

B.3. Coherent states

The coherent states introduced by Schrödinger [1926] to simulate the motion of a (near)classical particle in a harmonic potential are usually defined by the eigenvalue problem¹²⁷

$$\hat{a} |\alpha\rangle = \alpha |\alpha\rangle \quad (\text{B.8})$$

¹²⁷The coherent states were recovered in the 1960's (Klauder [1960, 1963a,b]; Glauber [1963a]; Sudarshan [1963]; Klauder and Sudarshan [1968]).

(α , complex). Equivalently,

$$|\alpha\rangle = \hat{D}(\alpha)|0\rangle, \quad (\text{B.9})$$

where $\hat{D}(\alpha)$ is the coherent displacement operator,

$$\hat{D}(\alpha) = \exp(\alpha\hat{a}^\dagger - \alpha^*\hat{a}) \quad (\text{B.10})$$

[note that $\hat{D}(\alpha)\hat{a}\hat{D}^\dagger(\alpha) = \hat{a} - \alpha$]. The coherent states are not orthogonal,

$$\langle\alpha'|\alpha\rangle = \exp\left(-\frac{1}{2}|\alpha - \alpha'|^2\right) \exp\left[\frac{1}{2}(\alpha\alpha'^* - \alpha^*\alpha')\right], \quad (\text{B.11})$$

and they are overcomplete (Cahill [1965]; Bacry, Grossmann and Zak [1975]), so that there are various possibilities of representing the density operator. In particular, it can be expanded as

$$\hat{\rho} = \frac{1}{\pi^2} \int d^2\alpha \int d^2\alpha' |\alpha\rangle\langle\alpha|\hat{\rho}|\alpha'\rangle\langle\alpha'| \quad (\text{B.12})$$

($d^2\alpha = d\text{Re}\alpha d\text{Im}\alpha$).

Equation (B.9) can be extended in order to define generalized coherent states by the action of the displacement operator on arbitrary states of the Hilbert space (see, e.g., Perelomov [1986]). In particular, the action of $\hat{D}(\alpha)$ for all values of α on a set of states $|\Psi_\lambda\rangle$ that resolve the unity introduces a foliation of the Hilbert space into orbits such that each state belongs exactly to one orbit of generalized coherent states. For example, the Fock states can be used to define the generalized coherent states,

$$|n, \alpha\rangle = \hat{D}(\alpha)|n\rangle, \quad (\text{B.13})$$

which are also called displaced Fock states.¹²⁸ Their expansion in the ordinary Fock basis reads as

$$|n, \alpha\rangle = \sum_m |m\rangle\langle m|n, \alpha\rangle, \quad (\text{B.14})$$

where the expansion coefficients $\langle m|n, \alpha\rangle$ can be given by

$$\langle m|n, \alpha\rangle = \left(m!n!e^{-|\alpha|^2}\right)^{\frac{1}{2}} \sum_{l=0}^{\{m,n\}} (-1)^{m-l} \frac{|\alpha|^{m+n-2l} e^{-i(m-n)\varphi}}{l!(m-l)!(n-l)!} \quad (\text{B.15})$$

[$\{m, n\} = \min(m, n)$, $\alpha = |\alpha|e^{i\varphi}$] or

$$\langle m|n, \alpha\rangle = \exp\left(-\frac{1}{2}|\alpha|^2\right) \sqrt{\frac{n!}{m!}} \alpha^{m-n} L_n^{m-n}(|\alpha|^2) \quad (\text{B.16})$$

[$L_n^m(x)$, Laguerre polynomial].

¹²⁸Similar to the coherent states, these states correspond to wave packets of a particle in a harmonic potential which keep their shapes and follow the classical motion (Husimi [1953]; Senitzky [1954]; Plebanski [1954, 1955, 1956]; Epstein [1959]).

B.4. *s*-Parametrized phase-space functions

Representations of the density operator in terms of phase-space functions which are formally similar to classical probability distributions are used frequently. Defining an *s*-parameterized displacement operator by

$$\hat{D}(\alpha; s) = e^{s|\alpha|^2/2} \hat{D}(\alpha), \quad (\text{B.17})$$

the following expansion of the density operator can be proved correct:

$$\hat{\rho} = \frac{1}{\pi} \int d^2\alpha \text{Tr}\{\hat{\rho} \hat{D}(-\alpha; s)\} \hat{D}(\alpha; -s) \quad (\text{B.18})$$

(for details, see, e.g., Cahill and Glauber [1969a,b]; Agarwal and Wolf [1970]; Peřina [1991]).¹²⁹ Introducing the Fourier transform of $\hat{D}(\alpha; s)$,

$$\begin{aligned} \hat{\delta}(\alpha - \hat{a}; s) &= \frac{1}{\pi^2} \int d^2\beta \hat{D}(\beta; s) \exp[\alpha\beta^* - \alpha^*\beta] \\ &= \frac{2}{\pi(1-s)} \hat{D}(\alpha) \left(\frac{s+1}{s-1}\right)^{\hat{a}^\dagger \hat{a}} \hat{D}^{-1}(\alpha), \end{aligned} \quad (\text{B.19})$$

the expansion (B.18) can be rewritten as¹³⁰

$$\hat{\rho} = \pi \int d^2\alpha P(\alpha; s) \hat{\delta}(\alpha - \hat{a}; -s), \quad (\text{B.20})$$

where

$$P(\alpha; s) = \text{Tr}\{\hat{\rho} \hat{\delta}(\alpha - \hat{a}; s)\} \quad (\text{B.21})$$

is the *s*-parametrized phase-space function, which is normalized to unity.¹³¹ Cases of particular interest are the Glauber-Sudarshan *P* function, $P(\alpha) \equiv P(\alpha; 1)$ (Glauber [1963b, 1963c]; Sudarshan [1963]), the Wigner function $W(\alpha) \equiv P(\alpha; 0)$ (Wigner [1932]) and the *Q* function $Q(\alpha) \equiv P(\alpha; -1)$ (Husimi [1940]). Note that $\hat{\delta}(\alpha - \hat{a}, -1) = \pi^{-1} |\alpha\rangle\langle\alpha|$, which implies that $Q(\alpha) = \pi^{-1} \langle\alpha|\hat{\rho}|\alpha\rangle$. The expectation value of an operator \hat{F} can then be given by

$$\langle\hat{F}\rangle = \int d^2\alpha P(\alpha; s) F(\alpha; s), \quad (\text{B.22})$$

where $F(\alpha; s)/\pi$ is defined according to eq. (B.21) with \hat{F} in place of $\hat{\rho}$.

From eqs. (B.19) and (B.21) we see that

$$\Phi(\alpha; s) = \text{Tr}\{\hat{\rho} \hat{D}(\alpha; s)\}, \quad (\text{B.23})$$

can be regarded as the characteristic function of the phase-space function $P(\alpha; s)$,

$$P(\alpha; s) = \frac{1}{\pi^2} \int d^2\beta \exp(\alpha\beta^* - \alpha^*\beta) \Phi(\beta; s). \quad (\text{B.24})$$

¹²⁹For $s=0$ the expansion (B.18) is known from Weyl's quantization method (Weyl [1927]).

¹³⁰Note that eqs. (B.20) and (B.21) also apply to other than density operators. Let \hat{F} be an operator function of \hat{a} and \hat{a}^\dagger . Then it can be shown that $\hat{F} = \int d^2\alpha F(\alpha; s) \hat{\delta}(\alpha - \hat{a}; s)$, where $F(\alpha; s) = \pi \text{Tr}\{\hat{F} \hat{\delta}(\alpha - \hat{a}; -s)\}$ is the associated *c*-number function in *s* order.

¹³¹Frequently the definition $P(q, p; s) \equiv 2^{-1} P[\alpha = 2^{-1/2}(q + ip)]$ is used, so that $P(q, p; s)$ can be regarded as a function of "position" and "momentum", with $\int dq \int dp P(q, p; s) = 1$.

Using eqs. (B.17), (B.23), and (B.24), the phase-space functions $P(\alpha; s)$ can be related to each other as

$$P(\alpha; s) = \frac{1}{\pi^2} \int d^2\beta \exp\left[\frac{1}{2}(s-s')|\beta|^2\right] \times \int d^2\gamma \exp[(\alpha-\gamma)\beta^* - (\alpha^* - \gamma^*)\beta] P(\gamma; s'). \quad (\text{B.25})$$

It should be noted that the formalism can be extended to finite dimensional Hilbert spaces (Opatrný, Welsch and Bužek [1996]; for the Wigner function, see Wootters [1987], Leonhardt [1995,1996]; for the Q function, see Opatrný, Bužek, Bajer and Drobný [1995] and Galetti and Marchioli [1996]).¹³²

B.5. Quantum state and quadrature components

It is worth noting that there is a one-to-one correspondence between the phase-space function $P(\alpha; s)$ and the set of quadrature-component distributions $p(x, \varphi)$ for all values of φ within a π interval (Vogel, K., and Risken [1989]). Introducing the characteristic function $\Psi(z, \varphi)$ of the quadrature-component distribution $p(x, \varphi)$,

$$\Psi(z, \varphi) = \int dx e^{izx} p(x, \varphi), \quad (\text{B.26})$$

it can be shown that

$$\Psi(z, \varphi) = e^{-sz^2/4} \Phi\left(iz2^{-1/2}e^{i\varphi}; s\right). \quad (\text{B.27})$$

Equations (B.24), (B.26), and (B.27) reveal that

$$p(x, \varphi) = \frac{1}{2\pi} \int dz \exp\left(-izx - \frac{1}{4}sz^2\right) \times \int d^2\alpha \exp[iz\langle\alpha|\hat{x}(\varphi)|\alpha\rangle] P(\alpha; s) \quad (\text{B.28})$$

and

$$P(\alpha; s) = \frac{1}{2\pi^2} \int_0^\pi d\varphi \int dz \left\{ |z| e^{sz^2/4} \times \exp[-iz\langle\alpha|\hat{x}(\varphi)|\alpha\rangle] \int dx e^{izx} p(x, \varphi) \right\}. \quad (\text{B.29})$$

In other words, knowledge of $p(x, \varphi)$ for all values of φ within a π interval is equivalent to knowledge of the quantum state.¹³³ In particular, the expansion of the density operator as given in eq. (B.18) can be rewritten, on using eqs. (B.23) and (B.27), as

$$\hat{\rho} = \frac{1}{2\pi} \int_0^\pi d\varphi \int dz |z| e^{sz^2/4} \Psi(-z, \varphi) \hat{D}\left(iz2^{-1/2}e^{i\varphi}; -s\right), \quad (\text{B.30})$$

which offers the possibility of relating $\hat{\rho}$ to $p(x, \varphi)$ as

$$\hat{\rho} = \int_0^\pi d\varphi \int dx \hat{K}(x, \varphi) p(x, \varphi), \quad (\text{B.31})$$

¹³²For an approach to phase-space functions for systems with finite-dimensional Hilbert spaces which uses a continuous phase space, see Várilly and Gracia-Bondía [1989]; Dowling, Agarwal and Schleich [1994].

¹³³Note that the φ integral in eq. (B.29) can be performed over any π interval.

provided that the operator kernel

$$\hat{K}(x, \varphi) = \frac{1}{2\pi} \int dz |z| \exp\{iz [\hat{x}(\varphi) - x]\}, \quad (\text{B.32})$$

exists (D'Ariano [1995]; D'Ariano, Leonhardt and Paul, H., [1995]).

C. Photodetection

In order to give an introduction into the quantum theory of photoelectric detection of light (Mandel [1958, 1963], Kelley and Kleiner [1964], Glauber [1965]), let us consider, as a simple example of a photodetection device, a large sample of atomic systems that are capable of absorbing light through the photoemission of electrons in a certain time interval $t, t + \Delta t$. Next suppose that the photoemission of the actual number m of photoelectrons is dominated by the process in which exactly m atomic systems are involved, so that each emits just one electron. We further assume that the total number N of atomic systems is much larger compared with the mean number of emitted electrons, so that for any (relevant) actual value m the inequality $m < N$ may be assumed. Under these assumptions, the main features of the theory may be developed by applying Dirac's perturbation theory to the basic process of light absorption and combining the corresponding results with methods of classical statistics with respect to the ensemble of photoelectrons generated by the absorption processes (see, e.g., Vogel, W., and Welsch [1994]).

Here, we will give a more intuitive analysis rather than an exact derivation. When each photon that falls – in the chosen time interval – on the detector gives rise to exactly one emitted electron, then the number of counted electrons agrees exactly with the number of photons, and the statistics of the counted electrons reflect exactly the photon-number statistics; i.e., the probability P_m of detecting m photoelectrons is equal to the probability p_m of m photons being in the field,

$$P_m = p_m = \langle m | \hat{\rho} | m \rangle. \quad (\text{C.1})$$

However owing to losses, the probability η of converting a photon to an electron is less than unity in general ($0 \leq \eta \leq 1$). This probability is also called detection (or quantum) efficiency. Since (under the assumptions made) the individual events of emission of a photoelectron can be regarded as being independent of each other, the probability $P_{m|n}(\eta)$ of observing m photoelectrons under the condition that n photons are present corresponds to a Bernoulli process,

$$P_{m|n}(\eta) = \binom{n}{m} \eta^m (1 - \eta)^{n-m} \quad \text{if } m \leq n, \quad (\text{C.2})$$

and $P_{m|n}(\eta) = 0$ if $m > n$. The joint probability that n photons are present and m photoelectrons are counted is then $P_{m|n}(\eta)p_n$, and hence the prior probability of detecting m photoelectrons is given by

$$P_m = \sum_n P_{m|n}(\eta) p_n = \sum_{n=m}^{\infty} \binom{n}{m} \eta^m (1 - \eta)^{n-m} p_n \quad (\text{C.3})$$

which for $\eta \rightarrow 1$ (perfect detection) reduces to eq. (C.1). Note that eq. (C.3) can be inverted in order to obtain p_n from P_m by simply replacing η with η^{-1} ,

$$p_n = \sum_{m=n}^{\infty} \binom{m}{n} \left(\frac{1}{\eta}\right)^n \left(1 - \frac{1}{\eta}\right)^{m-n} P_m. \quad (\text{C.4})$$

Equation (C.3) can be rewritten as¹³⁴

$$P_m = \left\langle : \frac{(\eta \hat{n})^m}{m!} e^{-\eta \hat{n}} : \right\rangle, \quad (\text{C.5})$$

and the characteristic function

$$\Omega(y) = \sum_m P_m e^{imy} \quad (\text{C.6})$$

can be given by

$$\Omega(y) = \left\langle : \exp[\eta \hat{n}(e^{iy} - 1)] : \right\rangle, \quad (\text{C.7})$$

where the symbol $::$ indicates normal ordering, with the operator \hat{a}^\dagger to the left of the operator \hat{a} . So far, we have assumed that the photons are effectively associated with a single (nonmonochromatic) mode. The extension of the above given formulae to multimode fields is straightforward. In particular, the multi-mode version of the single-mode photocounting formula (C.5) reads as

$$P_{m_1, m_2, \dots} = \left\langle \prod_k : \frac{(\eta_k \hat{n}_k)^{m_k}}{m_k!} e^{-\eta_k \hat{n}_k} : \right\rangle, \quad (\text{C.8})$$

where \hat{n}_k is the photon-number operator of the k th mode, and η_k is the quantum efficiency which with the photons of this mode are detected.

D. Elements of least-squares inversion¹³⁵

Let \mathbf{f} be a (possibly unknown) n_0 dimensional ‘‘state’’ vector and consider a stochastic linear transform,

$$\mathbf{y} = \mathbf{A} \mathbf{f} + \mathbf{n}, \quad (\text{D.1})$$

yielding an m_0 dimensional ($m_0 \geq n_0$) ‘‘data’’ vector \mathbf{y} available from measurements. Here, \mathbf{A} is a given $m_0 \times n_0$ matrix, and \mathbf{n} is an m_0 dimensional vector whose random elements with zero means and covariance matrix \mathbf{W}^{-1} describe the noise associated with realistic measurements. The probability of a state vector \mathbf{f} being realized under the condition that there is a data vector \mathbf{y} can be given by

$$P(\mathbf{f}|\mathbf{y}) \sim P(\mathbf{y}|\mathbf{f}) P(\mathbf{f}), \quad (\text{D.2})$$

¹³⁴Note that the identity $|n\rangle\langle n| = : (\hat{n}^n/n!) e^{-\hat{n}} :$ is valid, which can easily be proved correct from the associated c -number function $|\langle \alpha|n\rangle|^2$ of $|n\rangle\langle n|$ in normal order.

¹³⁵For details, see, e.g., Golub and van Loan [1989]; Robinson [1991]; Press, Teukolsky, Vetterling and Flannery [1995].

where for Gaussian noise the conditional probability $P(\mathbf{y}|\mathbf{f})$ of observing the data vector \mathbf{y} is

$$P(\mathbf{y}|\mathbf{f}) \sim \exp\left[-\frac{1}{2}(\mathbf{y} - \mathbf{A}\mathbf{f})^\dagger \mathbf{W}(\mathbf{y} - \mathbf{A}\mathbf{f})\right]. \quad (\text{D.3})$$

The probability $P(\mathbf{f})$ is a measure of *a priori* knowledge of the state and can be set constant if no state is preferred. The most probable state $\tilde{\mathbf{f}}$ can then be found by minimization of¹³⁶

$$C(\mathbf{f}) = (\mathbf{y} - \mathbf{A}\mathbf{f})^\dagger \mathbf{W}(\mathbf{y} - \mathbf{A}\mathbf{f}), \quad (\text{D.4})$$

from which

$$\mathbf{A}^\dagger \mathbf{W} \mathbf{A} \tilde{\mathbf{f}} = \mathbf{A}^\dagger \mathbf{W} \mathbf{y}, \quad (\text{D.5})$$

and when $\mathbf{A}^\dagger \mathbf{W} \mathbf{A}$ is not singular, then

$$\tilde{\mathbf{f}} = (\mathbf{A}^\dagger \mathbf{W} \mathbf{A})^{-1} \mathbf{A}^\dagger \mathbf{W} \mathbf{y}. \quad (\text{D.6})$$

Otherwise, the inversion of eq. (D.5) is not unique and further criteria must be used to select a solution. When the matrix \mathbf{W} is not known, then it may be set a multiple of a unity matrix, so that eq. (D.6) reduces to

$$\tilde{\mathbf{f}} = (\mathbf{A}^\dagger \mathbf{A})^{-1} \mathbf{A}^\dagger \mathbf{y}, \quad (\text{D.7})$$

provided that $\mathbf{A}^\dagger \mathbf{A}$ is not singular. Equation (D.7) still gives the correct averaged inversion, but the statistical fluctuation of the result may be (slightly) enhanced.

If the data are not sensitive enough to some state-vector components, then these components can hardly be determined with reasonable accuracy. Mathematically, $\mathbf{A}^\dagger \mathbf{W} \mathbf{A}$ becomes (quasi-)singular and regularizations, such as Tikhonov regularization and singular-value decomposition, are required to solve approximately eq. (D.5). For simplicity let us set $\mathbf{W} = \mathbf{I}$ (\mathbf{I} , unity matrix). Using Tikhonov regularization, it is assumed that some components of the state vector can be preferred by a properly chosen *a priori* probability $P(\mathbf{f})$, such as

$$P(\mathbf{f}) \sim \exp\left(-\frac{1}{2}\lambda^2 \mathbf{f}^\dagger \mathbf{f}\right), \quad (\text{D.8})$$

the parameter λ ($\lambda \geq 0$) being a measure of the strength of regularization. Maximization of $P(\mathbf{f}|\mathbf{y})$ then yields, on recalling eqs. (D.2) and (D.3),

$$\tilde{\mathbf{f}} = (\lambda^2 \mathbf{I} + \mathbf{A}^\dagger \mathbf{A})^{-1} \mathbf{A}^\dagger \mathbf{y}. \quad (\text{D.9})$$

Note that $\lambda^2 \mathbf{I} + \mathbf{A}^\dagger \mathbf{A}$ has only positive eigenvalues and is thus always invertible. A possible choice of λ is based on the so-called *L* curve, which is a log-log plot of $\|\mathbf{f}\|$ versus $\|\Delta\mathbf{y}\|$, $\Delta\mathbf{y} = \mathbf{y} - \mathbf{A}\mathbf{f}$, for different values of λ . The points on the horizontal branch correspond to large noise, whereas the points on the vertical branch correspond to large data misfit. Optimum choice of λ corresponds to points near the corner of the *L* curve.

¹³⁶If \mathbf{W} is diagonal (i.e., the noise is uncorrelated), then eq. (D.4) represents a sum of weighted squares of the differences between the components of the data vector \mathbf{y} and the components of the transformed vector $\mathbf{A}\mathbf{f}$, each term of the sum being multiplied by a weight given by the corresponding element of \mathbf{W} .

Applying singular-value decomposition, the inversion of the matrix $\mathbf{A}^\dagger \mathbf{A}$ is performed such that their eigenvalues whose absolute values are smaller than the (positive) parameter of regularization σ_0 are treated as zeros, but the inversions are set zero (instead to infinity). This operation is called “pseudoinverse” of a matrix,

$$\tilde{\mathbf{f}} = \text{Pseudoinverse}(\mathbf{A}^\dagger \mathbf{A}; \sigma_0) \mathbf{A}^\dagger \mathbf{y}. \quad (\text{D.10})$$

For σ_0 close to zero the result of eq. (D.10) is similar to that of eq. (D.7). With increasing σ_0 , smaller absolute values of components of $\tilde{\mathbf{f}}$ are preferred.

The effect of the regularization parameters λ and σ_0 is similar. The statistical error of the reconstructed state vector $\tilde{\mathbf{f}}$ is decreased, but bias towards zero is produced simultaneously. Hence, optimum parameters are those for which the bias is just below the statistical fluctuation. The bias can be estimated, e.g., by Monte Carlo generating new sets of “synthetic” data from the reconstructed state. From these sets one can again reconstruct new sets of $\tilde{\mathbf{f}}$. The difference between the mean value of the states reconstructed from the synthetic data and the originally reconstructed state estimates the bias.

References

- Abbas, G.L., V.W.S. Chan and T.K. Yee, 1983, *Opt. Lett.* **8**, 419.
- Agarwal, G.S., and S. Chaturvedi, 1994, *Phys. Rev.* **A49**, R665.
- Adams, C.S., M. Sigel, and J. Mlynek, 1994, *Phys. Rep.* **240**, 143.
- Agarwal, G.S., and E. Wolf, 1970, *Phys. Rev.* **D2**, 2161.
- Aharonov, Y., and L. Vaidman, 1993, *Phys. Lett.* **A178**, 38.
- Aharonov, Y., D.Z. Albert and C.K. Au, 1981, *Phys. Rev. Lett.* **47**, 1029.
- Aharonov, Y., J. Anandan and L. Vaidman, 1993, *Phys. Rev.* **A47**, 4616.
- Akulin, V.M., Fam Le Kien and W.P. Schleich, 1991, *Phys. Rev.* **A44**, R1462.
- Alter, O., and Y. Yamamoto, 1995, *Phys. Rev. Lett.* **74**, 4106.
- Anderson, M.H., J.R. Ensher, M.R. Matthews, C.E. Wieman and E.A. Cornell, 1995, *Science* **269**, 198.
- Andrews, M.R., M.-O. Mewes, N.J. van Druten, D.S. Durfee, D.M. Kurn and W. Ketterle, 1996, *Science* **273**, 84.
- Andrews, M.R., C.G. Townsend, H.-J. Miesner, D.S. Durfee, D.M. Kurn and W. Ketterle, 1997, *Science* **275**, 637.
- Arthurs, E., and J.L. Kelly Jr., 1965, *Bell. Syst. Tech. J.* **44**, 725.
- Ashburn, J.R., R.A. Cline, P.J.M. van der Burgt, W.B. Westerveld and J.S. Risley, 1990, *Phys. Rev.* **A41**, 2407.
- Ashburn, J.R., R.A. Cline, C.D. Stone, P.J.M. van der Burgt, W.B. Westerveld and J.S. Risley, 1989, *Phys. Rev.* **A40**, 4885.
- Assion, A., M. Geisler, J. Helbing, V. Seyfried and T. Baumert, 1996, *Phys. Rev.* **A54**, R4605.
- Bacry, H., A. Grossmann and J. Zak, 1975, *Phys. Rev.* **B12**, 1118.
- Ban, M., 1991a, *Phys. Lett.* **A152**, 223.
- Ban, M., 1991b, *Phys. Lett.* **A155**, 397.
- Ban, M., 1991c, *J. Math. Phys.* **32**, 3077.
- Ban, M., 1991d, *Physica* **A179**, 103.
- Ban, M., 1992, *J. Opt. Soc. Am.* **B9**, 1189.
- Ban, M., 1993, *Phys. Lett.* **A176**, 47.
- Banaszek, K., and K. Wódkiewicz, 1996, *Phys. Rev. Lett.* **76**, 4344.
- Banaszek, K., and K. Wódkiewicz, 1997a, *Phys. Rev.* **A55**, 3117.
- Banaszek, K., and K. Wódkiewicz, 1997b, *J. Mod. Opt.* **44**, 2441.
- Banaszek, K., and K. Wódkiewicz, 1998, *Optics Express* **3**, 141.
- Band, W., and J.L. Park, 1970, *Found. Phys.* **1**, 133.
- Band, W., and J.L. Park, 1971, *Found. Phys.* **1**, 339.
- Band, W., and J.L. Park, 1979, *Am. J. Phys.* **47**, 188.
- Bandilla, A., and H. Paul, 1969, *Ann. Phys. (Leipzig)* **23**, 323.
- Bandilla, A., and H. Paul, 1970, *Ann. Phys. (Leipzig)* **24**, 119.
- Bardroff, P.J., E. Mayr and W.P. Schleich, 1995, *Phys. Rev.* **A51**, 4963.
- Bardroff, P.J., C. Leichtle, G. Schrade and W.P. Schleich, 1996, *Phys. Rev. Lett.* **77**, 2198.
- Bardroff, P.J., E. Mayr, W.P. Schleich, P. Domokos, M. Brune, J.M. Raimond and S. Haroche, 1996, *Phys. Rev.* **A53**, 2736.
- Baseia, B., M.H.Y. Moussa and V.S. Bagnato, 1997, *Phys. Lett.* **A231**, 331.
- Beck, M., D.T. Smithey and M.G. Raymer, 1993, *Phys. Rev.* **A48**, R890.

- Bergquist, J.C., R.G. Hulet, W.M. Itano and D.J. Wineland, 1986, Phys. Rev. Lett. **57**, 1699.
- Barnett, S.M., and D.T. Pegg, 1996, Phys. Rev. Lett. **76**, 4148.
- Bergou, J., and B.-G. Englert, 1991, Ann. Phys. (NY) **209**, 479.
- Bertrand, J., and P. Bertrand, 1987, Found. Phys. **17**, 397.
- Białynicka-Birula, Z., and I. Białynicki-Birula, 1994, J. Mod. Opt. **41**, 2203.
- Białynicka-Birula, Z., and I. Białynicki-Birula, 1995, Appl. Phys. B**60**, 275.
- Blockley, C.A., D.F. Walls and H. Risken, 1992, Europhys. Lett. **17**, 509.
- Blow, K.J., R. Loudon, S.J.D. Phoenix and T.J. Shepherd, 1990, Phys. Rev. **A42**, 4102.
- Bodendorf, C.T., G. Antesberger, M.S. Kim and H. Walther, 1998, Phys. Rev. **A57**, 1371.
- Bohn, J., 1991, Phys. Rev. Lett. **66**, 1547.
- Bolda, E.L., S.M. Tan and D.F. Walls, 1997, Phys. Rev. Lett. **79**, 4719.
- de Boer, C., 1987, *A Practical Guide to Spines* (Springer, New York).
- Bradley, C.C., C.A. Sackett, J.J. Tollett and R.G. Hulet, 1995, Phys. Rev. Lett. **75**, 1687.
- Braginsky, V.B., and F.Y. Khalili, 1992, *Quantum Measurement*, (Cambridge University Press, Cambridge).
- Braginsky, V.B., Y.I Vorontsov and F.Y. Khalili, 1977, Sov. Phys.-JETP **46**, 705.
- Braunstein, S.L., 1990, Phys. Rev. **A42**, 474.
- Braunstein, S.L., C.M. Caves and G.J. Milburn, 1991, Phys. Rev. **A43**, 1153.
- Breitenbach, G., and S. Schiller, 1997, J. Mod. Optics **44**, 2207.
- Breitenbach, G., S. Schiller and J. Mlynek, 1997, Nature **387**, 471.
- Breitenbach, G., T. Müller, S.F. Pereira, J.-Ph. Poizat, S. Schiller and J. Mlynek, 1995, J. Opt. Soc. Am. **B12**, 2304.
- Hanbury Brown, R., and R.Q. Twiss, 1956a, Nature **177**, 27.
- Hanbury Brown, R., and R.Q. Twiss, 1956b, Nature **178**, 1046.
- Hanbury Brown, R., and R.Q. Twiss, 1957a, Proc. Roy. Soc. (London) **A242**, 300.
- Hanbury Brown, R., and R.Q. Twiss, 1957b, Proc. Roy. Soc. (London) **A243**, 291.
- Brown, L.S., and G. Gabrielse, 1986, Rev. Mod. Phys. **58** 233.
- Brune, M., and S. Haroche, 1994, in: *Quantum Dynamics of Simple Systems, The Forty Forth Scottish Universities Summer School in Physics*, Stirling, eds G.-L. Oppo, S.M. Barnett, E. Riis and M. Wilkinson (Institute of Physics Publishing, Bristol and Philadelphia, 1996) p. 49.
- Brune, M., S. Haroche, V. Lefevre, J.M. Raimond and N. Zagury, 1990, Phys. Rev. Lett. **65**, 976.
- Brune, M., S. Haroche, J.M. Raimond, L. Davidovich and N. Zagury, 1992, Phys. Rev. **A45**, 5193.
- Brune, M, J.M. Raimond, P. Goy, L. Davidovich and S. Haroche, 1987, Phys. Rev. Lett. **59** 1899.
- Brune, M., F. Schmidt-Kaler, A. Maali, J. Dreyer, E. Hagley, J.M. Raimond and S. Haroche, 1996, Phys. Rev. Lett. **76**, 1800.
- Brunner, W., H. Paul and G. Richter, 1965, Ann. Phys. (Leipzig) **15**, 17.
- Busch, P., and P.J. Lahti, 1989, Found. Phys. **19**, 633.
- Bužek, V., and M. Hillery, 1996, J. Mod. Opt. **43**, 1633.
- Bužek, V., and P.L. Knight, 1995, in: *Progress in Optics XXXIV*, ed. E. Wolf (North-

- Holland, Amsterdam).
- Bužek, V., G. Adam and G. Drobný, 1996a, Ann. Phys. (NY) **245**, 37.
- Bužek, V., G. Adam and G. Drobný, 1996b, Phys. Rev. **A54**, 804.
- Bužek, V., C.H. Keitel and P.L. Knight, 1995a, Phys. Rev. **A51**, 2575.
- Bužek, V., C.H. Keitel and P.L. Knight, 1995b, Phys. Rev. **A51**, 2594.
- Bužek, V., G. Drobný, G. Adam, R. Derka and P.L. Knight, 1997, J. Mod. Opt. **44**, 2607.
- Cahill, K.E., 1965, Phys. Rev. **138B**, 1566.
- Cahill, K.E., and R.J. Glauber, 1969a, Phys. Rev. **177**, 1857.
- Cahill, K.E., and R.J. Glauber, 1969b, Phys. Rev. **177**, 1882.
- Campos, R.A., B.E.A. Saleh and M.C. Teich, 1989, Phys. Rev. **A40**, 1371.
- Carmichael, H.J., 1987, J. Opt. Soc. Am. **B4**, 1588.
- Carnal, O., and J. Mlynek, 1991, Phys. Rev. Lett. **66**, 2689.
- Caves, C.M., 1982, Phys. Rev. **D 26**, 1817.
- Caves, C.M., and P.D. Drummond, 1994, Rev. Mod. Phys. **66**, 481.
- Caves, C.M., and B.L. Schumaker, 1985, Phys. Rev. **A31**, 3068.
- Chaturvedi, S., G.S. Agarwal and V. Srinivasan, 1994, J. Phys. **A27**, L39.
- Chen, X., and J.A. Yeazell, 1997, Phys. Rev. **A56**, 2316.
- Cirac, J.I., R. Blatt, A.S. Parkins and P. Zoller, 1994, Phys. Rev. **A49**, 1202.
- Cline, R., P.J.M. van der Burgt, W.B. Westerveld and J.S. Risley, 1994, Phys. Rev. **A49**, 2613.
- Collett, M.J., R. Loudon and C.W. Gardiner, 1987, J. Mod. Opt. **34**, 881.
- Cook, R.J., 1978, Phys. Rev. Lett. **41**, 1788.
- Corbett, J.V., and C.A. Hurst, 1978, J. Austral. Math. Soc. **B20**, 182.
- Dakna, M., L. Knöll and D.-G. Welsch, 1997a, Quantum Semiclass. Opt. **9**, 331.
- Dakna, M., L. Knöll and D.-G. Welsch, 1997b, Phys. Rev. **A55**, 2360.
- Dakna, M., T. Opatrný and D.-G. Welsch, 1998, Opt. Commun. **148**, 355.
- D'Ariano, G.M., 1995, Quantum. Semiclass. Opt. **7**, 693.
- D'Ariano, G.M., 1997a, in: *Quantum Optics and Spectroscopy of Solids*, eds T. Hakioglu and A.S. Shumovsky (Kluwer Academic Publisher, Amsterdam) p. 175.
- D'Ariano, G.M., 1997b, in: *Quantum Communication, Computing and Measurement*, eds O. Hirota, A.S. Holevo and C.M. Caves (Plenum, New York) p. 253.
- D'Ariano, G.M., 1997c, Private communication.
- D'Ariano, G.M., and C. Macchiavello, 1998, Phys. Rev. **A57**, 3131.
- D'Ariano, G.M., and M.G.A. Paris, 1997a, Phys. Lett. **A233**, 49.
- D'Ariano, G.M., and M.G.A. Paris, 1997b, in: *5th Central-European Workshop on Quantum Optics*, Prague, eds I. Jex and G. Drobný (Acta Physica Slovaca **47**, 281).
- D'Ariano, G.M., and L. Maccone, 1997, in: *Fifth International Conference on Squeezed States and Uncertainty Relations*, Balatonfüred, eds D. Han, J. Janszky, Y.S. Kim and V.I. Man'ko (NASA/CP-1998-206855) p. 529.
- D'Ariano, G.M., and N. Sterpi, 1997, J. Mod. Opt. **44**, 2227.
- D'Ariano, G.M., and H.P. Yuen, 1996, Phys. Rev. Lett. **76**, 2832.
- D'Ariano, G.M., U. Leonhardt and H. Paul, 1995, Phys. Rev. **A52**, R1801.
- D'Ariano, G.M., C. Macchiavello and M.G.A. Paris, 1994a, Phys. Rev. **A50**, 4298.
- D'Ariano, G.M., C. Macchiavello and M.G.A. Paris, 1994b, Phys. Lett. **A195**, 31.
- D'Ariano, G.M., C. Macchiavello and M.G.A. Paris, 1995, Phys. Lett. **A198**, 286.
- D'Ariano, G.M., C. Macchiavello and N. Sterpi, 1997, Quantum Semiclass. Opt. **9**,

929.

D'Ariano, G.M., S. Mancini, V.I. Man'ko and P. Tombesi, 1996, *Quantum Semiclass. Opt.* **8**, 1017.

Davidović, and D.M., D. Lalović, 1993, *J. Phys.* **A26**, 5099.

Davidovich, L., M. Orszag and N. Zagury, 1996, *Phys. Rev.* **A54**, 5118.

Davies, E.B., 1976, *Quantum theory of open systems* (Academic Press, New York).

Davies, E.B., and J.T. Lewis, 1970, *Commun. Math. Phys.* **17**, 239.

Davies, K.B., M.-O. Mewes, M.R. Andrews, N.J. van Druten, D.S. Durfee, D.M. Kurn and W. Ketterle, 1995, *Phys. Rev. Lett.* **75**, 3969.

Derka, R., V. Bužek and G. Adam, 1996, in: *4th Central-European Workshop on Quantum Optics*, Budmerice, ed. V. Bužek (*Acta Physica Slovaca* **46**, 355).

Derka, R., V. Bužek, G. Adam and P.L. Knight, 1996, *J. Fine Mechanics Optics* **11-12**, 341.

D'Helon, C., and G.J. Milburn, 1996, *Phys. Rev.* **A54**, R25.

Dhirani, Al-A., D.A. Kokorowski, R.A. Rubenstein, T.D. Hammond, B. Rohwedder, E.T. Smith, A.D. Roberts, and D.E. Pritchard, 1997, *J. Mod. Opt.* **44**, 2583.

Dodonov, V.V., I.A. Malkin, and V.I. Man'ko, 1974, *Physica* **72**, 597.

Dodonov, V.V., and V.I. Man'ko, 1997, *Phys. Lett.* **A229**, 335.

Dowling, J.P., G.S. Agarwal and W.P. Schleich, 1994, *Phys. Rev.* **A49**, 4101.

Drummond, P.D., 1989, in: *Fifth New Zealand Symposium on Quantum Optics*, eds J.D. Harvey and D.F. Walls (Springer-Verlag, Berlin) p. 57.

Drummond, P.D., and C.W. Gardiner, 1980, *J. Phys.* **A13**, 2353.

Dunn, T.J., I.A. Walmsley and S. Mukamel, 1995, *Phys. Rev. Lett.* **74**, 884.

Dutra, S.M., P.L. Knight and H. Moya-Cessa, 1993, *Phys. Rev.* **A48**, 3168.

Dutra, S.M., and P.L. Knight, 1994, *Phys. Rev.* **A49**, 1506.

Epstein, S.T., 1959, *Am. J. Phys.* **27**, 291.

d'Espagnat, B., 1976, *Conceptual Foundations of Quantum Mechanics*, (Benjamin, Reading, MA).

Fano, U., 1957, *Rev. Mod. Phys.* **29**, 74.

Fearn, H., and R. Loudon, 1987, *Opt. Commun.* **64**, 485.

Feenberg, E., 1933, Ph.D. thesis, Harvard University.

Feynman, R.P., R.B. Leighton and M. Sands, 1965, *The Feynman Lectures on Physics* (Addison-Wesley, Reading, MA).

Freyberger, M., 1997, *Phys. Rev.* **A55**, 4120.

Freyberger, M., S.H. Kienle, and V.P. Yakovlev, 1997, *Phys. Rev. A* **56**, 195.

Freyberger, M., and W.P. Schleich, 1993, *Phys. Rev.* **A47**, R30.

Freyberger, M., K. Vogel and W.P. Schleich, 1993a, *Quantum Opt.* **5**, 65.

Freyberger, M., and A.M. Herkommer, 1994, *Phys. Rev. Lett.* **72**, 1952.

Freyberger, M., K. Vogel and W.P. Schleich, 1993b, *Phys. Lett.* **A176**, 41.

Friedman, C.N., 1987, *J. Austral. Math. Soc.* **B30**, 289.

Gale, W., E. Guth and G.T. Trammel, 1968, *Phys. Rev.* **165**, 1434.

Galetti, D., and M.A. Marchioli, 1996, *Ann. Phys. (NY)* **249**, 454.

Gardiner C.W., 1983, *Handbook of Stochastic Methods* (Springer, Berlin).

Gardiner, C.W., 1991, *Quantum Noise* (Springer, Berlin).

Gauss, C.F., 1809, *Theoria motus corporum coelestium in sectionibus conicis solem ambientum* (Perthes and Besser, Hamburg).

Gauss, C.F., 1821, *Theoria combinationis observationum erroribus minimis obnoxiae*

- (Societati regiae scientiarum exhibita, Göttingen).
- Gerlach, W., and O. Stern, 1921, *Z. Phys.* **8**, 110.
- Gerlach, W., and O. Stern, 1922, *Z. Phys.* **9**, 349.
- Glauber, R.J., 1963a, *Phys. Rev.* **130**, 2529.
- Glauber, R.J., 1963b, *Phys. Rev. Lett.* **10**, 84.
- Glauber, R.J., 1963c, *Phys. Rev.* **131**, 2766.
- Glauber, R.J., 1965, in: *Quantum Optics and Electronics*, eds C. DeWitt, A. Blandin and C. Cohen-Tannoudji (Gordon and Breach, New York) p. 144.
- Glauber, R.J., and M. Lewenstein, 1991, *Phys. Rev.* **A43**, 467.
- Golovchenko, J.A., D.R. Kaplan, B. Kincaid, R. Levesque, A. Meixner, M.P. Robbins, and J. Felsteiner, 1981, *Phys. Rev. Lett.* **46**, 1454.
- Golub, G.H., and C.F. van Loan, 1989, *Matrix Computations* (J. Hopkins University Press, Baltimore and London).
- Greene, B.I., J.F. Federici, D.R. Dykaar, R.R. Jones and P.H. Bucksbaum, 1991, *Appl. Phys. Lett.* **59**, 893.
- Gruner, T., and D.-G. Welsch, 1996, *Phys. Rev.* **A53**, 1818.
- Havener, C.C., N. Rouze, W.B. Westerveld and J.S. Risley, 1986, *Phys. Rev.* **A33**, 276.
- Helstrom, C.W., 1976, *Quantum Detection and Estimation Theory* (Academic, New York).
- Herkommer, A.M., V.M. Akulin and W.P. Schleich, 1992, *Phys. Rev. Lett.* **69**, 3298.
- Herzog, U., 1996a, *Phys. Rev.* **A53**, 1245.
- Herzog, U., 1996b, *Phys. Rev.* **A53**, 2889.
- Ho, S.T., A.S. Lane, A. La Porta, R.E. Slusher and B. Yurke, 1990, in: *International Quantum Electronics Conference, Technical Digest Series Vol. 7* (Optical Society of America, Washington).
- Holevo, A.S., 1973, *J. Multivar. Anal.* **3**, 337.
- Holevo, A.S., 1982, *Probabilistic and Statistical Aspects of Quantum Theory* (North-Holland, Amsterdam).
- Hradil, Z., 1992, *Quantum Opt.* **4**, 93.
- Hradil, Z., 1993, *Phys. Rev.* **A47**, 2376.
- Hradil, Z., 1997, *Phys. Rev.* **A55**, R1561.
- Husimi, K., 1940, *Proc. Phys. Math. Soc. Jpn.* **22**, 264.
- Husimi, K., 1953, *Proc. Theor. Phys.* **9**, 381.
- Huttner, B., J.J. Baumberg, J.F. Ryan and S.M. Barnett, 1992, *Opt. Commun.* **90**, 128.
- Imamoğlu, A., 1993, *Phys. Rev.* **A47**, R4577.
- Ivanović, I.D., 1981, *J. Phys.* **A14**, 3241.
- Ivanović, I.D., 1983, *J. Math. Phys.* **24**, 1199.
- Ivanović, I.D., 1993, *J. Phys.* **A26**, L579.
- Jain, A., C.D. Lin and W. Fritsch, 1987a, *Phys. Rev.* **A35**, 3180.
- Jain, A., C.D. Lin and W. Fritsch, 1987b, *Phys. Rev.* **A36**, 2041.
- Jain, A., C.D. Lin and W. Fritsch, 1988, *Phys. Rev.* **A37**, 3611(E).
- Janicke, U., and M. Wilkens, 1995, *J. Mod. Opt.* **42**, 2183.
- Janszky, J., and Y.Y. Yushin, 1986, *Opt. Commun.* **59**, 151.
- Janszky, J., P. Adam and Y. Yushin, 1992, *Opt. Commun.* **93**, 191.
- Javanainen, J., 1994, *Phys. Rev. Lett.* **72**, 2375.

- Jaynes, E.T., 1957a, Phys. Rev. **106**, 620.
Jaynes, E.T., 1957b, Phys. Rev. **108**, 171.
Jaynes, E.T., and F.W. Cummings, 1963, Proc. IEEE **51**, 89.
Jex, I., S. Stenholm and A. Zeilinger, 1995, Opt. Commun. **117**, 95.
Jones, K.R.W., 1991, Ann. Phys. (NY) **207**, 140.
Jones, K.R.W., 1994, Phys. Rev A**50**, 3682.
Jones, R.R., 1996, Phys. Rev. Lett. **76**, 3927.
Jones, R.R., D. You and P.H. Bucksbaum, 1993, Phys. Rev. Lett. **70**, 1236.
Kano, Y., 1965, J. Math. Phys. **6**, 1913.
Kazantsev, A.P., 1975, Zh. Eksp. Teor. Fiz. **67**, 1660; (Sov. Phys. JETP **40**, 825).
Kazantsev, A.P., 1978, Usp. Fiz. Nauk **124**, 113; (Sov. Phys. Usp. **21**, 58).
Keith, D.W., C.R. Ekstrom, Q.A. Turchette, and D.E. Pritchard (1991), Phys. Rev. Lett. **66**, 2693.
Kelley, P.L., and W.H. Kleiner, 1964, Phys. Rev. **136**, A316.
Kemble, E.C., 1937, *Fundamental Principles of Quantum Mechanics*, (McGraw-Hill, New York).
Kienle, S.H., D. Fischer, W.P. Schleich, V.P. Yakovlev and M. Freyberger, 1997, Appl. Phys. B**65**, 735.
Kim, M.S., 1997a, Phys. Rev. A**56**, 3175.
Kim, M.S., 1997b, J. Mod. Opt. **44**, 1437.
Kim, M.S., and N. Imoto, 1995, Phys. Rev. A**52**, 2401.
Kim, M.S., and B.C. Sanders, 1996, Phys. Rev. A**53**, 3694.
Kim, C., and P. Kumar, 1994, Phys. Rev. Lett. **73**, 1605.
Kiss, T., U. Herzog and U. Leonhardt, 1995, Phys. Rev. A**52**, 2433.
Klauder, J.R., 1960, Ann. Phys. (NY) **11**, 123.
Klauder, J.R., 1963a, J. Math. Phys. **4**, 1055.
Klauder, J.R., 1963b, J. Math. Phys. **4**, 1058.
Klauder, J.R., and E.C.G. Sudarshan, 1968, *Fundamentals of Quantum Optics* (Benjamin, New York).
Knöll, L., W. Vogel and D.-G. Welsch, 1987, Phys. Rev. A**36**, 3803.
Kochański, P., and K. Wódkiewicz, 1997, J. Mod. Opt. **44**, 2343.
Kokorowski, D.A., and D.E. Pritchard, 1997, J. Mod. Opt. **44**, 2575.
Kowalczyk, P., C. Radzewicz, J. Mostowski and I.A. Walmsley, 1990, Phys. Rev. A**42**, 5622.
Krähmer, D.S., and U. Leonhardt, 1997a, Phys. Rev. A**55**, 3275.
Krähmer, D.S., and U. Leonhardt, 1997b, J. Phys. A**30**, 4783.
Krähmer, D.S., and U. Leonhardt, 1997c, Appl. Phys. B**65**, 725.
Kreinovitch, V.Ja., 1977, Theor. Math. Phys. **28**, 623.
Kühn, H., D.-G. Welsch and W. Vogel, 1994, J. Mod. Opt. **41**, 1607.
Kühn, H., W. Vogel and D.-G. Welsch, 1995, Phys. Rev. A**51**, 4240.
Kurtsiefer, Ch., T. Pfau and J. Mlynek, 1997, Nature **386**, 150.
Kwiat, P.G., A.M. Steinberg, R.Y. Chiao, P.H. Eberhard and M.D. Petroff, 1993, Phys. Rev. A**48**, R867.
Lai, Y., and H.A. Haus, 1989, Quantum Opt. **1**, 99.
Lalović, D., D.M. Davidović and N. Bijedić, 1992] Phys. Rev. A**46**, 1206.
Lambrecht, A., T. Coudreau, A.M. Steinberg and E. Giacobino, 1996, Europhys. Lett. **36**, 93.

- Legendre, A.M., 1805, *Nouvelles méthodes pour la détermination des orbites des comètes* (Firmin–Didot, Paris).
- Lee, C.T., 1992, Phys. Rev. **A46**, 6097.
- Lehner, J., U. Leonhardt and H. Paul, 1996] Phys. Rev. **A53**, 2727.
- Leibfried, D., D.M. Meekhof, B.E. King, C. Monroe, W.M. Itano and D. Wineland, 1996, Phys. Rev. Lett. **77**, 4281 (1996).
- Leichtle, C., W.P. Schleich, I.Sh. Averbukh and M. Shapiro, 1998, Phys. Rev. Lett. **80**, 1418.
- Leonhardt, U., 1993, Phys. Rev. **A48**, 3265.
- Leonhardt, U., 1994, Phys. Rev. **A49**, 1231.
- Leonhardt, U., 1995, Phys. Rev. Lett. **74**, 4101.
- Leonhardt, U., 1996, Phys. Rev. **A53**, 2998.
- Leonhardt, U., 1997a, Phys. Rev. **A55**, 3164.
- Leonhardt, U., 1997b, J. Mod. Opt. **44**, 2271.
- Leonhardt, U., 1997c, *Measuring the Quantum State of Light* (Cambridge University Press, Cambridge).
- Leonhardt, U., and P.J. Bardroff, 1997, in: *5th Central-European Workshop on Quantum Optics*, Prague, eds I. Jex and G. Drobný (Acta Physica Slovaca **47**, 225).
- Leonhardt, U., and I. Jex, 1994, Phys. Rev. **A49**, R1555.
- Leonhardt, U., and M. Munroe, 1996, Phys. Rev. **A54**, 3682.
- Leonhardt, U., and S. Schneider, 1997, Phys. Rev. **A56**, 2549.
- Leonhardt, U., and H. Paul, 1993a, Phys. Rev. **A47**, R2460.
- Leonhardt, U., and H. Paul, 1993b, Phys. Rev. **A48**, 4598.
- Leonhardt, U., and H. Paul, 1994a, Phys. Rev. Lett. **72**, 4086.
- Leonhardt, U., and H. Paul, 1994b, J. Mod. Opt. **41**, 1427.
- Leonhardt, U., and H. Paul, 1995, Progr. Quantum Electron. **19**, 89.
- Leonhardt, U., and M.G. Raymer, 1996, Phys. Rev. Lett. **76**, 1985.
- Leonhardt, U., H. Paul and G.M. D’Ariano, 1995, Phys. Rev. **A52**, 4899.
- Leonhardt, U., J.A. Vaccaro, B. Böhmer and H. Paul, 1995, Phys. Rev. **A51**, 84.
- Leonhardt, U., M. Munroe, T. Kiss, Th. Richter and M.G. Raymer, 1996, Opt. Commun. **127**, 144.
- Lohmann, A.W., 1993, J. Opt. Soc. Am. **A10**, 2181.
- London, F., 1926, Z. Phys. **37**, 915.
- London, F., 1927, Z. Phys. **40**, 193.
- Loudon, R., 1986, in: *Coherence, Cooperation and Fluctuations*, eds F. Haake, L.M. Narducci and D.F. Walls (Cambridge University Press, Cambridge) p. 240.
- Luis, A., and J. Peřina, 1996a, Quantum Semiclass. Opt. **8**, 873.
- Luis, A., and J. Peřina, 1996b, Quantum Semiclass. Opt. **8**, 887.
- Luis, A., and L.L. Sánchez-Soto, 1995, Quantum Semiclass. Opt. **7**, 153.
- Lukš, A., and V. Peřinová, 1994, Quantum Opt. **6**, 125.
- Lutterbach, L.G., and L. Davidovich, 1997, Phys. Rev. Lett. **78**, 2547.
- Lynch, R., 1995, Phys. Rep. **256**, 367.
- Mancini, S., and P. Tombesi, 1997a, Phys. Rev. **A56**, 3060.
- Mancini, S., and P. Tombesi, 1997b, Europhys. Lett. **40**, 351.
- Mancini, S., V.I. Man’ko and P. Tombesi, 1995, Quantum Semiclass. Opt. **7**, 615.
- Mancini, S., V.I. Man’ko and P. Tombesi, 1996, Phys. Lett. **A213**, 1.
- Mancini, S., V.I. Man’ko and P. Tombesi, 1997, J. Mod. Opt. **44**, 2281.

- Mancini, S., P. Tombesi and V.I. Man'ko, 1997, Europhys. Lett. **37**, 79.
- Mandel, L., 1958, Proc. Phys. Soc. Lond. **72**, 1037.
- Mandel, L., 1963, in: *Progress in Optics*, Vol. 2, ed. E. Wolf (North-Holland, Amsterdam) p. 181.
- Mandel, L., 1982, Phys. Rev. Lett. **49**, 136.
- Mandel, L., and E. Wolf, 1995, *Optical Coherence and Quantum Optics* (Cambridge University Press).
- Man'ko, O.V., 1996, J. Russ. Laser Research **17**, 579.
- Man'ko, O.V., 1997, Phys. Lett. **A228**, 29.
- Marchioli, M.A., S.S. Mizrahi and V.V. Dodonov, 1997, Phys. Rev. **A56**, 4278.
- Marks, J.R., 1991, *Introduction to Shannon Sampling and Interpolation Theory* (Springer, New York).
- de Matos Filho, R.L., and W. Vogel, 1996, Phys. Rev. Lett. **76**, 4520.
- Mattle, K., M. Michler, H. Weinfurter, A. Zeilinger and M. Zukowski, 1995] Appl. Phys. **B60**, S111.
- McAlister, D.F., and M.G. Raymer, 1997a, Phys. Rev. **A55**, R1609.
- McAlister, D.F., and M.G. Raymer, 1997b, J. Mod. Opt. **44**, 2359.
- Meekhof, D.M., C. Monroe, B.E. King, W.M. Itano and D.J. Wineland, 1996, Phys. Rev. Lett. **76**, 1796.
- Meschede, D., H. Walther and G. Müller, 1985, Phys. Rev. Lett. **54**, 551.
- Mewes, M.-O., M.R. Andrews, D.M. Kurn, D.S. Durfee, C.G. Townsend and W. Ketterle, 1997, Phys. Rev. Lett. **78**, 582.
- Mogilevtsev, D., Z. Hradil and J. Peřina, 1997, J. Mod. Opt. **44**, 2261.
- Mollow, B.R., and R.J. Glauber, 1967a, Phys. Rev. **160**, 1076.
- Mollow, B.R., and R.J. Glauber, 1967b, Phys. Rev. **160**, 1097.
- Monroe, C., D.M. Meekhof, B.E. King and D.J. Wineland, 1996, Science **272**, 1131.
- Moroz, B.Z., 1983, Int. J. Theor. Phys. **22**, 329.
- Moroz, B.Z., 1984, Int. J. Theor. Phys. **23**, 497(E).
- Moya-Cessa, H., and P.L. Knight, 1993, Phys. Rev. A **48**, 2479.
- Munroe, M., D. Boggavarapu, M.E. Anderson and M.G. Raymer, 1995] Phys. Rev. **A52**, R924.
- Munroe, M., D. Boggavarapu, M.E. Anderson, U. Leonhardt and M.G. Raymer, 1996, in: *Coherence and Quantum Optics VII*, eds J.H. Eberly, L. Mandel and E. Wolf (Plenum, New York) p. 53.
- Nagourney, W., J. Sandberg, and H. Dehmelt, 1986, Phys. Rev. Lett. **56**, 2797.
- Natterer, F., 1986, *The Mathematics of Computerized Tomography* (Wiley, Chichester).
- Neuhauser, W., M. Hohenstatt, P.E. Toschek and H.G. Dehmelt, 1980, Phys. Rev. **A22**, 1137.
- von Neumann, J., 1932, *Mathematische Grundlagen der Quantenmechanik* (Springer, Berlin).
- Newton, R.G., and B. Young, 1968, Ann. Phys. (NY) **49**, 393.
- Noel, M.W., and C.R. Stroud, Jr., 1996, Phys. Rev. Lett. **77**, 1913.
- Noh, J.W., A. Fougères and L. Mandel, 1991, Phys. Rev. Lett. **67**, 1426.
- Noh, J.W., A. Fougères and L. Mandel, 1992a, Phys. Rev. **A45**, 424.
- Noh, J.W., A. Fougères and L. Mandel, 1992b, Phys. Rev. **A46**, 2840.
- Noh, J.W., A. Fougères and L. Mandel, 1993a, Phys. Rev. Lett. **71**, 2579.

- Noh, J.W., A. Fougères and L. Mandel, 1993b, Phys. Rev. **A47**, 4535.
- Noh, J.W., A. Fougères and L. Mandel, 1993c, Phys. Rev. **A47**, 4541.
- Noordam, L.D., and R.R. Jones, 1997, J. Mod. Opt. **44**, 2515.
- O'Connell, R.F., and A.K. Rajagopal, 1982, Phys. Rev. Lett. **48**, 525.
- Opatrný, T., and D.-G. Welsch, 1997, Phys. Rev. **A55**, 1462.
- Opatrný, T., M. Dakna and D.-G. Welsch, 1997, in: *Fifth International Conference on Squeezed States and Uncertainty Relations*, Balatonfüred, eds D. Han, J. Janszky, Y.S. Kim and V.I. Man'ko (NASA/CP-1998-206855) p. 621.
- Opatrný, T., M. Dakna and D.-G. Welsch, 1998, Phys. Rev. **A57**, 2129.
- Opatrný, T., D.-G. Welsch and V. Bužek, 1996, Phys. Rev. **A53**, 3822.
- Opatrný, T., D.-G. Welsch and W. Vogel, 1996, in: *4th Central-European Workshop on Quantum Optics*, Budmerice, ed. V. Bužek (Acta Physica Slovaca **46**, 469).
- Opatrný, T., D.-G. Welsch and W. Vogel, 1997a, Phys. Rev. **A55**, 1416.
- Opatrný, T., D.-G. Welsch and W. Vogel, 1997b, Optics Commun. **134**, 112.
- Opatrný, T., D.-G. Welsch and W. Vogel, 1997c, Phys. Rev. **A56**, 1788.
- Opatrný, T., V. Bužek, J. Bajer and G. Drobný, 1995, Phys. Rev. **A52**, 2419.
- Opatrný, T., D.-G. Welsch, S. Wallentowitz and W. Vogel, 1997, J. Mod. Opt. **44**, 2405.
- Orłowski, A., and H. Paul, 1994, Phys. Rev. **A50**, R921.
- Ou, Z.Y., C.K. Hong and L. Mandel, 1987a, Opt Commun. **63**, 118.
- Ou, Z.Y., C.K. Hong and L. Mandel, 1987b, Phys. Rev. **A36**, 192.
- Ou, Z.Y., and H.J. Kimble, 1995, Phys. Rev. **A52**, 3126.
- Paris, M.G.A., 1996a, Phys. Lett. **A217**, 78.
- Paris, M.G.A., 1996b, Phys. Rev. **A53**, 2658.
- Paris, M.G.A., 1996c, Opt. Commun. **124**, 277.
- Paris, M.G.A., A.V. Chizhov and O. Steuernagel, 1997, Opt. Commun. **134**, 117.
- Park, J.L., and W. Band, 1971, Found. Phys. **1**, 211.
- Park, J.L., W. Band and W. Yourgrau, 1980, Ann. Phys. (Leipzig) **37**, 189.
- Parkins, A.S., P. Marte, P. Zoller, O. Carnal and H.J. Kimble, 1995, Phys. Rev. **A51**, 1578.
- Paul, H., 1963, Ann. Phys. (Leipzig) **11**, 411.
- Paul, H., 1974, Fortschr. Phys. **22**, 657.
- Paul, H., W. Brunner and G. Richter, 1966, Ann. Phys. (Leipzig) **17**, 262.
- Paul, H., P. Törmä, T. Kiss and I. Jex, 1996a, Phys. Rev. Lett. **76**, 2464.
- Paul, H., P. Törmä, T. Kiss and I. Jex, 1996b, J. Opt. Fine Mechanics **41**, 338.
- Paul, H., P. Törmä, T. Kiss and I. Jex, 1997a, Phys. Rev. **A56**, 4076.
- Paul, H., P. Törmä, T. Kiss and I. Jex, 1997b, J. Mod. Opt. **44**, 2395.
- Paul, W., O. Osberghaus and E. Fischer, 1958, *Forschungsberichte des Wirtschafts- und Verkehrsministeriums Nordrhein-Westfalen*, Nr. 415 (Westdeutscher Verlag, Köln und Opladen).
- Pauli, W., 1933, in: *Handbuch der Physik*, Vol. 24, Part 1, eds H. Geiger and K. Scheel (Springer, Berlin); for an English translation, see Pauli, W., *General Principles of Quantum Mechanics* (Springer, Berlin, 1980) p. 17.
- Pavičić, M., 1987, Phys. Lett. **A122**, 280.
- Pegg, D.T., and S.M. Barnett, 1988, Europhys. Lett. **6**, 483.
- Pegg, D.T., and S.M. Barnett, 1997, J. Mod. Opt. **44**, 225.
- Pegg, D.T., S.M. Barnett and L.S. Phillips, 1997, J. Mod. Opt. **44**, 2135.

- Penning, F.M., 1936, *Physica* **3**, 873.
- Perelomov, A., 1986, *Generalized Coherent States and Their Applications* (Springer, Berlin).
- Peřina, J., 1985, *Coherence of Light* (Reidel, Dordrecht).
- Peřina, J., 1991, *Quantum Statistics of Linear and Nonlinear Optical Phenomena* (Reidel, Dordrecht).
- Pfau, T., and Ch. Kurtsiefer, 1997, *J. Mod. Opt.* **44**, 2551.
- Plebanski, J., 1954, *Bull. Acad. Polon.* **11**, 213.
- Plebanski, J., 1955, *Bull. Acad. Polon.* **14**, 275.
- Plebanski, J., 1956, *Phys. Rev.* **101**, 1825.
- Polzik, E.S., J. Carri and H.J. Kimble, 1992, *Phys. Rev. Lett.* **68**, 3020.
- Popper, K.R., 1982, *Quantum Theory and the Schism in Physics* (Hutchinson, London).
- Poyatos, J.F., R. Walser, J.I. Cirac, P. Zoller and R. Blatt, 1996, *Phys. Rev.* **A53**, R1966.
- Prasad, S., M.O. Scully and W. Martienssen, 1987, *Opt. Commun.* **62**, 139.
- Press, W.H., S.A. Teukolsky, W.T. Vetterling and B.P. Flannery, 1995, *Numerical Recipes in C* (Cambridge University Press, New York).
- Prugovečki, E., 1977, *Int. J. Theor. Phys.* **16**, 321.
- Radon, J., 1917, *Berichte über die Verhandlungen der Königlich-Sächsischen Gesellschaft der Wissenschaften zu Leipzig, Mathematisch-Physikalische Klasse* **69**, 262.
- Rajagopal, A.K., 1983, *Phys. Rev.* **A27**, 558.
- Raman, C., C.W.S. Conover, C.I. Sukenik and P.H. Bucksbaum, 1996, *Phys. Rev. Lett.* **76**, 2436.
- Ramsey, N.F., 1956, *Molecular Beams* (Clarendon Press, Oxford).
- Raymer, M.G., 1994, *Am. J. Phys.* **62**, 986.
- Raymer, M.G., 1997, *J. Mod. Opt.* **44**, 2565.
- Raymer, M.G., M. Beck, and D.F. McAlister, 1994, *Phys. Rev. Lett.* **72**, 1137.
- Raymer, M.G., D.F. McAlister and U. Leonhardt, 1996, *Phys. Rev.* **A54**, 2397.
- Raymer, M.G., J. Cooper, H.J. Carmichael, M. Beck and D.T. Smithey, 1995, *J. Opt. Soc. Am.* **B12**, 1801.
- Raymer, M.G., D.T. Smithey, M. Beck, M.E. Anderson and D.F. McAlister, 1993, *Third International Wigner Symposium*, Oxford.
- Reck, M., A. Zeilinger, H.J. Bernstein and P. Bertani, 1994, *Phys. Rev. Lett.* **73**, 58.
- Reichenbach, H., 1946, *Philosophical Foundations of Quantum Mechanics* (University of California Press, Berkeley).
- Rempe, G., H. Walther and N. Klein, 1987, *Phys. Rev. Lett.* **58**, 353.
- Renwick, S.P., E.C. Martell, W.D. Weaver and J.S. Risley, 1993, *Phys. Rev.* **A48**, 2910.
- Richter, Th., 1996a, *Phys. Lett.* **A211**, 327.
- Richter, Th., 1996b, *Phys. Rev.* **A53**, 1197.
- Richter, Th., 1996c, *Phys. Rev.* **A54**, 2499.
- Richter, Th., 1997a, *J. Mod. Opt.* **44**, 2385.
- Richter, Th., 1997b, *Phys. Rev.* **A55**, 4629.
- Richter, Th., and A. Wünsche, 1996a, *Phys. Rev.* **A53**, R1974.
- Richter, Th., and A. Wünsche, 1996b, in: *4th Central-European Workshop on Quan-*

- tum Optics*, Budmerice, ed. V. Bužek (Acta Physica Slovaca **46**, 487).
- Richter, G., W.H Brunner and H. Paul, 1964, Ann. Phys. (Leipzig) **14**, 239.
- Robinson, D.J.S., 1991, *A Course in Linear Algebra with Applications* (World Scientific, Singapore).
- Royer, A., 1977, Phys. Rev. **A15**, 449.
- Royer, A., 1985, Phys. Rev. Lett. **55**, 2745.
- Royer, A., 1989, Found. Phys. **19**, 3.
- Royer, A., 1994, Phys. Rev. Lett. **73**, 913.
- Royer, A., 1995, Phys. Rev. Lett. **74**, 1040(E).
- Royer, A., 1996, Phys. Rev. **A53**, 70.
- Sauter, Th., W. Neuhauser, R. Blatt and P.E. Toschek, 1986, Phys. Rev. Lett. **57**, 1696.
- Schiller, S., G. Breitenbach, S.F. Pereira, T. Müller and J. Mlynek, 1996, Phys. Rev. Lett. **77**, 2933.
- Schneider, S., A.M. Herkommer, U. Leonhardt and W.P. Schleich, 1997, J. Mod. Opt. **44**, 2333.
- Schrödinger, E., 1926, Naturwiss. **14**, 664.
- Schubert, M., and W. Vogel, 1978a, Wiss. Zeitschr. FSU Jena, Math.–Nat. R. **27**, 179.
- Schubert, M., and W. Vogel, 1978b, Phys. Lett. **A68**, 321.
- Schülke, W., 1988, Portugal. Phys. **19**, 421.
- Schülke, W., and S. Mourikis, 1986, Acta Cryst. **A42**, 86.
- Schülke, W., U. Bonse, and S. Mourikis, 1981, Phys. Rev. Lett. **47**, 1209.
- Schumaker, B.L., 1984, Opt. Lett. **9**, 189.
- Seifert, N., N.D. Gibson and J.S. Risley, 1995, Phys. Rev. **A52**, 3816.
- Senitzky, I.R., 1954, Phys. Rev. **95**, 1115.
- Shapiro, J.H., 1985, IEEE J. Quant. Electron. **21**, 237.
- Shapiro, J.H., and S.S. Wagner, 1984, IEEE J. Quant. Electron. **20**, 803.
- Shapiro, J.H., and H.P. Yuen, 1979, IEEE Trans. Inform. Theor. **25**, 179.
- Shapiro, J.H., H.P. Yuen and J.A. Machado Mata, 1979, IEEE Trans. Inform. Theor. **24**, 657.
- Shapiro, M., 1995, J. Chem. Phys. **103**, 1748.
- Shore, B.W., and P.L. Knight, 1993, J. Mod. Opt. **40**, 1195.
- Sleator, T., T. Pfau, V. Balykin, O. Carnal and J. Mlynek, 1992, Phys. Rev. Lett. **68**, 1996.
- Smithey D.T., M. Beck, J. Cooper and M.G. Raymer, 1993, Phys. Rev. **A48**, 3159.
- Smithey, D.T., M. Beck, M.G. Raymer and A. Faridani, 1993, Phys. Rev. Lett. **70**, 1244.
- Smithey, D.T., M. Beck, J. Cooper, M.G. Raymer and A. Faridani, 1993, Phys. Scr. **T48**, 35.
- Song, S., C.M. Caves and B. Yurke, 1990, Phys. Rev. **A41**, 5261.
- Stenholm, S., 1992, Ann. Phys. (N.Y.) **218**, 233.
- Stenholm, S., 1995, Appl. Phys. **B60**, 243.
- Stern, O., 1921, Z. Phys. **7**, 249.
- Steuernagel, O., and J.A. Vaccaro, 1995, Phys. Rev. Lett. **75**, 3201.
- Stulpe, W., and M. Singer, 1990, Found. Phys. Lett. **3**, 153.
- Sudarshan, E.C.G., 1963, Phys. Rev. Lett. **10**, 277.

- Susskind, L., and J. Glogower, 1964, *Physics* **1**, 49.
- Takahashi, K., and N. Saitô, 1985, *Phys. Rev. Lett.* **55**, 645.
- Tan, S.M., 1997, *J. Mod. Opt.* **44**, 2233.
- Tanguy, C., S. Reynaud and C. Cohen-Tannoudji, 1984, *J. Phys.* **B17**, 4623.
- Tegmark, M., 1996, *Phys. Rev. A* **54**, 2703.
- Titulaer, U.M., and R.J. Glauber, 1966, *Phys. Rev.* **145**, 1041.
- Törmä, P., S. Stenholm and I. Jex, 1995, *Phys. Rev.* **A52**, 4853.
- Törmä, P., I. Jex and S. Stenholm, 1996, *J. Mod. Opt.* **43**, 245.
- Trippenbach, M., and Y.B. Band, 1996, *J. Chem. Phys.* **105**, 8463.
- Turski, L.A., 1972, *Physica* **57**, 432.
- Ueda, M., and M. Kitagawa, 1992, *Phys. Rev. Lett.* **68**, 3424.
- Vaccaro, J.A., and S.M. Barnett, 1995, *J. Mod. Opt.* **42**, 2165.
- Várilly, J.C., and J.M. Gracia-Bondía, 1989, *Ann. Phys. (NY)* **190**, 107.
- Vogel, K., and H. Risken, 1989, *Phys. Rev.* **A40**, 2847.
- Vogel, W., 1991, *Phys. Rev. Lett.* **67**, 2450.
- Vogel, W., 1995, *Phys. Rev.* **A51**, 4160 (1995).
- Vogel, W., and J. Grabow, 1993, *Phys. Rev.* **A47**, 4227.
- Vogel, W., and R.L. de Matos Filho, 1995, *Phys. Rev.* **A52**, 4214.
- Vogel, W., and W. Schleich, 1991, *Phys. Rev.* **A44**, 7642.
- Vogel, W., and D.-G. Welsch, 1994, *Lectures on Quantum Optics* (Akademie Verlag, Berlin).
- Vogel, W., and D.-G. Welsch, 1995, in: *3th Central-European Workshop on Quantum Optics*, Budmerice, ed. V. Bužek (*Acta Physica Slovaca* **45**, 313).
- Vogel, W., D.-G. Welsch and L. Leine, 1987, *J. Opt. Soc. Am.* **B4**, 1633).
- Vogt, A., 1978, in: *Mathematical Foundations of Quantum Theory*, ed. A.R. Marlow (Academic, New York) p. 365.
- Walker, N.G., 1987, *J. Mod. Opt.* **34**, 15.
- Walker, N.G., and J.E. Carroll, 1984, *Electron. Lett.* **20**, 981.
- Wallentowitz S., and W. Vogel, 1995, *Phys. Rev. Lett.* **75**, 2932.
- Wallentowitz, S., and W. Vogel, 1996a, *Phys. Rev.* **A53**, 4528.
- Wallentowitz S., and W. Vogel, 1996b, *Phys. Rev.* **A54**, 3322.
- Wallentowitz, S., R.L. de Matos Filho, and W. Vogel, 1997, *Phys. Rev.* **A56**, 1205.
- Wallis, H., A. Röhrli, M. Naraschewski and A. Schenzle, 1997, *Phys. Rev.* **A55**, 2109.
- Walser, R., 1997, *Phys. Rev. Lett.* **79**, 4724.
- Walser, R., J.I. Cirac and P. Zoller, 1996, *Phys. Rev. Lett.* **77**, 2658.
- Waxer, L.J., I.A. Walmsley and W. Vogel, 1997, *Phys. Rev.* **A56**, R2491.
- Weigert, S., 1992, *Phys. Rev.* **A45**, 7688.
- Weyl, H., 1927, *Z. Phys.* **46**, 1.
- Wiedemann, H., 1996, unpublished.
- Wiesbrock, H.-W., 1987, *Int. J. Theor. Phys.* **26**, 1175.
- Wigner, E.P., 1932, *Phys. Rev.* **40**, 749.
- Wigner, E.P., 1959, *Group Theory* (Academic Press, New York).
- Wilkens, M., and P. Meystre, 1991, *Phys. Rev.* **A43**, 3832.
- Wineland, D.J., J.J. Bollinger, W.M. Itano, F.L. Moore, and D.J. Heinzen, 1992, *Phys. Rev. A* **46**, R6797.
- Wódkiewicz, K., 1984, *Phys. Rev. Lett.* **52**, 1064.
- Wódkiewicz, K., 1986, *Phys. Lett.* **A115**, 304.

- Wódkiewicz, K., 1988, Phys. Lett. **A129**, 1.
- ten Wolde, A., L.D. Noordam, A. Lagendijk and H.B. van Linden van den Heuvell, 1988, Phys. Rev. Lett. **61**, 2099.
- Wootters, W.K., 1987, Ann. Phys. (NY) **176**, 1.
- Wootters, W.K., and B.D. Fields, 1989, Ann. Phys. (NY) **191**, 363.
- Wootters, W.K., and W.H. Zurek, 1979, Phys. Rev. **D19**, 473.
- Wünsche, A., 1990, Quantum Opt. **2**, 453.
- Wünsche, A., 1991, Quantum Opt. **3**, 359.
- Wünsche, A., 1996a, Quantum Semiclass. Opt. **8**, 343.
- Wünsche, A., 1996b, Phys. Rev. **A54**, 5291.
- Wünsche, A., 1997, J. Mod. Opt. **44**, 2293.
- Wünsche, A., and V. Bužek, 1997, Quantum Semiclass. Opt. **9**, 631.
- Yeazell, J.A., and C.R. Stroud, Jr., 1988, Phys. Rev. Lett. **60**, 1494.
- Yuen, H.P., 1982, Phys. Lett. **A91**, 101.
- Yuen, H.P., and V.W.S. Chan, 1983, Opt. Lett. **8**, 177.
- Yuen, H.P., and J.H. Shapiro, 1978b, IEEE Trans. Inf. Theory **24**, 657.
- Yuen, H.P., and J.H. Shapiro, 1978b, in: *Coherence and Quantum Optics IV*, eds L. Mandel and E. Wolf (Plenum, New York) p. 719.
- Yuen, H.P., and J.H. Shapiro, 1980, IEEE Trans. Inf. Theory **26**, 78.
- You, D., R.R. Jones, P.H. Bucksbaum and D.R. Dykaar, 1993, Opt. Lett. **18**, 290.
- Yurke, B., 1985, Phys. Rev. **A32**, 300, 311.
- Yurke, B., and D. Stoler, 1987, Phys. Rev. **A36**, 1955.
- Yurke, B., S.L. McCall and J.R. Klauder, 1986, Phys. Rev. **A33**, 4033.
- Yurke, B., P. Grangier, R.E. Slusher and M.J. Potasek, 1987, Phys. Rev. **A35**, 3586.
- Zaugg, T., M. Wilkens and P. Meystre, 1993, Found. Phys. **23**, 857.
- Zucchetti, A., W. Vogel and D.-G. Welsch, 1996, Phys. Rev. **A54**, 856.
- Zucchetti, A., W. Vogel, M. Tasche and D.-G. Welsch, 1996, Phys. Rev. **A54**, 1678.